

Climate impacts on hydrometric variables in the Mackenzie River Basin

by

Queenie Kwan Yi Yip

A thesis
presented to the University of Waterloo
in fulfillment of
the thesis requirement for the degree of
Master of Applied Science
in
Civil Engineering

Waterloo, Ontario, Canada, 2008

© Queenie Kwan Yi Yip 2008

I hereby declare that I am the sole author of this thesis. This is a true copy of the thesis, including any required final revisions, as accepted by my examiners.

I understand that my thesis may be made electronically available to the public.

Abstract

The research described in this thesis examines how the hydrologic cycle is affected by climate changes in the Mackenzie River Basin (MRB) in northern Canada. The study focuses on five hydro-meteorological variables; runoff, evapotranspiration, storage, temperature and precipitation. Two different climate input data sets were used: Environment Canada gridded observed data and the European Center for Medium range Weather Forecasting (ECMWF) Re-Analysis climate data (ERA-40). In both data sets, runoff and evapotranspiration were modelled using the WATFLOOD hydrological model for the period of 1961 to 2002 on a 20 by 20 km grid.

Trends were assessed on a monthly and annual basis using the Mann-Kendall non-parametric trend test. The hydrologic cycle in the MRB appears to be strongly influenced by climate change. The results reveal a general pattern of warming temperatures, and increasing precipitation and evapotranspiration. Overall decreases in runoff and in storage were detected from the Environment Canada data set while increases in runoff and in storage were detected from the ECMWF data set.

The trends in runoff and evapotranspiration reflected changes in both precipitation and temperature. The spatial pattern of changes in runoff followed the pattern of change in precipitation very closely in most of the months, with the exception of March and October. The effect of changes in temperature is much more noticeable than that of changes in precipitation in March and October. The change in spatial distribution of evapotranspiration, on the other hand, matched the pattern of changes in temperature better; yet its seasonal pattern follows more closely to that of precipitation.

The sensitivity of annual runoff to changes in climate was also estimated using a nonparametric estimator. Among the most important findings are: 1) runoff was more sensitive to precipitation and less sensitive to temperature; 2) runoff was positively correlated with precipitation and evapotranspiration; 3) runoff was negatively correlated with temperature, implying any increase in melt runoff from glaciers caused by increases in temperature were offset by losses due to

evapotranspiration within the basin; 4) soil moisture storage may play an important role in the runoff and evapotranspiration processes; and 5) the sensitivity of mean annual runoff to changes in precipitation and evapotranspiration is typically lower along the Rocky Mountain chain, higher in the central zone of the Interior Plain, and highly varied in the Canadian Shield region in the basin.

Correlation analysis suggested that the agreement between the two data sets is very weak at the grid-cell level. However, there was broad degree of consistencies in the seasonal and spatial patterns of trends between the two data sets, suggesting that the data are more reliable for identifying hydrological changes on a regional scale than at grid-cell level.

Acknowledgements

First and foremost, I would like to thank my supervisor, Dr. Donald H. Burn, for his support, wisdom, encouragement, and limitless patience throughout my research. His advice and comments on my thesis drafts have been valuable. I thank him for having his office door open whenever I need! I was lucky to have such an enthusiastic and all-around great person as my advisor. I would also want to thank my supervisor's wife, Joanne, for her delicious dishes.

I would also like to extend my gratitude to Dr. Eric D. Soulis. He has been abundantly helpful and supportive during my two years of research. He has shared his wealth of knowledge and experience on many aspects of work and life with me. I am also grateful to him for being the second reader. Also, thank him for his trust and confidence on me. I can never forget the strength and courage I received from him during the difficult times.

In addition, a number of people lent their expertise to this research. In particular, the assistance of Frank Seglenieks was invaluable. Frank assisted in many ways throughout the process of this thesis. I thank him for his time and assistance on the project. I would like to also thank Environment Canada and European Center for Medium range Weather Forecasting (ECMWF) for providing me the climate data that I regard as the backbone of this research.

I am also grateful for the research funding from the Mackenzie GEWEX Study (MAGS), Environment Canada, and the Natural Sciences and Engineering Research Council (NSERC) of Canada.

I would like to express my heartiest thanks to my friends, Edwin Wong, Gigi Ching, Aaron Chong, Jeremy Chan, and Heather Mustard, for helping me through the difficult times, and for all the emotional support and caring they provided.

Lastly, and most importantly, I wish to thank my parents. I owe my parents, Regina and Ping Yip, much of what I have become. I thank them for raised me, supported me, taught me, and loved me. To them I dedicate this thesis.

Table of Contents

	Page No.
Abstract.....	iii
Acknowledgements.....	v
Table of Contents.....	vi
List of Figures.....	ix
List of Tables.....	xi
1 INTRODUCTION.....	1
1.1 Background.....	1
1.2 Research needs	2
1.3 Research goals and objectives	4
1.4 Research scope	5
1.5 Thesis organization.....	5
2 THEORETICAL BACKGROUND AND LITERATURE REVIEW	7
2.1 Introduction	7
2.2 Climate change	9
2.3 Greenhouse effect and climate change	10
2.4 Impact of climate change.....	12
2.4.1 Hydrology and water resources.....	12
2.4.2 Coastal systems	15
2.4.3 Ecosystem	16
2.4.4 Food and fibre production	17
2.4.5 Human health	18
2.4.6 Feedbacks on greenhouse warming.....	18
2.5 Detection and attribution	18
2.5.1 Data for hydrological change detection	19
2.5.2 Hydrological modelling and impacts of climatic change.....	19

2.6	Trend detection.....	20
2.7	Trend detection research.....	24
2.7.1	Interpreting test results.....	30
2.8	Attribution research.....	31
2.9	Application of detection and attribution.....	34
2.9.1	Global.....	34
2.9.2	United States.....	35
2.9.3	Canada.....	37
2.9.4	Other regions.....	44
2.10	Climate change impacts in the MRB.....	45
2.10.1	Future climate scenarios generated by GCMs.....	45
2.10.2	Detection and attribution research in the MRB.....	45
2.11	Large-scale climate anomalies and hydrological trends.....	48
3	TECHNICAL APPROACH/ METHODOLOGY	51
3.1	Variable selection and data collection.....	51
3.2	Mann-Kendall test for trend detection.....	52
3.3	Local trend detection.....	54
3.4	Regional trend detection.....	55
3.5	Relationship of runoff with climate.....	56
3.6	Interpretation of test results.....	57
4	THE STUDY SITE.....	60
4.1	Climatic regions.....	62
4.2	Natural and anthropogenic influences on the streamflow regime.....	67
5	DATA SOURCES.....	68
5.1	Description of data sets.....	68
5.2	Variables selection.....	69
5.3	The WATFLOOD hydrological model.....	70
5.3.1	Performance of WATFLOOD.....	71
5.3.2	Data processing.....	72
5.3.3	Model Calibration.....	75

6	RESULTS	76
6.1	Trends	76
6.1.1	Temperature	76
6.1.2	Precipitation	81
6.1.3	Runoff	85
6.1.4	Evapotranspiration	91
6.1.5	Storage.....	97
6.1.6	Summary of trend results	99
6.2	Climate elasticity	104
6.3	Comparisons of the two data sets	113
6.3.1	Original data.....	113
6.3.2	Partial correlation	118
7	COMPARISONS WITH OTHER STUDIES.....	126
8	DISCUSSION	129
9	CONCLUSIONS AND RECOMMENDATIONS.....	133
	REFERENCES.....	137
	APPENDIX A Box plots of estimated monthly trend magnitude.....	148
	APPENDIX B Spatial distribution of monthly trend.....	174
	APPENDIX C Location of 60 sample sites used in the comparison of the two data sets....	187
	APPENDIX D Summary of monthly original data.....	188

List of Figures

Figure 1	The Hydrologic Cycle	13
Figure 2	Climatic regions in the Mackenzie River Basin	41
Figure 3	Categories of PDO and ENSO from 1961 to 2002	49
Figure 4	Technical Approach Flow Chart	51
Figure 5	The Mann-Kendall test procedure	52
Figure 6	Trend Free Pre-whitening Procedure	55
Figure 7	The Mackenzie River Basin and its geographic features and population centers	61
Figure 8	Ecozones in the Mackenzie River Basin	62
Figure 9	The Mackenzie River Basin location and its major sub basins	63
Figure 10	Physiographical subdivisions in the Mackenzie River Basin	64
Figure 11	Grouped response unit and runoff routing concept	71
Figure 12	Environment Canada – Box plots of 4667 estimated trend magnitude for every month and for the annual temperature records	78
Figure 13	ECMWF – Box plots of 4635 estimated trend magnitude for every month and for the annual temperature records	79
Figure 14	Spatial distribution of significant ($p=0.1$) annual mean temperature trends	80
Figure 15	Environment Canada – Box plots of 4667 estimated trend magnitude for every month and for the annual precipitation records	82
Figure 16	ECMWF – Box plots of 4667 estimated trend magnitude for every month and for the annual precipitation records	83
Figure 17	Spatial distribution of significant ($p=0.1$) annual precipitation trends	84
Figure 18	Environment Canada – Box plots of 4667 estimated trend magnitude for every month and for the annual runoff records	87
Figure 19	ECMWF – Box plots of 4667 estimated trend magnitude for every month and for the annual runoff records	88
Figure 20	Plots of regional median trend magnitude for runoff records	89
Figure 21	Spatial distribution of significant ($p=0.1$) annual runoff trends	91
Figure 22	Environment Canada – Box plots of 4667 estimated trend magnitude for every month and for the annual evapotranspiration records	94
Figure 23	ECMWF – Box plots of 4667 estimated trend magnitude for every month and for the annual evapotranspiration records	95
Figure 24	Spatial distribution of significant ($p=0.1$) annual evapotranspiration trends	96
Figure 25	Box plots of 4667 estimated trend magnitude for the annual storage records	98
Figure 26	Spatial distribution of significant ($p=0.1$) annual storage trends	99
Figure 27	Probability level associated with trends for Environment Canada data set and ECMWF data	

	set	101
Figure 28	Summary of annual trends for each water balance component.....	104
Figure 29	Box plots of 4667 estimated precipitation elasticity of runoff for the Mackenzie River Basin	106
Figure 30	Box plots of 4667 estimated evapotranspiration elasticity of runoff for the Mackenzie River Basin.....	106
Figure 31	Box plots of 4635 estimated temperature elasticity of runoff for the Mackenzie River Basin	107
Figure 32	Environment Canada – Map of precipitation elasticity of runoff for the Mackenzie River Basin.....	108
Figure 33	ECMWF – Map of precipitation elasticity of runoff for the Mackenzie River Basin.....	109
Figure 34	Environment Canada – Map of evapotranspiration elasticity of runoff for the Mackenzie River Basin.....	111
Figure 35	ECMWF – Map of evapotranspiration elasticity of runoff for the Mackenzie River Basin.....	112
Figure 36	Environment Canada – Map of temperature elasticity of runoff for the Mackenzie River Basin.....	114
Figure 37	ECMWF – Map of temperature elasticity of runoff for the Mackenzie River Basin.....	115
Figure 38	Box plots of original data from 60 sample site for annual runoff.....	116
Figure 39	Box plots of original data from 60 sample site for annual precipitation	116
Figure 40	Box plots of original data from 60 sample site for annual evapotranspiration	117
Figure 41	Box plots of original data from 60 sample site for annual storage.....	117
Figure 42	Box plots of original data from 60 sample site for annual temperature	118
Figure 43	Box plots of 4635 estimated partial correlation of the Environment Canada data set with the ECMWF data set.....	120
Figure 44	Partial correlation of the Environment Canada data set with the ECMWF data set for the runoff records.....	121
Figure 45	Partial correlation of the Environment Canada data set with the ECMWF data set for the precipitation records.....	122
Figure 46	Partial correlation of the Environment Canada data set with the ECMWF data set for the evapotranspiration records.....	123
Figure 47	Partial correlation of the Environment Canada data set with the ECMWF data set for the storage records.....	124
Figure 48	Partial correlation of the Environment Canada data set with the ECMWF data set for the temperature records.....	125

List of Tables

Table 1	Interpretation of errors of type I and II.....	21
Table 2	Summary of Nash values for both data sets.....	75
Table 3	Summary of trend analyses using the MK test for Temperature (in °C/year)	77
Table 4	Summary of trend analyses using the MK test for Precipitation (mm/year)	81
Table 5	Summary of trend analyses using the MK test for Runoff (mm/year)	86
Table 6	Summary of trend analyses using the MK test for Evapotranspiration (mm/year)	92
Table 7	Summary of trend analyses using the MK test for Storage	97
Table 8	Summary of trends showing the percentage of grid squares with a trend that is significant at the 10% significance level.....	100
Table 9	Summary of the climate elasticity of runoff.....	104
Table 10	Summary of the regional partial correlation of Environment Canada data set with ECMWF data set.....	119

1 INTRODUCTION

1.1 Background

Water is an essential component to life on earth. Its importance to humans is more than simply sustaining life. Water has been used in activities such as industrial production, waste removal, irrigation, residential uses and production of hydroelectric power (Blarcum *et al.*, 1995). Yet, disasters can also result from the change of quantity and quality of water. For example, the 1998 flood of China's Yangtze River, the 1930s North American Dust Bowl, and the 2000 Walkerton Tragedy have caused serious life and economic losses, and severe health problems.

Over the last few decades, development interventions have focused on issues such as economic growth and political interest. This has put further pressure on the functioning of the earth system in the face of climate change, leading to global changes in soil moisture, an increase in global mean sea level, and prospects for more severe extreme high-temperature events, floods and droughts in some places (IPCC, 1997). IPCC (2007a) has further concluded that many natural systems are being affected by climate changes and that human activity has "very likely" been the driving force in that change over the last 50 years. This strong consensus has raised attention from governments, organizations, media, and public. Such awareness has led to a growing interest in the study of the impacts of climate change.

Climate change can affect all the natural processes in the biosphere. While the movement of water through the hydrologic cycle is the largest flow among any material in the biosphere, the hydrologic cycle is intricately linked with climate (Chahine, 1992). For example, IPCC (2007a) has documented two types of hydrological systems that are affected around the world:

- "increased run-off and earlier spring peak discharge in many glacier- and snow-fed rivers" (IPCC, 2007a: 3);
- "warming of lakes and rivers in many regions with effects on thermal structure and water quality" (IPCC, 2007a: 3).

Numerous authors have examined the impacts of climate change on water resources (Mimikou *et al.*, 2000; Jackson *et al.*, 2001; Schindler, 2001; White *et al.*, 2005). Although the results vary,

all of them concluded that climate change will adversely affect water quality and quantity. Further, IPCC (1997) noted that water quality and quantity in North America are particularly sensitive to climate change. While Canada contains about nine percent of the world's renewable water, any change in water quantity and/ or quality would have consequences far beyond Canada's border (Environment Canada, 2004).

The Mackenzie River Basin (MRB) covers one-fifth of the total land area of Canada. As the tenth largest basin in the world by drainage area, the basin plays an important part in regulating the thermohaline circulation of the world's oceans (Environment Canada, 2001). The basin is also the largest North American source of freshwater draining into the Arctic Ocean (Environment Canada, 2001).

Previous studies have concluded that the MRB has undergone a significant warming trend over the last few decades (Shabbar *et al.*, 1997; Stewart *et al.*, 1998; Zhang *et al.*, 2000; Cao *et al.*, 2002; Abdul Aziz, 2004). Moreover, Nicholls *et al.* (1996) noted that the climatic change signal for high-latitude basins such as the MRB are projected to be stronger than elsewhere. Relatively small changes in climate can result in relatively large changes in the amount of discharge to the Arctic Ocean, and thus drastically influence the net freshwater balance of the Arctic Ocean such as sea-ice production and oceanic salinity (Cao *et al.*, 2002).

1.2 Research needs

The Global Energy and Water Cycle Experiment (GEWEX) developed by World Climate Research Programme (WCRP) coordinates researchers all around the world aimed at improving the understanding and predicting the water and the energy cycle and their role in the climate system (Environment Canada and NSERC CRSNG, 2004). The MRB, located in the northern portion of western Canada, is a study area for the GEWEX in North America. This contribution is referred to as the Mackenzie GEWEX Study (MAGS).

As part of the MAGS, the objective of this research is to improve the understanding and quantify some aspects of the water cycle of the MRB under climate warming. According to IPCC (1995), climate change is likely to increase river runoff in high latitude regions, such as the MRB,

because of increased precipitation. Furthermore, increasing surface temperature will tend to increase evapotranspiration (Dingman, 2002). One of the major consequences will be an intensification of the water cycle.

The Mackenzie Basin Impact Study (MBIS) focuses on the impacts of potential climate changes on the land and water resource in the MRB (Cohen, 1996). It is a six-year collaborative research program which initiated by Environment Canada in 1990. This study suggested that the effects of climate warming are evident in the MRB. It also concluded that the region will undergo dramatic changes because of global warming (Environment Canada, 1997). Soulis *et al.* (1994) further found that changes in runoff in the MRB are expected under climate change in the MBIS.

Previous studies on the analysis of hydrological trends in the MRB have focused on streamflow variables (Burn, 1994; Blarcum *et al.*, 1995; Spence, 2002; Woo and Thorne, 2003; Abdul Aziz, 2004; Burn *et al.*, 2004a; Burn *et al.*, 2004b). Streamflow variables are commonly used because they are one of the most readily accessible observed data with reasonable accuracy. Streamflow is a spatially and temporally integrated response to meteorological inputs (e.g. rainfall, evaporation, precipitation, and temperature), and physiographic features (e.g. topography, lithology, soil, and vegetation cover heterogeneities) on the surrounding drainage basin area (Westmacott and Burn, 1997; Labat *et al.*, 2004).

However, any changes on the basin and/or on the waterways can influence the magnitude and/ or timing of streamflow events. For example, Lettenmaier *et al.* (1994) suggested that the nature of streamflow responses to trends in antecedent precipitation is more complex than changes in direct runoff, and is likely to be catchment specific. These impacts should be identified from the time series to differentiate between the effects of climate (including both natural variability and anthropogenic climate change) and non-climatic factors (e.g. land use and land-cover change, storage modification, water consumption, and irrigation) (Labat *et al.*, 2004). As established later, Woo and Thorne (2003) described some natural and anthropogenic influences on the streamflow regimes in the MRB.

The MRB has a sparse distribution of gauging stations. Resources are often limited to provide

and maintain an appropriate density of stream gauges and weather stations in this large and remote area (Soulis *et al.*, 2005). The majority of the stations are located in the southern basin. To cope with this dilemma, some authors increased the spatial coverage of some stations (Zhang *et al.*, 2001a; Abdul Aziz, 2004). Abdul Aziz (2004), for example, studied the hydrological regime in the MRB. The drainage areas within the network are up to 606,000 km², which is 30% of the total area of the studied basin. Woo and Thorne (2003) studied the streamflow in the MRB and used regression relationships to estimate the flow for the ungauged basin. However, some gauging stations in the basin have closed down in the mid-1990s (Spence *et al.*, 2007). The reductions of gauging stations will increase the extrapolation error by around 16% for all flow regimes (Spence *et al.*, 2007).

Moreover, the quality of the available data is highly variable. Many gauging stations in the basin have short records and gaps within the time series (Woo and Thorne, 2003). Since the representativeness of the time series is very important in the study of climate impacts, a compromise between the length of record and station density is required.

An alternative approach consists of an extensive analysis of individual hydrologic components of the water cycle, such as precipitation, runoff, evapotranspiration, and soil moisture, and the possible correlation between these hydrological parameters and measured climate. This approach eliminates the impacts of non-climatic factors on the natural hydrological regime from the analysis (Bouwer *et al.*, 2006). However, obtaining an adequate spatial representation of these parameter values through direct observation is always impractical. This study utilizes a hydrological model to simulate these hydrological parameters from historical changes in climate. The advantage of this approach is that hydrological models can generate output of different variables at various spatial scales (Xu, 1999) and temporal resolution (Gleick, 1986), which overcomes the limitation of using observed streamflow data.

1.3 Research goals and objectives

Runoff in North America is most sensitive to the recent climatic change among other continents in the world (Labat *et al.*, 2004). Therefore, a clear understanding of the trends and characteristics of each hydrological process in high latitude basins, such as the MRB, is an

important starting point to better understand the cause of pressure on water resources in a cold region climate system. The goal of this research was to examine the impact of climate change on the hydrologic cycle in the MRB, and thereby advance our understanding of the high latitude water cycle. The research focused on five hydro-meteorological variables; runoff, evaporation, storage, temperature and precipitation. To meet the goal, the following specific objectives were defined:

- generate monthly and annually time series for the five hydro-meteorological variables;
- identify trends in the time series;
- estimate sensitivity of runoff and evaporation to changing climate;
- assess the quality of the data sets used in this study; and
- compare findings with other studies.

1.4 Research scope

The current research focuses only on the impacts of climatic factor on the hydrologic cycle. Other relevant non-climatic factors, such as deforestation, solar dimming, land-use, irrigation, and direct atmospheric carbon dioxide effects on plant transpiration (Gedney *et al.*, 2006), are not considered in this research. However, the final section of this research compares the findings from Abdul Aziz (2004), who studied the streamflow trends in the MRB, for evidence of changes in hydrological regime from non-climatic drivers.

1.5 Thesis organization

In light of the emerging issues concerning global warming, the first part of Chapter 2 reviews some of the current information on the topic of global warming. The remainder of Chapter 2 reviews literature, background information and theories associated with this study. A fundamental concept of climate change and its impacts to the earth system are presented in accordance to the conceptual framework developed by the IPCC (1997). This is followed by a review of the methodology of change detection in time series of hydrological data. A method to estimate the sensitivity of hydrological variables to climate change is also reviewed. Case studies of related research are summarized, with particular emphasis on trend detection and hydrologic sensitivity research. This chapter ends with a discussion of the use of hydrologic

models for assessing the impacts of climate change. The technical approach that is used in this research is outlined in Chapter 3. This chapter also includes a brief discussion of the hydrological model used in this research, and the benefits of this model applying to the context of the MRB, the case study site which is described in Chapter 4. In Chapter 5, the data are described in detail. In particular, the description focuses on the quality of the input climate data, the computational process, and the quality of the simulated data. The approach outlined in Chapter 3 is then applied and the results are presented in Chapter 6. Chapter 7 compares the findings from this research to other related studies of North America and the MRB. This information will provide better insight to the changing hydrologic system under climate warming, and will form the foundation for future research and sustainable management of watersheds in the MRB. Chapter 8 discusses and summarizes the major findings in this study. This research ends with conclusions and recommendations from this research study.

2 THEORETICAL BACKGROUND AND LITERATURE REVIEW

2.1 Introduction

There is increasing evidence that climate change is occurring. Since the 19th century, scientists have noticed that human emissions of CO₂ have impacts on global climate. The topic of climate change, however, had simply remained as a scientific topic rather than a global issue that affects everyone. The Kyoto Protocol to the United Nations Framework Convention on Climate Change (UNFCCC), the first binding climate change agreement, targeted reductions in greenhouse gases by an average of 5.2% below the 1990's level during the five-year period (2008-2012) (Wikipedia, 2007b). However, according to Mittelstaedt (2007), increasing emission of greenhouse gases have been recorded in most of the countries, such as Canada, United States, Britain, Italy, South Africa, Brazil, China, Mexico and India. Although emissions from Russia, which account for about 6.5 percent of total world emission, declined in the early 1990s, they are now increasing again. Mittelstaedt (2007) claimed that Russia has “hardly any policy in place to curb emissions.”

One of the reasons for inaction is scientific uncertainty about the human impacts on the climate (PEW Center on Global Climate Change, 2004; Anonymous, 2007a). In 1990, the IPCC First Assessment Report states that “the size of this warming is...of the same magnitude as natural climate variability...observed [temperature] increase could be largely due to this natural variability.” The second IPCC Assessment Report (1995: 5) suggested “a discernible human influence on global climate.” The words were never strong enough to raise attention from public, governments nor media. Another barrier is economic interest of status quo. For example, there were some claims about scientist bribes to raise doubt about climate change by an oil company (Guggenheim, 2006; Anonymous, 2007c; Zabarenko, 2007).

A once scientific idea is now becoming an ethical (Stern, 2006), economical (Stern, 2006) and political issue (Blarcum *et al.*, 1995; Cororan, 2006). The release of Al Gore's documentary, *An Inconvenient Truth* (2006), provides a prologue to what Attenborough (2007) termed as “moral change” in public's attitude toward climate change (Dispatch, 2006). According to a report by

Nielsen Company and Oxford University (2007), a survey of more than 26000 Internet users in 47 nations in March, 2007 indicated that sixteen percent of them would have “major concern” on climate change (compared to only 7 percent in a survey in October, 2006). Another widely known report, The Stern’s (2006) report, discusses the effect of climate change on the world economy. This report has brought up the discussions on costs and policy responses to climate change (Norwich Union, 2007). The IPCC (2007a) report, which affirms that global warming is “unequivocal”, has justified the doubts and destroyed excuses for inaction.

Global warming has been put as one of the top agenda items in the Group of Eight nations (G8) summit in June, 2007 (Mittelstaedt, 2007). However, “while climate changes run like a rabbit, world politics move like a snail...” (Borenstein, 2007). Most of the countries still fail to control their emissions. According to the study commissioned jointly by WWF and Allianz Group (2007), United States, Canada, and Russia have been ranked as having the poorest performance record among the advanced countries (Mittelstaedt, 2007). Australia and United States have refused to join the Kyoto Protocol. Large developing countries such as China, India and Brazil, although exempt from the Kyoto Protocol’s rule, their emissions, as of the year of 2000, represent about 25 percent of the total world emissions. York (2007) even predicted that China will potentially become the world’s top producer of greenhouse gases in 2009 due to the extensive use of coal as energy source. These countries (United States, Russia, Australia, China, Brazil, and India) represent about 59 percent of the total world greenhouse gas emissions (USGCRP, 2000; WRI, 2007b). All of them, however, have refused to ratify the Kyoto Protocol targets (Anonymous, 2007b; Anonymous, 2007d; Gorrie, 2007; Mittelstaedt, 2007; York, 2007).

The main objective of the Kyoto Protocol is the “stabilization of greenhouse gas concentrations in the atmosphere at a level that would prevent dangerous anthropogenic interference with the climate system” (UNFCCC, 2007). Yet, greenhouse gases are not the only driving force of climate change. Why did UNFCCC make such an objective statement when other factors may also contribute to climate change? The remainder of this chapter discusses the concept of climate change, its impact, and the detection work.

2.2 Climate change

The climate system varies due to internal variability and external forces (IPCC, 2007b). The internal variability is caused by the chaotic dynamics of the climate system (IPCC, 2001b). It occurs naturally on all time-scales from weeks to centuries and even millennia (IPCC, 2001b). Some of the known internal variations include Pacific Interdecadal Climate Oscillation (PDO) and El Niño-Southern Oscillation (ENSO). The external forcings, on the other hand, include both natural and anthropogenic influences. Examples of natural external forcings include solar variation (IPCC, 2007b), volcanic emissions (IPCC, 2007b), forest fires, orbital forcing (Dingman, 2002), and plate tectonics (Wikipedia, 2007a). Human activities also influence the climate by changing atmospheric composition (IPCC, 2007b) and land use (Wikipedia, 2007a). Most of these forcings altered the radiation balance of the earth, and thereby alter various natural systems, such as climate systems, ecosystems, and hydrologic systems, on earth.

Radiation from the sun travels to Earth through space. About 20 percent of the incoming solar radiation arriving at the top of the Earth's atmosphere is reflected back into space by clouds and aerosols (IPCC, 2007b). Once the radiation reaches the Earth's surface, an additional 10 percent of this radiation is reflected by high albedo surfaces, such as snow, ice, and deserts (IPCC, 2007b). The remaining radiation is changed into heat energy. About 60 percent of this heat energy is absorbed by different parts of the climate system and warms the land and water. The water cycle, winds and ocean currents, and photosynthesis use the remaining 40 percent of energy to drive their processes (Viau, 2003). To balance the incoming energy, the Earth itself must radiate, on average, the same amount of energy back to space by emitting outgoing longwave radiation (IPCC, 2007b). This heat energy is entrapped by greenhouse gases in the lower atmosphere to maintain the surface warmth of Earth (Smith and Smith, 2000).

The source of the energy that drives the climate system is the sun. Thus, any changes to the solar radiation balance of the earth would have direct impact on the climate. IPCC (2007b) document three fundamental ways to alter this balance:

- 1) "by changing the incoming solar radiation [by orbital forcing]" (IPCC, 2007b: 96);
- 2) "by changing the fraction of solar radiation that is reflected (called 'albedo') [by changes in cloud cover, atmospheric composition or land use]" (IPCC, 2007b: 96); and

- 3) “by altering the longwave radiation from Earth back towards space [by changing greenhouse gas concentrations]” (IPCC, 2007b: 96).

These changes can lead to a warming or cooling of the climate system, and thus impact other natural systems on the earth. As established later, these responses may interact and form feedback loops that can amplify or dampen an external forcing factor (Steffen, 2006).

Human activities have seriously altered the radiative balance of the atmosphere. The major radiative forcing resulting from human activities include greenhouse gases, ozone, stratospheric water vapour, surface albedo by altering land use, and aerosol (IPCC, 2007b). IPCC (2007b) has pointed out two important points. First, natural forcings are very small compared to the radiative forcing resulting from human activities. As a result, the radiative forcing from human activities is much more important for current and future climate change. The second point is that the primary driver of climate change from human activities is increasing greenhouse gas concentration in the atmosphere. This has significantly contributed to the warming trend since the start of the industrial era.

2.3 Greenhouse effect and climate change

Some greenhouse gases occur naturally in the atmosphere, while others result from anthropogenic activities. Naturally occurring greenhouse gases includes water vapor, carbon dioxide (CO₂), methane (CH₄), nitrous oxide (N₂O), and ozone (O₃). Since the atmosphere is generally cooler than the Earth’s surface, gas molecules in the atmosphere absorb the longwave radiation (also called infrared radiation) emitted from Earth to keep Earth’s climate warm and habitable. Without greenhouse gases, Earth’s average surface temperature would be about 30°C lower (Dingman, 2002). This phenomenon is called the greenhouse effect.

The earliest discovery of the greenhouse effect can be found as early as 1824 by Joseph Fourier (John F. Kennedy School of Government, 2001). He found that the atmosphere absorbs longwave radiation emitted from Earth more effectively than shorter wavelength radiation from the sun (Stern, 2006). In the 1860s John Tyndall identified that water vapor and carbon dioxide in the atmosphere would absorb thermal radiation (John F. Kennedy School of Government, 2001). In 1896, Svante Arrhenius investigated the relationship between greenhouse gases and

climate. He suggested that carbon dioxide in the atmosphere could substantially alter the surface temperature (John F. Kennedy School of Government, 2001). He also realized that the ongoing combustion of coal could lead to global warming through increase of greenhouse gases. In 1938, Guy Stewart Callendar quantitatively investigated the impacts to climate with rising atmospheric carbon dioxide concentration (John F. Kennedy School of Government, 2001). He found that an increase of 2°C in mean global temperature would result from a doubled carbon dioxide climate (IPCC, 2007b). However, scientists have ignored these ideas. Callendar has also overlooked this idea and thought this warming would be beneficial by delaying the return of glaciers (Wikipedia, 2007c). The speculations were vindicated during the 1950s when a few researchers (Ahlmann, Gilbert N. Plass, Roger Revelle, Hans Suess, Bert Bolin, Erik Eriksson, and Charles David Keeling) extensively studied atmospheric carbon dioxide concentration and its impacts on climate (John F. Kennedy School of Government, 2001; Weart and American Institute of Physics, 2007). Researchers began to pursue interests on this topic from that point. These studies have provided more insight into the greenhouse effect and its relationship with Earth's climate. For example, other greenhouse gases, such as methane, nitrogen, and chlorofluorocarbons, in the atmosphere have been identified (IPCC, 2007b). Researchers also found that these gases are a crucial factor in climate change. Recent scientific development of complex computer models, General Circulation Models (GCM), can aid in determination of the impacts of increasing greenhouse gases on the global climate (Smith and Smith, 2000).

Many human activities have changed the earth's atmospheric composition. UNFCCC (2007) document some of the main contributions of anthropogenic greenhouse gases including burning of fossil fuels, deforestation, livestock, production of halocarbons and sulphur hexafluoride, transportation, and industrial processes. Among these contributions, burning of fossil fuels is the largest contribution to the anthropogenic greenhouse gases.

Four important greenhouse gases resulting from human activities are carbon dioxide (CO₂), methane (CH₄), nitrous oxide (N₂O), halocarbons (CFCs), and ozone (O₃). Increasing concentrations of these gases has led to increases of 0.56 to 0.92°C (from 1906-2005) in the mean global temperature (IPCC, 2007b). Furthermore, this warming trend is expected to continue in the near future (Stern, 2006).

2.4 Impact of climate change

The intensification of global warming has heightened concern over responses of natural systems and the impacts on humans. Many studies have concluded that the recent warming in the troposphere is mainly due to anthropogenic forcings (Tett *et al.*, 2002; Scafetta and West, 2006; IPCC, 2007a). Many impacts due to this warming would be irreversible (Sparks, 2007). For example, reduction of ice sheet, such as Arctic Sea Ice, Greenland and West Antarctic Ice Sheets, and the associated sea level rise would be irreversible (IPCC, 2007b). In addition, an increasing trend of extreme climate events has been reported. A significant proportion of the global land area has been increasingly affected by a significant change in climatic extremes during the second half of the twentieth century (Frich *et al.*, 2002). Understanding the responses of different systems to climate change is important for sustainable development and protection of natural resources.

IPCC (1997) has developed a conceptual framework in the assessment of climate change impacts into ecosystems, hydrology and water resources, food and fiber production, coastal systems, and human health categories. Among these categories, changes to hydrology and water resources will affect nearly every aspect of human well-being (Gleick, 1986). The following discussion follows a similar framework, and in turn looks at impact of climate change on hydrology and water resources, coastal system, and impacts of these hydrologic changes and climate on ecosystem, food and fibre production, and human health aspects. Feedback mechanisms are introduced at the end of this section.

2.4.1 Hydrology and water resources

The impact to hydrology and water resources is likely to have direct and/ or indirect impacts on the other categories (i.e. ecosystem, food and fibre production, and human health). As Smith and Smith (2000) indicated, “ecosystem could not function” and “life could not persist” without the cycling of water.

Although 70% of the earth’s surface is covered by water (Loaiciga *et al.*, 1996), only less than

3% can be used for drinking and to irrigate crops. Of that fresh water, 69% is locked in solid form of glaciers; only 1% is in freshwater lakes and rivers (Dingman, 2002). As of 2002, 1.1 billion people lack access to safe drinking water and 2.6 billion people lack adequate sanitation (WHO, 2007).

The hydrologic cycle makes fresh water available to sustain current human population. Figure 1 shows an abstraction of the hydrologic cycle. The hydrologic cycle is a continuous process from:

1. evaporation losses from the oceans exceed the gain by precipitation;
2. moist air masses move inland and if the right conditions exist, precipitation occurs; and
3. finally the excess of water on land returns to the oceans as runoff, balancing the deficit in the ocean-atmosphere exchange.

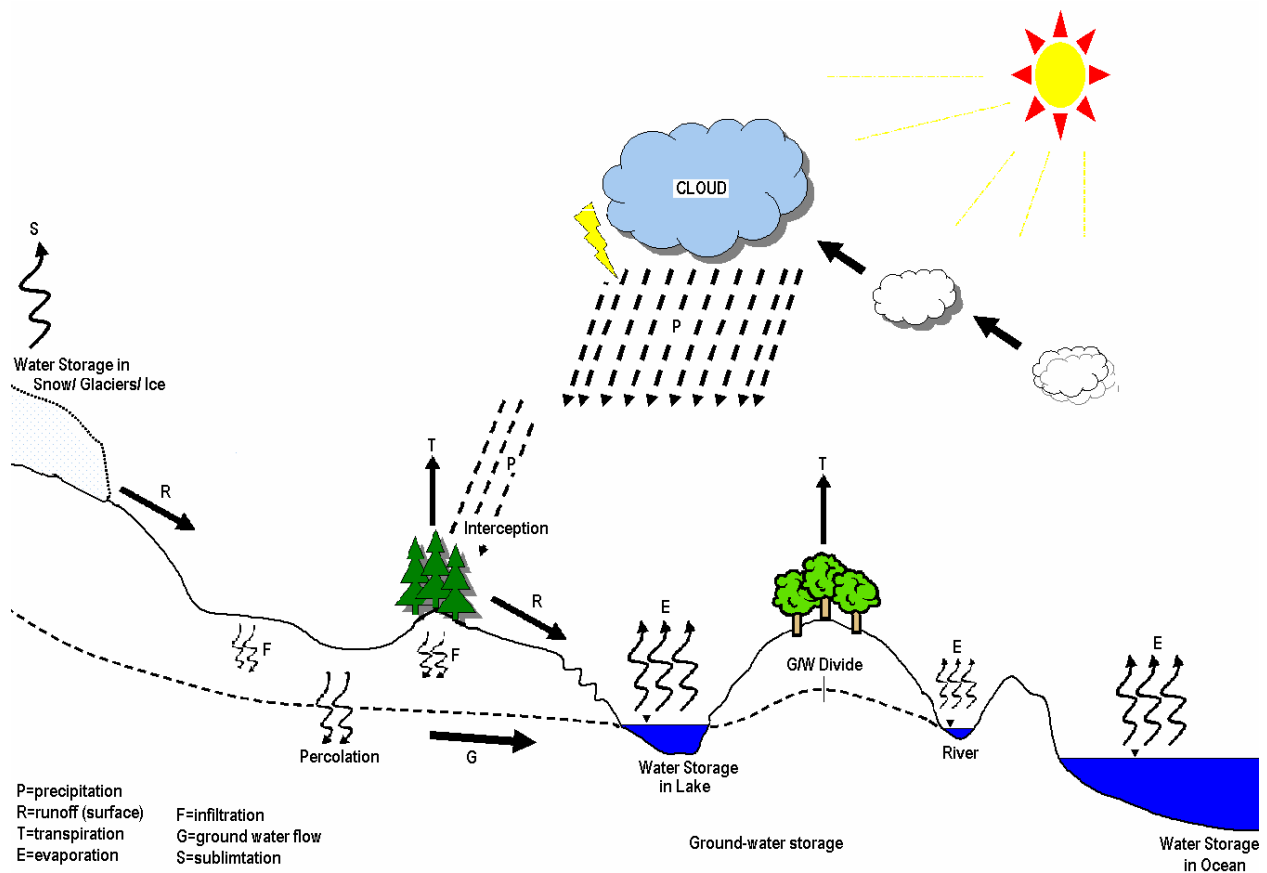


Figure 1 The Hydrologic Cycle
 Source: adapted from Colorado State University (2005)

However, climate change is expected to cause an intensification of the earth's hydrological cycle in the next 100 years (Jackson *et al.*, 2001), with general increase in ocean evaporation (Labat *et al.*, 2004), and increase in precipitation (Huntington, 2006) or decrease in continental evapotranspiration (Labat *et al.*, 2004). This process finally leads to an increase of fresh water running to the ocean via rivers (Matthews, 2006), leading to changes in water availability as well as in competition for water resources. This effect is expected to be particularly noticeable at high latitudes (USGCRP, 2000).

Another aspect of an intensified water cycle is increase in occurrence, extent, intensity and duration of extreme hydrologic events (Loaiciga *et al.*, 1996). Changes in flood frequencies are expected particularly in northern latitudes and in regions experiencing snowmelt-induced flood events (IPCC, 1995). IPCC (2007a) has further projected an increase in the extent of drought-affected areas, some of which are currently water-stressed areas. Increase of tropical storms will affect human health directly through catastrophic damage or indirectly through damage to crops (Huntington, 2006).

One of the major components of the hydrologic cycle is snow and ice. Glaciers contain about 69% of the global fresh water (Dingman, 2002). More than one-sixth of the world population currently lives in an area that depends upon meltwater from snow and glaciers as their water supply (IPCC, 2007a). During the last century, the reductions in mass, volume, area and length of snow and glaciers have been clearly observed on the global scale (Singh *et al.*, 2006).

Groisman *et al.* (1994) reported a 10% decline of areal snow cover from 1973 to 1992 in the northern hemisphere. Deglaciation has led to decreasing availability of water and has seriously affected agricultural and livestock production in some parts of the world (Chalise, 2002). Many natural systems are being affected by deglaciation including enlargement and increased numbers of glacial lakes; increasing ground instability in permafrost regions, and rock avalanches in mountain regions; and changes in some Arctic and Antarctic ecosystems (IPCC, 2007a).

Deglaciation has also led to increase in runoff and thereby influence water flows in rivers, and finally resulted in rising sea level. Dowdeswell *et al.* (1997) reported the melting of arctic glaciers contributed 0.13 mm/year sea-level rise (or 30% of total) since 1940. Sea ice and glaciers are involved in three important feedback mechanisms. First, a decrease in the areal

extent of ice and glaciers affects albedo thereby increasing the absorption of solar radiation (Steffen, 2006). Secondly, melting of permafrost will release the carbon stored and increase the concentration of CO₂ or CH₄ in the atmosphere (Steffen, 2006). Both of these feedback mechanisms would accelerate warming. Finally, as established later, reduced salinity due to increasing runoff to the ocean would result in a drop in surface temperature in higher latitudes.

Degradation of water quality is also expected in a changing climate. IPCC (2001a) noted a degradation of freshwater quality in higher water temperature. Increasing of water temperature by climate warming would increase the rate of chemical and biochemical reactions of the water and reduce the amount of essential dissolved gases such as oxygen in the water (Tchobanoglous and Schroeder, 1985). Another example is more frequent heavy rainfall events would flush more pollutants and sediments into lakes and rivers (USGCRP, 2000). In addition, flood damage of some services, such as storm and wastewater systems, water filtration facilities, and landfills, would increase the risks of contaminating freshwater. On the other hand, regions facing increasing summer drying or decreasing streamflow would likely have degradation of water quality because of increased salinity and concentration of pollutants by reducing stream dilution capacity (Mimikou *et al.*, 2000).

Groundwater is another important freshwater resource. About 30% of total global freshwater is groundwater (Dingman, 2002). Globally, groundwater accounts for at least 25% of the drinking water supply (Jackson *et al.*, 2001). Unlike surface water, groundwater supply is generally more stable, both in quality and quantity. Groundwater is more affected by long-term climate trends than short-term climate variability (USGCRP, 2000). Climate change will shorten the length of recharge period because of increasing water demand from longer growing seasons (Holman, 2006). USGCRP (2000) noted falling of groundwater levels in many areas in the United States. In terms of water quality, increase of flooding and rising sea level will increase the likelihood of saltwater intrusion into aquifers (Holman, 2006).

2.4.2 Coastal systems

During the 20th century, the sea level has risen at a rate of 1 to 2 mm per year (IPCC, 2001a).

This is largely attributed to 20th century warming and the associated thermal expansion of ocean waters and melting of glaciers (IPCC, 2001a). The 2001 report of the IPCC estimates that under all the scenarios of IPCC emissions, global mean sea level will rise from 0.09 to 0.88 m above the 1990 levels by 2100. In addition, there is potential for sea level rise of 4 to 6 m or more if partial deglaciation of the Greenland ice sheet and the West Antarctic ice sheet were to occur (IPCC, 2007a).

Coastal ecosystems and human populations in coastal environments would be seriously affected by rising sea level. Coastal ecosystems, such as coastal wetlands and marshes, can be affected by direct inundation and changes in water quality (i.e. water depth, temperature, salinity, and turbidity) (Smith and Smith, 2000). Saltwater intrusion would increase salinity of estuaries and aquifers thereby decreasing freshwater availability and affect coastal fisheries (IPCC, 2001a). Coastal flooding and other coastal hazards will increase the risk and damage to human population, particularly to people who live in coastal areas and small islands (Smith and Smith, 2000).

2.4.3 Ecosystem

Broadly, an ecosystem is a functioning unit where organisms (biotic component) interact with their environment (abiotic component) (Smith and Smith, 2000). Since climate is an integral part of the environment, many levels in the ecosystems are highly sensitive to climate change (U.S. EPA, 2007). It has been suggested that if increases in global temperature exceed 1.5-2.5°C, major changes in ecosystem structure and function are projected to occur (IPCC, 2007a). For example, IPCC (2007a) noted that up to 30 percent of species would face extinction if increases in global average temperature exceed 1.5-2.5°C. Global ecosystems will also reorganize in terms of their location, character and expanse as the warming trend continues (Rizzo and Wiken, 1992). As an example, IPCC (1997) suggested that vegetation boundaries are expected to shift into higher latitudes and elevations as the warming trend continues.

Climate change can also alter the balance of hydrologic processes and lead to more severe impacts on ecosystems than caused by warming alone. For example, inland aquatic ecosystems

will be influenced by climate change through altered water temperatures, flow regimes, water levels, and water quality (Jackson *et al.*, 2001). Durance and Ormerod (2007) reported several impacts on the macroinvertebrates community in a central Welsh upland due to climate forcing stream temperature changes. Another example is drought-induced declines in vegetation. Frank (2007) examined the impacts drought had on grassland production in Yellowstone National Park. He concluded that drought strongly influenced the below-ground productivity of the grassland.

Another major concern of changes in water quality and quantity would be the direct influences on habitat for aquatic biota. Smith and Smith (2000) emphasized the importance of habitat to the future survival rate of the world's wildlife. Tynan and DeMaster (1997) document some potential effects on loss of ice-associated habitat to marine mammals, such as seals, polar bears, and walruses, in the Arctic. They suggested that the distributions, densities, and foraging success of these arctic mammals would be greatly affected with decreasing sea-ice habitat. Another example is changes in hydrology of wetlands. Wetlands are among the richest ecosystems. Many plants, organisms, and wildlife depend upon wetlands as their habitat (Smith and Smith, 2000). Some hydrologic conditions are necessary for a wetland to exist in the first place. Changes in any of these hydrologic conditions, such as increase in frequency and duration of flood or drought, and changing the chemistry and/ or temperature of the water, would seriously affect the structure and function of wetlands (Smith and Smith, 2000). It is also realized that wetland's hydrologic conditions provide additional benefits in terms of water resources management. One of the major wetland functions in hydrology of a region is groundwater recharge.

2.4.4 Food and fibre production

Agriculture, water resources and climate are highly interrelated with each other. Changes in temperature, precipitation, length of growing season, timing of extreme events, and water availability will directly affect crop yield (IPCC, 1997). Existing water supplies are only marginally adequate to maintain acceptable levels of food production (Gleick, 1986). As an example cited in Merz *et al.* (2003), in Nepal, shortage of water for agricultural and domestic purposes during the dry months of the year is of particular concern. Moreover, they also

revealed that intensified agriculture is adding to concerns about quality of water in Nepal. IPCC (2007a) has projected a decrease in global food production if increases of local average temperature above 3°C occur.

2.4.5 Human health

In addition to the impacts of human health by the three aspects discussed above, human health could be affected by climate change through heat-stress mortality, tropical vector-borne disease, urban air pollution problems, and decreases in cold-related illnesses (IPCC, 1997). Other indirect health effects include increased incidence of communicable diseases, and increased mortality and injury due to increased extreme hydrologic events (Smith and Smith, 2000).

2.4.6 Feedbacks on greenhouse warming

Processes and responses as a result of changing climate can interact to form feedback loops that either amplify (*positive feedback*) or dampen (*negative feedback*) the effects of a change in climate forcing (Loaiciga *et al.*, 1996). There are many feedback loops present in the earth system. General circulation models (GCMs) predict that global climatic change will likely be amplified in northern high latitude regions largely due to positive feedback mechanisms (Overpeck *et al.*, 1997; Serreze *et al.*, 2000). Several of the most important ones operating in high latitudes include water vapor feedback, surface albedo feedback, carbon cycle physiological feedback, and ocean-atmospheric interactions.

2.5 Detection and attribution

Sufficient corroborative evidence is required to prove “beyond a reasonable doubt” that climate change is contributing to a particular change. In recent decades, many quantitative estimates are available to associate observed changes such as hydrology and water resources with climate change. Detection and attribution use statistical tests to assess whether observed changes contain evidence of the expected responses to external forcing that is distinct from internal variability (IPCC, 2007a). The detection and attribution of past trends, changes, and variability is essential for understanding the potential future changes resulting from anthropogenic activities (Zhang *et*

al., 2001a).

Detection and attribution are always linked together in climate change study. Nonetheless, their objectives are different. According to IPCC (2001b), “detection” is the process of identifying variability and trends in a variable that cannot be explained by natural internal variability. However, detection does not provide a reason for that change. “Attribution”, on the other hand, ascribes the most likely causative factor to the change.

The detection and attribution processes require a set of time-series data, either from observational or model output. The data must be of sufficient quality and duration. Kundzewicz and Robson (2004) urged that records of 30 years or less are too short; at least 50 years of record is necessary.

2.5.1 Data for hydrological change detection

There are several ways to generate hydrologic time-series data. The two broad categories are observational or hydrological model outputs. Most studies of the hydrological impacts of climate change are based on historical streamflow data. The major drawback of this approach is that the quality of data largely depends upon the measurement instrument. Examples of problems are: instrumental malfunction; and change in measurement techniques, in instrumentation, or in instrument location (Kundzewicz and Robson, 2004). Moreover, missing values and gaps are a common problem in most historical time-series (Kundzewicz and Robson, 2004).

2.5.2 Hydrological modelling and impacts of climatic change

Another approach involves calibrating a hydrological model and then inputting climate data to simulate hydrologic output. Such models simulate hydrological output by perturbing an historical time-series data, downscaling data from a GCM, or by utilizing weather-generated data (Jones *et al.*, 2006). There are several attractive characteristics in this approach. First, the most appropriate models can be chosen for any specific region (Gleick, 1986). Second, hydrology models can be tailored to fit the characteristic of available data (Gleick, 1986) and generate

spatial output of different variables (Bouwer *et al.*, 2006). Third, regional-scale hydrologic models are considerably easier to manipulate than GCMs (Gleick, 1986). Fourth, such regional models can be used to evaluate the sensitivity of hydrologic conditions of specific watersheds to changes in climate (Gleick, 1986). Fifth, methods that can incorporate both detailed regional hydrology characteristics and output from large-scale GCMs will be well situated to take advantage of continuing improvements in the resolution, regional geography, and hydrology of global climate models (Gleick, 1986). Sixth, effects of man-made hydrological developments and climate variability, or between different contributors, can be distinguished (Gedney *et al.*, 2006; Jones *et al.*, 2006). Finally, variables that are difficult to obtain through direct measurement, such as evapotranspiration, can be generated (Bouwer *et al.*, 2006).

2.6 Trend detection

Changes in hydrological records may sometimes be difficult to detect, even if a suitable statistical test is employed. For example, a subtle change that has not lasted long or just recently occurred might be easily overlooked (Radziejewski and Kundzewicz, 2004). Cunderlik and Burn (2004) further demonstrated that the location and the length of a given observation period have a crucial impact on trend results. Radziejewski and Kundzewicz's (2004) study evaluated the impact of intensity of change, duration of the reference period, and duration of the change period on detectability of hydrological trends. They examined five tests in their study: the Mann-Kendall (MK) test, Spearman's rank correlation, normal scores linear regression, distribution-free CUSUM (Chiew and McMahon, 1993), and cumulative deviations (Buishand, 1982) applied to normal scores. Some of the important findings that relate to this research include:

- to detect changes at the 99% significance level as compared to 95%, the intensity must be at least 44% higher.
- to achieve a 95% mean significance level, the slope of linear trend must be at least 0.28 for reference periods of 30 years, to be detectable within 10 years after its initiation.
- to detect a trend within 20 years after its initiation, a linear trend must be strong (at least 0.1 of the standard deviation of the base process per year).
- to detect weak to moderate intensity trends, shorter reference period is recommended, since using a longer reference period may weaken the detectability.

They concluded that changes that are weak or have not lasted long are not detectable. However, even if a change has not been detected by statistical tests, it doesn't necessarily demonstrate an absence of a change. Examination of the growing time series of hydrological data should be a permanent exercise as impacts of climate change on hydrological processes are likely to be stronger and last longer. Even though the change has not yet been detected, the likelihood of detection may grow.

A statistical test is an usual technique to detect and quantify the change in a hydrological time series. The purpose is to determine if a variable in question contains statistically significant trend in the data and estimate the value of the slope. The hypothesis test consists of a null hypothesis in which there is no trend in the data or the variation is due to random natural variability. This null hypothesis is to be tested against the alternative hypothesis, that there is a trend.

An appropriate test statistic is selected to evaluate the significance of the alternative hypothesis. A criterion is specified for the probability of a Type I error (Table 1). Type I error is the probability that the null hypothesis is true (i.e. no trend is present) but incorrectly rejected. This probability is also called the significance level, which measures whether the test statistic is very different from the range of values that would typically occur under the null hypothesis. Another type of error occurs when the null hypothesis is false (i.e. a trend exists) but not rejected (Table 1). This error is called type II error. This probability also represents the power of a statistical test. When the probability of Type II error is low, the risk of incorrectly accepting the null hypothesis is low, and thus the test is said to be powerful (Kundzewicz and Robson, 2004).

Table 1 Interpretation of errors of type I and II
Source: Kundzewicz and Robson (2004)

		Does a trend exist?	
		Yes	No
Has a trend been detected	Yes	Correct decision Probability = $1 - \alpha$	Error of type I: false trend detected when none exists Probability = α
	No	Type II error: failure to detect an existing trend (e.g. due to weakness of the trend, or of the methodology, or shortness of the record) Probability = β	Correct decision Probability = $1 - \beta$

Both parametric and non-parametric tests can be used for evaluating the significance levels. Parametric tests are more powerful than nonparametric test (Johnson, 2000). However, parametric tests such as linear regression are based on the assumption that the random variable is normally distributed (Önöz and Bayazit, 2002), homoscedastic (homogenous variance) (Önöz and Bayazit, 2002), and independent (Kundzewicz and Robson, 2004). However, hydrological data are often strongly non-normal (Kundzewicz and Robson, 2004). Moreover, hydrological and climatological data are often highly correlated spatially (Lettenmaier *et al.*, 1994) and, therefore, data values are not independent (Kundzewicz and Robson, 2004). The data may also display seasonality or other cycles, which violates the homoscedastic assumption.

Since there are many situations where it is doubtful whether the assumptions for parametric tests can be justified for hydrological time-series, nonparametric tests are usually preferred (Cunderlik and Burn, 2002). Nonparametric tests are based on less stringent assumptions and are more robust with respect to missing values, censored data, tied values, seasonality, non-normality, non-linearity and serial dependence (Cunderlik and Burn, 2002). Although the serial independence of a time series is still required (Yue *et al.*, 2002a), the major benefit of nonparametric tests lies in the exact level of significance even when the populations are quite non-normal (Johnson, 2000).

Many tests for trend are now available. Kundzewicz and Robson (2004) documented some common statistical techniques for change detection:

- 1) **Spearman's rho** is a nonparametric rank-based statistical test that measures the monotonic trend between two variables. The Spearman's rho is similar to the Pearson product-moment correlation except that it measures trend when the data are in ordinal form and not necessarily normally distributed. Although Yue *et al.* (2002a) showed that the Spearman's rho test provides results almost identical to those obtained for the Mann-Kendall test, the Spearman's rho test is seldom used in hydro-meteorological trend analysis.
- 2) **Kendall's tau/ Mann-Kendall (MK) test** (Mann, 1945; Kendall, 1975) is another nonparametric rank-based test that is most widely used for detecting monotonic trends in

hydro-meteorological time-series data (Yue *et al.*, 2002a). It is similar to Spearman's rho in terms of power and underlying assumptions. Both of these rank-based tests (the Spearman's rho and MK) have the advantage that they are less affected by outliers because its statistics are not directly based on the values of the random variables (Önöz and Bayazit, 2002). They are different since the MK test uses a different measure of correlation which has no parametric analogue (Kundzewicz and Robson, 2004). This test is discussed in detail in Chapter 3.

- 3) **Seasonal Kendall test** (Hirsh *et al.*, 1982) is a modified version of the MK test that accounts for data with significant seasonal component. This test compares relative ranks of data values from the same season and then performs the MK trend test on the sum of the statistics from each season (Hamed and Rao, 1998). The effect of seasonality can be eliminated using this test, however, it does not account for the correlation in the series within seasons. The Seasonal Kendall test was later modified by Hirsch and Slack (1984) to account for serial correlation (also called autocorrelation) in the time series.
- 4) **Linear regression** is a parametric test that describes the linear trend of a random variable over time. This test requires the assumptions of normality and independence of observations (Robson *et al.*, 1998). When the normal assumption is met, this standard test will have greater power than nonparametric tests (Yue *et al.*, 2002a). The test statistics for this test is the linear regression gradient.
- 5) **Other robust regression tests** are also available for estimating trend in series. Kundzewicz and Robson (2004) gave several examples of alternative measures of trend: least absolute deviation regression, M-estimates of regression, and trimmed regression.

When choosing a statistical test, it is necessary to consider the characteristics of the data. Duration of reference data (Radziejewski and Kundzewicz, 2004), sample size (Yue *et al.*, 2002a), sample variations (Yue *et al.*, 2002a), distribution and shape of the data (Yue *et al.*, 2002a), or shape of trend (Yue and Pilon, 2004) can affect the power of a statistical test. Furthermore, if assumptions made in a statistical test are not met, the estimates of significance level could be grossly incorrect (Radziejewski and Kundzewicz, 2004).

2.7 Trend detection research

A Monte Carlo experiment was performed by Önöz and Bayazit (2002) to investigate the power of the t-test against the MK test for trend analysis. As expected, they found that the t-test is more powerful in the normally distributed case. Yet, the power of the t-test is a decreasing function of the coefficient of skewness. They concluded that when the coefficient of skewness is high, the MK test is more powerful.

Yue and Pilon (2004) assessed, using Monte Carlo simulation, the power of the parametric t-test, nonparametric MK test, bootstrap-based slope (BS-slope), and bootstrap-based-MK (BS-MK) test to detect monotonic (linear and nonlinear) trends in both normal and non-normal time series. For normally-distributed data, the slope-based tests (the t-test and the BS-slope test), which have the same power, perform slightly better than the rank-based tests (the MK and the BS-MK), which also have the same power, irrespective of whether a trend is linear or nonlinear. For non-normally distributed data, the power of the rank-based tests for detecting the trend is much higher than the slope-based tests, irrespective of whether a trend is linear or nonlinear. The power of the tests is much more sensitive to the probability distribution of the sample data in comparison to the shape of trend.

Yue *et al.* (2002a) investigated the power of the MK and Spearman's rho tests by Monte Carlo simulation. The experiment demonstrated that the power of these tests increases with magnitude of trend, sample size, and the pre-assigned significance level. On the other hand, the power of these tests decreases when there are more variations in the time series. Both of the tests exhibit a similar dependency on the distribution type and its shape parameter. They also found that site's characteristics can dramatically affect the power of the test when a trend exists. Although they concluded that both tests have similar power and are indistinguishable in practical point of view, they cited a study by Daniel (1978), which revealed that:

- 1) "S [Kendall statistics] approaches normality more rapidly than does D [Spearman's rho]" (Yue *et al.*, 2002a: 260); and
- 2) "S provides an unbiased estimate of the population parameter, while D does not, and therefore, S is more interpretable" (Yue *et al.*, 2002a: 260).

The MK test and Spearman's rho test are used for detecting monotonic trends in many hydrological studies (Yue *et al.*, 2002a). However, the MK test has become the most frequently used nonparametric test after the appearance of the paper of Hirsch *et al.* (1982) (Yue *et al.*, 2002a). This section reviews research that focuses on the trend detection technique of the MK test.

The Kendall statistic was originally devised by Mann (1945) as a nonparametric test for trend. The exact distribution of this test statistic was derived later by Kendall (1975). In 1980s, the Seasonal Kendall test for trend was developed for determining the existence of trend in water quality time series (Helsel *et al.*, 2006).

Yue *et al.* (2002a) found that the power of the MK test is dependent upon the distribution types when a trend exists. The MK test has highest power on the EV3 (type 3 generalized extreme value) distribution and has lowest power on the lognormal distribution. Thus, the MK test is not a true distribution-free test.

Level of significance

There are two kinds of significance levels that must be considered: local (nominal) significance and field (global) significance. Local significance tests the significance of a trend in a data set for an individual site. Field significance, on the other hand, determines the percentage of sites that are expected to show a trend, at a given local significance level, purely by chance (Burn and Hag Elnur, 2002).

Robson *et al.* (1998) compared the conventional approach and permutation approach (sampling with no replacement) for determining the local significance level. The permutation approach generates a distribution of the test statistic from the data. A local significance level is estimated from this distribution and compared to the test statistic to determine the significance of the detected trend. They suggested that the use of permutation to determine local significance level avoids making distributional assumption and is able to preserve the serial and spatial structure of the data. From this experiment, they found that the conventional approach detected a trend more frequently than the permutation approach.

Kundzewicz and Robson (2004) advised that one should pay attention to the assumptions made in the trend test. Assuming a 10% significance level means that an error will occur, on average, for 10 out of 100 times. Even if a test is highly significant, it may only be a weak indication of change.

Hydrological data are often correlated both in space and time (Burn and Hag Elnur, 2002). However, many trend tests such as the MK test are based on the basic assumption of independent data (Douglas *et al.*, 2000). The presence of correlation, both spatial and serial, reduces the effective size of a sample used for hypothesis test (Douglas *et al.*, 2000).

Spatial correlation/ cross-correlation

When there is no cross-correlation (also called spatial correlation) among sites, the field significance can be approximated by the binomial distribution (Livezey and Chen, 1983). However, spatial correlation is a source of error that is present in any spatial analysis of trend (Yue *et al.*, 2001). Ignoring spatial correlation can result in misleading and erroneous interpretations of the climate and/ or streamflow records (Douglas *et al.*, 2000). It can affect the trend test in two ways. First, spatial correlation creates a duplicate of information contained in each site, and thereby reduces the effective sample size of the data set (Douglas *et al.*, 2000). Secondly, this correlation causes difficulties in deriving an exact probability distribution for the test statistics (Douglas *et al.*, 2000). When the data are cross-correlated, Matalas and Langbein (1962) found that there are severe limits on substituting density of sites with length of record.

Livezey and Chen (1983) demonstrated the importance to assess the field significance of trends in a region. They proposed a Monte Carlo procedure to resolve the issue of spatial correlation. The procedure estimates the number of rejections in a set of tests required to reject the null hypothesis (i.e. no trend is present). Lettenmaier *et al.* (1994) applied the same procedure to determine the field significance of the trend test. The data that are assumed to be spatially uncorrelated were assessed against the same set of data that are assumed to be perfectly correlated. They found that spatial correlation would increase the critical value for rejecting the null hypothesis.

Douglas *et al.* (2000) showed that ignoring spatial correlation would dramatically affect the interpretation of hypothesis test. They proposed a bootstrap method (sampling with replacement) to develop an empirical cumulative density function of regional average Kendall statistics in each region to determine the field significance of that region at a given significance level. Bootstrapping method can adapt to various types of data and requires relatively few assumptions regarding the sample data (Kundzewicz and Robson, 2004). This approach also enables the MK test to account for cross-correlation while still preserving the cross-correlation structure in the data. However, Yue *et al.* (2001) noted that this approach may miss significant trend in smaller regions because upward trends cancel downward trends in the calculation of the regional average Kendall statistics. Yue *et al.* (2001) further suggested that when there is a large number of both upward and downward trends, it is desirable to assess separately the field significance of upward and downward trends.

To extend the approach developed by Douglas *et al.* (2000), Yue *et al.* (2001) proposed a new bootstrapping approach that will separately assess upward and downward trends. The procedure conducts the MK test on the data series from each site which has been re-arranged according to the new order of year set. The new year set is formed by resampling with replacement of the selected period or range of years. This procedure is repeated for 1000 times to estimate bootstrap empirical cumulative distributions for upward and downward trend to estimate the field significance for that region. They compared the results obtained using this procedure with the one obtained using binomial distribution and concluded that the results are dramatically different.

Burn and Hag Elnur (2002) also modified the bootstrap approach developed by Douglas *et al.* (2000). Similar to the bootstrap approach proposed by Yue *et al.* (2001), this bootstrap approach conducts the MK test to a resampled data set from each site at a specified local significance level. The percentage of sites that are significant is then determined. This procedure is repeated by a targeted number of times to generate a distribution for the percentage of sites that are significant. Finally, a critical value is obtained from this distribution. Variables with a larger percentage of stations showing a significant trend than this critical value are considered to be

globally significant.

Serial correlation/ autocorrelation

Similar to positive cross-correlation, for the series with short record length ($n \leq 50$) (Yue and Wang, 2002), positive serial correlation in the data increases the probability of falsely rejecting the null hypothesis (i.e. no trend is present) (Douglas *et al.*, 2000), while negative serial correlation decreases the rejection rate (Yue and Wang, 2002). Kulkarni and Von Storch (1995) demonstrated, by Monte Carlo experiments, that the result of the MK test depends strongly on the serial correlation. Yue *et al.* (2002b) examine the influence of serial correlation on trend detection. They found that the presence of positive (negative) serial correlation increases (decreases) the magnitude of the variance of the Kendall statistics, whereas it does not change the mean and the distribution type of the Kendall statistics. The presence of a trend, on the other hand, can also influence the magnitude of the estimate of serial correlation.

Von Storch (1995) and Kulkarni and Von Storch (1995) proposed a “pre-whitening” method to reduce the effect of serial correlation. In this method, the serial component is first removed from the time series before conducting the MK test. Douglas *et al.* (2000) used this pre-whitening method and noted that fewer regions were interpreted as having statistically significant trends. However, while pre-whitening can effectively remove a serial component from a series, removal of positive serial correlation also removes part of the existing trend and removal of negative serial correlation inflates the existing trend (Yue *et al.*, 2002b). The slope of trend estimated from the pre-whitened series is not the true one that a series has (Yue and Wang, 2002), thus leading to biased estimation of the probability of trend (Yue *et al.*, 2002b). A similar conclusion was drawn by Fleming and Clarke (2002) who also suggested that the pre-whitening approach should not be used unless there is a strong site-specific basis for the assumption of autoregressive noise presence in the hydrological time series. They recommended using multi-stage techniques to eliminate the effect of serial correlation. Yue and Wang (2002) have suggested to use the MK test directly on the original data rather than after pre-whitening when sample size and magnitude of trend are large enough.

Another method to reduce the influences of serial correlation was proposed by Hamed and Rao

(1998). They evaluated the mean and variance of the MK trend test statistic in the presence of serial correlation. Furthermore, they have quantitatively proven that the existence of positive (negative) autocorrelation in the data increases (decreases) the probability of falsely detected trend by inflating (reducing) the variance of the Kendall statistics. Similarly to the findings from Yue *et al.* (2002b), they found that the variance of the Kendall statistic is underestimated when the data are positively autocorrelated. They derived, from Bayley and Hammersley's (1946) effective sample size formula, an approximate formula to calculate the variance of the MK test statistics for autocorrelated data. Based on this modified value of variance, they proposed a modified MK trend test for autocorrelated data. Their experiment showed that the proposed modified test is as powerful as the original MK test. However, Yue *et al.* (2002b) argued that although this procedure reduced the false rejection rate compared with the classical MK test, the false rejection rate is still much higher than it should be.

Yue *et al.* (2002b) indicated that the two approaches mentioned above (the pre-whitening approach by Kulkarni and Von Storch (1995), and the modified MK test by Hamed and Rao (1998)) fail to address the potential interaction between a trend and a serial component when both are present in a time series. To avoid this, Yue *et al.* (2002b) proposed the trend free pre-whitening (TFPW) procedure to detect a significant trend in a serially correlated series. As the name implies, the estimated trend is first removed from the time series prior to pre-whitening the series. The identified trend is then added back to this residual series to perform the MK test. They compared the MK, the MK with the pre-whitening approach by Kulkarni and Von Storch (1995), and the modified MK test by Hamed and Rao (1998) with the MK-TFPW. They concluded that the MK-TFPW provided the best estimate of trend among the other three tests.

Yue *et al.* (2001) studied spatial patterns of trend in Canadian streamflow. They incorporated the trend free pre-whitening (TFPW) procedure developed by Yue *et al.* (2002b) to reduce the effect of serial correlation. They also compared the results from 1) the MK test without considering serial correlation and 2) the MK test with Kulkarni and Von Storch (1995) pre-whitening with 3) the MK test with TFPW. Among the three approaches, the MK test with Kulkarni and Von Storch (1995) pre-whitening is the most conservative. The results from the MK test and the MK with TFPW are not greatly different. Only about 10% of the sites show

contradictory results. They showed that the TFPW procedure can effectively remove the serial component from the data.

Darken *et al.* (2000) compared different methods of estimating the variance for use in hypothesis test to detect changes in water quality trend. They have first compared the variances of the mean estimated by the effective sample size bootstrap with the Theibaux and Zwiers (1984) method and with the ignorance method of estimating the effective sample size (Darken *et al.*, 2000: 427), the moving blocks bootstrap (Hall *et al.*, 1995), and the standard bootstrap. They found that effective sample size bootstrap with the Theibaux and Zwiers (1984) method of estimating the effective sample size is the best of the methods considered. These bootstrap methods, the delta method (Seber, 1982), and the null case formula (Kendall, 1975) were then applied to the hypothesis test. All of these methods provide reasonable estimates in various circumstances. For data that are independent and non-normal, the bootstrap provides the best test. They also concluded that the effective sample size bootstrap was the only method explored which allows the hypothesis test to consistently hold its level. When serial correlation is also present in the time series, the effective sample size bootstrap with the Theibaux and Zwiers (1984) method of estimating the effective sample size performs the best.

Yue and Wang (2004) demonstrated the ability of incorporating the effective sample size (ESS) approach in the MK test to eliminate the effect of serial correlation. In the study, the Monte Carlo simulation experiment has shown that the ESS approach can effectively limit the effect of serial correlation on the MK test when no trend exists within the time series. Yet, when trend is present in the time series, the existence of trend will contaminate the magnitude of sample serial correlation. They suggested to incorporate a multi-stage technique such as the one proposed in Yue *et al.*'s (2002b) study, but using the ESS approach to replace the pre-whitening approach.

2.7.1 Interpreting test results

A statistical test detects statistically significant changes from the data. If the data are not representative, then test results can be meaningless. For example, observational data can be affected by instrumental error. Data from model output can also be affected by low-quality input

data or hydrological uncertainty within the model itself. Therefore, when interpreting test results, one should keep an eye out for possible data quality problems that may previously have been missed (Kundzewicz and Robson, 2004).

Kundzewicz and Robson (2004) argued that no statistical test is perfect, even if all test assumptions are met. For a 5% significant level, 5% of test results are expected to be significant but incorrect. Unless many tests show significant change, a small number of significant test results may only provide weak evidence of change.

The incorporation of historical or local knowledge about the data into the analysis is very important (Kundzewicz and Robson, 2004). When test results indicate a significant change in a variable, then it is important to attribute such a change to the cause. Many possible explanations can be used to explain the change, such as changes caused by direct anthropogenic effects (urbanization, construction of large reservoirs, dam, drainage systems, changes in land-use etc.) (Burn *et al.*, 2004b), natural catchment changes (e.g. natural changes in channel morphology) (Kundzewicz and Robson, 2004), climate variability (Kundzewicz and Robson, 2004), and large-scale oceanic and atmospheric process (Burn *et al.*, 2004b). These changes can hinder the ability to understand the impact climate change may have on a water resource system.

2.8 Attribution research

There is still no standard procedure for attributing a detected hydrological change to possible causative factors. Common approaches currently employed in trend attribution studies are empirical relationship, statistical approach, modelling approach, and sensitivity analysis.

Empirical relationship

An empirical relationship is derived from a large sample of observations. A famous empirical formula applied in climate impact research is from Langbein (1949). He related the mean annual runoff from 22 drainage basins in the United States to the mean annual precipitation and the weighted temperature. Many studies have used his formula in assessing the runoff impacts of changes of temperature and precipitation (Stockton and Boggess, 1979; Revelle and Waggoner, 1983; Callaway and Currie, 1985). However, empirical relationships are usually derived from

conditions that are too broad or too specific. Langbein's (1949) climate-runoff relationship, for example, cannot provide a reliable estimate for a specific drainage basin because it is derived from observed differences across space (Karl and Riebsame, 1989). Moreover, in a lot of cases, it is impossible to incorporate all the factors in an empirical relationship; some of the important factors might be omitted. For example, Langbein's (1949) climate-runoff relationship has ignored many macro-climatic factors and surface characteristics (Karl and Riebsame, 1989) that have a profound effect on the estimation of evapotranspiration. Thus, this relationship can often only provide a quick estimate of the change.

Statistical approach

Many studies have employed statistical approaches to analyze the possible relationship between measured climate and hydrological parameters. Karl and Riebsame (1989) used scatterplots and simple correlations to relate runoff to temperature, precipitation and other factors. They also conducted a multiple regression analysis of changes of temperature, precipitation, runoff, and various basin characteristics. Neal *et al.* (2002) used standard statistical methods to compare deviations in warm- and cold-PDO average streamflows from the long-term mean. Labat *et al.* (2004) performed linear regression analysis between annual runoff and annual temperature at a global scale and at a continental scale (Africa, Asia, Europe, North America, and South America). Other examples of the use of the correlation analysis for trend attribution include the works by Burn and Hag Elnur (2002), Burn *et al.* (2004b), Abdul Aziz (2004), Chingombe *et al.* (2005), Déry and Wood (2005), and Karabörk (2007).

Johnson (2000) argued that high observed correlation does not necessarily imply a direct cause-and-effect relationship. He advised that, when using the correlation coefficient as a measure of relationship, attention should be focused on the possibility that an important lurking variable is influencing the calculation. Kingston *et al.* (2006) also emphasized a similar concern. They suggested detrending the time series of interest before undertaking statistical analysis for countering spurious correlation induced by similar trends in time series. Cunderlik and Burn (2004) have used a similar approach. They linked the identified regional trend of monthly maximum flows by means of trend significance index and then verified these linkages by cross-correlation analysis applied on records with all serially dependent components removed.

Modelling approach

Another method suggested by Kingston *et al.* (2006) is to utilize simulation modelling as a tool for process-based understanding of the hydroclimatological system. This method can also complement the associations highlighted by statistical or empirical methods (Kingston *et al.*, 2006). Hydrological models are capable of reproducing the hydrological condition accurately in flexible spatial and/ or temporal scale. As a result, they can break down the contribution of hydrological changes into components. For example, Gedney *et al.* (2006) isolated various effects (climate change and variability, aerosol concentration, atmospheric CO₂, and land use) by carrying out five simulations using a mechanistic land-surface model. In the first simulation, all factors varied throughout the fully transient simulation. In the other four simulations, one of the factors was fixed to its initial condition while the other components varied throughout the twentieth century. Trend in each simulation is compared with the observed trend using a standard optimal fingerprinting technique to attribute the most likely contribution to the change. Similarly, Bouwer *et al.* (2006) quantitatively differentiate the effect of man-made hydrological developments with climate variability on river runoff using a hydrological model.

Sensitivity Analysis

Many hydrologic climate sensitivity studies also utilize a hydrological model to observe the resulting changes in streamflow from varying the model's atmospheric input. For example, Jones *et al.* (2006) and Singh *et al.* (2006) have performed this type of study. They estimated the hydrological sensitivity of three hydrological models to climate change. A common problem associated with this approach is that sensitivity results for the same basin using different models can be significantly different (Sankarasubramanian *et al.*, 2001). Worst yet, Sankarasubramanian *et al.* (2001) noted that sensitivity results for the same basin using identical models can be remarkably different. To mitigate this problem, Sankarasubramanian *et al.* (2001) developed a nonparametric estimator that can produce unbiased estimates of the sensitivity of streamflow to climate under different model assumptions or a calibration strategy. Through a Monte Carlo experiment, they have proven that this nonparametric estimator has low bias and is as robust as or more robust than alternate model-based approaches.

2.9 Application of detection and attribution

2.9.1 Global

Mitchell (1989), by using a GCM, projected the average temperature will increase from 1 to 5°C in a doubled CO₂ environment, with the largest increases at high latitudes. Warmer temperatures tend to increase evapotranspiration and the amount of water vapor in the atmosphere, intensifying the hydrologic cycle (Karl and Riebsame, 1989) and increasing global precipitation by from 3% to 15% (Mitchell, 1989).

Blarcum *et al.* (1995) examined the monthly changes in runoff for nine of the world's major high latitude rivers where snow melt is an important component of river runoff. The nine rivers examined in the study are Yenesei River, Lena River, Ob River, Amur River, Mackenzie River, Yukon River, Severnaya Dvina River, Kolyma River, and Indigirka River. In the doubled CO₂ climate, the model estimated increase in annual precipitation and runoff for all the rivers. The spring months were predicted to have greatest change in runoff. The model further predicted the increased outflow at the river mouths begins earlier in the spring, and the maximum outflow occurs approximately one month sooner.

Nijssen *et al.* (2001) used four climate models and a macroscale hydrological model to predict the hydrologic response from nine of the world's major basins: Amazon, Amur, Mackenzie, Mekong, Mississippi, Severnaya Dvina, Xi, Yellow, Yenisei. In general, GCMs predicted a warming and increase of precipitation for all the basins, with greatest warming in the highest latitudes during the winter months. These higher latitude basins are also predicted to have the largest changes in the hydrologic cycle particularly during early to mid spring. The GCMs predicted a reduction in annual streamflow for most tropical and mid-latitude basins, and an increase in streamflow for high-latitude basins.

Labat *et al.* (2004) examined the impact of climatic changes on global and continental hydrological cycle. They found that North America runoff is particularly sensitive to climatic change. They also concluded that the sensitivity of global runoff to global temperature is 0.039 and the sensitive of runoff to temperature in North America is 0.110. However, Legates *et al.*

(2005) have criticized their findings based on the non-climatic influences on the reliability of the discharge records in Labat *et al.*'s (2004) study, findings from previous studies, and Labat *et al.*'s (2004) approach to interpret test results.

Gedney *et al.* (2006) examined both global and continental river runoff changes, and evaluated the impact that each of the four possible contributions (climate, aerosol concentration, atmospheric CO₂, and land use) and their combination have on changes in runoff. The major findings in their study are:

- 1) Global runoff has increased throughout the 20th century; while global precipitation increased prior to 1960 and decreased thereafter.
- 2) The post-1960 global runoff increase was double the rate of the entire 20th century.
- 3) Among all the contributions, only climate and the direct CO₂ effect were detected at the 5% significance level.
- 4) Twentieth-century climate alone is insufficient to explain the changes in global runoff.
- 5) The main contribution to global runoff change is the direct CO₂ effect.
- 6) Increasing CO₂ causes partial closure of stomatal apertures on plant leaves and suppresses transpiration, leading to increases in global runoff.
- 7) Runoff increased in South America, North America and Asia, and decreased in Africa and Europe.
- 8) The largest increase in runoff is observed in South America; North America is the next largest.
- 9) In North America, both precipitation and runoff have increased throughout the 20th century but the rate of post-1960 increase is more than double the entire 20th century.
- 10) In North America, the rate of runoff increase is very close to the rate of precipitation increase (i.e. sensitivity of runoff to climate is close to 1)
- 11) In North America, climate change alone can explain more than 75% of the changes in runoff; the remainder is mostly explained by the direct CO₂ effect.

2.9.2 United States

Changes in runoff can be estimated from changes in precipitation and evapotranspiration via the

water-balance equation. Nemec and Schaake (1982) estimated the sensitivity of runoff to climate variation by applying the Sacramento Watershed model to an arid basin and a humid basin in the United States. For the arid basin, 4% increase of evapotranspiration (with constant precipitation) yields only a 5 to 10% decrease in runoff, but a 10% increase of precipitation would amplify the increase of runoff by a factor of 6. They also found that runoff is less sensitive to both evapotranspiration and precipitation in the humid basin. For the humid basin, a 4% increase of evapotranspiration only decreases runoff by 1 to 2% and a 10% increase of precipitation only amplifies runoff by a factor of 2.5.

Similar results were found by Wigley and Jones (1985), who have shown by theory from the water-balance equation and empirical modelling that:

- 1) Changes in runoff are everywhere more sensitive to changes in precipitation than to changes in evapotranspiration.
- 2) The relative change in runoff is always greater than the relative change in precipitation.
- 3) Runoff is most sensitive to climatic change in regions with small runoff ratio.
- 4) The relative change in runoff exceeds the relative change in evapotranspiration only in regions where the runoff ratio is less than 0.5.

From the scenarios generated by GCMs for the Sacramento River Basin in California, Gleick (1987) concluded that climate change generally decreases summer runoff, increases winter runoff, and shifts the timing of the monthly runoff. In his study, he further found that annual runoff is affected primarily by precipitation changes while the seasonal distribution of runoff is affected by changes in mean monthly temperature. He also observed an increase in winter runoff when he increased the ratio of snowfall to total precipitation in the water balance model. He attributed this seasonal effect of runoff to increasing temperature.

These conclusions are in general agreement with Karl and Riebsame's (1989) study. Karl and Riebsame (1989) examined the sensitivity of runoff to changes in precipitation and temperature using historical data across the United States. They concluded that average temperature changes of 1 to 2°C typically have little effect on annual runoff whereas precipitation changes may be amplified one to six times in relative runoff changes.

Lettenmaier *et al.* (1994) detected strong increasing trends in the average temperature, the precipitation and the streamflow, and a decreasing trend in the temperature range across the United States. Lins and Slack (1999) found that the increase of streamflow is not geographically nor seasonally uniform. Most increases were found to occur in low to moderate streamflows, particularly during the late summer and autumn period. This period is consistent with the reported precipitation increase from Lettenmaier *et al.* (1994). From Lins and Slack's (1999) study, the increase of streamflows were most widespread in the Upper Mississippi, Ohio valley, Texas-Gulf, and the Mid-Atlantic, which is also roughly the same vicinity as the upward trends in precipitation found by Lettenmaier *et al.* (1994).

Douglas *et al.* (2000) examined the trends in flood and low flows in the United States. They did not find significant trends in flood flows but found significant upward trend in low flows. The area of concentrated upward trends in this study is consistent with the area of upward trend in low to moderate flow reported by Lins and Slack (1999). Two major conclusions can be drawn from the results of Lettenmaier *et al.* (1994), Lins and Slack (1999), and Douglas *et al.* (2000). First, the United States is getting wetter but less extreme. Secondly, there are some correlations between the locations of upward trends in low flows and upward trends in annual precipitation.

Sankarasubramanian *et al.*'s (2001) findings also confirmed these results. Sankarasubramanian *et al.* (2001) estimated the climate elasticity of streamflow in the United States. The sensitivity of streamflow to climate ranged from 1.0 to 2.5. The highest values of the climate sensitivity occur primarily in the arid and semiarid regions of the Midwest and Southwest, which is consistent with the findings from Lins and Slack (1999) and Douglas *et al.* (2000).

2.9.3 Canada

Kite (1993) examined long-term temperature, precipitation and streamflow data from sites across Canada to investigate the possibility of identifying impacts from climate change. He was able to detect some significant linear trends but no apparent spatial pattern was observed.

Kwong and Gan (1994) investigated the permafrost distribution along the Mackenzie Highway from south of the Great Slave Lake, Canada, to the southern limit of the sporadic discontinuous permafrost zone. The permafrost has migrated northward by 120 km in 26 years. They related the melting of permafrost to climatic warming by analyzing monthly temperature records from nine weather stations. A significant warming trend was detected for the period 1949-1989. Gan (1995) extended this research to detect climate trend across Canada and northeastern USA for the same period. He reported significant warming trends only in western Canada in January and March, and to a limited extent in April, May and June. Some cooling trends in October were also reported across Canada and in northeastern USA.

Zhang *et al.* (2000) examined temperature and precipitation trends in Canada during the 20th century. From 1900-1998, the mean annual temperature over southern Canada (latitudes below 60°) has increased by an average of 0.9°C. This trend was dominated by rises of temperature prior to the 1940s and after the 1970s. For the period of 1940-1970, there was a modest decrease of mean annual temperature. The warming trend is the strongest in the west, particularly in the Canadian Prairies during winter and early spring. For the east coast, some cooling trends were observed in the recent portion of the data. During the 1940s to 1960s, night-time temperatures have increased more than day-time temperatures, thus resulting in a significant decrease in daily temperature range (Zhang *et al.*, 2000; Vincent and Mekis, 2006).

Zhang *et al.* (2000) observed the annual maximum temperature has significantly increase by 1.5 to 2°C in northern British Columbia and in the MRB from 1950 to 1998. In addition, the increase in winter maximum temperature is statistically significant only in some parts of the MRB. These strong changes in climate might be explained by the interdecadal variation of atmospheric-oceanic circulation over the North Pacific because it is known to impact climate over North America, particularly in the west coast (Zhang *et al.*, 2001a). This prediction is further supported by the findings in Cunderlik and Burn's (2004) analysis, which has revealed a good correspondence between long-term air-temperature records and the PDO index.

According to Zhang *et al.* (2000), the annual precipitation has significantly increased by 5% to 30% in southern Canada, with the exception of southern Alberta and Saskatchewan where

decreasing precipitation was detected. The greatest increase of precipitation occurred in eastern Canada; the Canadian Prairies have the least increase. In the recent portion of the data, precipitation has increased most significantly in the northern regions and decreased in the southern regions of the country. The ratio of snowfall to total precipitation has also increased during the same period with significant negative trends occurring mostly in southern Canada during spring.

In Canada, the pattern of climate change is distinct in winter and spring: drier and warmer in the southwestern regions and wetter and cooler in the northeastern regions (Zhang *et al.*, 2000). Overall, Canada “is not getting hotter, but rather ‘less cold’” (Bonsal *et al.*, 2001) and the number of smaller rainfall events increased more than that of larger events, and the frequency of heaviest events did not increase at all (Zhang *et al.*, 2001b).

From analyzing historical streamflow data across Canada for the period of 1957-1997, Yue *et al.* (2001) reported a general downward trend between approximately 50° and 58° latitude, and a general upward trend above latitude of 58°, which stretches from northern British Columbia and the Yukon Territory through the Northwest Territories and into Nunavut. Another band of upward trend was observed between the latitude of 44° to 50°.

Zhang *et al.* (2001a) also investigated Canadian streamflow for three study periods: 1967-1996, 1957-1996, and 1947-1996. The results for the period of 1957-1996 are consistent with Yue *et al.* (2001). Zhang *et al.* (2001a) concluded that the annual mean streamflow has generally decreased, with greatest decrease in the southern part of the country. The monthly mean streamflow significantly decreased in summer and autumn, and increased in spring. In northern British Columbia and the Yukon Territory, significant increases were observed only in the low flow. In southern Canada, significant decreases were observed in annual maximum, mean, and minimum streamflow. These results indicated that “Canada is not experiencing more extreme hydrological events” (Zhang *et al.*, 2001a). They also noted that the beginning of the freshet season has advanced by more than a month. This trend is particularly strong in British Columbia. In fact, the strongest changes in all hydroclimatic variables analyzed in this study were observed in British Columbia and the Yukon Territory. They attributed this result to the

interdecadal variation of atmospheric-oceanic circulation over the North Pacific.

Burn and Hag Elnur (2002) summarized streamflow trends across Canada by nine climatic regions: the Pacific climatic region, the South British Columbia Mountains, the Yukon North British Columbia Mountains, the Prairies, the North West Forest, the North East Forest, the Great Lakes St. Lawrence, and the Atlantic climatic regions. Since the MRB is covered by part of the Yukon North British Columbia Mountains, the Prairies, the North West Forest, and the South British Columbia Mountains climatic regions (Figure 2), only findings for these four climatic regions from this study will be summarized here.

- **“The Yukon North British Columbia Mountains** climatic region displays particular sensitivity in the variables related to the timing of events. The ice start dates and the ice end dates exhibit decreasing trends implying earlier occurrence of freeze up and break up of river ice in the more recent years. Increasing flows are noted for February through May” (Burn and Hag Elnur, 2002: 117).

Only the relationship between the ice start date and the November temperature was analyzed in this region. The two series exhibit a similar pattern over the period of record.

- **“The Prairies** climatic region exhibits a decreasing trend for the ice end date implying earlier occurrence of this event in more recent years. Increasing flow are noted for the months of January – March, again likely related to an earlier onset of spring runoff” (Burn and Hag Elnur, 2002: 117).
- **“The Northwest Forest** climatic region exhibits a decreasing trend in the end of ice conditions implying earlier occurrence of the spring melt period. The months of February and March exhibit increasing trends while December exhibits a decreasing trend” (Burn and Hag Elnur, 2002: 117).

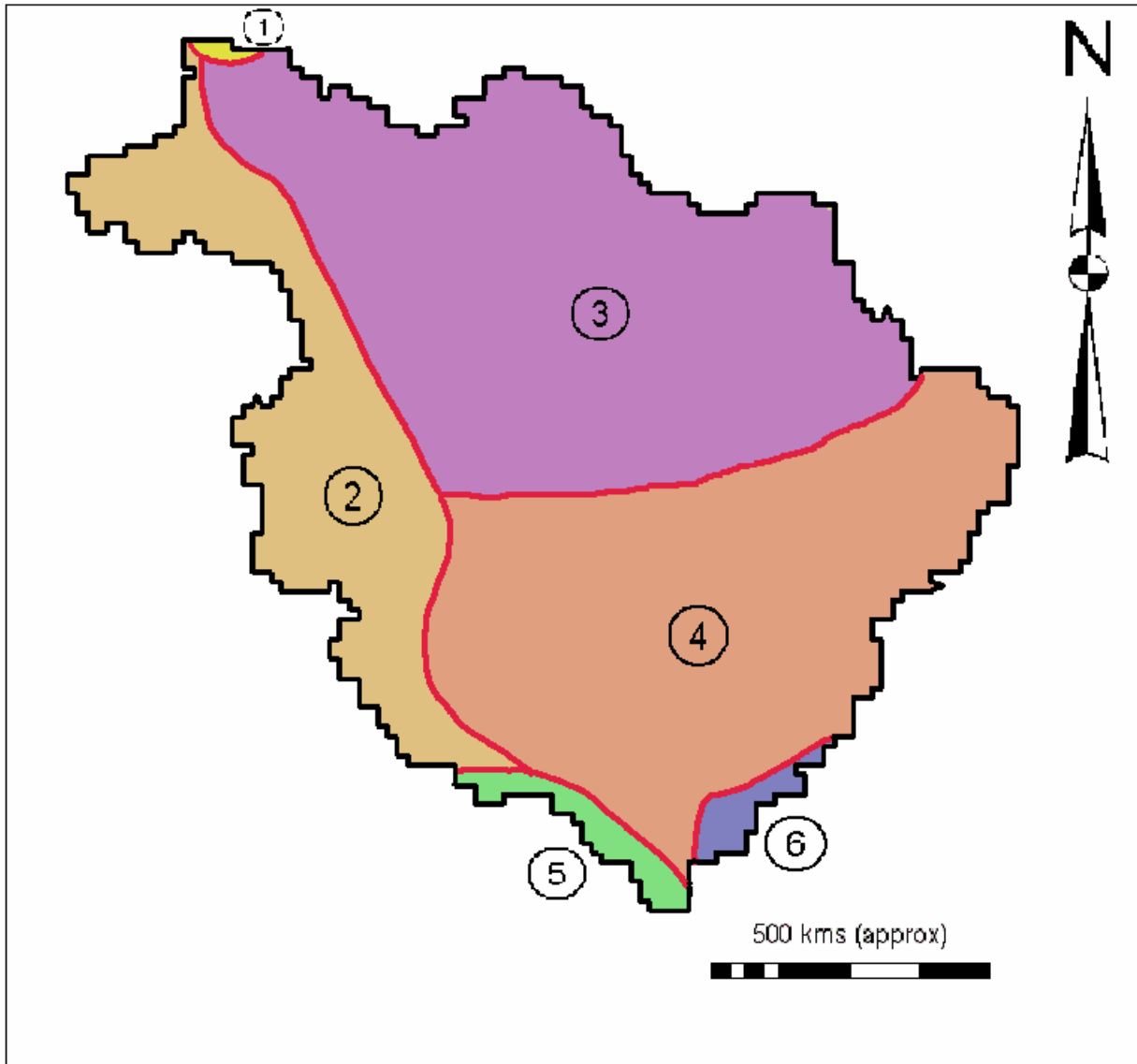


Figure 2 Climatic regions in the Mackenzie River Basin
 (1) Delta, (2) The Yukon/ North British Columbia Mountains, (3) Mackenzie, (4) The Northwest Forest, (5) The South British Columbia Mountains, and (6) Prairies
Source: adapted from Burn and Hag Elnur (2002)

- **“The South British Columbia Mountains** climate region has decreasing monthly flows in February, and June – October. Increasing flow is noted for the months of April and May, which is likely attributable to a shift in the timing of the runoff for this region. The main runoff period for catchments in this region typically starts in April. The date on which ice conditions start exhibits a decreasing trend implying that freeze-up is occurring earlier in the more recent years” (Burn and Hag Elnur, 2002: 117).

The correlation between the annual maximum flow data and the annual temperature data is strongly significant. Burn and Hag Elnur (2002) concluded that increase of temperature is strongly associated with decreasing maximum flows.

Déry and Wood (2005) noted a 10% decrease in the total annual river discharge from northern Canada to the Arctic and North Atlantic Oceans from 1964 to 2003. In the analysis, they divided the Canadian landmass by 5 separate drainage basins (from east to west): the Labrador Sea, Eastern Hudson Bay (including Ungava Bay), Western Hudson Bay, the Arctic Ocean (which includes the MRB), and the Bering Strait. Although they observed changes in river discharge for the Arctic Ocean and Bering Strait, no significant trends have been detected from 1964 to 2003.

Canadian Prairies

Burn (1994) and Westmacott and Burn (1997) showed that climate change can affect both the magnitude and timing of hydrologic events in the Churchill-Nelson River Basin in west-central Canada, which includes the provinces of Alberta, Saskatchewan, Manitoba and Ontario. Burn (1994) found a large number of rivers exhibit earlier spring runoff particularly in the recent portion of the data (from 1951 to 1991). A similar result was also obtained in Westmacott and Burn (1997). They have additionally evaluated the effect of climate change on the mean monthly, mean annual, and extreme annual flow for the period of 1920-1990. The magnitude of all streamflow variables were decreasing except for spring streamflow. They attributed the increasing of spring streamflow to the potential for snow melting.

Yulianti and Burn (1998) investigated the impacts of temperature change on low flow in the same region. They found that the magnitude of low flow is decreasing while the temperature is increasing in the study period. Moreover, they found that the low flow events have occurred more frequently.

Gan (1998) identified hydroclimatic trends and possible climatic warming in the Canadian Prairies for the period of 1949-1989. The Canadian Prairies are generally getting warmer and drier in these 4 decades. This result is consistent with the findings of Zhang *et al.* (2000).

Although the Prairies are getting drier, no significant trend has detected in drought duration, severity, and magnitude (Gan, 1998).

Burn and Hesch (2006) compared trends in potential and pan evaporation for the Canadian Prairies. Many significant decreasing trends have been detected for both evaporation measures and these trends are mainly concentrated in the summer months of June and July. Burn and Hesch (2007) conducted a similar analysis on lake and pan evaporation in the same region. They found field significant decreasing trends in June, July, October, and warm season evaporation for the two measures of evaporation.

British Columbia

Loukas and Quick (1996) used a hydrological model to assess the hydrologic response to climate change in the Upper Campbell, which is a maritime watershed, and the Illecillewaet, which is an interior watershed. The model predicted a larger increase of annual precipitation and mean annual runoff in the interior watershed than in the maritime watershed. However, the magnitude and frequency of mean annual maximum daily flow is predicted to decrease only in the interior watershed. Although the magnitude and frequency of annual maximum precipitation in the maritime watershed is predicted to increase, the relative increase of mean annual runoff was predicted to be lower than in the interior watershed. Loukas and Quick (1999) extended this research and concluded that the magnitude, volume, frequency and duration of floods would increase in the maritime watershed while decreasing in the interior watershed.

After the findings from the Burn and Hag Elnur's (2002) study regarding the South British Columbia Mountains region, Cunderlik and Burn (2002) further investigated the trend of the maximum flows in this region. They found an increasing trend of spring maximum flow, with largest increase in April. Cunderlik and Burn (2004) found the spring air temperatures, particularly the April temperature, triggers the onset of snowmelt earlier in spring, resulting in an increase of maximum flow in April. All other months showed a regional decrease in monthly maximum flows; this was most pronounced in October. This significant change was attributed to the summer temperature, which increased soil moisture deficit leading to lower maximum flows (Cunderlik and Burn, 2002). Cunderlik and Burn (2002) also noted the shifting of snowmelt

induced maximum flow from June – July to March – May resulting in decreasing flow in the beginning of summer.

2.9.4 Other regions

Jones *et al.* (2006) estimated the sensitivity of runoff to changes in rainfall and potential evaporation for 22 Australian catchments from different climatic zones. The mean sensitivity of flow to mean annual rainfall ranges from 2.1 to 2.5; sensitivity to mean annual potential evaporation ranges from only -0.5 to -1.0. They further noted that a higher runoff coefficient corresponds to a lower annual potential evaporation.

Chiew (2006) also estimated the rainfall elasticity of streamflow across Australia. He included data from 219 catchments and used the nonparametric estimator proposed by Sankarasubramanian *et al.* (2001) for estimating the rainfall elasticity. The rainfall elasticity of streamflow is about 2.0 to 3.5. He further noted that the rainfall elasticity of streamflow is strongly correlated to runoff coefficient, where streamflow is more sensitive to rainfall in drier catchments, and those with low runoff coefficient. He also performed the sensitivity analysis for 22 Australian catchments using the same hydrological models as Jones *et al.* (2006). Chiew (2006) concluded that the rainfall elasticity from the hydrological modelling approach was found to be slightly higher than the nonparametric estimator.

Singh *et al.* (2006) studied the effect of climate change on runoff in the Himalayan Basin in India. The Himalayan Basin encompasses a very large number of glaciers where snowmelt process is an important component of runoff in this basin – about 87% of total runoff is contributed by glacier melting. Unlike most other literature reviewed here, they found that changes in runoff are more sensitive to changes in temperature compared with rainfall. For a 2°C warming and a 10% increase in rainfall, the increase in summer streamflow is about 28% and 3.5%, respectively. They also noted that the streamflow increased linearly with both temperature and rainfall.

2.10 Climate change impacts in the MRB

2.10.1 Future climate scenarios generated by GCMs

The GCM in the Blarcum *et al.* (1995) study has predicted a small increase of the maximum Mackenzie flow in a doubled CO₂ climate. The increase is mainly due to increased spring precipitation in the doubled CO₂ climate. The model predicted 21% increases in both precipitation and runoff in the doubled CO₂ climate. Again, the sensitivity of runoff to precipitation is 1.0, which is closed to the model prediction from Gedney *et al.* (2006). However, Blarcum *et al.* (1995) were not confident about this result because the modelled annual basin-wide precipitation and runoff for the baseline condition were nearly twice the observed. The model further predicted a decrease in the monthly snowmass throughout the snow season, and the melting season began sooner in the Mackenzie River.

The GCMs in the Dornes *et al.* (undated) study have predicted an increasing average factor of nearly two for both temperature and precipitation in the MRB for the 2020s, the 2050s and the 2080s. That is, in the next century, the GCMs predicted that temperature and precipitation in the MRB could increase by as much as 4°C and 20%, respectively.

2.10.2 Detection and attribution research in the MRB

Louie *et al.* (2002) studied the relationship between the observed annual discharge in the MRB and climate using a simple water balance. They found that

- precipitation and net surface moisture supply (precipitation minus evapotranspiration) are strongly correlated with annual discharge with a lag of 3 months;
- evapotranspiration is not significantly (negatively) correlated with discharge; and
- mean annual temperature is also not significantly (negatively) correlated with discharge.

Gibson and Edwards (2002) calculated the catchment-weighted evaporation losses in northern Canada. They found that the evaporation typically ranges from 10-15% in tundra areas draining into the Arctic Ocean to as high as 60% in forested subarctic areas draining to the Mackenzie River via Great Bear or Great Slave Lakes. They also found that open-water evaporation generally decreases with increasing latitude and accounts for 5-50% of total evapotranspiration.

Woo and Thorne (2003) analyzed the streamflow trend for the mountainous sub-basins in the west of the MRB. In the analysis of flow patterns for the major sub-basins in the MRB, they found that the mountainous sub-basins contribute about 60% of runoff for the Mackenzie River. Furthermore, the data record for this sub-basin is more extensive. Thus, this sub-basin is representative of the streamflow trend in the MRB. Significant warming was detected in the past three decades, especially in April. This spring warming has caused the date of snowmelt initiation to advance by about three days per decade. Although they did not detect statistically significant trend in annual flows nor peak flow within the record, they observed significant increases of the year-to-year variations of annual flow and arrival of the spring peaks in some sub-basins for the last 10-years of record.

In a study of Liard River Basin, Burn *et al.* (2004b) have detected a weak decreasing trend in annual mean streamflow for the 40-year study period. Although results varied between different duration of study period, generally, they detected increasing flows from December to April, an increasing annual minimum flow, a decreasing summer flow, and earlier occurrence of the spring freshet, the spring maximum flood event and the annual maximum flood event. Several relationships were found between trends in hydrological variables and both meteorological variables and the PDO process: the spring freshet decreases with the spring temperatures, the winter flows increase with the PDO index, the annual minimum flow increases with both the timing of the spring freshet and the timing of the spring maximum flow events.

Burn *et al.* (2004a) examined the trends and variability of streamflow for the Liard and Athabasca Rivers. In general, both basins exhibit increasing trends in the annual minimum, the winter and spring flows, and decreasing trends in the annual maximum flood events and the date of occurrence of the spring freshet. They attributed the increasing trend in the annual minimum flow to increasing winter temperature, and the earlier spring freshet to increasing spring temperature. For the Athabasca River Basin, more trends have been detected; these trends are usually larger in magnitude relative to the Liard River Basin. They predicted this contrast may indicate other changes, such as changes of land-use, have placed additional stresses on the hydrological regime in the Athabasca River Basin.

Nijssen *et al.* (2001) summarized the average water balance components simulated by a macroscale hydrological model for the MRB from 1980 to 1993. They found that precipitation, evaporation, and runoff are larger during the summer months; while storage decreases from April to July. In the year of 2045, the predicted changes in monthly water balance component in the MRB are:

- increase in storage occurred in winter months because of the increased precipitation stored as snow;
- the snowmelt runoff was predicted to begin in April; it began in May in the baseline condition.

To observe the impact of climate change on evapotranspiration and runoff, they adjusted the temperature and precipitation independently by 2°C warmer and 10% increase, respectively. For the change in temperature, significant increase of evapotranspiration was observed particularly in the spring and summer months. Moreover, runoff has generally decreased when temperature increases, with the exception of spring runoff. They also noted that although both evapotranspiration and runoff increased when precipitation increased, runoff is more sensitive to change in precipitation. As in many other sensitivity studies done on North America, runoff is more sensitive to the change in precipitation than to the change in temperature.

Abdul Aziz (2004) assessed the impacts of climate change on the hydrological regime in the MRB using both historical data and hydrological model output for a 40-year study period. He observed a general increase in the maximum, mean, and minimum temperatures. The maximum and mean temperature increases were most prevalent in winter months of December to April, and the minimum temperature increased in all months except in autumn. Strong decreases in January and December precipitation were observed. As expected in a warmer climate, the ratio of rainfall to precipitation increases in April; the ratio of snowfall to precipitation has strongly increased in the winter months and decreased in spring. The results also indicated strong increasing streamflow trends for the winter months of December to April, and for the annual minimum flow. He also detected a weak decrease of early summer and late fall streamflows, and annual mean flow. The observed warming in late winter and early spring has triggered earlier onset of spring freshet over the basin. Abdul Aziz (2004) also noted that the southern portion of

the basin within the headwaters and mainstem Athabasca as well as the mainstem Peace were characterized mostly by the lack of trends or occasionally different behaviours compared to the other parts of the basin. The author related this behaviour to meltwater of glaciers running from the Columbia Ice Field into the southern end of the basin.

Several relationships were found between the hydrological variables and meteorological variables in Abdul Aziz's (2004) study. The results are in close agreement with Gleick's (1987) findings: the annual runoff is affected primarily by precipitation changes while the seasonal distribution of runoff is affected by changes in mean monthly temperature. Abdul Aziz (2004) found that all monthly flows, except January flow, are strongly correlated to changes in mean monthly temperature while the correlation between annual mean flow and changes in annual total precipitation is much stronger than between annual mean flow and temperature.

Abdul Aziz (2004) also assessed the change in hydrological regime using a hydrological model, WATFLOOD. He found significant discrepancies between the modelled results and the observed, as well as between the modelled results and other previous studies. He examined the probable cause of the discrepancies and concluded that the European Center for Medium range Weather Forecasting (ECMWF) Re-analysis climate data were not of sufficient quality to generate accurate streamflow data.

2.11 Large-scale climate anomalies and hydrological trends

Déry and Wood (2005) investigated the possible role of large-scale climate anomalies such as the Arctic Oscillation (AO), the ENSO, the PDO, and the Pacific North American (PNA) pattern on high-latitude river discharge. Significant correlation was found between the river runoff to the Arctic Ocean and the ENSO (0.68), and anti-correlation was found between the river runoff and both the PDO (-0.53) and the PNA (-0.51).

ENSO is a coupled ocean-atmosphere phenomenon primarily active over the tropics and subtropics of the Pacific and Indian Oceans. "El Niño" is Spanish for the "Christ's Child". It is associated with warm waters in the eastern Pacific Ocean along the coast of Ecuador and Peru. While "The Little Girl", "La Niña", represents the opposite of El Niño (USDA, 2005). Figure 3

categorizes ENSO from 1961 to 2002.

PDO is an interdecadal fluctuation that has been shown to have regional climate signatures similar to those associated with ENSO. Mantua *et al.* (1997) found that warm-PDO (positive value) phases are generally associated with warmer temperature and drier than normal condition during winter. During opposite conditions, winter temperature and precipitation is usually cooler and higher, respectively. Cool PDO phases occurred from 1900 to 1924 and from 1947 to 1976, and warm phases from 1925 to 1946 and from 1977 to 1996 (Mantua *et al.*, 1997). Figure 3 categorizes PDO from 1961 to 2002.

	1961	1962	1963	1964	1965	1966	1967	1968	1969	1970	1971	1972	1973	1974	1975	1976	
ENSO				El Nino	La Nina	El Nino			El Nino	El Nino	La Nina	La Nina	El Nino	La Nina	La Nina	La Nina	
PDO	+	-	-	-	-	-	-	-	-	+	-	-	-	-	-	-	
	1977	1978	1979	1980	1981	1982	1983	1984	1985	1986	1987	1988	1989	1990	1991	1992	
ENSO	El Nino	El Nino		El Nino			El Nino		La Nina		El Nino	El Nino	La Nina			El Nino	
PDO	+	+	-	+	+	+	+	+	+	+	+	+	-	+	-	+	
	1993	1994	1995	1996	1997	1998	1999	2000	2001	2002							
ENSO			El Nino	La Nina		El Nino	La Nina										
PDO	+	+	-	+		+											

Figure 3 Categories of PDO and ENSO from 1961 to 2002
Source: adapted from Harshburger *et al.* (2002)

Mantua *et al.* (1997) also found that the strongest PDO coefficient is located in north-western North America. During warm-PDO phase, the annual water year discharge in Columbia Rivers is on average 14% lower (Mantua *et al.*, 1997). Neal *et al.* (2002) further observed that warm-PDO winter flows being typically higher than the cold-PDO winter flows and the warm-PDO summer flows being typically lower than the cold-PDO flows in Southeast Alaska from 1947 to 1998. Furthermore, they observed that the ratio of snowfall to total precipitation is much lower during the warm-PDO, causing higher than normal winter streamflow. During cold-PDO, on the other hand, more precipitation (as compared to the warm-PDO) was stored as snow, thus causing greater summer streamflows (Neal *et al.*, 2002).

Harshburger *et al.* (2002) examined the regional pattern of associations between climate anomalies (and their interactions) and winter precipitation and streamflow variability in Idaho from 1960 to 1999. They noted that the Pacific Northwest tend to experience below (above) normal precipitation during the El Nino (La Nina) phase. Spring discharge showed a similar

negative relationship to El Nino and PDO. They also found that La Nina phase has greater impact on winter precipitation and spring streamflow than the El Nino phase. Yet, the combination of El Nino-positive PDO and La Nina-negative PDO years has higher correlation to winter precipitation and streamflow than that of any single event; the greatest anomalies occurred during the combination of La Nina-negative PDO. These effects of ENSO are regional-specific (Hamlet and Lettenmaier, 1999) and depend on topography (Redmond and Koch, 1991).

Cunderlik and Burn (2004) demonstrated that PDO has a crucial role in the air-temperature records in the Southern British Columbia Mountains climate region. They have varied the scenarios of 40-year-long periods starting with 1900-1939 and ending with 1960-1999. This experiment illustrated that very contrasting trend results can be obtained from the different scenarios of 40-year-long periods. They suggested the trend results were dependent upon the location of the period relative to the given PDO phase.

Specifically in the Liard Sub-basin in the MRB, Burn *et al.* (2004b) investigated the relationship of the streamflow data from 1960-1999 with the PDO. They found that minimum flows were positively correlated to the PDO and maximum flows were negatively correlated to the PDO. The results also indicated that during the warm-PDO phase, the occurrences of annual maximum and spring maximum floods shift towards the spring and shift towards the summer during the cold-PDO phase. They attributed this to higher spring temperatures during the warm-PDO phase triggered by early onset of snowmelt.

3 TECHNICAL APPROACH/ METHODOLOGY

Climate input data were supplied into a watershed model to simulate hydrologic variables on a grid basis. A statistical test was then employed to identify trends in these variables. The major steps in this research are summarized in the flow chart in Figure 4, and are described in the following sections.

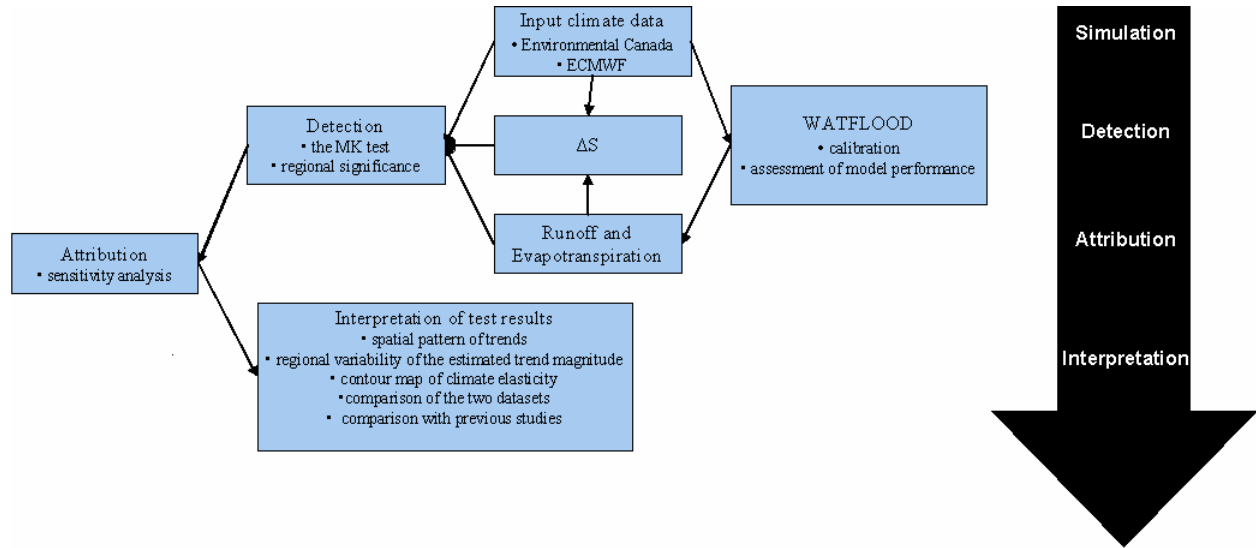


Figure 4 Technical Approach Flow Chart

3.1 Variable selection and data collection

As depicted in Figure 1 in Section 2.4.1, the major components in the hydrologic cycle are evapotranspiration, precipitation, storage, and runoff. Moreover, while the model does not simulate flow in large rivers (lakes) well, it is likely to give better simulations of the amount of runoff generated within each grid and thus potentially available for use. Therefore, evapotranspiration (ET), precipitation (P), storage (S), and runoff (R), as well as temperature (T), were included in the analysis. Two different data sets were used in this study. One of the data sets was chosen for calibrating the WATFLOOD hydrological model. The WATFLOOD model is discussed in more detail in Chapter 5.

In both data sets, runoff and evapotranspiration were modelled using WATFLOOD on a 20 by 20 km grid. The change in storage was estimated from the water-balance equation.

$$P - ET - R = \frac{\Delta S}{\Delta t} \quad (1)$$

where the right side of the equation represents the change in water storage within the grid over a time step Δt . In the analysis, the cumulative change in storage was used, that is, the change in total water storage (ΔS) in a grid. The storage term is assumed to equal zero at an annual time-step under stationary conditions (Douglas *et al.*, 2000). However, climate change may cause the random variables on the left-hand side of the equation to become non-stationary. Consequently, the other terms in the water balance also become non-stationary (Douglas *et al.*, 2000). Climate change may be impacting the storage term and/ or the runoff term.

After the time series of all the hydrologic variables were collected, the trends in the time series were assessed using a statistical test for trend. The relationships between runoff and climatic factors were examined using sensitivity analysis.

3.2 Mann-Kendall test for trend detection

The Mann-Kendall non-parametric test was selected for determining the existence of trend in hydrologic and temperature time series. The major procedures of trend detection are summarized in the flow chart in Figure 5, and described in section 3.2 to 3.4.

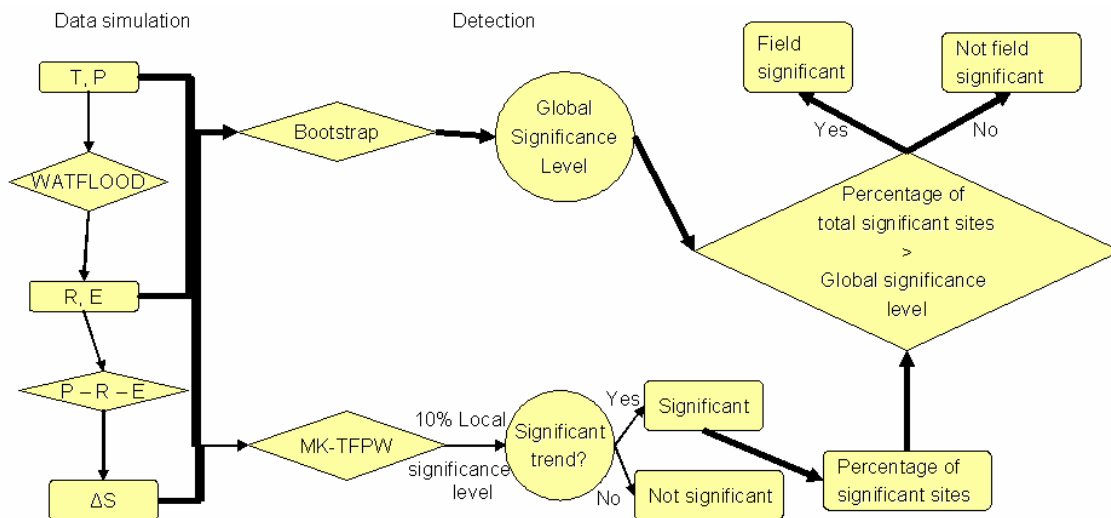


Figure 5 The Mann-Kendall test procedure

According to Cunderlik and Burn (2002) and Burn *et al.* (2004b), the hypothesis test is described

as follows:

The null hypothesis, H_0 : the data are a sample of N independent and identically distributed random variables (i.e. no existing trend in the data set), is tested against

The alternative hypothesis, H_1 : the distribution of x_i and x_j is not identical for all $i, j \leq N$ with $i \neq j$, where i and j are the sequential data values and N is the length of the data set record.

For a two-sided test, at the pre-selected level of significance, α , reject H_0 if the standardized test statistic, $Z < -Z_{\alpha/2}$ or $Z > Z_{\alpha/2}$, where the standardized MK statistic Z follows the standard normal distribution with mean of zero and variance of one:

$$Z = \begin{cases} \frac{S-1}{\sqrt{\text{var}(S)}} & \text{if } S > 0 \\ 0 & \text{if } S = 0 \\ \frac{S+1}{\sqrt{\text{var}(S)}} & \text{if } S < 0 \end{cases} \quad (2)$$

where the MK test statistic, S is given by:

$$S = \sum_{j=1}^{N-1} \sum_{i=j+1}^N \text{sgn}(x_i - x_j) \quad (3)$$

where,

$$\text{sgn}(\theta) = \begin{cases} 1 & \text{if } \theta > 0 \\ 0 & \text{if } \theta = 0 \\ -1 & \text{if } \theta < 0 \end{cases} \quad (4)$$

For independent, identically distributed random variables (i.e. no trend), the theoretical mean and variance of S is

$$E(S) = 0 \quad (5)$$

$$\text{var}(S) = \frac{N(N-1)(2N+5) - \sum_t^N t(t-1)(2t+5)}{18} \quad (6)$$

where t = extent of any tie.

There are two important parameters in trend tests. The local significance levels, also termed as the p-values, indicate the amount of evidence for rejecting the H_0 . This value

can reveal extra information about the strength of the trend when no significant trend is detected. Another characteristic of a trend that is of interest is its magnitude and the direction. The non-parametric robust slope estimator, β , determined by Hirsch *et al.* (1982), indicates the magnitude and tendency of the slope. The β value can be determined using:

$$\beta = \text{Median} \left\{ \frac{x_i - x_j}{i - j} \right\} \text{ for all } j < i \quad (7)$$

3.3 Local trend detection

Many hydrological time series exhibit significant serial correlation. To reduce the effect of serial correlation in the data, this study incorporated the TFPW approach developed by Yue *et al.* (2002b) with a slight modification by Burn *et al.* (2004b). The procedures are summarized in Figure 6, and are described in Burn *et al.* (2004b) as follows:

Step 1. The MK statistic, S , was estimated, and the local significance level, α , of the trend in the original data series was also evaluated. The non-parametric slope, β , was calculated using Eq. 7. The TFPW procedure is only implemented if the slope differs from zero.

Step 2. The monotonic trend, β , was removed using:

$$y_t = x_t - \beta t \quad (8)$$

where x_t is the series value at time t and y_t is the de-trended series.

Step 3. The lag-1 serial correlation coefficient r_1 of the de-trended series y_t was computed using the following formula (Salas *et al.*, 1980)

$$r_1 = \frac{\frac{1}{N-1} \sum_{t=1}^{N-1} [y_t - E(y_t)][y_{t+1} - E(y_{t+1})]}{\frac{1}{N} \sum_{t=1}^N [y_t - E(y_t)]^2} \quad (9)$$

$$\text{where } E(y_t) = \frac{1}{N} \sum_{t=1}^N y_t \quad (10)$$

If the value of r_1 is not statistically significant (at the 5% level), the trend results from Step 1 are used and the calculations for the data set are complete. If the serial correlation is significant (at the 5% level), the de-trended series is pre-whitened through:

$$y'_t = y_t - r_1 y_{t-1} \quad (11)$$

where y'_t is the residual series. The residual series should be an independent series.

Step 4. The monotonic trend was added to the residual series through:

$$y''_t = y'_t + \beta t \quad (12)$$

where y''_t is the trend free pre-whitened series.

Step 5. The Mann-Kendall statistic, S, and the local significance of the calculated S for the y''_t series were evaluated.

The results of the MK test were then evaluated at the 10% local significance level in this study.

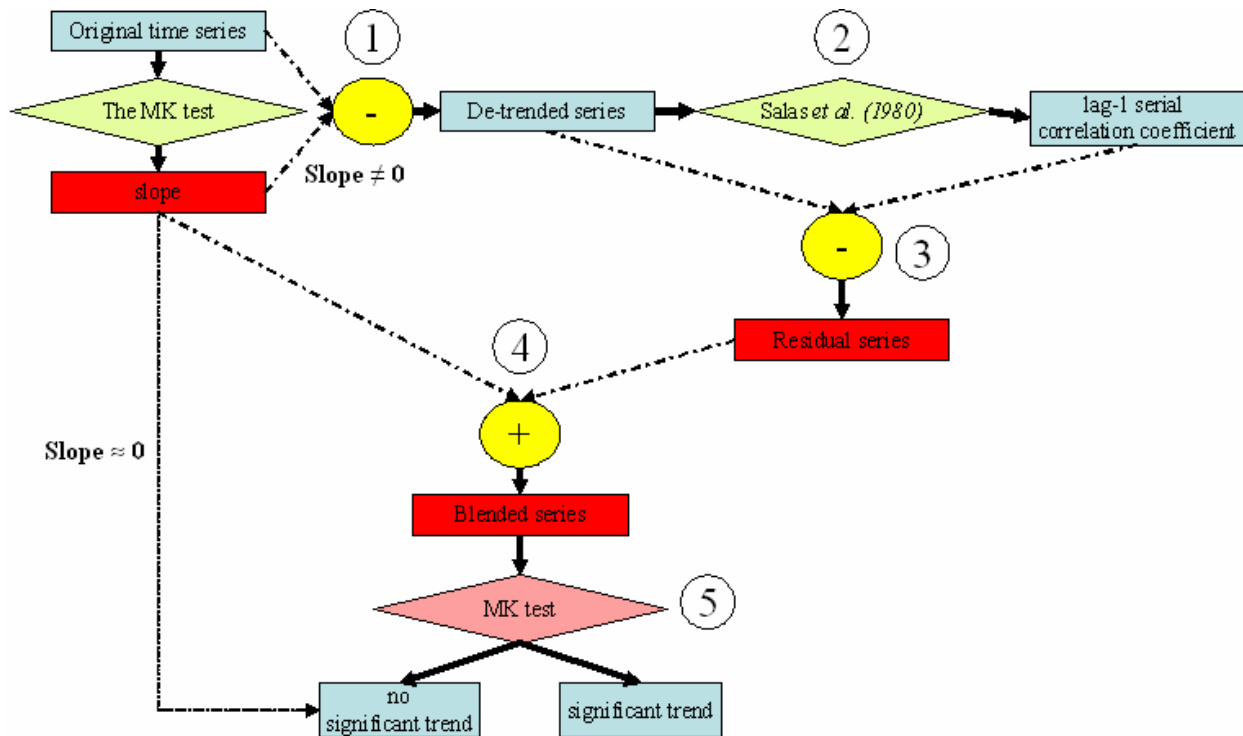


Figure 6 Trend Free Pre-whitening Procedure

3.4 Regional trend detection

To determine if a given variable is significant at a regional scale, one has to determine the effect of cross-correlation in the data set. In this study, a modified bootstrap resampling approach developed by Burn and Hag Elnur (2002) was used to account for cross-correlation. This procedure determines the critical value for the percentage of sites where significant trend would

be expected to occur by chance. According to Burn and Hag Elnur (2002), the procedures are described as follow:

Step 1. A year was randomly selected from a specified range of years. The specified range is a defined period of record for which the analysis is to be conducted.

Step 2. The data value for each site for the selected year was entered in the data set being assembled.

Step 3. Step 1 and 2 were repeated until the resampled data set has the target number of station-years of data.

Step 4. The MK test is applied to the data from each station in the resampled data set and the percentage of results that are significant at the $\alpha\%$ level is determined, where α is the local significance level.

Step 1—4 are repeated a total of NS times (NS was set to 1000) resulting in a distribution for the percentage of results that are significant at the $\alpha\%$ level. From this distribution, the value that is exceeded $\alpha_f\%$ of the time is selected as the critical value, p_{crit} ; α_f is referred to as the field, or global significance level. Results obtained with a percentage of sites showing a significant trend larger than p_{crit} are considered significant at the $\alpha_f\%$ level.

Results obtained from the trend tests were analyzed using a local significance level of 10% and a field significance level of 10%.

3.5 Relationship of runoff with climate

The potential impacts of climate change on the hydrologic cycle can be assessed using the nonparametric estimator proposed by Sankarasubramanian *et al.* (2001). Sankarasubramanian *et al.* (2001) found that this estimator has low bias and is as robust as or more robust than alternate model-based approaches. Chiew (2006) further found that this elasticity estimator is not affected by catchment size, length of data or the quality of model calibration.

Climate-runoff relationships were identified by this nonparametric estimator, ϵ , for each grid.

The nonparametric estimator can be expressed as:

$$\varepsilon_p = \text{median}\left(\frac{R_t - \bar{R}}{P_t - \bar{P}} \cdot \frac{\bar{P}}{\bar{R}}\right) \quad (13)$$

where R_t is the annual runoff, P_t can be any annual climatic variable, \bar{R} and \bar{P} are the long-term sample means.

Each pair of R_t and P_t in the time series were used to estimate a value of the $\left(\frac{R_t - \bar{R}}{P_t - \bar{P}} \cdot \frac{\bar{P}}{\bar{R}}\right)$, and

the median of these values is the nonparametric estimate of ε_p for that site. The sensitivity of runoff to changing climate (temperature and precipitation), as well as the sensitivity between runoff and evapotranspiration were assessed using this approach in this study.

3.6 Interpretation of test results

The trend detection and the climate elasticity of runoff identify the monotonic trends and the relationship between variables within a referenced timeframe. In this study, the analysis was conducted in a grid-by-grid basis as difficulties arose when interpreting large amounts of test results. Furthermore, trends are focused on a relationship with time while hydrological time series are correlated both in time and space. Thus, when interpreting test results, the goals are 1) identifying spatial patterns, 2) obtaining useful information, and 3) examining if there is any problem in the test results or in the original data. Theoretical knowledge on the variables, historical knowledge about the data and the study site, and other extra information were incorporated with graphs, maps, and statistical techniques to achieve the aforementioned goals.

Spatial distribution of trends

Maps were created for displaying the spatial distribution of trends. The sites with significant positive and negative trends at 10% level, and sites with no significant trend at 10% level, were illustrated using different colours. Spatial distribution of trends was visually examined to identify if any spatial patterns dominated in a specific climatic zone, sub-basin or region or if the trends are distributed randomly across the basin. Moreover, maps of different variables can assist in visually identifying and interpreting possible relationships between variables. These maps might also assist in explaining results from sensitivity analysis, and/ or comparing with

previous studies.

Regional variability of the estimated trend magnitude

The slope estimate for all the grid squares were summarized using box-plots. The plots can reveal the regional variability of the estimated trend magnitude for the entire basin. Moreover, they exhibit the overall trend, the range of slope values, and the distribution of the slope values. These plots can also aid in the comparison between results from different months, different seasons, and different data sets.

Map of climate elasticity

Maps were used to illustrate the spatial variability of the climate elasticity. Regions that are relatively sensitive or relatively insensitive to climate can be immediately identified on these maps.

Box-plots of climate elasticity

These plots summarized the climate elasticity for the entire basin. The climate elasticities of runoff to precipitation, evapotranspiration, and temperature were plotted separately for each data set.

Comparison of the two data sets

Data are the backbone of a trend detection and attribution study. In this study, two sets of climate data were obtained from two different sources. Detailed discussions of each data set are provided in Chapter 5. To compare the two data sets, partial correlation, box-plots, and maps were employed.

Partial correlation method was employed because hydroclimatic variables are often correlated with time. Partial correlation was calculated for each grid point based on the annual time series of each data set as follows:

$$r_{12.3} = \frac{r_{12} - r_{13}r_{23}}{\sqrt{(1 - r_{13}^2)(1 - r_{23}^2)}} \quad (14)$$

where $r_{12.3}$ is the partial correlation between the two data sets, subscript 1 represents the first data

set, subscript 2 represents the other data set, subscript 3 represents the time sequence. Then r_{12} is the ordinary correlation coefficient. The partial correlations were then summarized using box-plots and maps.

Even if variables from both data sets exhibit similar trends and are highly correlated, they can still be very different in magnitude. To compare the magnitude of each variable from the two data sets, 60 sample sites were randomly selected in the basin to compare the magnitude of each variable from the two data sets. Data values of a variable for a selected year from each sample site were displayed in a box-plot.

Comparison with other studies

The results of trend detection and nonparametric estimator were compared with results from other detection studies done on North America, specifically in the MRB. The attempts were made to compare the modelled results with the observed and validate the findings from each data set.

4 THE STUDY SITE

Stretching over 15° (from about 52° to 70°) of latitude from Jasper, Alberta in the south to the coast of the Beaufort Sea in the north (Figure 7) (Environment Canada and NSERC CRSNG, 2004), the MRB is home to nearly 400000 people (MRBB, 2004) and influences the life of mammals, birds and fish. The population density in most of the basin is less than one person/km² (WRI, 2007b). Unlike the usual settlement pattern, the majority of the population and development is located in the upstream area in the south (WRI, 2007a). The northern part of the MRB is a vast land where aboriginal people live, speaking eleven different languages (MRBB, 2001).

The basin covers an area of approximately 1.8 million km² (Environment Canada and NSERC CRSNG, 2004) that includes parts of three provinces (British Columbia, Alberta and Saskatchewan) and two territories (Yukon and the Northwest Territories). The mainstem of the basin, the Mackenzie River, flows approximately 4240 km from the headwaters of the Finlay River to the Arctic Ocean (Louie *et al.*, 2002). The basin is the longest river system with the largest drainage area in Canada (Stewart *et al.*, 2002). The southern basin is dominated by boreal forest and cropland with alpine areas in its mountains, and the north is arctic tundra (Louie *et al.*, 2002, Figure 8).

The MRB is composed of six main sub-basins (Figure 9), three large lakes (Figure 7) and, three major deltas (Figure 7) including one of the world's largest freshwater deltas, the Peace-Athabasca Delta (Stewart *et al.*, 2002). Permafrost underlies more than 75% of the basin while the economic activities, such as agriculture and forestry, are concentrated in the remaining area of the basin in the south (Environment Canada and NSERC CRSNG, 2004) and occupy less than 2 percent of the total basin area (WRI, 2007a). As the largest source of fresh water for the Arctic Ocean from North America, the basin plays an important part in regulating the thermohaline circulation of the world's oceans (Environment Canada and NSERC CRSNG, 2004). The basin also encompasses a diversity of abundant potential resources (Woo and Thorne, 2003). The Mackenzie River is a major transportation corridor for transporting these renewable and non-renewable resources to the southern markets (Louie *et al.*, 2002), and delivering supplies to the northern communities and industries (Sung *et al.*, 2006).



Figure 7 The Mackenzie River Basin and its geographic features and population centers
Source: used with permission of Environment Canada and NSERC CRSNG (2004)

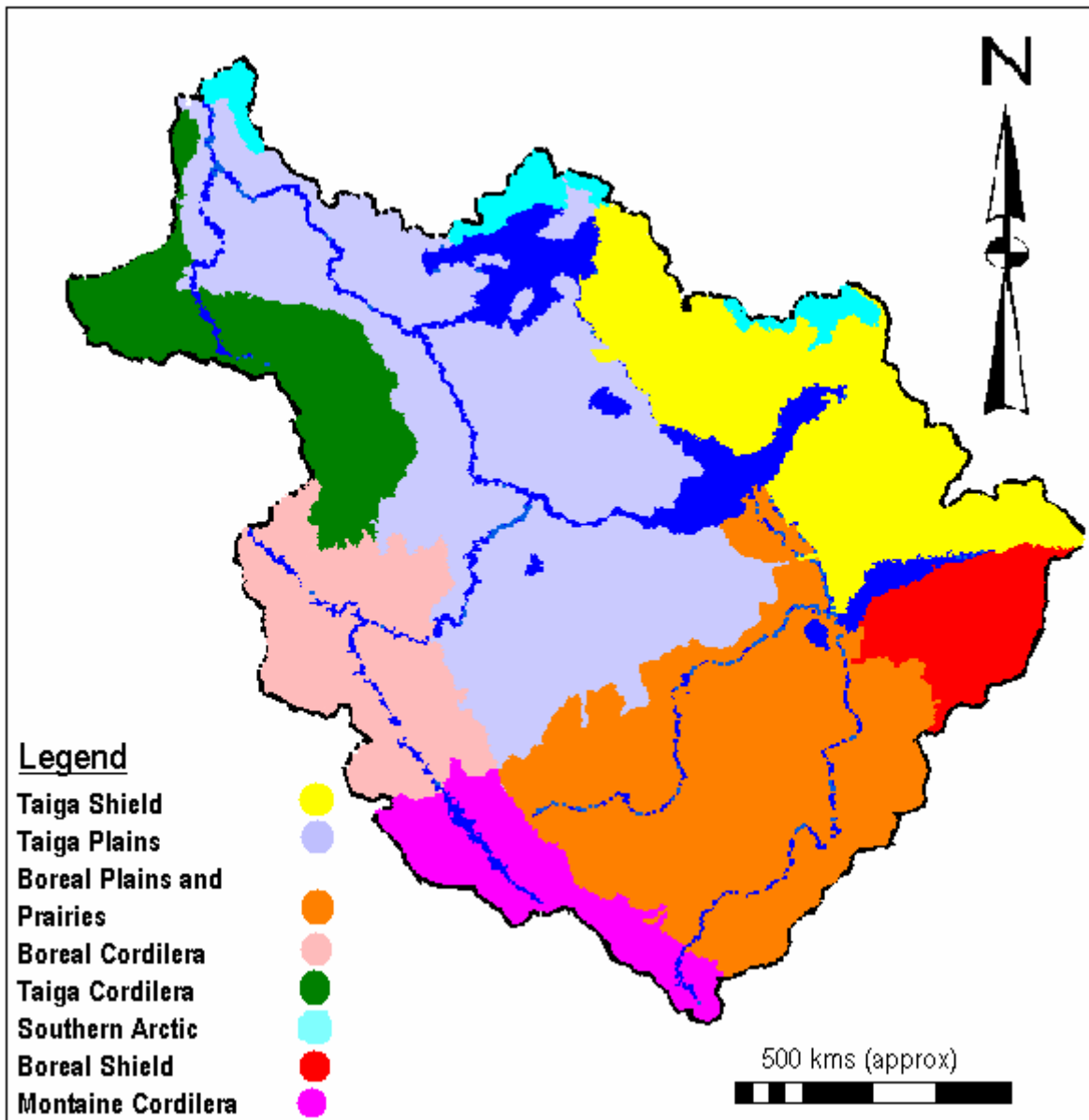


Figure 8 Ecoregions in the Mackenzie River Basin
 Source: adapted from MRBB (2001)

4.1 Climatic regions

Four major physiographic regions influence the climatological and hydrological regime of the basin: the Western Cordillera, the Interior Plain, the Precambrian Shield, and the Arctic Coastal Plain (Woo and Thorne, 2003, Figure 10). The effect of climate change in different geographic regions is expected to vary from region to region.

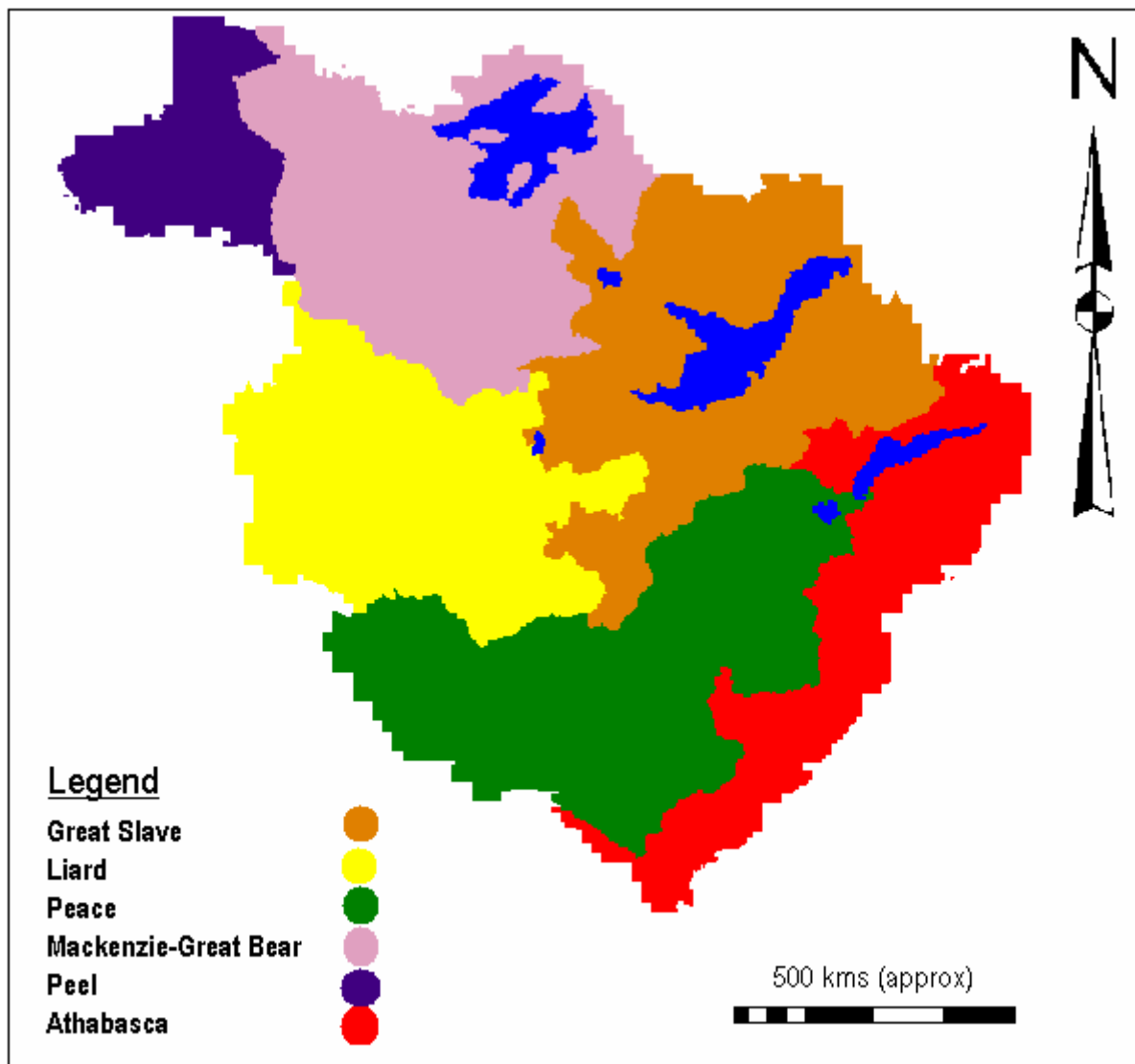


Figure 9 The Mackenzie River Basin location and its major sub basins
 Source: adapted from Louie *et al.* (2002)

The Western Cordillera (Regions 2 and 5 in Figure 10) consists of a series of mountain chains along the west side of the basin (Woo and Thorne, 2003). The Rocky Mountain chain exceeds 3000 m in the south but is only 1800 to 2100 m in the north (Louie *et al.*, 2002) with some glaciers occupying the mountain tops and high valleys (Woo and Thorne, 2003). This region dominates the flow to the Mackenzie whereas the Shield and the plains have relatively lower runoff (Woo and Thorne, 2003).

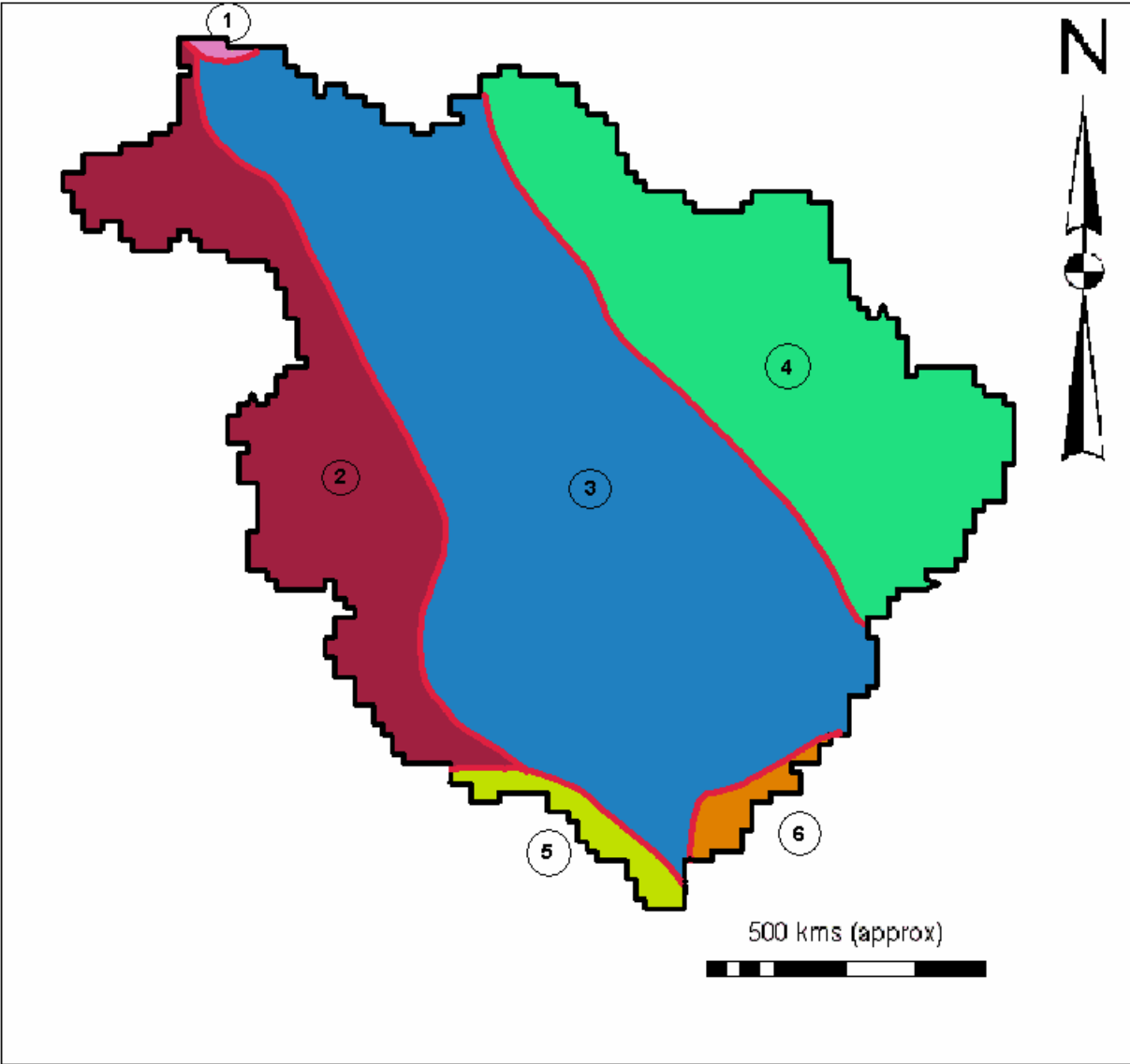


Figure 10 Physiographical subdivisions in the Mackenzie River Basin
 (1) Delta, (2) West Cordillera, (3) Interior Plains, (4) Canadian Shield, (5) West
 Cordillera, and (6) Interior Plain
Source: adapted from Woo and Thorne (2003)

The Canadian Shield (Region 4 in Figure 10) in the east is a rolling terrain with Precambrian bedrock uplands (Woo and Thorne, 2003) separated by soil-filled valleys that also contain lakes and wetlands (Woo and Marsh, 2005). This region contains discontinuous permafrost and encompasses the three large lakes of the MRB (Stewart *et al.*, 1998). The lake storage tremendously attenuates outflow in this region (Woo and Marsh, 2005). Furthermore, rock

fractures and patches allow water seepage and gradually release the moisture to bedrock infiltration or to evaporation (Woo and Marsh, 2005). Thus, the runoff ratio is highly variable in the Shield upland (Woo and Marsh, 2005). A fill-and-spill mechanism is the most appropriate description of the runoff process in the region because snowmelt runoff is generated only after the storage requirements are satisfied (Woo and Marsh, 2005).

The Interior Plains run through the central zone of the basin (Regions 3 and 6 in Figure 10). The region constitutes approximately one-third of the basin area and encompasses a series of gently rolling plateaus and lowlands as well as many wetlands and lakes (Louie *et al.*, 2002). The Alberta Plateau in the south is covered by prairie grassland and the Mackenzie Lowlands in the north are covered by tundra with boreal and subarctic forest separating these two areas (Louie *et al.*, 2002).

At the mouth of the Mackenzie is its delta (Region 1 in Figure 10), an assemblage of distributaries, levees, wetlands, and lakes (Woo and Thorne, 2003). The region supports a unique and vulnerable arctic ecosystem. For example, the wetlands in this region are hydrogeomorphologically self-sustaining due to the insulating properties of the organic layer and the large ground ice content, which helps to raise the water table in the summer and ensure frequent saturation of the organic layer in the wetlands (Woo and Marsh, 2005).

The several climatic regions encompassed by this basin include the cold temperate, mountain, subarctic, and arctic zones (Woo and Thorne, 2003). The mean annual basin temperature is approximately -3.4°C with approximately -25°C to -30°C in winter and 15°C in summer (Stewart *et al.*, 2002). The greatest interannual temperature variability occurs in the winter (Stewart *et al.*, 2002).

Annual precipitation in the basin declines from southwest (> 1000 mm) to the north (approximately 200 mm) (Woo and Thorne, 2003). One of the reasons is the presence of the Pacific Ocean and Rocky Mountains to the west, which enhance the moisture advection from southwest of the basin (Cao *et al.*, 2002). The average annual total precipitation is approximately 421 mm (Louie *et al.*, 2002), with snowfall dominated for 6-8 months (Stewart *et*

al., 2002). Minimum precipitation occurs during the winter months of February to April and the maximum occurs during the summer months of June to August (Stewart *et al.*, 2002). For over half the year, snow stays on the ground in many parts of the basin and snowmelt usually triggers major high-flow events in the spring (Woo and Thorne, 2003). In the summer and autumn, convectional and frontal rainfall is the important source of water for streamflow generation (Woo and Thorne, 2003). Evapotranspiration mainly occurs between May to October and is approximately 250 to 277 mm/year (Louie *et al.*, 2002). However, the evapotranspiration estimate has great uncertainty because of changes in basin storage space (Stewart *et al.*, 2002).

The hydrological regime in most rivers is characterized by high flows generated from snowmelt and river ice breakup (Woo and Thorne, 2003). Following the peak flow in the snowmelt period are declining flows in the summer and low flow in the winter. Some researchers (Searcy *et al.*, 1996, for example) reported some advanced ice breakups by the massive river discharge in the spring, which implies an effect on the water balance and runoff generation in the basin.

The hydrological characteristics for each sub-basin are different. The Laird is a large mountainous basin with no large lakes within the sub-basin (Burn *et al.*, 2004b). The Athabasca is located in the cold, temperate zone of the southern Mackenzie Basin and has an intermediate flow (Woo and Thorne, 2003). The Great Slave includes the drainage from the Canadian Shield as well as several basins on the high plains (Woo and Thorne, 2003). The Great Bear in the Shield region is dominated by the large Great Bear Lake (Woo and Thorne, 2003). The mountainous sub-basins in the west (the Liard, the Peace, and the Peel) constitute the largest flow (60%) to the Mackenzie (Woo and Thorne, 2003). The Great Slave and the Great Bear, although covering approximately the same total area as the mountainous sub-basins, produce lower runoff and only contribute about 25% of the Mackenzie flow (Woo and Thorne, 2003).

The mean annual residual (precipitation – evapotranspiration – discharge) is -28.4 mm from 1972 to 1995 (Louie *et al.*, 2002). This residual is a combination of errors in the three water balance components and the assumption of zero annual storage (Louie *et al.*, 2002).

4.2 Natural and anthropogenic influences on the streamflow regime

The streamflow regime can be altered by natural and anthropogenic influences. The major anthropogenic influence to the flow regime is the reservoir operation to generate hydroelectric power in the Peace River at Hudson Hope (Woo and Thorne, 2003). There are two major dams in the basin (IUCN *et al.*, 2003). One of them is the W.A.C. Bennett Dam, which impounds the Peace River to form the Williston Reservoir for hydroelectric power generation at Hudson Hope. The dam effectively reduces the snowmelt and summer flows at Peace Point (Woo and Thorne, 2003). The other dam, located 23 km downstream of W.A.C. Bennett Dam, is the Peace Canyon Dam. The two dams supply 40% of British Columbia's hydroelectric power (Official Tourism Site of British Columbia, 2007). Storage in wetlands and lakes across the basin naturally attenuate the high flows and extend the low flows. Large lakes (i.e. the Great Slave Lake, the Great Bear, and Lake Athabasca) have great effects in modifying the high flows (Woo and Thorne, 2003).

5 DATA SOURCES

5.1 Description of data sets

Two sets of climate data were used in this study. Data were obtained from Environment Canada and ECMWF for the period 1961-2002. The Environment Canada data were obtained from the National Climate Data and Information Archive (National Climate Data and Information Archive, 2005), operated and maintained by the Meteorological Service of Canada (MSC). The MSC is a division of Environment Canada, which is responsible for collection of meteorological data in Canada. The MSC has operated a network of climate stations throughout Canada since 1840. The climate network is one of the longest running monitoring networks in the country. Currently, there are approximately 2200 stations that provide at least daily temperature and/ or precipitation data. A rudimentary climate network, measuring temperature and precipitation, has existed in the MRB since the 1890s. This climate network has poor spatial distribution with the number of stations decreasing with increasing latitude and increasing elevation. In addition, the loss of stations due to closure beginning in the 1990s has increased the extrapolation error by around 16% for all flow regimes (Spence *et al.*, 2007). There are now approximately 330 stations within the MRB or within 200 km of the basin. From this station set, only 100 stations have the full 40 years of record and 250 stations have over 30 years of record. The climate data used in this study are gridded using all available stations. With limited high elevations stations, we are forced to rely on lower elevation stations and make assumptions with respect to how precipitation and temperature change with elevation. In this study, the daily precipitation data were interpolated using a simple inverse distance algorithm while the daily temperature data were first normalized using a lapse rate of 0.6 degrees Celsius for each 100 m of elevation change before using the inverse distance algorithm. Potentially large errors are expected in the precipitation data because 1) precipitation measurements are prone to significant systematic measurement errors due to wind, wetting losses and evaporation losses (Louie *et al.*, 2002); 2) precipitation is extremely variable and is more difficult to predict and extrapolate between sites than temperature; and 3) snowfall is generally underestimated, particularly in the mountainous and windswept Arctic terrain (Metcalf *et al.*, 1994).

ECMWF produced reanalysis data sets for the period 1957-2002 using the ERA-40 data

assimilation system (ECMWF, 2006). The reanalysis climate data covers the entire world on 125 km grid spacing (Kållberg *et al.*, 2005). Reanalysis differs from the traditional climatological approach in that it processes a wide variety of observations simultaneously, using the physical laws embodied in the forecast model and observations to interpret conflicting or indirect observations and fill gaps in observational coverage (ECMWF, 2006). The data were produced by three-dimensional variational data assimilation using six-hourly cycling (Kållberg *et al.*, 2005). The temperature and precipitation data for the 42-year study period have been collected in six hour intervals for all months of the year (ECMWF, 2006).

Two different data sets were used because precipitation and temperature calculated using station and gridded data could be different. For example, gridding averages station precipitation and may lead to a smoothing of the precipitation field (i.e. increasing the frequency but reducing the intensity).

5.2 Variables selection

The major components of the water cycle include precipitation (P), evapotranspiration (ET), runoff (R), and storage (S). The annual value and monthly mean of these four variables and temperature (T) were selected for this study. The annual values for P, ET, and R are the total mm of water for the particular year, whereas, the annual values for T is the monthly averaged values in °C over the particular year. The monthly mean represents the magnitude of daily averaged values over the particular month. Only the year-end cumulative S (in mm) for each year were used in the analysis.

The precipitation and temperature of the interpolated MSC data and ECMWF data were directly used for the analysis. The temperature and precipitation data were also used as inputs into the WATFLOOD hydrological model. The model calculates all elements of the hydrologic cycle including evapotranspiration and runoff at a spatial resolution of 20 km. The change in storage for each grid square was calculated using Eq. 1. These three fields were then used for the analysis.

5.3 The WATFLOOD hydrological model

The requirement for this project was a modelling approach capable of providing monthly average outputs at a resolution of 20 km. R and ET modelling was performed using the WATFLOOD model (Kouwen, 1972). Kouwen (1996) has presented a detailed description of the model structure. A brief description of the model is given below.

WATFLOOD is a hybrid simulation model of the watershed hydrologic budget. It is used for flow forecasting and stream modelling through an integrated set of computer programs that can simulate any watershed's response times ranging from one hour to several weeks. The model has four vertical layers (surface, upper zone, saturated zone, and saturated lower zone) and horizontal resolutions from 1 to 25 km. The basic structure of WATFLOOD is shown in Figure 11. In general, the vertical water-budget (within a single grid) is modelled with conceptual equations, while the routing from grid to grid is modelled with physically-based equations. WATFLOOD treats each cell as a separate catchment and calculates each component of the water balance at a daily time-step. This concept is named Grouped Response Unit (GRU). The GRU is based on the concept that similar land cover groups respond in a similar way (Kouwen *et al.*, 1993). The model assumed uniform meteorological inputs and watershed characteristics over a particular grid cell. Within a single grid, vertical water budget processes include snow accumulation and ablation, evaporation, surface storage, infiltration, interception storage and evaporation, surface runoff, interflow, groundwater recharge, baseflow, glacier runoff, and wetland routing. Horizontal water budget processes from grid to grid include overland and channel routing.

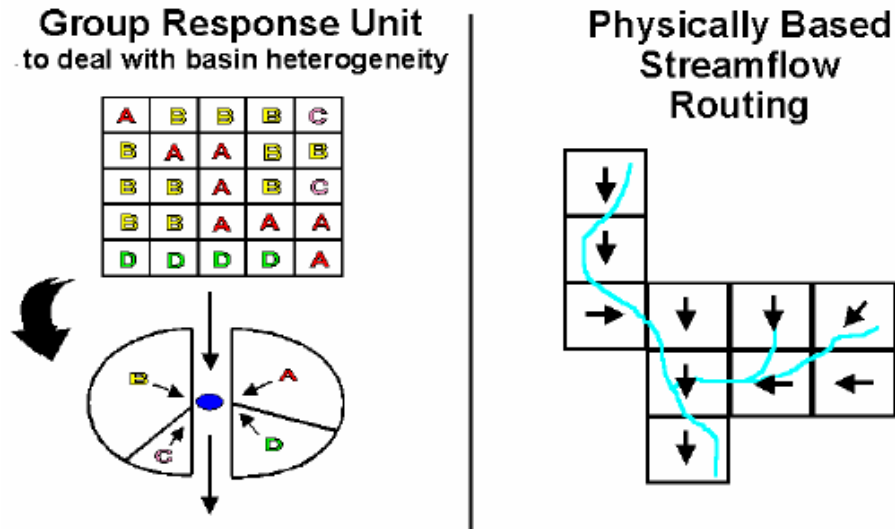


Figure 11 Grouped response unit and runoff routing concept
 Source: used with permission of Kouwen (1996)

5.3.1 Performance of WATFLOOD

Gleick (1986) has suggested six important limiting factors that must be considered when selecting and using a hydrologic model to study the impacts of changes in climate on regional water resources:

- 1) “the inherent accuracy of the model” (Gleick, 1986: 105);
- 2) “the degree to which model accuracy depends upon the existing climatic conditions for which the model was initially developed and calibrated” (Gleick, 1986: 105);
- 3) “the availability of input data, including comparative historical climatic data” (Gleick, 1986: 105);
- 4) “the accuracy of the input data” (Gleick, 1986: 105);
- 5) “model flexibility, ease of use, and adaptability to diverse climatic and hydrologic conditions” (Gleick, 1986: 105); and
- 6) “compatibility with existing general circulation model” (Gleick, 1986: 105).

The performance of WATFLOOD is assessed based on these factors.

Kouwen *et al.* (2000) have investigated the utility of WATFLOOD for the evaluation of atmospheric simulation. They have demonstrated that the hydrological model is sufficiently sensitive to improve the atmospheric models. As a major component of the MAGS,

WATFLOOD is currently coupled with an atmospheric model, CLASS, to produce a hydrology-land-surface scheme model, WATCLASS (Soulis and Seglenieks, 2007), which is part of the Canadian Mesh water modelling system (Soulis and Seglenieks, 2007).

Moreover, the WATFLOOD model has been successfully applied in various forms for climate and hydrology studies in a number of river basins. Although WATFLOOD has been used most extensively in the MRB, the GRU method has made the model capable of being applied in many different watersheds by only calibrating to streamflow (Bingeman *et al.*, 2006). Examples of use of WATFLOOD for climate and hydrology studies include the works by Cranmer *et al.* (2001), Abdul Aziz (2004), Dibike and Coulibaly (2004), Bingeman *et al.* (2006), Sung *et al.* (2006), and Toth *et al.* (2006). These studies have confirmed that the WATFLOOD model can estimate various components of the water cycle with sufficient accuracy. As discussed later, the Nash values from both data sets are reasonable in this study thus indicating that the model provides accurate estimate of streamflow from interpolated or gridded input data. The two data sets were also compared and the results are discussed in Chapter 6.

5.3.2 Data processing

In WATFLOOD, the water balance is calculated for each grid-cell using all the vertical water budget processes that are included in the model. Daily rainfall first fills the interception storage and surface storage, and they are emptied by evaporation. The excess rainfall is then subjected to infiltration. The infiltrated water percolates downward, is subjected to interflow, groundwater recharge, baseflow, and moisture storage.

The evapotranspiration from the soil moisture storage can be estimated by Priestley and Taylor (1972), Hargreaves and Samani (1982) (Eq. 17), or pan evaporation. When radiation data are available, the Priestley and Taylor (1972) equation can be used to estimate the potential evapotranspiration (PET). When only temperature data are available, as in this study, the Hargreaves equation is used to estimate the PET (in mm/day):

$$PET = 0.0075 \cdot R_a \cdot C_t \cdot \delta_t^{1/2} \cdot T_{avg,d} \quad (17)$$

where δ_t is the difference between the mean monthly maximum and mean monthly minimum

temperature (°F), and $T_{avg,d}$ is the mean temperature (°F) in the time step. WATFLOOD uses a modified version of this equation to account for measurements of temperature in °C. C_t is a temperature reduction coefficient which is a function of relative humidity (w_a):

$$\begin{aligned} C_t &= 0.035(100 - w_a)^{1/3} & w_a \geq 54\% \\ C_t &= 0.125 & w_a < 54\% \end{aligned} \quad (18)$$

R_a is the total incoming extraterrestrial solar radiation (in mm):

$$R_a = 15.392 \cdot d_t (w_s \cdot \sin \phi \cdot \sin \delta \cdot \cos \phi \cdot \cos \delta \cdot \sin w_s) \quad (19)$$

where ϕ is latitude in degrees, and the relative distance between the earth and the sun,

$$d_t = 1 + 0.033 \cdot \cos\left(\frac{2\pi \cdot J}{365}\right) \quad (20)$$

where J is the Julian day, the solar declination (in radians),

$$\delta = 0.4093 \cdot \sin\left(\frac{2\pi \cdot J}{365} - 1.405\right) \quad (21)$$

and the sunset hour angle (in radians),

$$w_s = \arccos(-\tan \phi \cdot \tan \delta) \quad (22)$$

Where neither temperature nor radiation data are available, the published pan evapotranspiration values can be used to estimate the PET. However, since the evapotranspiration cannot exceed the atmospherically controlled rate (i.e. limited by available energy and water supply) to areal PET, the actual evapotranspiration (AET) is a function of PET and soil moisture content and is reduced from the PET by:

$$\begin{aligned} AET &= PET && \text{if } PET < IET \\ AET &= (PET - IET) \cdot UZSI \cdot FPET2 \cdot FTALL \cdot ETP && \text{if } PET > IET \\ AET &= PET && \text{for water (rivers/ lakes)} \end{aligned} \quad (23)$$

where IET is the interception evaporation, $FTALL = \begin{cases} 0.7 & \text{Tall Vegetation} \\ 1 & \text{Short Vegetation} \end{cases}$

$$FPET2 = \frac{TTO - TTOMIN}{Temp3} \quad 0.02 < FPET2 < 1.0 \quad (24)$$

where TTO are the accumulated degree-days after January 1 of each year and TTOMIN is the lowest value reached during the winter, and the Upper Zone Storage Indicator,

$$UZSI = \left[\frac{UZS - PWP}{SAT - PWP} \right]^{1/2} \quad (25)$$

where UZS is the upper zone soil moisture, the permanent wilting point,

$$PWP = FCAP \times FULL \quad (26)$$

and the level of saturation,

$$SAT = SPORE \times FULL \quad (27)$$

where FCAP is the field capacity, SPORE is the saturation point, and a theoretical depth at which 100% of the soil pores are full of water,

$$FULL = \frac{RETN}{FCAP} \quad (28)$$

where RETN is the retention factor and this variable is optimized during the calibration of the model. In a study in the Boreal Ecosystem Atmosphere Study (BOREAS) sites, Bingeman *et al.* (2006) showed that WATFLOOD estimates the timing of evaporation well but tends to overestimate the evaporation.

The excess rainfall that exceeds the infiltration capacity becomes surface runoff. The surface runoff from the grid is calculated using the Manning's formula:

$$Q_r = (D_1 - D_s)^{1.67} S_i^{0.5} A / R_3 \quad (29)$$

where Q_r is the channel inflow in m^3/s , D_1 is the surface storage in mm, A is the area of the basin element in m^2 , D_s is the depression storage capacity in mm, and R_3 is the combined roughness and channel length parameter. The D_s and R_3 are optimized during the calibration of the model. Cranmer *et al.* (2001) have shown that WATFLOOD is capable of accurately modelling the nonlinear rainfall-runoff processes for increasing rainfall intensities.

The surface runoff, interflow, and baseflow in a grid are all added to the total inflow from upstream grid and routed through the grid to the next downstream grid.

In this study, the basin was divided into 4667 grid boxes. The model operates with input time series of daily precipitation and temperature and calculates all elements of the hydrologic cycle. It produces daily runoff and evapotranspiration, but monthly averages were used.

5.3.3 Model Calibration

The model was first calibrated using daily and monthly historic time series from Environment Canada for each station gauge using the Nash-Sutcliffe coefficient:

$$R_{NS}^2 \equiv 1 - \frac{\sum_{i=1}^N (Q_i - \hat{Q})^2}{\sum_{i=1}^N (Q_i - m_Q)^2} \quad (30)$$

where Q_i is the measured flow, \hat{Q} is the predicted flow, and m_Q is the average value of Q_i for the period being simulated. The R_{NS}^2 describes how well the magnitude and patterns of the simulated streamflow compares with the observed streamflow. The value of the Nash-Sutcliffe coefficient ranges from negative infinity ($-\infty$) to 1. After the model was calibrated, the ECMWF data for the same period (1961-2002) were used to validate the model. The Nash values for each data set at two of the stations are listed in Table 2. Numbers in the bracket are the Nash value using monthly values; the other numbers are Nash value using daily values. The result indicates that the model is capable of reasonably estimating the streamflow from both data sets.

Station	Environment Canada	ECMWF
Mackenzie at Arctic Red River	0.55 (0.58)	0.59 (0.61)
Liard River at Fort Liard	0.78 (0.86)	0.57 (0.75)

6 RESULTS

The following section presents the results of the MK test and the sensitivity analysis for the 1961-2002 study period. The results of the MK test are presented based on the 10% local and global significance levels. Maps showing the trend detection results for the hydrologic variables at the 10% significance level are also presented. Additionally, the sensitivity of runoff to changes in climate is summarized in the form of maps and box-plots. Finally, the results of partial correlations and comparison between the Environment Canada and the ECMWF data sets are also discussed.

6.1 Trends

6.1.1 Temperature

Regional trend

Table 3 summarizes the regional trend magnitude of temperature. Results that are field significant, at the 10% significant level, are shown in bold. The MRB has generally experienced regional warming between 1961 and 2002. These regional warming trends were statistically significant from January to April for both data sets. In both data sets, the regional annual mean temperature exhibited significant increasing trend. The annual mean temperature increased regionally by about 2.28°C per 42 years from the Environment Canada data set and by about 1.22°C per 42 years from the ECMWF data set.

There were more significant and stronger regional positive trends in the Environment Canada data set than in the ECMWF data set. The trends in September and from May to July are stronger and field significant for the Environment Canada data set but statistically insignificant at 10% global significant level for the ECMWF data set. Regional cooling was observed in the October records, but only the Environment Canada record was field significant. The other months showed increasing regional median trends, but with $p \geq 0.10$. The greatest warming over the entire basin is in January for both data sets, with regional temperature increased significantly by about 5.32°C for the Environment Canada data set and about 3.55°C for the ECMWF data for the 1961-2002 period. Among the four seasons, winter shows the greatest warming over the entire basin. The median regional increase during winter is well over 4.8°C and 2.8°C during

1961-2002 for the Environment Canada and the ECMWF data sets, respectively, followed by spring with regional increase of about 4°C and 2.4°C. Warming during summer and autumn is the least with less than 1°C regional increase for the Environment Canada data set and less than 0.5°C regional increase for the ECWMF data set in the 42-year study period. It is apparent that winter and spring temperature contributed the most to the positive trend in the annual mean temperature.

Table 3 Summary of trend analyses using the MK test for Temperature (in °C/year)

	Environment	
	Canada	ECMWF
Jan	0.13 (0.14)	0.08 (0.08)
Feb	0.12 (0.12)	0.07 (0.06)
Mar	0.11 (0.12)	0.08 (0.08)
Apr	0.06 (0.07)	0.04 (0.04)
May	0.02 (0.03)	0.02 (0.02)
Jun	0.03 (0.04)	0.01 (0.01)
Jul	0.03 (0.03)	0.01 (0.01)
Aug	0.02 (0.02)	0.00 (0.00)
Sep	0.04 (0.04)	0.03 (0.03)
Oct	-0.03 (-0.03)	-0.03 (-0.03)
Nov	0.05 (0.05)	0.02 (0.03)
Dec	0.10 (0.11)	0.05 (0.05)
Ann	0.05 (0.06)	0.03 (0.03)

Note: Entries in bold indicate results that are field significant at the 10% level. The numbers on the left represent the median trend magnitude, and the numbers in bracket represent the average trend magnitude. Positive values indicate increasing trends and negative value indicate decreasing trends.

Regional variability of the estimated trend

Figure 12 and Figure 13 illustrate the regional variability of the estimated temperature trend magnitude for the entire basin for the Environment Canada and the ECMWF data sets, respectively. The two plots exhibit a similar pattern: the regional variability of the estimated trend magnitude is low in the summer months and high in winter months. In addition, the summer months of May to August have weaker positive slope, but the winter months have stronger positive slope. In both data sets, over 90% of areas show increasing annual mean temperature during the study period.

For all of the months in the Environment Canada data set, more than 70% of sites have experienced warming trends, with the exception of October temperature. Temperature from

December to March even shows upward trend at over 90% of sites. The October temperature shows downward trend at over 70% of sites. For the ECMWF data set, over 90% of sites have experienced warming trends, with the exception of February and summer months of May to August, which has half or almost half of the basin with upward trends. The monthly comparison plots are illustrated in Appendix A. The plots indicate that the variability of slope values from Environment Canada data set is always wider in range and the median trend magnitude from Environment Canada data set is usually larger.

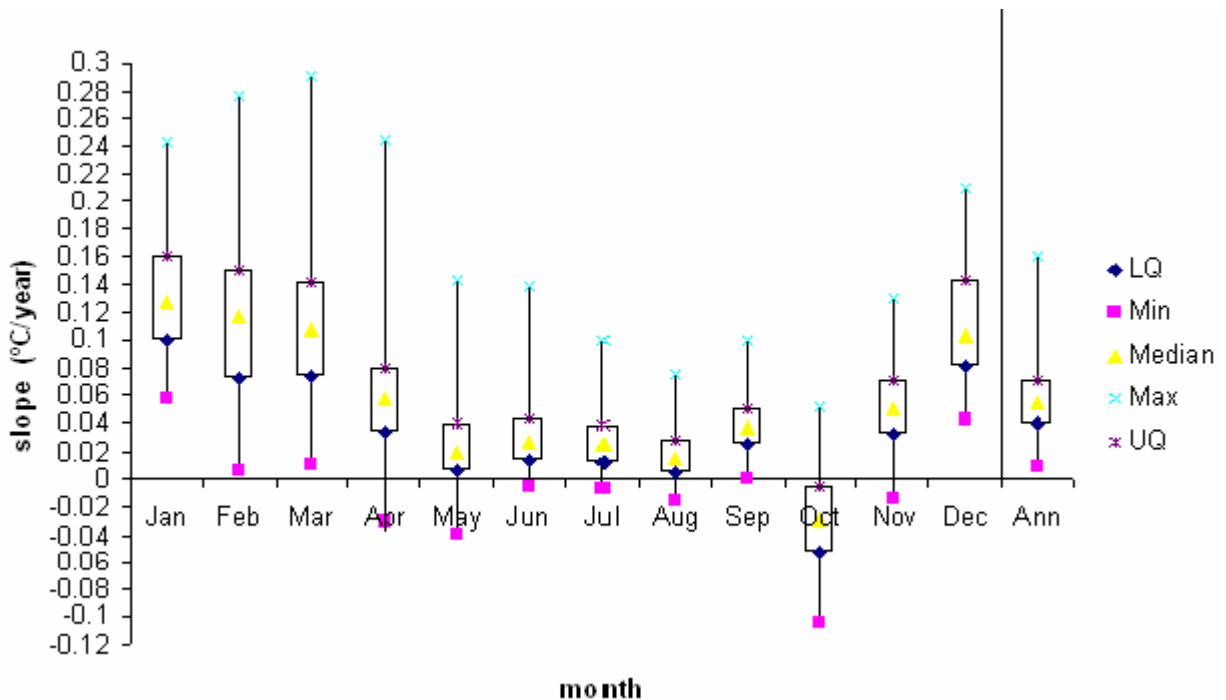


Figure 12 Environment Canada – Box plots of 4667 estimated trend magnitude for every month and for the annual temperature records

Note: The boxes show the first quartile, median, and the third quartile, which contains 50% of the values. The whiskers extend from the box to the five and 95 percentiles.

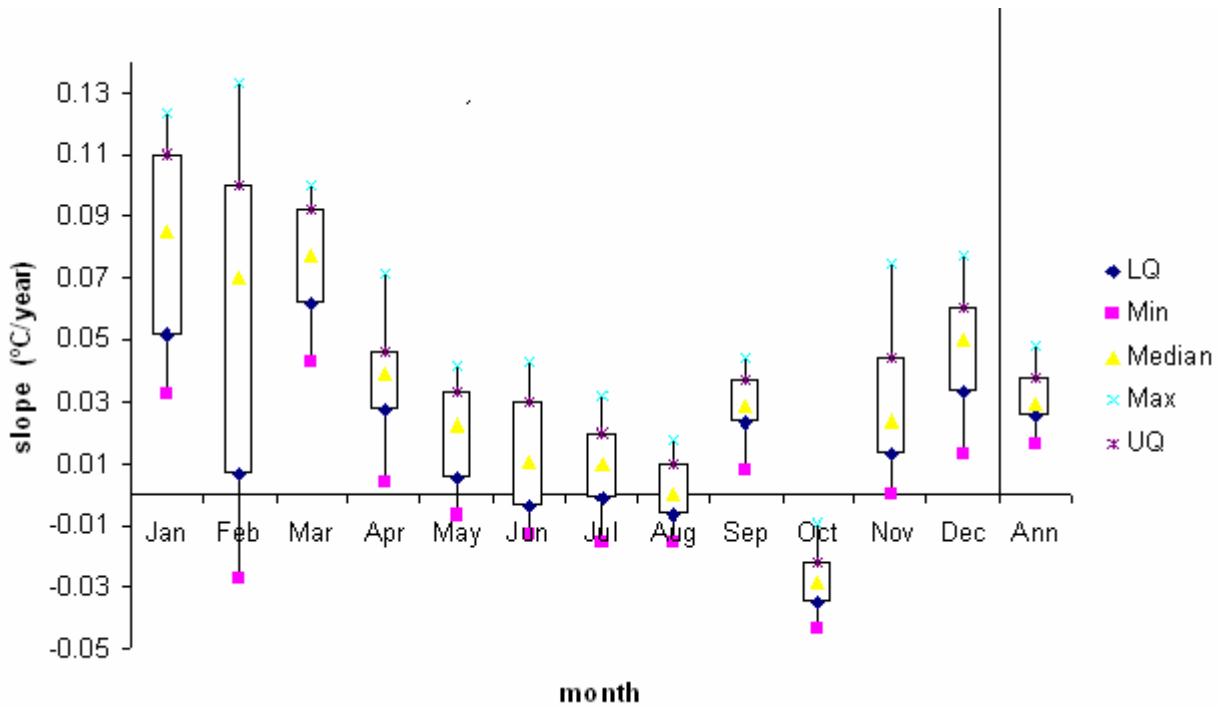


Figure 13 ECMWF – Box plots of 4635 estimated trend magnitude for every month and for the annual temperature records

Note: The boxes show the first quartile, median, and the third quartile, which contains 50% of the values. The whiskers extend from the box to the five and 95 percentiles.

Spatial distribution

Figure 14 shows the spatial distribution of trends in annual mean temperature from Environment Canada and the ECMWF data sets. Monthly plots can be found in Appendix B. In general, the annual mean temperature had significant increases across much of the basin. Similarly to the finding from Table 2, there are considerably larger numbers of trends for the annual mean temperature than would be expected to occur by chance. Moreover, as seen from Table 3 and Appendix B, both data sets are field significant in the winter months of January to April, and the number of trends for these months are far more than the other months in both data sets. Yet, there are pronounced differences in the distribution of trends between the two data sets and between months. For instance, only upward trends are observed from the ECMWF data set, with the exception of October temperature, while the Environment Canada data set has downward trends in some areas and upward trends in some other areas. Some significant downward trends were observed only during spring, summer and autumn for the Environment Canada data set. Only significant upward trends were observed in the winter months. When downward trends are

detected, they were always clustered at Great Bear Lake. On the other hand, although the ECMWF data set has less number of trends detected, the spatial patterns are more well-defined.

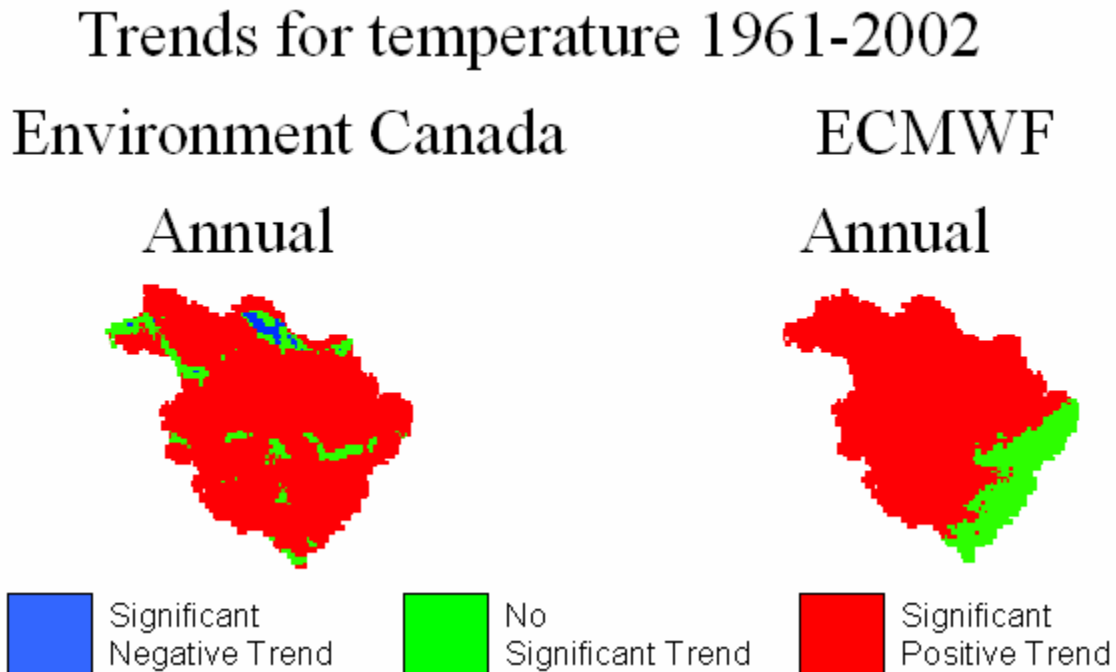


Figure 14 Spatial distribution of significant ($p=0.1$) annual mean temperature trends

Monthly temperature generally increased in most months for the both data sets. The greatest monthly increase is in January and February; however, the trends are statistically significant only in and around Peel, Bear, and Slave Sub-basin. Warming in March, similar to the annual one, has the greatest spatial extent, which covered most of the area in the MRB. August, November and December temperature has the least area with significant trends for both data sets; these months are also field insignificant as seen from Table 2. The spatial pattern in April is similar to May, except that April warming is stronger and the area with significant upward trend has expanded from west side of the Northwest Territories to include northeast British Columbia and part of Yukon Territory. The June and July warming are concentrated in and around the Bear Sub-basin for both data sets. These data show one contrary pattern, a regional cooling trend in October. These cooling trends are concentrated in the southern basin and account for over one-fourth of the total basin area.

6.1.2 Precipitation

Regional Trend

Table 4 presents the regional trend summary of precipitation. Results that are field significant, at the 10% significant level, are shown in bold. In general, the ECMWF data set showed stronger positive trends, and the Environment Canada data set showed stronger negative trends. Regional annual precipitation amount increased by about 6mm from the Environment Canada data set and by about 84 mm from the ECMWF data set during 1961-2002.

The regional trends of precipitation have shown a seasonal pattern. Summer months of May to August and early autumn of September showed the greatest regional positive trends in both data sets; winter months generally showed regional decreasing trends or no trends in the precipitation amount. Regional decreases in precipitation amounts were greatest in January, with about 6.46 mm for the Environment Canada data and about 2.1 mm for the ECMWF data per 42 years. Regional increases in precipitation amounts, on the other hand, were greatest in July, with about 14 mm and 26.5 mm for the Environment Canada and the ECMWF data set, respectively. The regional decreasing trend of winter precipitation amount was offset by the strong regional increasing trend of summer precipitation amount and resulted in overall increases in mean annual precipitation amount.

Table 4 Summary of trend analyses using the MK test for Precipitation (mm/year)

	Environment	
	Canada	ECMWF
Jan	-0.15(-0.16)	-0.05 (-0.04)
Feb	-0.10 (-0.09)	0.00 (-0.03)
Mar	-0.08 (-0.07)	0.06 (0.06)
Apr	-0.08 (-0.08)	0.05 (0.05)
May	0.18 (0.18)	0.31 (0.34)
Jun	0.08 (0.17)	0.46 (0.44)
Jul	0.33 (0.35)	0.63 (0.64)
Aug	0.12 (0.14)	0.33 (0.34)
Sep	0.09 (0.07)	0.21 (0.24)
Oct	0.00 (-0.01)	0.17 (0.16)
Nov	-0.08 (-0.06)	0.06 (0.08)
Dec	-0.08 (-0.09)	0.00 (-0.01)
Ann	0.14 (0.29)	2.00 (2.02)

Note: Entries in bold indicate results that are field significant at the 10% level. The numbers on the left represent the median trend magnitude, and the numbers in bracket represent the average trend magnitude. Positive values indicate increasing trends and negative value indicate decreasing trends.

Regional variability of the estimated trend

Figures 15 and 16 show that the regional variability of the estimated precipitation trend magnitude, as opposed to the variability of the estimated temperature trend magnitude, is high in summer and low in winter for both data sets. Although the seasonal pattern of both data sets is similar, the median slope for the Environment Canada data set is always slightly lower than for the ECMWF data set. However, some of their median slopes are opposite in direction, indicating that the Environment Canada data have weaker positive trend (particularly in the summer months) or stronger negative trend (particularly in the winter months). Also noteworthy is the zero median slope is inside the interquartile range or near the interquartile range for all months for the Environment Canada data set, including annual precipitation. The ECMWF data, on the other hand, has the zero median slope outside the interquartile range for annual and the summer precipitation. This result indicates that over 75% areas have experienced significant increases of precipitation amount annually and during the summer months. The monthly comparison plots are illustrated in Appendix A.

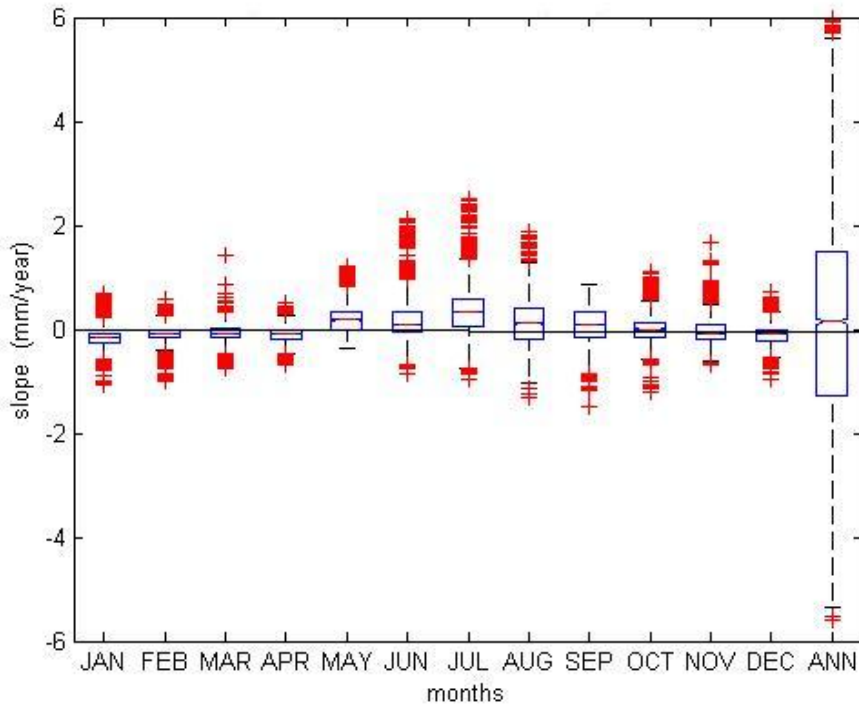


Figure 15 Environment Canada – Box plots of 4667 estimated trend magnitude for every month and for the annual precipitation records

Note: The boxes show the first quartile, median, and the third quartile, which contains 50% of the values. The whiskers extend from the box to the highest and lowest values, excluding outliers.

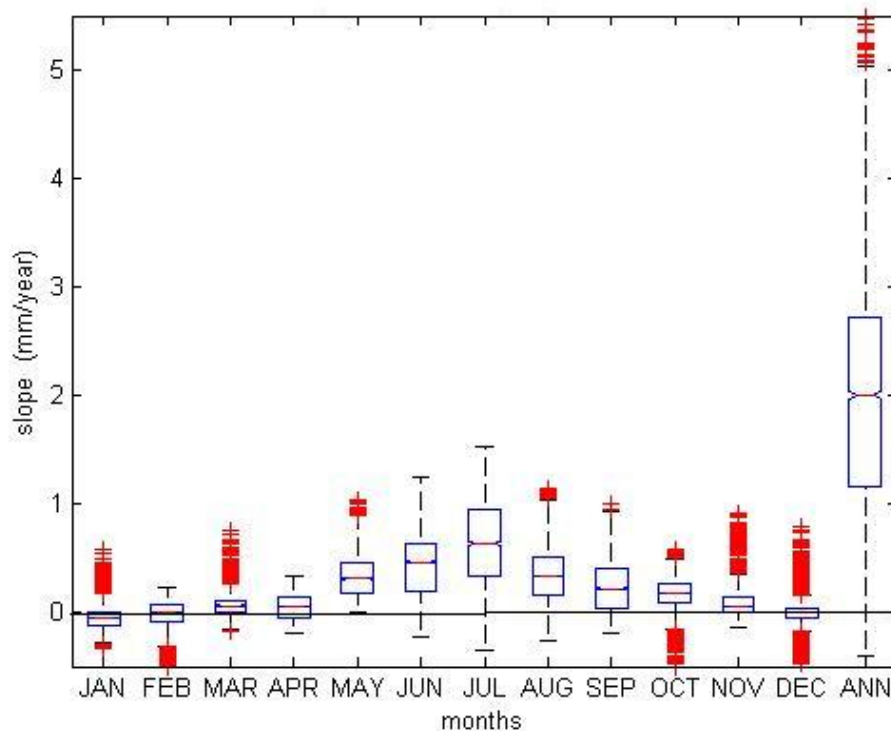


Figure 16 ECMWF – Box plots of 4667 estimated trend magnitude for every month and for the annual precipitation records

Note: The boxes show the first quartile, median, and the third quartile, which contains 50% of the values. The whiskers extend from the box to the highest and lowest values, excluding outliers.

Spatial distribution

The spatial distribution of trends in annual precipitation is plotted in Figure 17. Monthly plots can be found in Appendix B. On an annual basis, increasing trends were dominate in the central basin for both data sets, but the spatial extent of upward trends for the Environment Canada was much smaller. There were more than 65% of areas showing increasing trends in the ECMWF data set compared to only 25% for the Environment Canada data set. It is also apparent that annual precipitation for Environment Canada data set contains both significant upward and downward trends; only significant upward trends were observed for the ECMWF data set. There were other substantial spatial variabilities in the precipitation trends between the two data sets. In general, for the Environment Canada data set,

- 1) monthly mean precipitation has increased in some areas but decreased in other areas
- 2) positive trends are usually clustered in the central and northern basin
- 3) positive trends always clustered along the border of the Bear and Liard Sub-basins near

the west side of the Slave Sub-basins

- 4) more negative trends have been detected than for the ECMWF data set; these negative trends usually clustered in the southern basin and in the northern Bear Sub-basin on the northwest side of the Great Bear Lake
- 5) the southern basin is characterized by decreasing precipitation amount during winter
- 6) Summer precipitation was increasing in the central basin (Liard, Bear, and Slave Sub-basins)

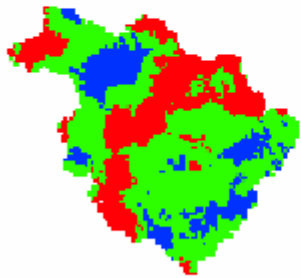
While the ECMWF data set

- 7) generally has less temporal coherence than the Environment Canada data
- 8) has more significant positive trends detected
- 9) has significant increases of summer precipitation amount that extended from the west side of the three large lakes to the west-end side of the basin
- 10) contains statistically significant trends only in upward direction from March to November.

Trends for precipitation 1961-2002

Environment Canada

Annual



Significant
Negative Trend



No
Significant Trend



Significant
Positive Trend

ECMWF

Annual



Figure 17 Spatial distribution of significant ($p=0.1$) annual precipitation trends

6.1.3 Runoff

Regional trend

Table 5 presents results for the regional runoff trends. There are large disagreements between the two data sets, both in terms of magnitude as well as direction. Runoff from the Environment Canada data set, for instance, has a range of median regional slope values from -0.19 to 0 mm/year while the ECMWF data set has the range from 0 to 1.23 mm/year. Regionally trends were field significance in all months for the Environment Canada data set. The ECMWF data set, on the other hand, are only field significance in spring, summer and autumn.

From the Environment Canada data set it is apparent that the regional runoff trend was generally decreasing, particularly in the summer months of May and June and autumn months of September to November. Yet, the ECMWF record has the greatest statistically significant regional runoff trend increase for the same months. The large disagreements between regional slope values for each month have accumulated to an even larger disagreement between the two annual regional slope values. The regional annual runoff has significantly decreased by about 8 mm for the Environment Canada record, as opposed to the significant regional increase of 50 mm for the ECMWF record. In the Environment Canada record, most of the regional monthly mean runoff trend magnitudes are equal to zero, but all monthly trends are field significant at the 10% level. In the ECMWF record, the regional monthly mean runoff trend magnitudes are equal to zero from November to March, and most of these monthly trends are not field significant at the 10% level. Possible cases for obtaining zero (or near-zero) for the median regional trend magnitude includes

- 1) all (or large number of) local trend magnitudes over the entire region equal (or nearly equal) to zero; and
- 2) upward trends cancel downward trends in the calculation of the median regional trend magnitude.

The two cases can be distinguished by assessing the critical value for the fraction of sites exhibiting a significant trend. This approach has been incorporated in this analysis and is described in Chapter 3 and by Burn and Hag Elnur (2002). In the Environment Canada data set, the regional monthly runoff trend magnitudes that are equal to zero, are also field significant at the 10% level. This situation is categorized to Case 1. Case 1 does not necessarily mean the

local trend is insignificant. Since most of the surface runoff is locked in solid form of ice, the baseline winter runoff is relatively small. Thus, small absolute changes in the runoff trend represent large relative changes in runoff during winter.

Table 5 Summary of trend analyses using the MK test for Runoff (mm/year)

	Environment	
	Canada	ECMWF
Jan	0.00 (0.00)	0.00 (0.01)
Feb	0.00 (0.00)	0.00 (0.00)
Mar	0.00 (0.02)	0.00 (0.05)
Apr	0.00 (0.05)	0.10 (0.23)
May	-0.18 (-0.19)	0.12 (0.15)
Jun	-0.04 (-0.04)	0.18 (0.19)
Jul	0.00 (0.03)	0.25 (0.27)
Aug	0.00 (0.02)	0.15 (0.18)
Sep	0.00 (0.00)	0.11 (0.15)
Oct	0.00 (-0.02)	0.08 (0.08)
Nov	0.00 (0.00)	0.01 (0.02)
Dec	0.00 (0.00)	0.00 (0.01)
Ann	-0.19 (-0.11)	1.23 (1.32)

Note: Entries in bold indicate results that are field significant at the 10% level. The numbers on the left represent the median trend magnitude, and the numbers in bracket represent the average trend magnitude. Positive values indicate increasing trends and negative value indicate decreasing trends.

Situations similar to the regional trend magnitude of the ECMWF data set where regional trend magnitude equal to zero but are not field significant, are categorized to Case 2. The two cases can also be distinguished or confirmed using plots of trend magnitudes and spatial pattern of trends over the entire region.

Regional variability of the estimated trend

Box plots of magnitude of the slope for the 4667 grid squares are depicted in Figures 18 and 19, to determine the regional variability of the estimated trend magnitude over the entire basin. The monthly comparison plots are illustrated in Appendix A.

The findings from the two data sets are almost opposite. For the Environment Canada data set, it was found that

- 1) the decrease in median regional trend magnitude was getting larger from April to May and getting smaller from May to June (Figure 20);

- 2) among the four seasons, the variability of slope values were usually wider in range during summer and autumn;
- 3) the variability of slope was also usually larger than from the ECMWF data set during summer and autumn;
- 4) the median trend magnitude were always the same as or lower than from the ECMWF data set; and
- 5) a preponderance of decreasing trends in the summer months, particularly the decreasing trend in May at over 60% of areas, contributed the most to the negative trend in regional annual runoff.

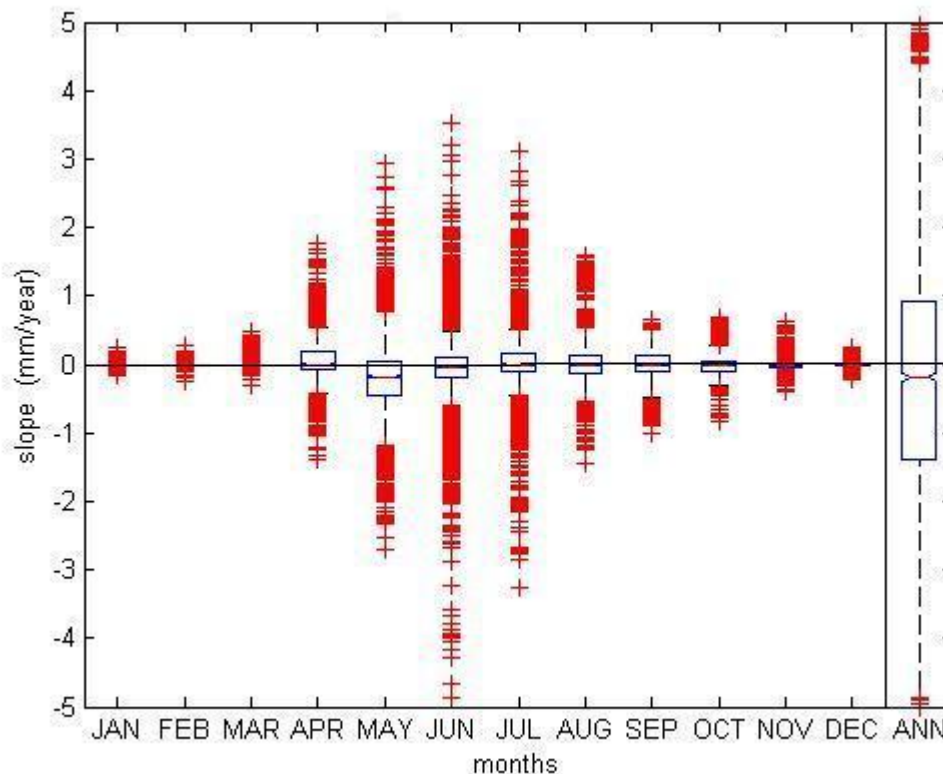


Figure 18 Environment Canada – Box plots of 4667 estimated trend magnitude for every month and for the annual runoff records

Note: The boxes show the first quartile, median, and the third quartile, which contains 50% of the values. The whiskers extend from the box to the highest and lowest values, excluding outliers

For the ECMWF data set, it was found that

- 1) the increase in median regional trend magnitude was getting larger from April to July and getting smaller from July to November (Figure 20);

- 2) among the four seasons, the variability of slope values were usually wider in range during spring and summer;
- 3) the variability of slope was usually larger than from the Environment Canada data set during spring and winter; and
- 4) the seasonal pattern of change generally follows the pattern of change in precipitation, with over 75% of areas showing increasing trend from April to November.

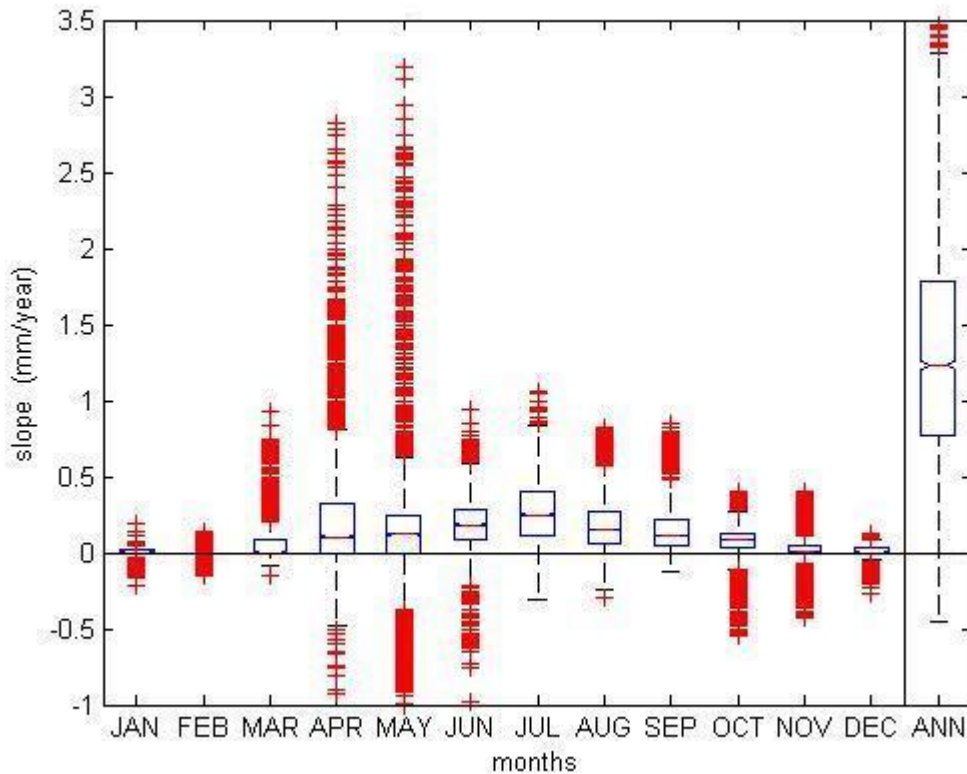


Figure 19 ECMWF – Box plots of 4667 estimated trend magnitude for every month and for the annual runoff records

Note: The boxes show the first quartile, median, and the third quartile, which contains 50% of the values. The whiskers extend from the box to the highest and lowest values, excluding outliers.

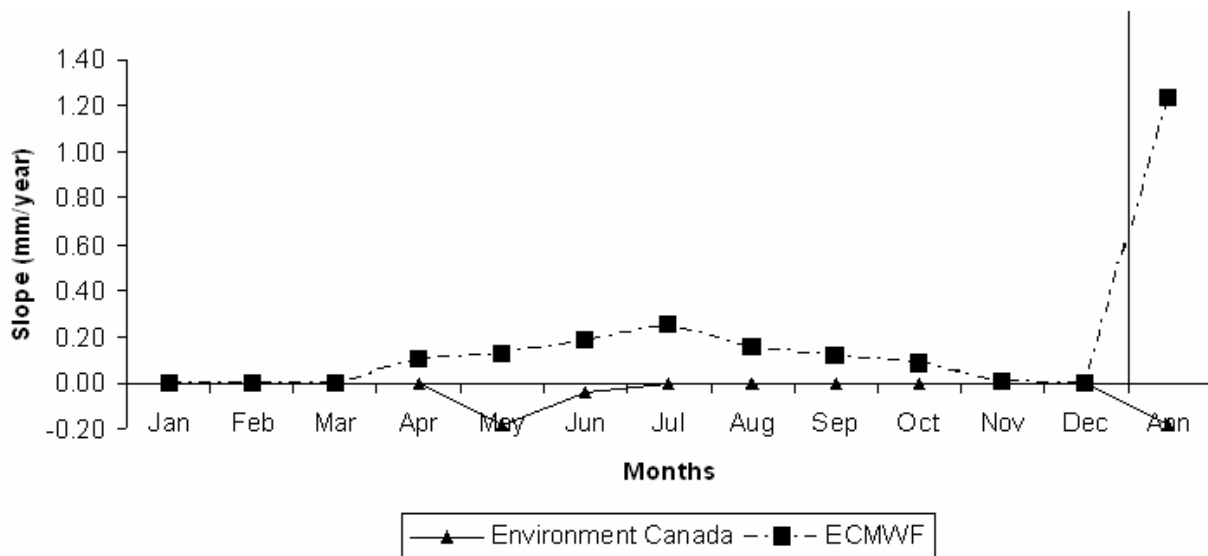


Figure 20 Plots of regional median trend magnitude for runoff records

Spatial distribution

The spatial distribution of trends in annual runoff is displayed in Figure 21. Note that there were significant positive and negative trends for the Environment Canada data set but only significant positive trends were detected for the ECMWF data set. There were around 65% of areas showing increasing trends in the ECMWF data set and 25% for the Environment Canada data set. The central basin generally showed positive trends for both data sets, with the larger spatial extent for the ECMWF data set.

The trends in runoff reflected changes in precipitation and temperature observed over the same periods. The runoff pattern broadly followed the precipitation pattern from July to November. Time lag between the changes in mean monthly precipitation and mean monthly runoff were not observed from the plot of spatial distribution. Yet, the pattern of change in runoff was generally larger in spatial extent for the ECMWF data set, and smaller for the Environment Canada data set compared to that of the precipitation pattern. The spatial pattern of annual runoff also follows the spatial pattern of annual precipitation, with ECMWF data set followed more closely with each other. The significant increases of temperature in March probably have caused earlier onset of snowmelt and melting of glacier, which contributed to significant increases in runoff, in the southeast part of the basin in the extensive glaciated Canadian Shield for the ECMWF data set. The increases of March temperatures in other northern areas in the basin, however, are

probably still not above the point that would cause significant increases of melting. This point was eventually reached by April and caused significant increases of runoff in other regions that are significantly glaciated, such as the mountain chains in the northwest and the west-central portion of the basin. The pattern of change in October runoff also follows the pattern of change in October temperature for the Environment Canada data set. However, an interesting pattern was observed for this month. Below latitudes of approximately 58°, decrease in temperature causes decrease in runoff. For the regions to the north, decrease in temperature causes increase in runoff.

Monthly plots can be found in Appendix B. There is obvious temporal coherence for only a few of the months. For each data set, the trends in the winter months were similar in spatial pattern, with a large number of upward trends in the north-central part of the basin, where the main contribution of runoff are from the mountain chains on the west. The summer, June and July, showed a cluster of upward trends in and near the Alberta Plateau for the ECMWF record, but the spatial extent of upward trends in June was much smaller. The summer months of May and June for the Environment Canada record consist of large number of sites with significant decreasing trend. The majority of these trends were located at areas where increasing April runoff have also been observed. This observation suggests that the decreasing trend in early-summer is probably linked to the reducing snowmelt process that used to occur more frequently in this month in the past.

Trends for runoff 1961-2002

Environment Canada

ECMWF

Annual

Annual

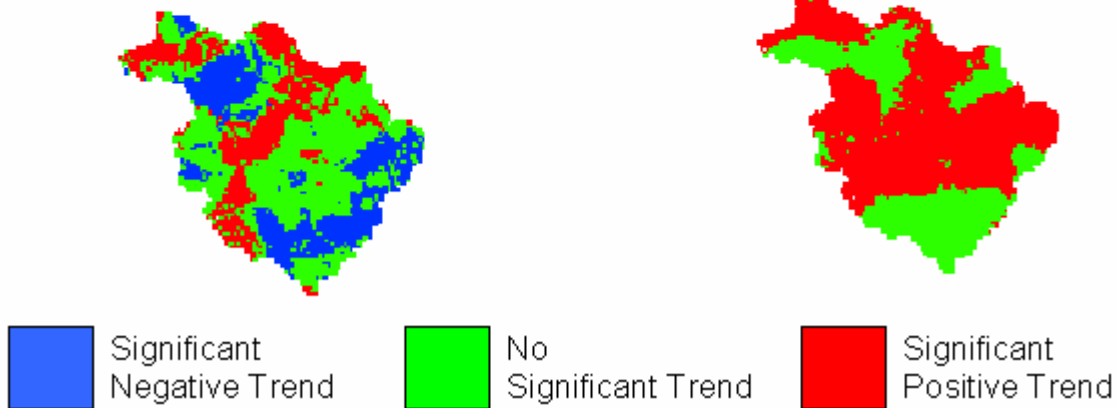


Figure 21 Spatial distribution of significant (p=0.1) annual runoff trends

Similar to the spatial pattern of precipitation, monthly mean runoff for most of the months for the Environment Canada data set always has few obvious clusters. There are sparse clusters of negative trends in the southern part of the basin (the southern Peace and the Athabasca Sub-basin) and in the northern Bear Sub-basin on the northwest side of Great Bear Lake. Another cluster of positive trends were observed along the Liard River at the mouth.

6.1.4 Evapotranspiration

Regional trend

In both data sets, evapotranspiration has generally increased in the MRB from 1961 to 2002 (Table 6). These increasing trends were statistically significant from March to September for both data sets, with most pronounced positive regional trends in the summer months of May to August. The regional increase during summer is well over 4.5 mm and 7 mm during the study period for the Environment Canada and the ECMWF data set, respectively, followed by autumn with regional increase of less than 1 mm for both data sets. Over the study period, the regional annual evapotranspiration increased at 21 mm and 31.5 mm per 42 years for the Environment

Canada and the ECMWF data sets, respectively.

From the results in Table 6, the seasonal pattern of the regional trend for both data sets is similar. However, when comparing the results of both data sets, all increasing regional trends for the Environment Canada data set are weaker. Moreover, the regional increasing trends in the winter months for the Environment Canada data set are also field significance. The greatest regional increase is in May for the Environment Canada data set (by about 5.73 mm) and in July for the ECMWF data set (by about 8.4 mm).

Table 6 Summary of trend analyses using the MK test for Evapotranspiration (mm/year)

	Environment	
	Canada	ECMWF
Jan	0.00 (0.00)	0.00 (0.00)
Feb	0.00 (0.00)	0.00 (0.00)
Mar	0.00 (0.01)	0.00 (0.01)
Apr	0.00 (0.03)	0.03 (0.05)
May	0.14 (0.13)	0.17 (0.17)
Jun	0.10 (0.12)	0.18 (0.18)
Jul	0.12 (0.14)	0.20 (0.23)
Aug	0.08 (0.09)	0.13 (0.14)
Sep	0.05 (0.06)	0.07 (0.07)
Oct	0.00 (-0.01)	0.00 (0.01)
Nov	0.00 (0.00)	0.00 (0.01)
Dec	0.00 (0.00)	0.00 (0.00)
Ann	0.50 (0.59)	0.75 (0.83)

Note: Entries in bold indicate results that are field significant at the 10% level. The numbers on the left represent the median trend magnitude, and the numbers in bracket represent the average trend magnitude. Positive values indicate increasing trends and negative value indicate decreasing trends.

Regional variability of the estimated trend

Figures 22 and 23 present box plots that compare the monthly and annual evapotranspiration trend slopes for the Environment Canada and the ECMWF data set, respectively. The monthly comparison plots are illustrated in Appendix A. It is apparent that the median slopes for the Environment Canada data set are always slightly lower than for the ECMWF data set and both are positive. Also note that the 25 percentile for both annual evapotranspiration is above zero, indicating a preponderance of increasing trends. The figures also indicate that there are more positive slopes detected from the ECMWF data set than for the Environment Canada data set, with over 85% of sites above zero. In general, the variability of slope values is larger during

summer and smaller during winter for both data sets. However, there is usually wider range of slope values for the Environment Canada data set than for the ECMWF data set, with the exception in spring months of March and April.

One interesting feature is that the seasonal pattern of the regional trends was of similar shape and direction as those for precipitation for both data sets. This result is physically reasonable because evapotranspiration depends on the availability of both energy and water (Louie *et al.*, 2002). Walsh *et al.* (1994) also found that the estimated evaporation had the same phase as that of precipitation. The possible reasons for obtaining this result may include:

- 1) the availability of water (i.e. the amount of precipitation) is a limiting factor, where when precipitation is less than potential evapotranspiration, the maximum actual evapotranspiration is limited by the amount of precipitation. Thus evapotranspiration increases when precipitation (the availability of water) increases;
 - For example, Nijssen *et al.* (2001) reported that evapotranspiration responds strongly to increasing precipitation in the MRB during summer because without a simultaneous increase in precipitation less water remains in storage and moisture stress is increased
- 2) the actual evapotranspiration is limited by moisture supply to the plant (Bedient and Huber, 2002: 46); and
 - water supply largely controls transpiration by affecting stomatal aperture (Raschke and Köhl, 1969)
 - precipitation increases the amount of moisture supply to vegetation, and thus increases transpiration
- 3) the amount of water vapor increases due to increasing regional evapotranspiration may lead to increasing precipitation within the basin. Thus the seasonal pattern of the regional precipitation follows the seasonal pattern of the regional evapotranspiration
 - For example, Cao *et al.* (2002) reported that during June of 1995, more of the moisture supply for precipitation came from the basin itself through evaporation or evapotranspiration than from outside the basin through advection
 - Cao *et al.* (2002) also cited a study conducted for some other water years in the MRB by Stewart *et al.* (1998), which also reported a similar finding

However, the spatial pattern of these two variables (evapotranspiration and precipitation) may still vary even though the seasonal patterns follow each other.

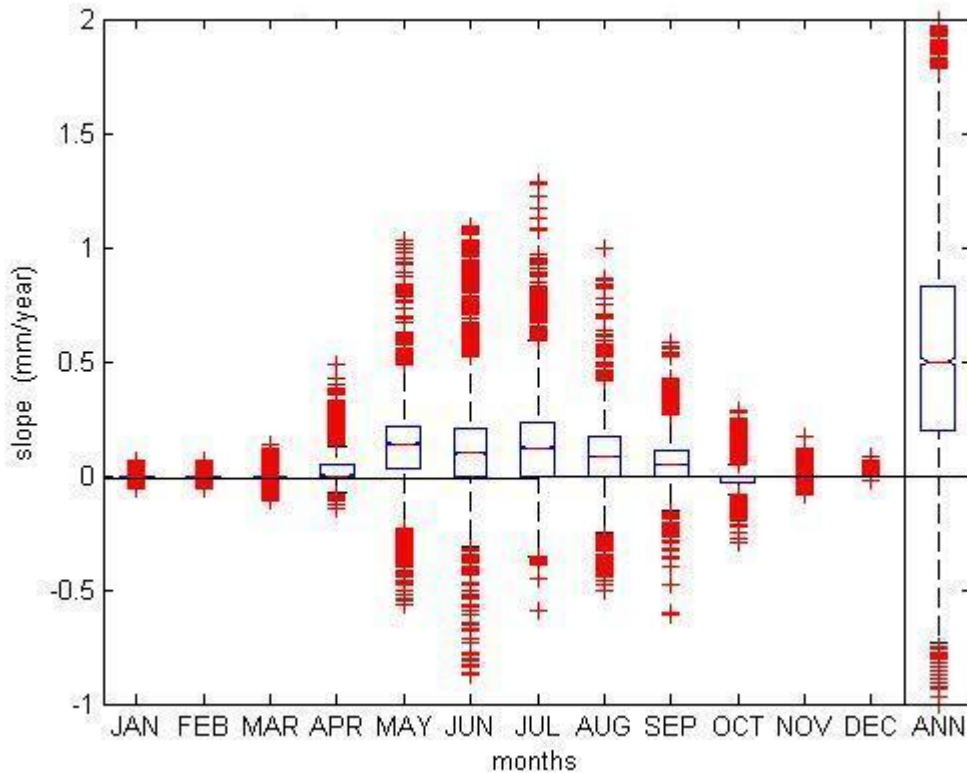


Figure 22 Environment Canada – Box plots of 4667 estimated trend magnitude for every month and for the annual evapotranspiration records

Note: The boxes show the first quartile, median, and the third quartile, which contains 50% of the values. The whiskers extend from the box to the highest and lowest values, excluding outliers

Spatial distribution

Figure 24 and Appendix B show maps with the trends in evapotranspiration from 1961 to 2002. Some clusters of downward trend were observed from the Environment Canada data set but none from the ECMWF data set. The spatial distribution between evapotranspiration and temperature was similar in most of the months, but the spatial extent of upward trends for temperature was usually larger. However, the spatial extent for the summer evapotranspiration is larger than that of temperature. This finding is not surprising since evapotranspiration is calculated according to Eq. 17 is based mainly on temperature, humidity and total incoming solar radiation. During the winter, spring and autumn months, variations in evapotranspiration depend primarily on the temperature changes. While there are increased amounts of incoming solar radiation in the

summer months over the basin (Voisin *et al.*, 2002) and thus increases in the latent heat flux for evapotranspiration, incoming solar radiation becomes another major driving force for evapotranspiration during the summer months. Therefore, the increasing trends for summer evapotranspiration are usually larger in spatial extent than that for summer temperature.

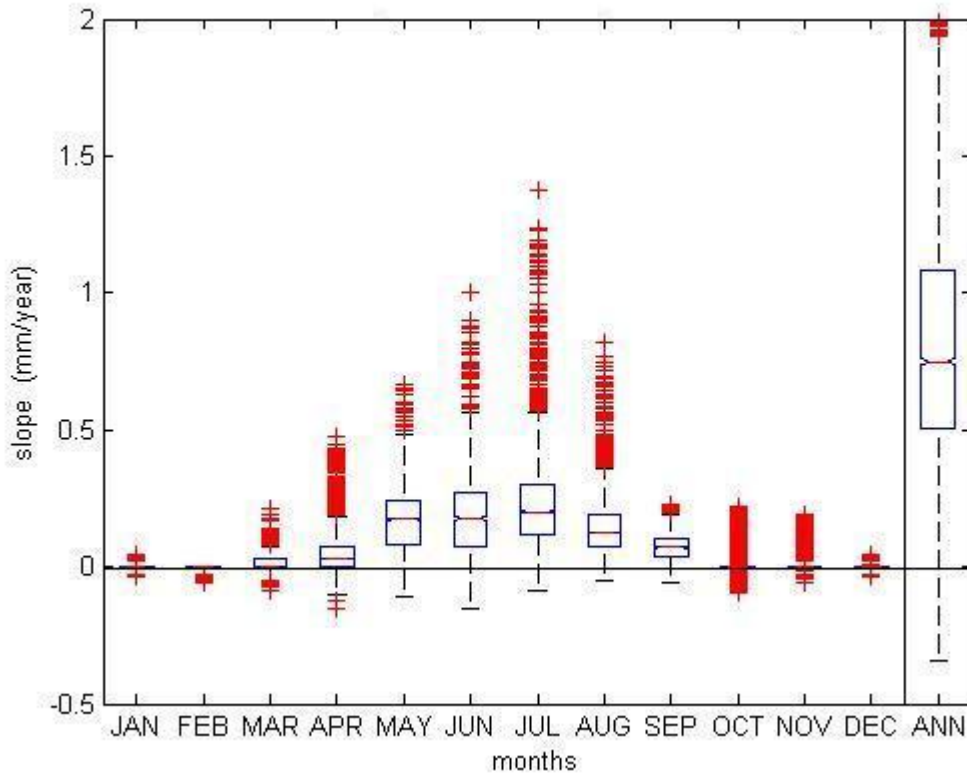


Figure 23 ECMWF – Box plots of 4667 estimated trend magnitude for every month and for the annual evapotranspiration records

Note: The boxes show the first quartile, median, and the third quartile, which contains 50% of the values. The whiskers extend from the box to the highest and lowest values, excluding outliers.

There is also evidence of some spatial coherence observed between the precipitation and evapotranspiration from the plots. Their spatial patterns followed closely with each other mainly during May to September. Time lag between the changes in mean monthly precipitation and mean monthly evapotranspiration were not observed from the mean monthly plot of spatial distribution.

Geographically, the pattern of trends from both data sets was similar in most of the months. It can be observed from Appendix B that the increasing trends during winter appear most dominant

in the east side of the Mackenzie River in the Northwest Territories, which covers the two large lakes (Great Bear Lake and Great Slave Lake). In early-spring of March, the increasing trends were clustered in the boreal and subarctic forest, and the southeast part of the basin. This may be due to the earlier beginning of the growing season inducing increased transpiration in the forested area. In April, increasing evapotranspiration was observed in the southern part of the basin. This result may suggest that the growing season of the prairie grassland, which used to occur in a later month in the past, switched earlier in April. Following in the summer months, the increasing evapotranspiration was most pronounced in the west side of the Mackenzie River. The greatest spatial extent is in July, with over 40% of sites and 65% of sites showing a significant increasing trend for the Environment Canada and the ECMWF data sets, respectively. The cluster of increasing trends in September has switched back to the east of the basin. They were dominated in the Peel, the Bear, and the northern Slave Sub-basins. The preponderance of upward trends in all months has led to large spatial extent of significant increasing trend in annual evapotranspiration.

Trends for evapotranspiration 1961-2002

Environment Canada

ECMWF

Annual

Annual

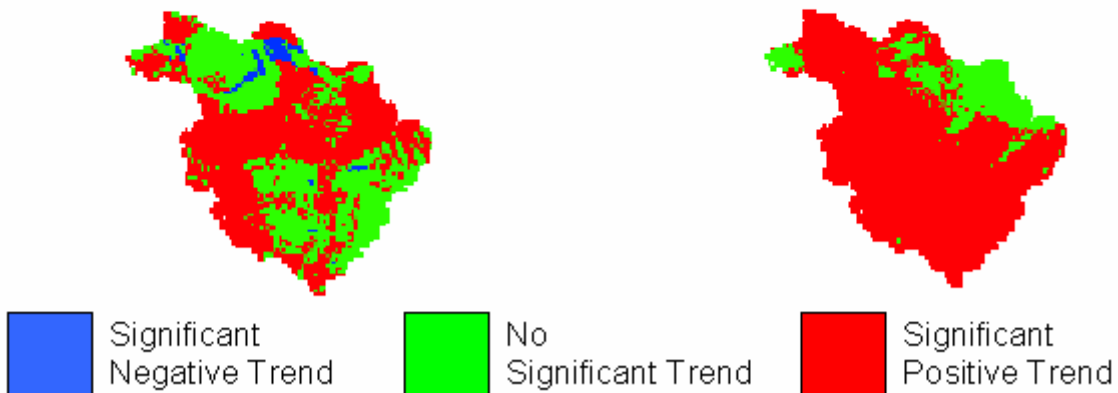


Figure 24 Spatial distribution of significant ($p=0.1$) annual evapotranspiration trends

6.1.5 Storage

Regional trend

The regional trend magnitudes for annual cumulative storage are displayed in Table 7. The annual storage for Environment Canada data set exhibits a regional significant decreasing trend of 7.88 mm per 42 years while the ECMWF data set exhibits a regional increasing trend of 18.82 mm per 42 years. For the Environment Canada data set, the observed increase in basin-averaged annual precipitation was compensated by strong increase in regional annual evapotranspiration, resulting in decreases in both regional annual runoff and storage. The regional residual for the changes in water balance over the 42-year period calculated from Eq. 1 (P-E-Q-S) is 0.017 mm/year. For the ECMWF data set, the observed increase in basin-averaged precipitation was compensated by increases in both runoff and evapotranspiration. The regional residual for the changes in water balance over the 42-year period is -0.431 mm/year. This residual is a combination of errors in the four water balance components and the imperfection in trend detection.

Table 7 Summary of trend analyses using the MK test for Storage

	Environment	
	Canada	ECMWF
Ann	-0.19 (0.14)	0.45 (0.47)

Note: Entries in bold indicate results that are field significant at the 10% level. The numbers on the left represent the median trend magnitude, and the numbers in bracket represent the average trend magnitude. Positive values indicate increasing trends and negative value indicate decreasing trends.

Regional variability of the estimated trend

Figure 25 presents box plots that compare the trend slopes for the annual storage from the Environment Canada data set and ECMWF data set. For the ECMWF data set, over 90% of sites have experienced the increasing storage of water. The 25 and 95 percentiles fall in the range between -0.23 and 1.18 mm/year. For the Environment Canada data set, on the other hand, over 60% of sites are below zero, indicating a preponderance of decreasing trend. However, its 95 percentile is above the 95 percentile for the ECMWF data set because the Environment Canada data set has wider range of slope values. The 25 and 95 percentiles for the Environment Canada data set fall in the range between -1.61 and 1.55 mm/year.

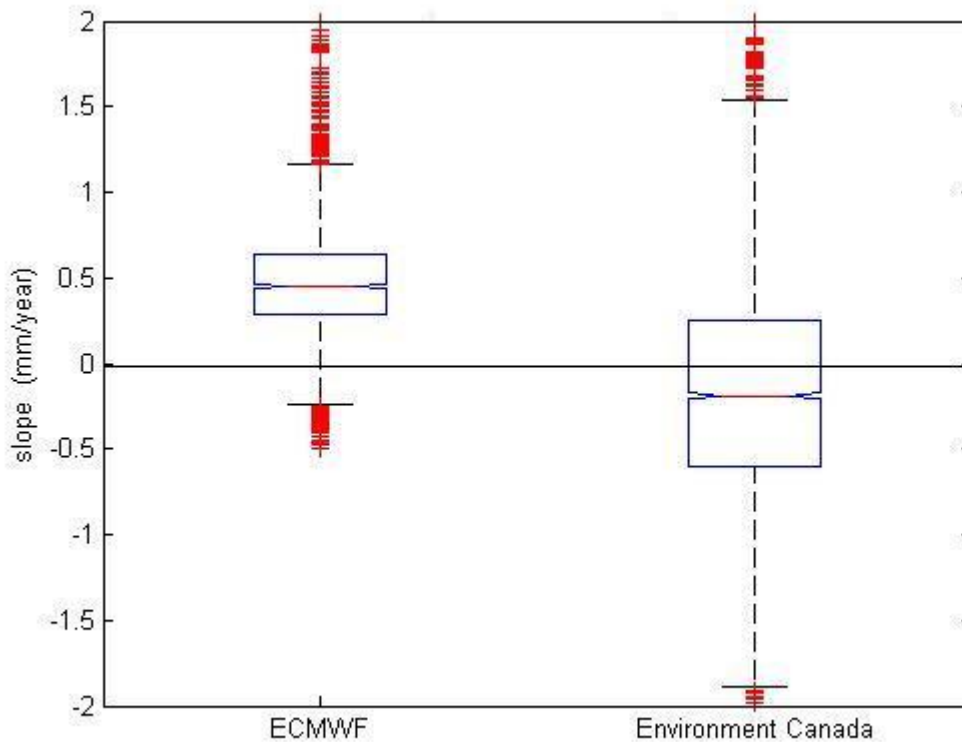


Figure 25 Box plots of 4667 estimated trend magnitude for the annual storage records
 Note: The boxes show the first quartile, median, and the third quartile, which contains 50% of the values. The whiskers extend from the box to the highest and lowest values, excluding outliers.

Spatial distribution

Geographically, the pattern of trends is quite different between the two data sets. Most of the significant trends detected from the Environment Canada data set are downward; less than 1% of sites have downward trends for the ECMWF data set. The general pattern is similar to that of annual runoff and annual precipitation. Yet, the spatial pattern of storage matched much better with annual runoff. The spatial extent for precipitation was usually larger than the annual runoff and annual storage.

For the Environment Canada data set, the decreasing trends were most pronounced in the Athabasca Sub-basin, and at Great Bear Lake and on the west side of Great Bear Lake in the Bear Sub-basin. For the ECMWF data set, regions that experienced the most widespread increases were the Peel Sub-basin, and in the west-central and central part of the basin. Also noteworthy is the reduced water storage in Great Bear Lake detected from both data sets.

Trends for storage 1961-2002

Environment Canada

ECMWF

Annual

Annual

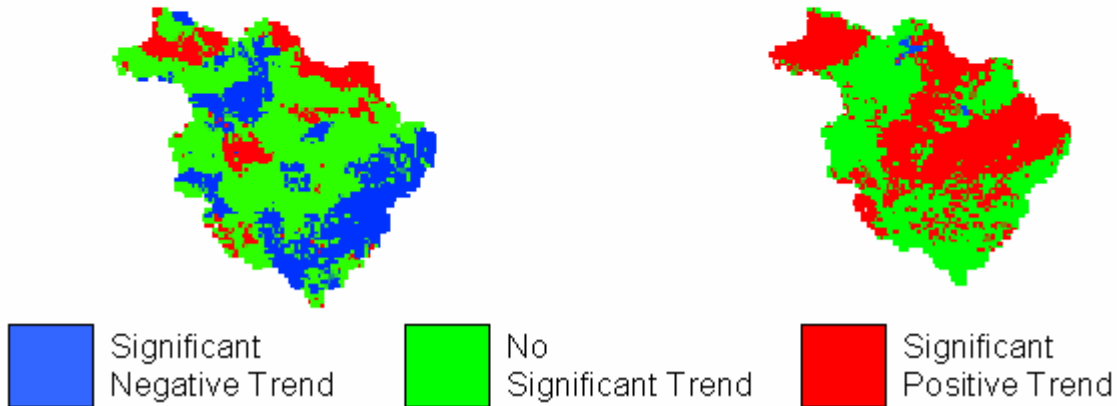


Figure 26 Spatial distribution of significant ($p=0.1$) annual storage trends

6.1.6 Summary of trend results

Table 8 and Figure 27 summarize the findings from the trend analysis. There are pronounced differences in the trend results between the two data sets. For the ECMWF data set, when a trend is detected, over 96% of the trends are increasing while the Environment Canada data set exhibits an increasing trend in about 76% of the cases where a trend is detected. The results are summarized in Table 8. Results that are field significant, at the 10% significance level, are shown in bold. For each variable, the values in the table give the percentage of areas that exhibited a locally significant trend (at the 10% significance level) while the signs indicate the direction of the trend. The table also shows the agreement and disagreement between trends in both data sets. From the results in Table 8, large number of significant increasing trends were detected in runoff in the spring and summer months of March to April and June to October from the ECMWF data set while there are mixes of increasing and decreasing trends from the Environment Canada data set. Temperature was significantly increasing during the winter months in both data sets. Precipitation and evapotranspiration were generally increasing,

Table 8

Summary of trends showing the percentage of grid squares with a trend that is significant at the 10% significance level

		Environment Canada		ECMWF	
	Month	Pos	Neg	Pos	Neg
runoff	Jan	17.9%	10.3%	26.3%	0.5%
	Feb	17.3%	6.8%	20.8%	1.1%
	Mar	25.7%	5.4%	34.8%	0.2%
	Apr	29.7%	9.5%	42.0%	0.0%
	May	11.1%	30.0%	9.1%	0.5%
	Jun	11.5%	12.6%	30.5%	0.0%
	July	17.3%	9.2%	50.8%	0.0%
	Aug	16.7%	8.0%	41.2%	0.0%
	Sep	21.6%	11.7%	46.0%	0.0%
	Oct	14.0%	25.8%	26.5%	0.1%
	Nov	16.8%	18.3%	15.6%	0.3%
	Dec	18.2%	13.7%	24.0%	0.4%
	Ann	24.4%	26.3%	64.1%	0.0%
precipitation	Jan	4.1%	34.4%	1.4%	4.3%
	Feb	7.2%	14.2%	9.7%	2.8%
	Mar	7.0%	14.5%	11.7%	0.0%
	Apr	3.4%	18.3%	6.6%	0.1%
	May	24.1%	1.1%	43.0%	0.0%
	Jun	11.3%	1.5%	35.3%	0.0%
	July	24.0%	4.0%	59.9%	0.0%
	Aug	18.0%	1.4%	28.5%	0.0%
	Sep	24.4%	4.6%	38.0%	0.0%
	Oct	5.5%	4.2%	17.7%	0.0%
	Nov	8.4%	15.9%	3.3%	0.0%
	Dec	7.3%	17.9%	0.0%	2.2%
	Ann	28.8%	16.0%	66.0%	0.0%
evapotranspiration	Jan	20.7%	5.9%	3.0%	7.5%
	Feb	16.0%	3.9%	1.8%	5.7%
	Mar	37.5%	0.2%	32.8%	1.1%
	Apr	26.0%	0.0%	32.5%	0.2%
	May	51.7%	0.0%	65.4%	0.0%
	Jun	33.7%	0.0%	51.2%	0.0%
	July	39.7%	0.0%	65.7%	0.0%
	Aug	31.9%	0.0%	36.6%	0.0%
	Sep	37.6%	0.0%	47.1%	0.0%
	Oct	20.9%	0.0%	1.6%	0.0%
	Nov	11.8%	0.7%	4.5%	0.0%
	Dec	20.6%	8.2%	1.7%	9.2%
	Ann	58.6%	0.0%	83.0%	0.0%
temperature	Jan	73.6%	0.0%	41.1%	0.0%
	Feb	65.3%	0.0%	30.4%	0.0%
	Mar	71.0%	0.9%	80.6%	0.0%
	Apr	47.1%	3.0%	47.6%	0.0%
	May	23.9%	4.3%	16.8%	0.0%
	Jun	50.1%	1.7%	30.3%	0.0%
	July	44.7%	1.2%	11.7%	0.0%
	Aug	17.6%	2.1%	0.0%	0.0%
	Sep	45.1%	1.1%	23.5%	0.0%
	Oct	5.4%	36.7%	0.0%	26.3%
	Nov	16.6%	0.5%	0.3%	0.0%
	Dec	57.2%	0.0%	0.0%	0.0%
	Ann	89.8%	1.2%	83.0%	0.0%
Storage	Month	Pos	Neg	Pos	Neg
	Ann	14.1%	28.8%	98.8%	1.0%

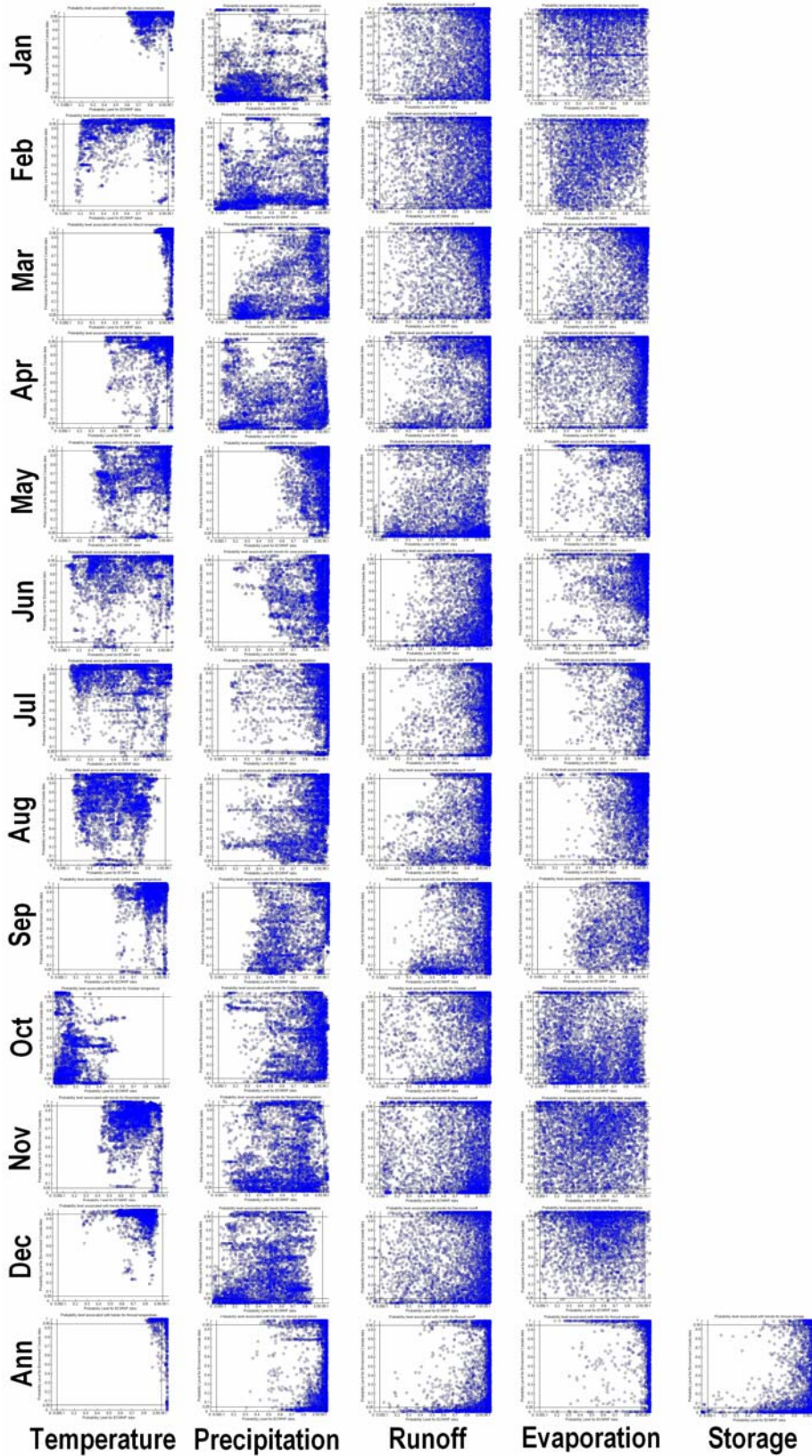


Figure 27 Probability level associated with trends for Environment Canada data set and ECMWF data set

Note: The x-axis represents the probability level for the ECMWF data set; the y-axis represents the probability level for the Environment Canada data set

particularly during the summer months. Also noteworthy is the significant increasing trend in the magnitude of the annual storage from the ECMWF data set but significantly decreasing from the Environment Canada data set.

Figure 27 is a plot of the probability level associated with the trend test for both data sets. A probability level of 0.05 or less indicates a decreasing trend, a probability level of 0.95 or greater indicates an increasing trend. Based on the 10% significance level, probability level between 0.05 and 0.95 indicates no trend.

An overall warming trend was observed with a high degree of confidence from 1961 to 2002. Mean monthly temperature records show a very apparent, strongly significant, positive trend, especially in the winter and early-spring months of December to March. Although their magnitudes of the warming were similar, the area with significant warming was much larger in early spring. From Figure 27, all the months, with the exception of the summer months and October, have large number of points clustered at the upper right-hand corner, indicating a large number of sites with significant or close to significant warming trend detected from both data sets. During summer, the points are scattered between 0.05 and 0.95 for both data sets, which indicates no obvious regional warming in general. The regional trend also indicates that temperature has increased the least in the summer months and was mainly clustered in the west-central portion of the basin. One contrary pattern was observed in October temperature. There were a relatively large number of sites (over 25%) with cooling trends in October; the majority of these sites are clustered in the southern basin.

A weak increase of precipitation was observed in the MRB. Figure 27 indicates a tendency toward increasing particularly during the summer months. One obvious cluster of statistically significant positive trends throughout the four seasons was observed around the border of Bear and Liard Sub-basins near the west side of the Slave Sub-basins. Although negative trends were also identified in some regions, particularly in the winter months, they were cancelled by the strong positive trends during summer, leading to overall increase in annual precipitation.

No conclusion can yet be made about the direction of the runoff trend. An overall decrease in

runoff was detected from the Environment Canada data set while an overall increase in runoff was detected from the ECMWF data set. In addition no general agreement can be found between the two data sets in Figure 27, except in March where a relatively large number of points clustered at the upper right-hand corner, implying an increasing trend in both data sets has been detected. The seasonal pattern in the regional trend of runoff was similar to that in the precipitation only for the ECMWF data set. Yet, the spatial pattern follows closely with the pattern of change in precipitation for both data sets. The effect of changes in precipitation is much more noticeable than that of change in temperature in most of the months, while the spatial distribution of runoff in spring (March) and autumn (October) was primarily affected by changes in temperature.

Evapotranspiration matched much better with temperature in terms of spatial distribution, but its seasonal regional pattern matched better with precipitation. The MRB has generally experienced increasing evapotranspiration, being most significant in the summer months from both data sets. Figure 27 also shows cluster of points at the upper right-hand corner. The variability of slopes values was also greater during summer, but with over 75% of sites showing increasing trends.

The graph for storage in Figure 27 is very similar to the graph for annual runoff. Moreover, the annual storage and annual runoff are very similar in terms of spatial distribution and direction of trends. These findings may suggest the two variables are positively correlated with each other or both of these variables are mainly affected by the change in precipitation.

Figure 28 summarizes the annual trends of each water balance component during 1961 to 2002. The regional residual for the changes in water balance over the 42-year period is stated in the middle of each figure.

The largest hydrological changes, in terms of magnitude, were manifested in the summer months of May to August. This is partly a result of the large increase in precipitation amount during that period. In addition, since most of the surface water is locked in solid form of ice and snow and the amount of energy available for evapotranspiration is limited in winter, a large change in a water balance component during winter represents only a small absolute change during summer.

Precipitation changes tend to be largest in winter for both data sets. Precipitation remained as the largest for all the other months in the ECMWF data set. For the Environment Canada data set, however, evapotranspiration changes were the largest in summer.

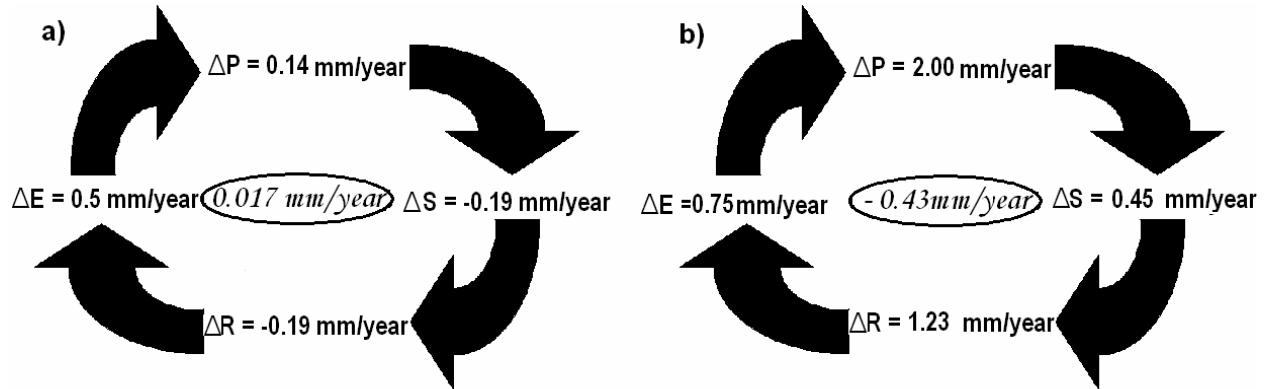


Figure 28 Summary of annual trends for each water balance component
a) Environment Canada and b) ECMWF

6.2 Climate elasticity

Regional climate elasticity

The precipitation elasticity of runoff (ϵ_P), the evapotranspiration elasticity of runoff (ϵ_{PET}), and the temperature elasticity of runoff (ϵ_T) are determined by Eq. 13. Table 9 summarizes the regional median climate elasticity of runoff over the entire basin. A value of >1.0 indicates that a 1% change in the climate variable can cause a $>1\%$ change in runoff. From the tabulated results, some general conclusions can be made:

- 1) Runoff was more sensitive to precipitation and less sensitive to temperature.
- 2) Runoff was positively correlated to precipitation and evapotranspiration; whereas runoff was negatively correlated to temperature.
- 3) The regional ϵ_P , ϵ_{PET} , and ϵ_T values from the ECMWF data set were stronger.

Table 9 Summary of the climate elasticity of runoff

	ϵ_P	ϵ_{PET}	ϵ_T
Environment Canada	1.275	0.872	-0.044
ECMWF	1.421	1.889	-0.173

The sensitivity of runoff to precipitation from the Environment Canada and the ECMWF data

sets is very similar (regional ϵ_P of 1.28 and 1.42, respectively). This result indicates a 1% change in regional precipitation results in a 1.28% and 1.42% change in regional runoff for the Environment Canada and the ECMWF data sets, respectively. Runoff was most sensitive to change in precipitation for the Environment Canada data set but it was most sensitive to change in evapotranspiration for the ECMWF data set.

The results for runoff change were -0.044% and -0.173% for every 1% increase in temperature. This behaviour indicates that any increases of glacier melt caused by increases in temperature were offset by losses due to evapotranspiration in the basin. Moreover, one interesting finding from Table 9 is that the regional runoff was changing along with the regional evapotranspiration for both data sets. This unexpected relationship may imply another variable, such as storage, lurking in the collective behaviour. Increases in soil moisture can cause more runoff generating in each grid due to less storage capacity to withhold meltwater and/ or rainfall (Woo and Marsh, 2005). It can also provide more soil moisture storage available for evapotranspiration (Douglas *et al.*, 2000).

Figures 29 to 31 present the box plots of the climate elasticity of runoff. The ϵ_P , ϵ_{PET} , and ϵ_T values from both data sets are very similar. It is apparent from Figure 29 that the relationships between precipitation and runoff were highly significant, with the five percentile above zero for both data sets. Over 90% of sites for the Environment Canada and the ECMWF data sets showed 0.4-2.15% and 0.76-2.11% change in mean annual runoff for every 1% change in mean annual precipitation, respectively. The results for ϵ_{PET} are 1.3-3.1 and -0.7-4.3, which were observed in over 90% of sites. For both data sets, the mean runoff was positively correlated to the mean annual evapotranspiration in over 75% of sites. Although runoff is less sensitive to temperature, the relationship found in a large number of sites (observed in 60% and 75% of sites for the Environment Canada and the ECMWF data sets, respectively) is a strong indication that such a relationship exists in the MRB.

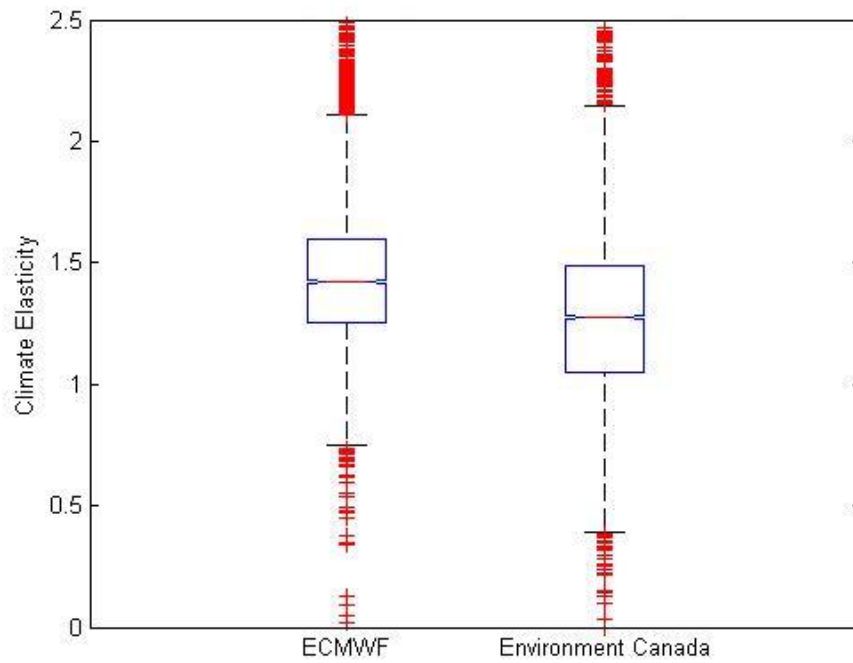


Figure 29 Box plots of 4667 estimated precipitation elasticity of runoff for the Mackenzie River Basin

Note: The boxes show the first quartile, median, and the third quartile, which contains 50% of the values. The whiskers extend from the box to the highest and lowest values, excluding outliers.

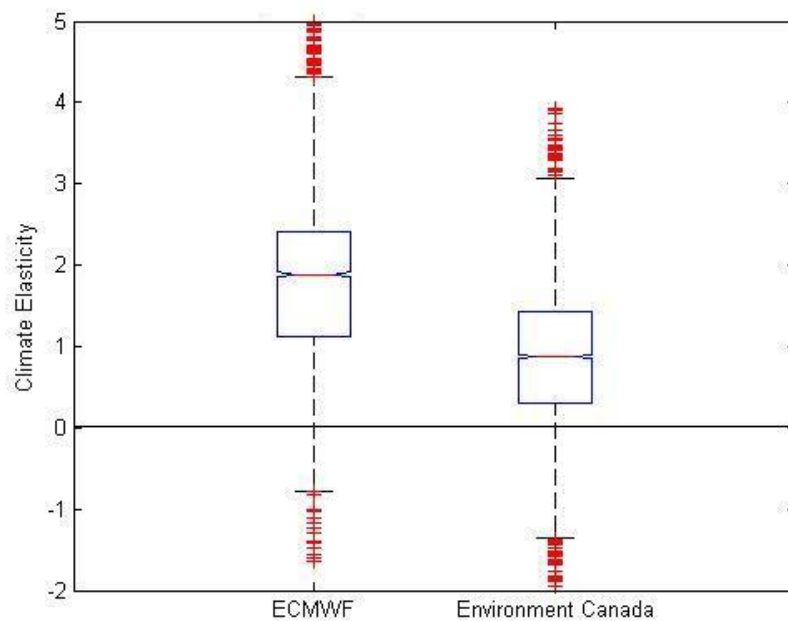


Figure 30 Box plots of 4667 estimated evapotranspiration elasticity of runoff for the Mackenzie River Basin

Note: The boxes show the first quartile, median, and the third quartile, which contains 50% of the values. The whiskers extend from the box to the highest and lowest values, excluding outliers.

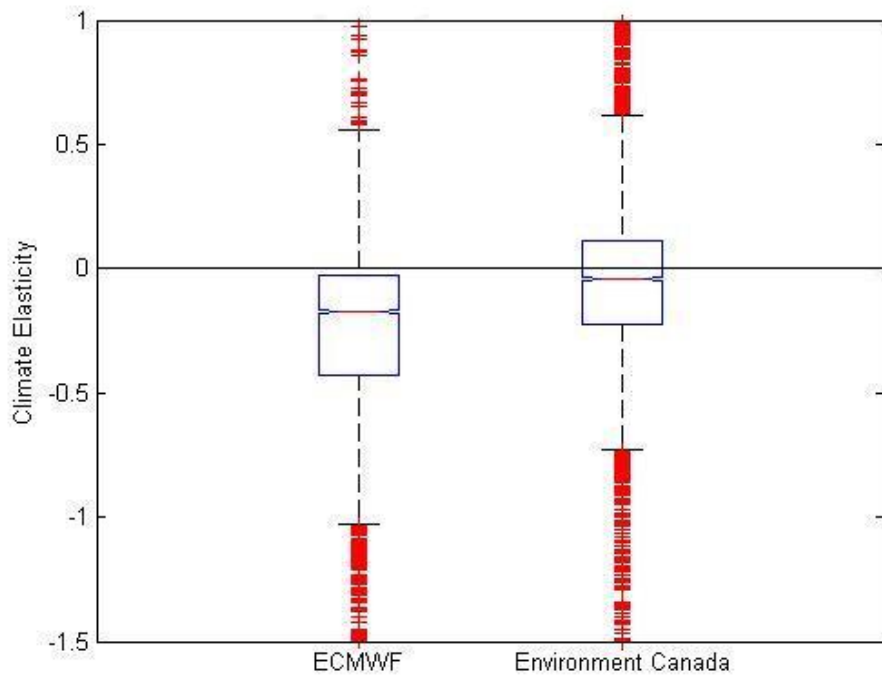
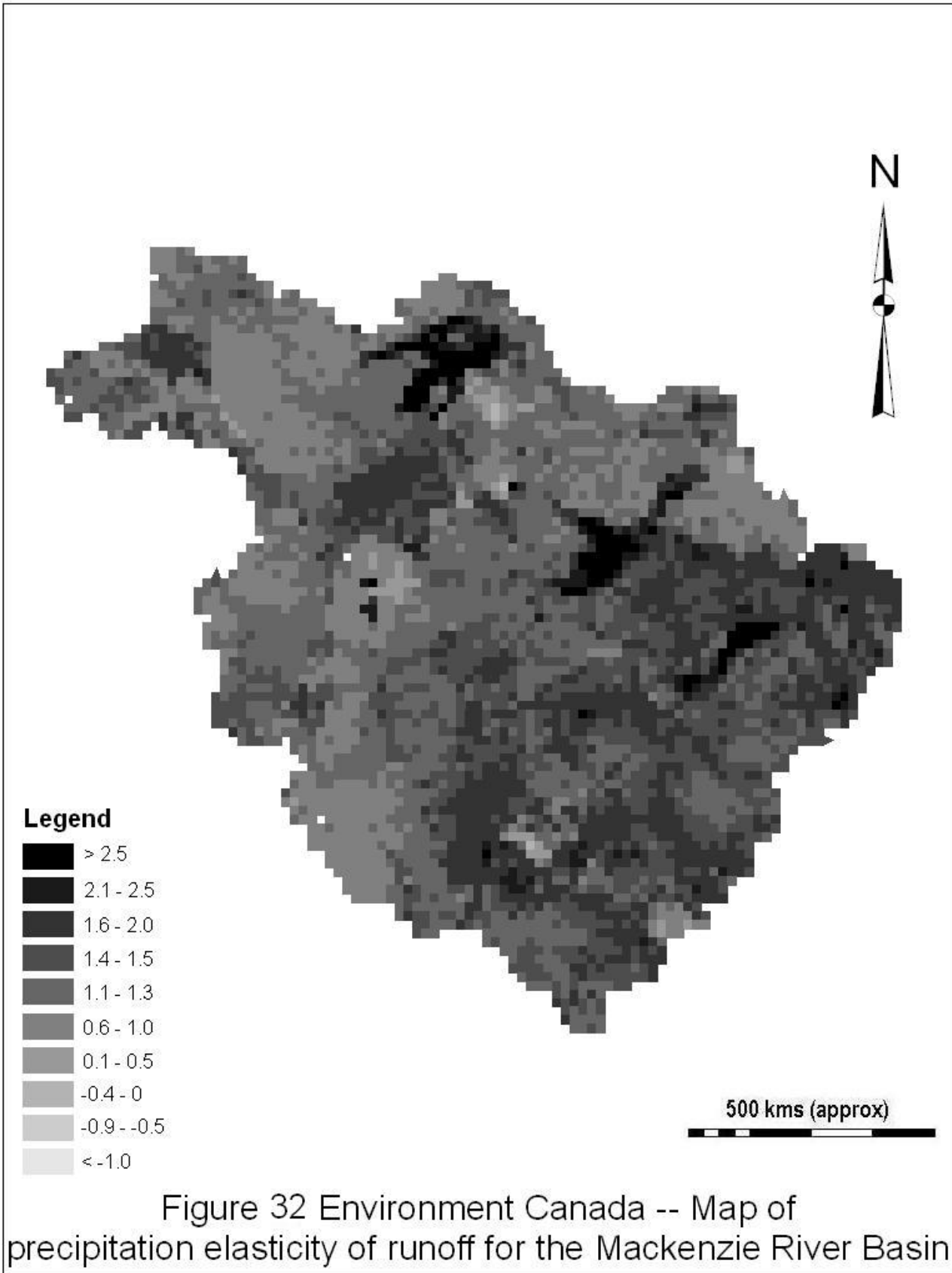


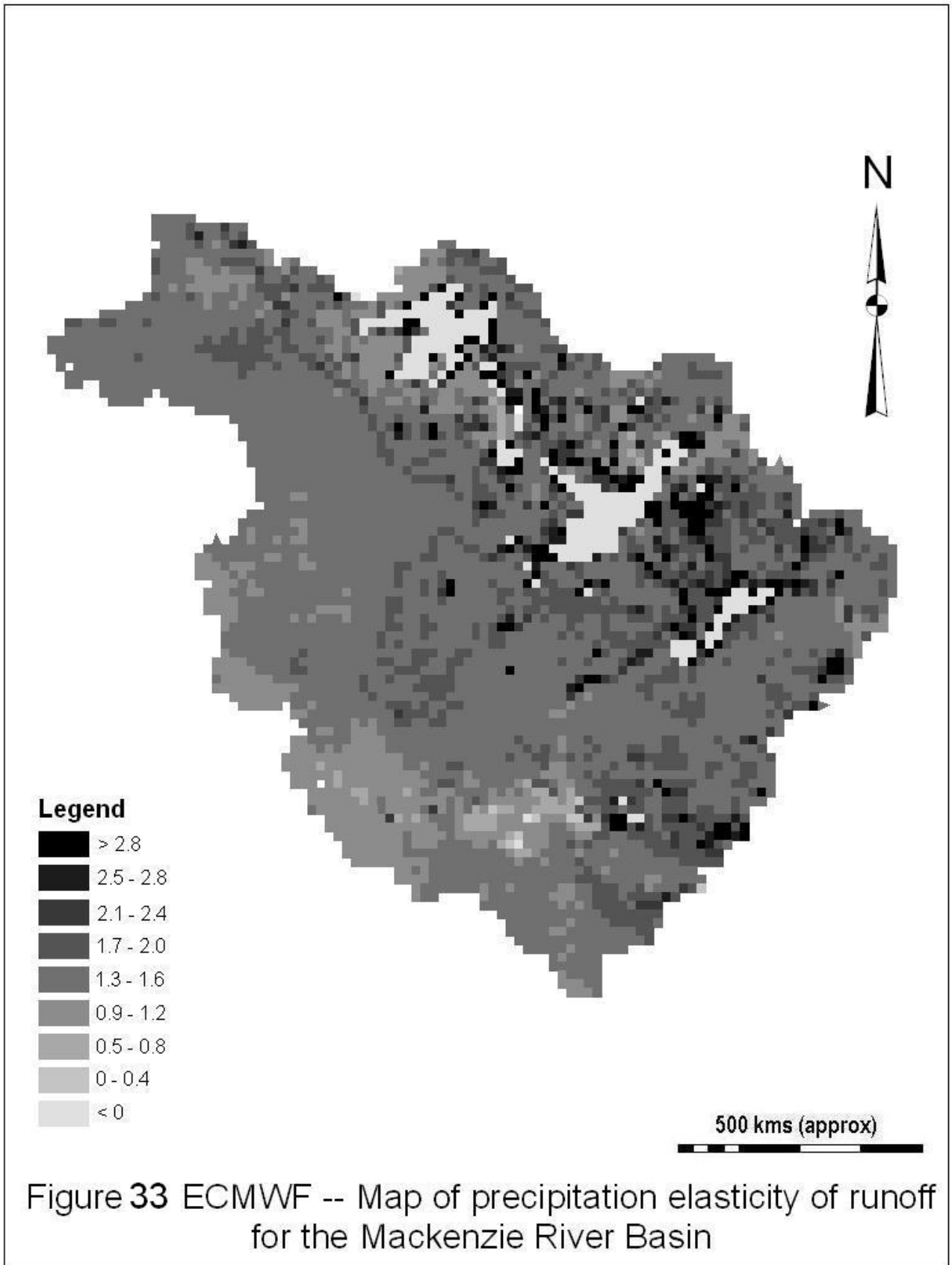
Figure 31 Box plots of 4635 estimated temperature elasticity of runoff for the Mackenzie River Basin

Note: The boxes show the first quartile, median, and the third quartile, which contains 50% of the values. The whiskers extend from the box to the highest and lowest values, excluding outliers.

Figures 32 and 33 illustrate maps of ε_P for the Environment Canada and the ECMWF data sets, respectively. The lakes and the areas around the lakes usually have extremely high absolute ε_P values. This behaviour may be due to the difficulties in obtaining runoff response in a grid with water land-cover type.

The ε_P values typically decrease from south to north in the Interior Plain. In Figure 32, it is apparent that the southern basin often consisted of larger values of ε_P ; they usually range from 1.6 to 2.2. The ε_P value on the Peel Sub-basin in the northern part of the basin, on the other hand, was usually much smaller; between 0 and 0.8 for the Environment Canada data set and between 1.2 and 1.6 for the ECMWF data set. The central zone of the basin usually has an intermediate ε_P value ranges from 1.2 to 1.6 for Environment Canada data set and 1.4 to 1.6 for the ECMWF data set.



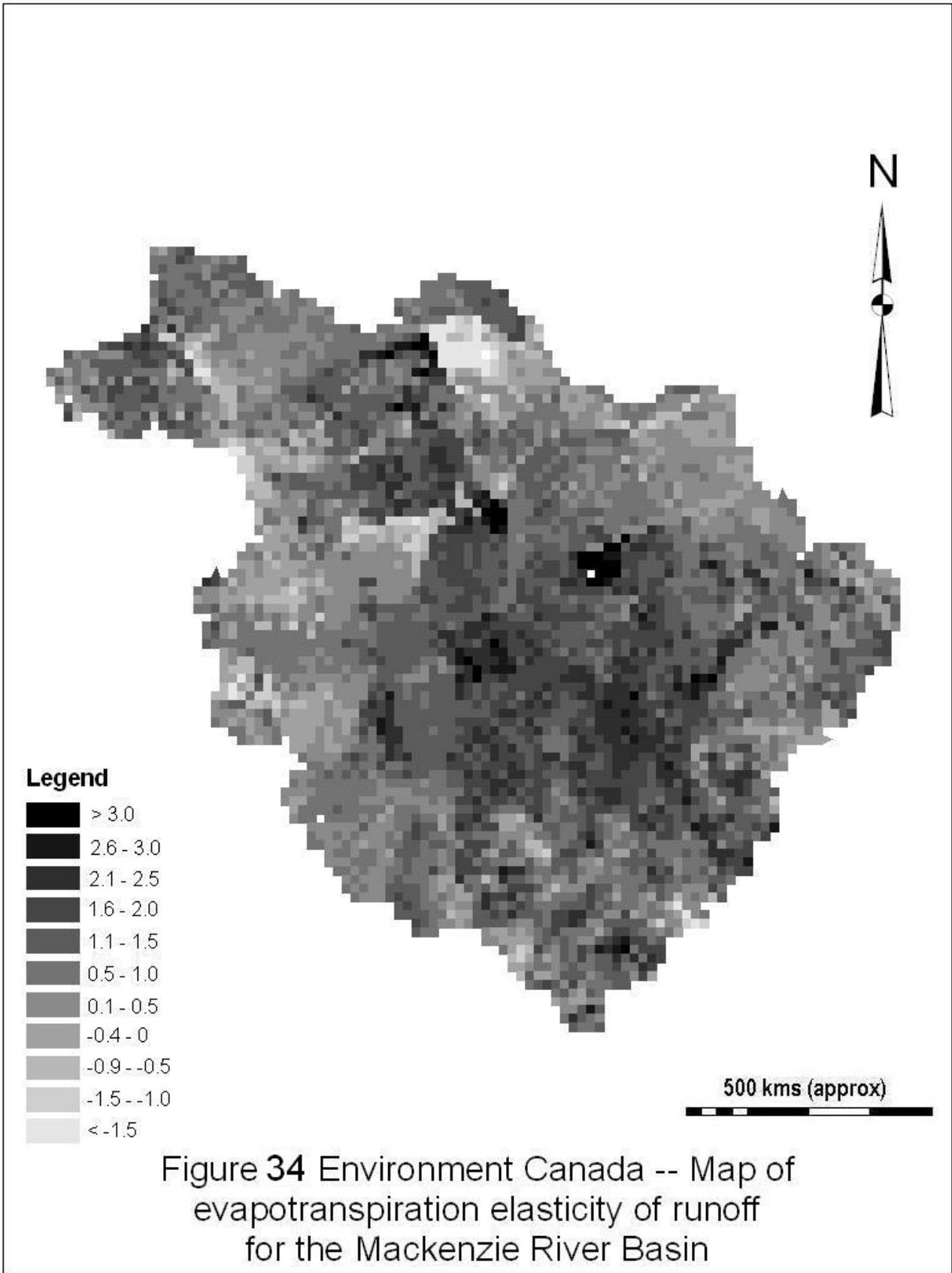


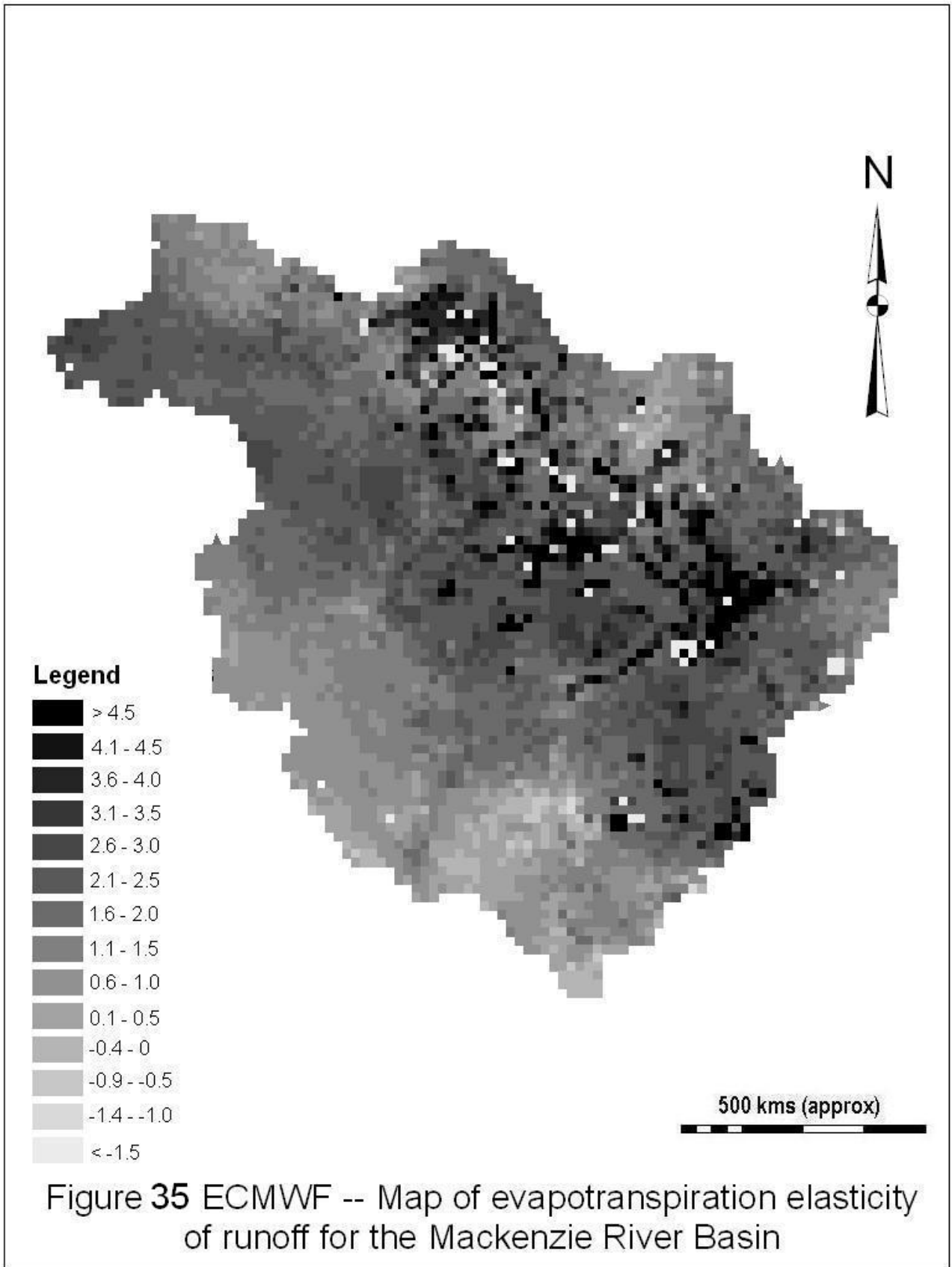
Along the Rocky Mountain chain on the west side of the basin was a region with lower ϵ_p . The ϵ_p values along the mountain chains typically range from 0.6 to 1.2 in the south and from 0.8 to 1.4 in the north for Environment Canada data set. For the ECMWF data set, the ϵ_p values range from 0.6 to 1.4 in the south and 1.2 to 1.4 in the north.

The ϵ_p value was quite varied on the Shield upland region in the east. For the Environment Canada data set, the ϵ_p values range from 0.6 to 1.2 in the Bear and the Slave Sub-basins and from 1.4 to 2.2 for the ECMWF data set. In the southeastern part of the basin, the ϵ_p values were typically larger. The ϵ_p values range from 1.6 to 2.2 for the Environment Canada data set and from 1.4 to over 4.0 for the ECMWF data set.

Figures 34 and 35 illustrate maps of ϵ_{PET} for the Environment Canada and ECMWF data sets, respectively. The ϵ_{PET} values were progressively increasing from the west to the central zone of the basin. Along the mountain chains in the west, the ϵ_{PET} values range from 0.8 to 1.0 for both data sets in the south, and from -0.8 to 0.6 for the Environment Canada data set and 2.0 to 3.0 for the ECMWF data set in the north. The greatest ϵ_{PET} was located on the east side of the Great Slave Lake in the central zone of the basin. The range of ϵ_{PET} values in this zone is 1.4-3 for the Environment Canada data set and 1.4-2.6 for the ECMWF data set. To the north of this zone was a region with relatively low ϵ_{PET} values, with ϵ_{PET} values of 0.4-1 for the Environment Canada data set and 0.8-1.4 for the ECMWF data set.

The spatial pattern of ϵ_p , ϵ_{PET} values in the Canadian Shield region was highly variable. The values of ϵ_{PET} in the southeastern part of the basin generally range from 0.2 to 1.6 and 1.0 to 1.8 for the Environment Canada and the ECMWF data sets, respectively. Areas to the north of this region generally have ϵ_{PET} values of 0 to 0.4 for the Environment Canada data. The values for the ECMWF data varied between 0-1.0 on the northeast side of the Great Slave Lake and 1.4-1.8 on the southeast side of the Great Slave Lake. To the east side of the Great Bear Lake, the range of ϵ_{PET} values was between 1.8 and 2.2.





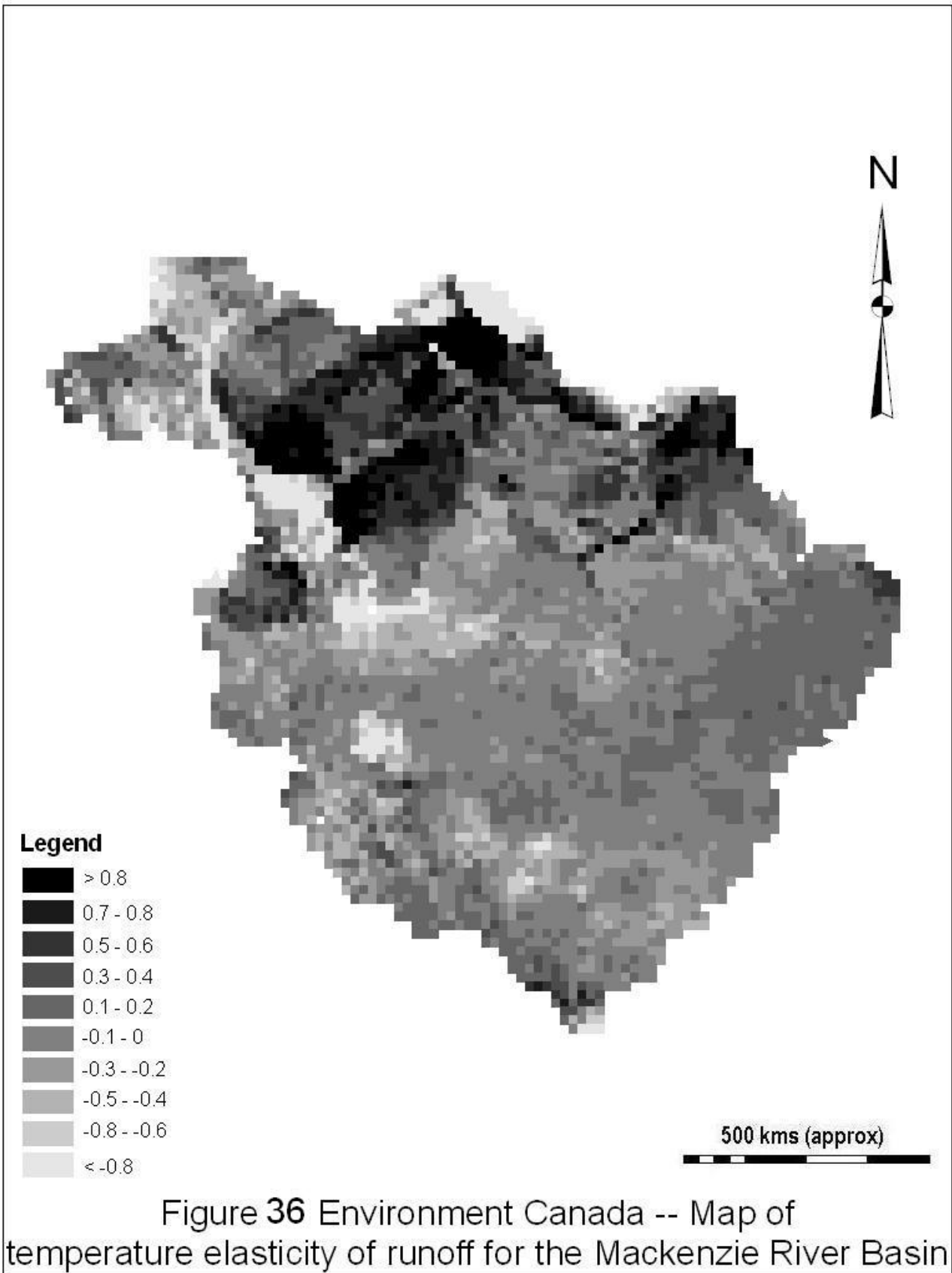
Figures 36 and 37 illustrate maps of ε_T for the Environment Canada and ECMWF data sets, respectively. Unlike ε_P and ε_{PET} which varied across the basin from west to east, ε_T varied with the latitude. At latitudes between approximately 55° to 63°, the range of ε_T values was -0.4-0 for the Environment Canada data set and the ε_T values was around 0 for the ECMWF data set. To the north is the region with stronger sensitivity but with opposite magnitude. The ε_T values in this region range from 0.4 to 0.6 for the Environment Canada data set and from -1.2 to -0.8 for the ECMWF data set. To the south, at the latitude of about 53°, is a small region with positive ε_T ranges between 0.2 to 0.4 for both data sets. Finally, around the Mackenzie Delta is a range of ε_T values between -0.6 and -0.2. Regions with negative ε_T indicate that any increase in glacier or permafrost melt due to increasing temperature were offset by losses due to evapotranspiration in that area. Similarly, regions with positive ε_T indicate that losses due to evapotranspiration is a more important process.

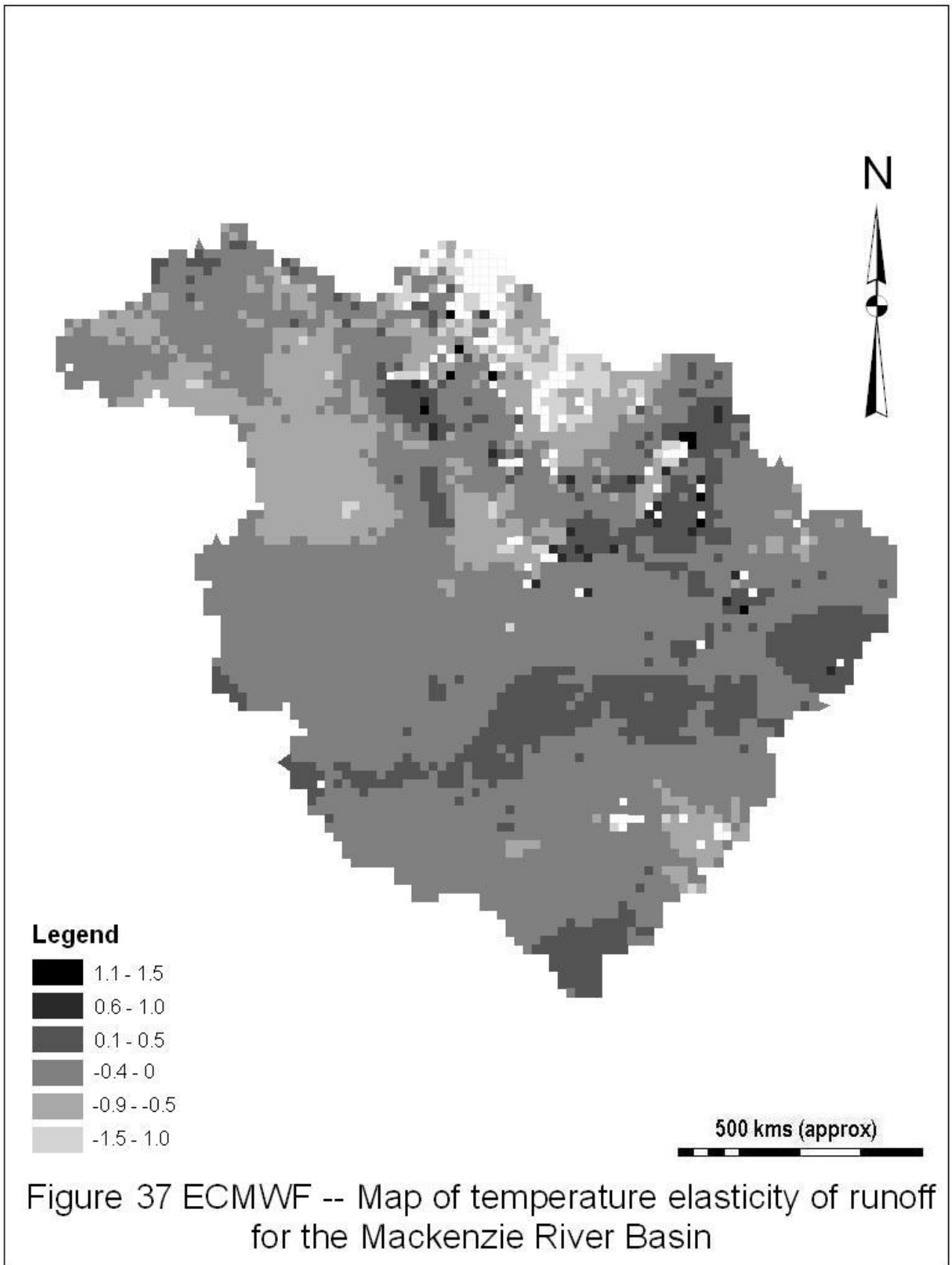
6.3 Comparisons of the two data sets

6.3.1 Original data

The year 1981 was chosen to compare the original data from 60 sample sites. Appendix C shows the location of these sample sites. Figures 38 to 42 summarize the data for annual runoff, precipitation, evapotranspiration, storage and temperature. The monthly results are summarized in tables in Appendix D. It is apparent that the magnitudes of each variable between the two data sets are similar, with the data from ECMWF usually larger both in annual and monthly records.

In the year of 1981, the seasonal monthly average temperatures were about -15° to -30°C in winter, and about 12° to 16°C in summer. Snowmelt starts in April and average temperatures again fell below the freezing point during October-November. The regional annual precipitation for the MRB is about 380 mm. Minimum precipitation over the basin occurred during the months of February, March and April for the Environment Canada data set and in January for the ECMWF data set. Maximum precipitation, on the other hand, occurred in the summer months of May to September. The regional annual runoff is 120.5 and 167 mm for the Environment Canada and the ECMWF data sets, respectively. The basin mean annual evapotranspiration is approximately 195.50 mm for the Environment Canada data set and 226.50 mm for the ECMWF





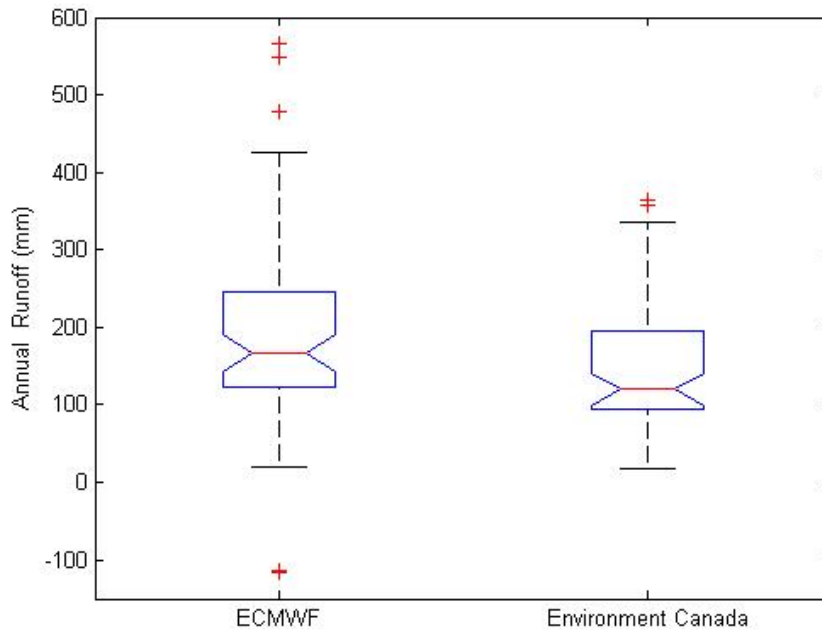


Figure 38 Box plots of original data from 60 sample sites for annual runoff
 Note: The boxes show the first quartile, median, and the third quartile, which contains 50% of the values. The whiskers extend from the box to the highest and lowest values, excluding outliers.

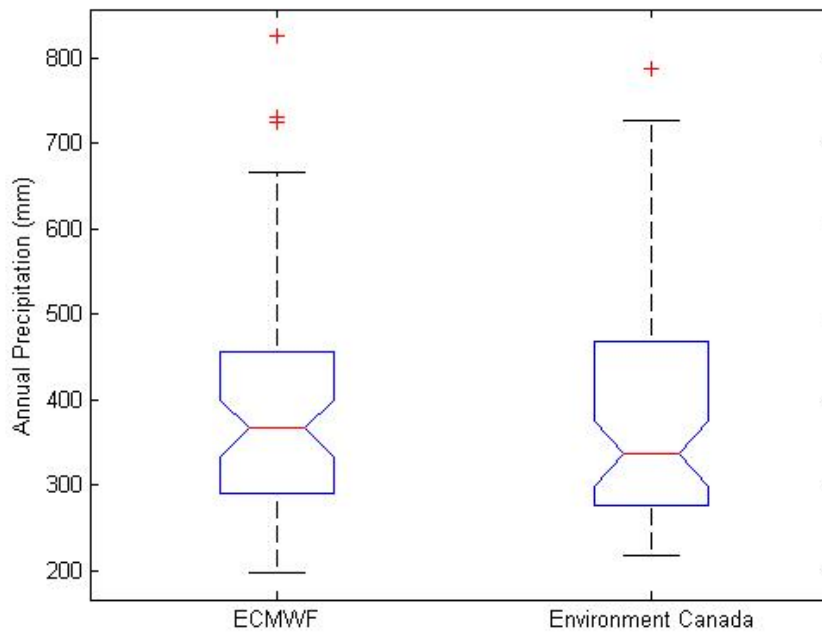


Figure 39 Box plots of original data from 60 sample sites for annual precipitation
 Note: The boxes show the first quartile, median, and the third quartile, which contains 50% of the values. The whiskers extend from the box to the highest and lowest values, excluding outliers.

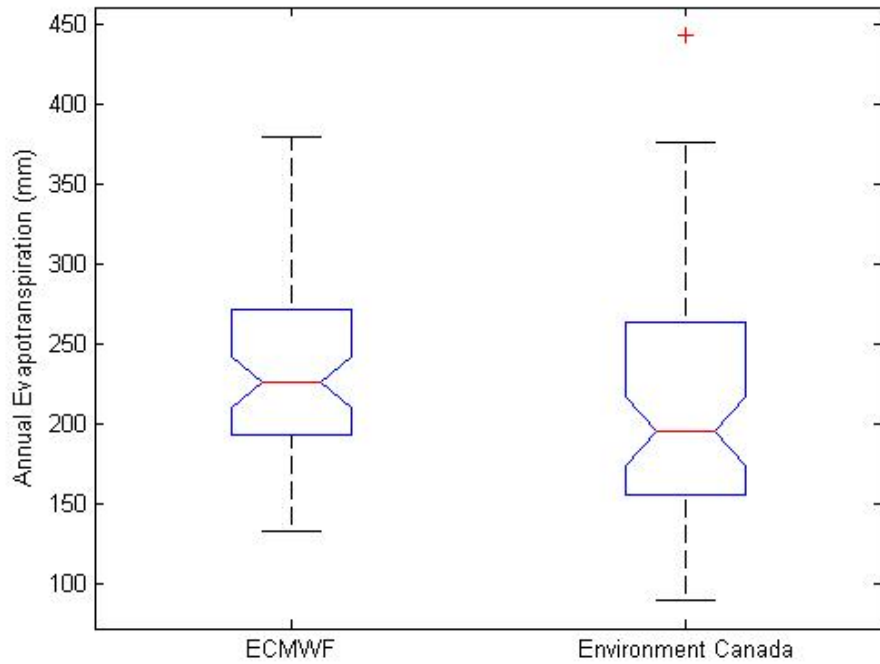


Figure 40 Box plots of original data from 60 sample sites for annual evapotranspiration
 Note: The boxes show the first quartile, median, and the third quartile, which contains 50% of the values. The whiskers extend from the box to the highest and lowest values, excluding outliers.

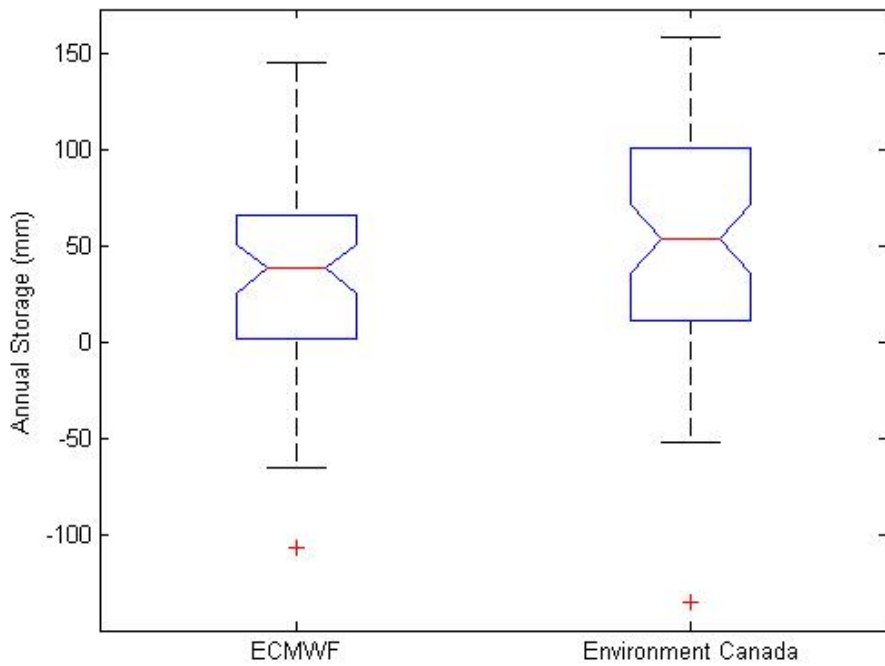


Figure 41 Box plots of original data from 60 sample sites for annual storage
 Note: The boxes show the first quartile, median, and the third quartile, which contains 50% of the values. The whiskers extend from the box to the highest and lowest values, excluding outliers.

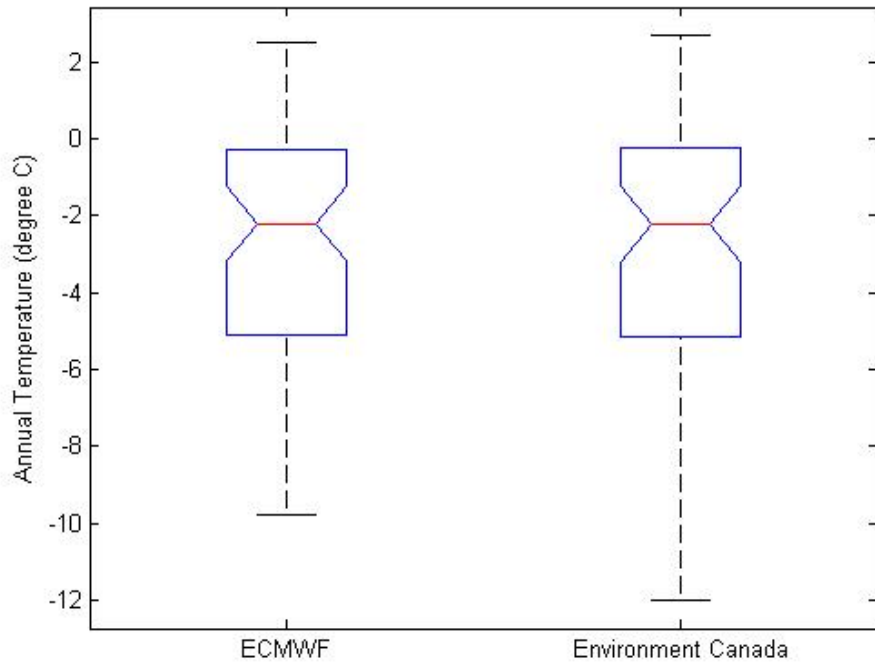


Figure 42 Box plots of original data from 60 sample sites for annual temperature
 Note: The boxes show the first quartile, median, and the third quartile, which contains 50% of the values. The whiskers extend from the box to the highest and lowest values, excluding outliers.

data set. The differences in storage between the two data sets were relatively large, with 53.5 mm for the Environment Canada data set and 38 mm for the ECMWF data set.

6.3.2 Partial correlation

Annual values of each variable have been used to calculate the partial correlation for each grid square. The results are summarized in Table 10 and Figure 43. Partial correlation ranges from -1 to 1. If partial correlation equals to 1 (-1), the two data sets are perfectly positively (negatively) correlated. Note that zero is inside the interquartile range for all the variables, indicating that the two data sets do not have much partial correlation with each other. The strongest positive correlation was between the storage terms, with only regional correlation of 0.07. The precipitation, runoff, and evapotranspiration records were negatively correlated between the Environment Canada data set and ECMWF data set, with precipitation data being the strongest.

Figures 44 to 48 show the relationship between the two data sets for the five variables for over 4600 sites in the basin. For precipitation, runoff and evapotranspiration records, the central zone is usually characterized by no or weak positive correlation, and negative correlation in other areas. Similar to these records, the storage records have no or weak positive correlation in the central zone. To the south of this zone is the zone with highest positive correlation, particularly at the southeastern side of the basin, which even exceeds 0.3. At the northern basin above the latitude of approximately 67°, the records are usually negatively correlated. For the temperature records, no obvious spatial pattern was observed. Most of the areas exhibit partial correlation between 0 and 0.1.

The low partial correlation values suggest that there are substantial local differences between the two data sets at grid-cell level. Yet, there are broad consistencies in the seasonal and spatial patterns of trends, the magnitude and spatial patterns of the climate elasticity, and the magnitude of the original data between the two data sets. Thus, the data are more reliable for identifying hydrological changes on a regional scale than at grid-cell level.

Table 10 Summary of the regional partial correlation of Environment Canada data set with ECMWF data set

R	P	ET	S	T
-0.015	-0.100	-0.016	0.070	0.047

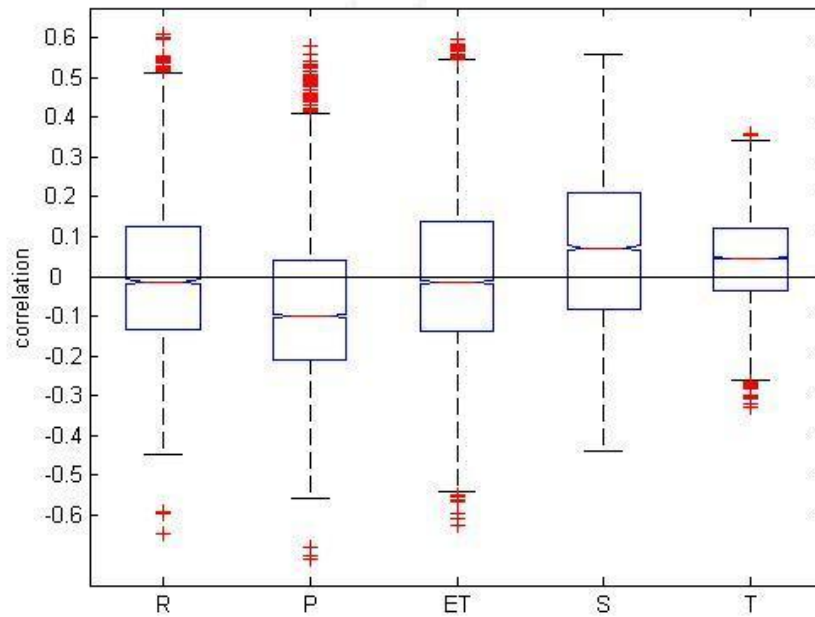
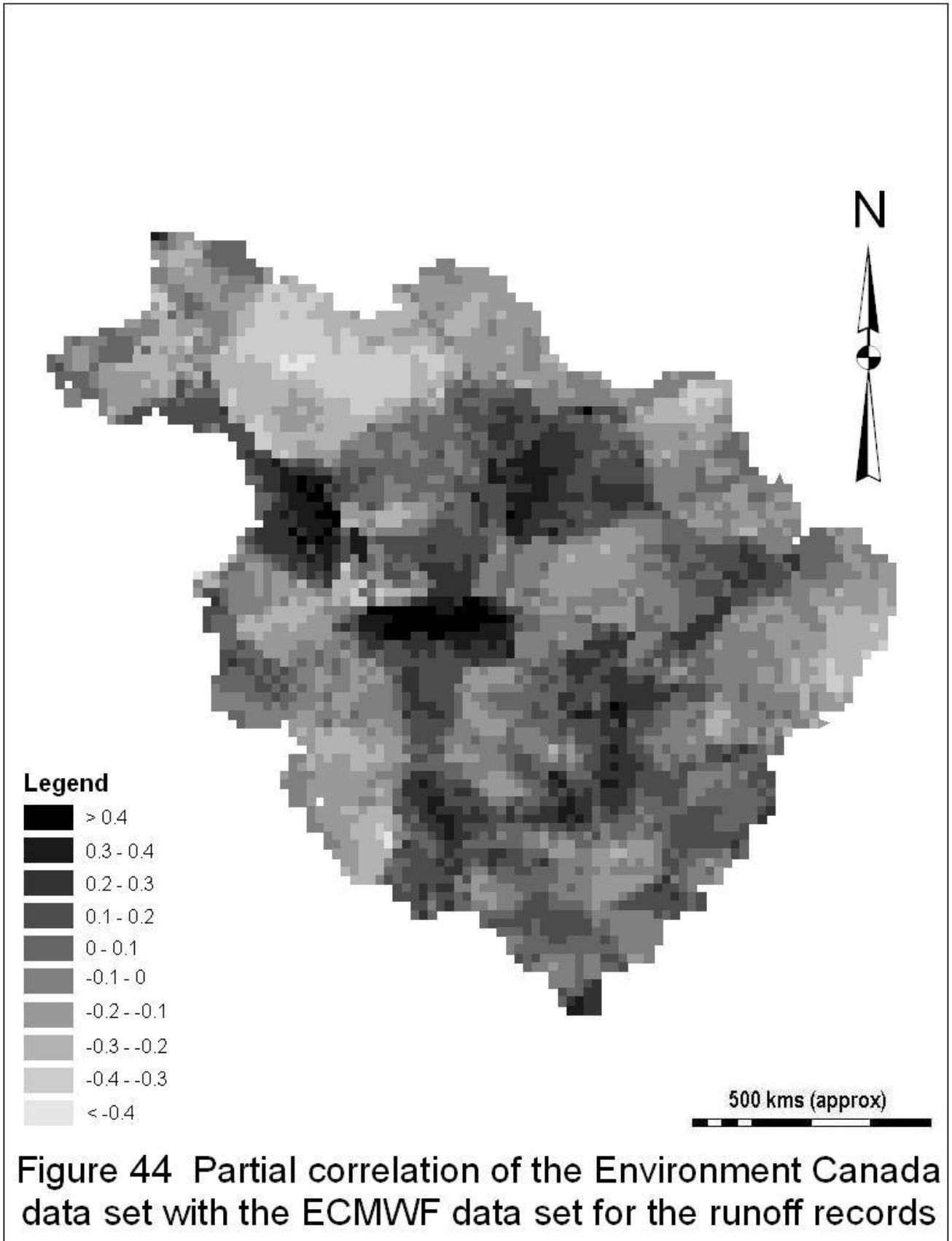
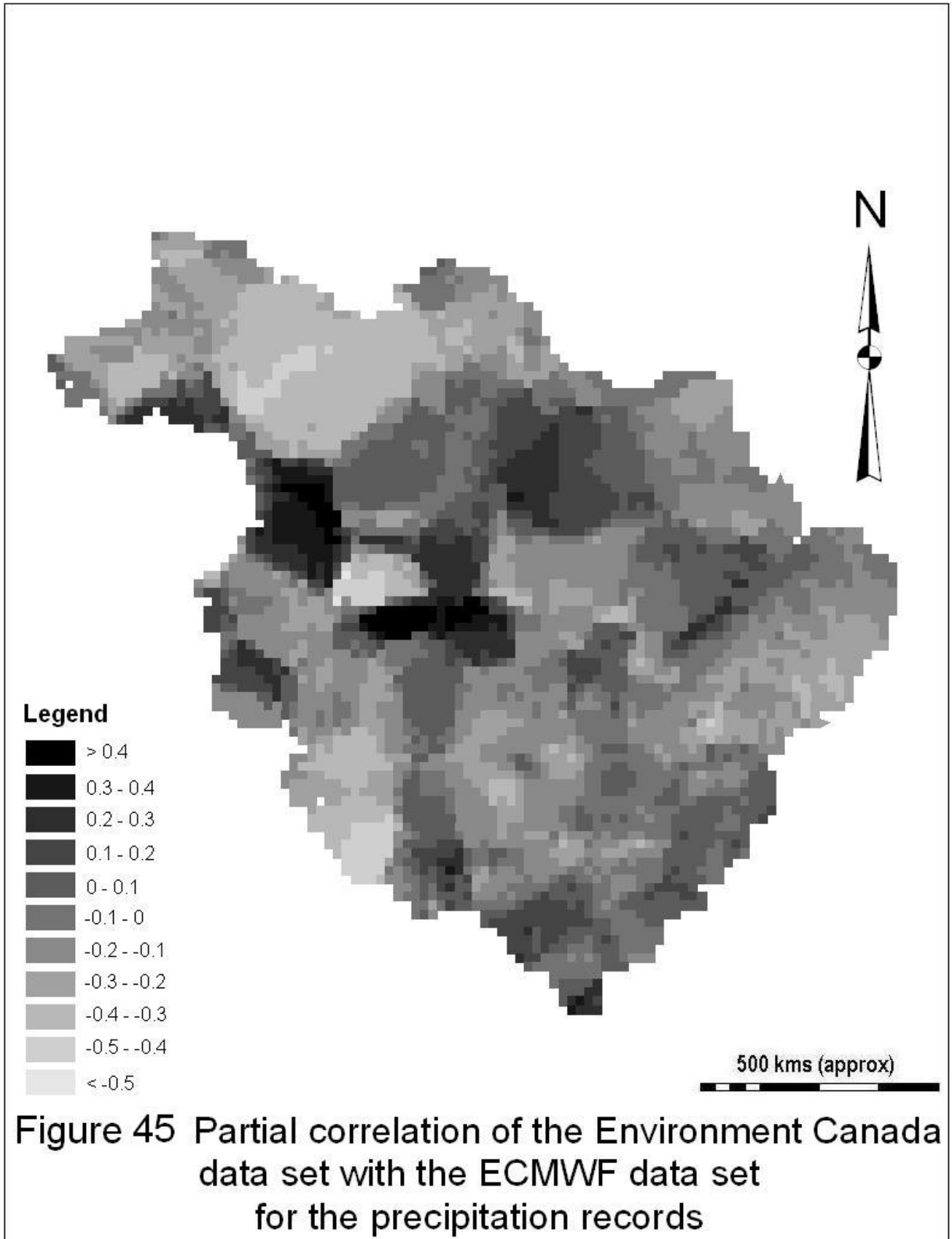
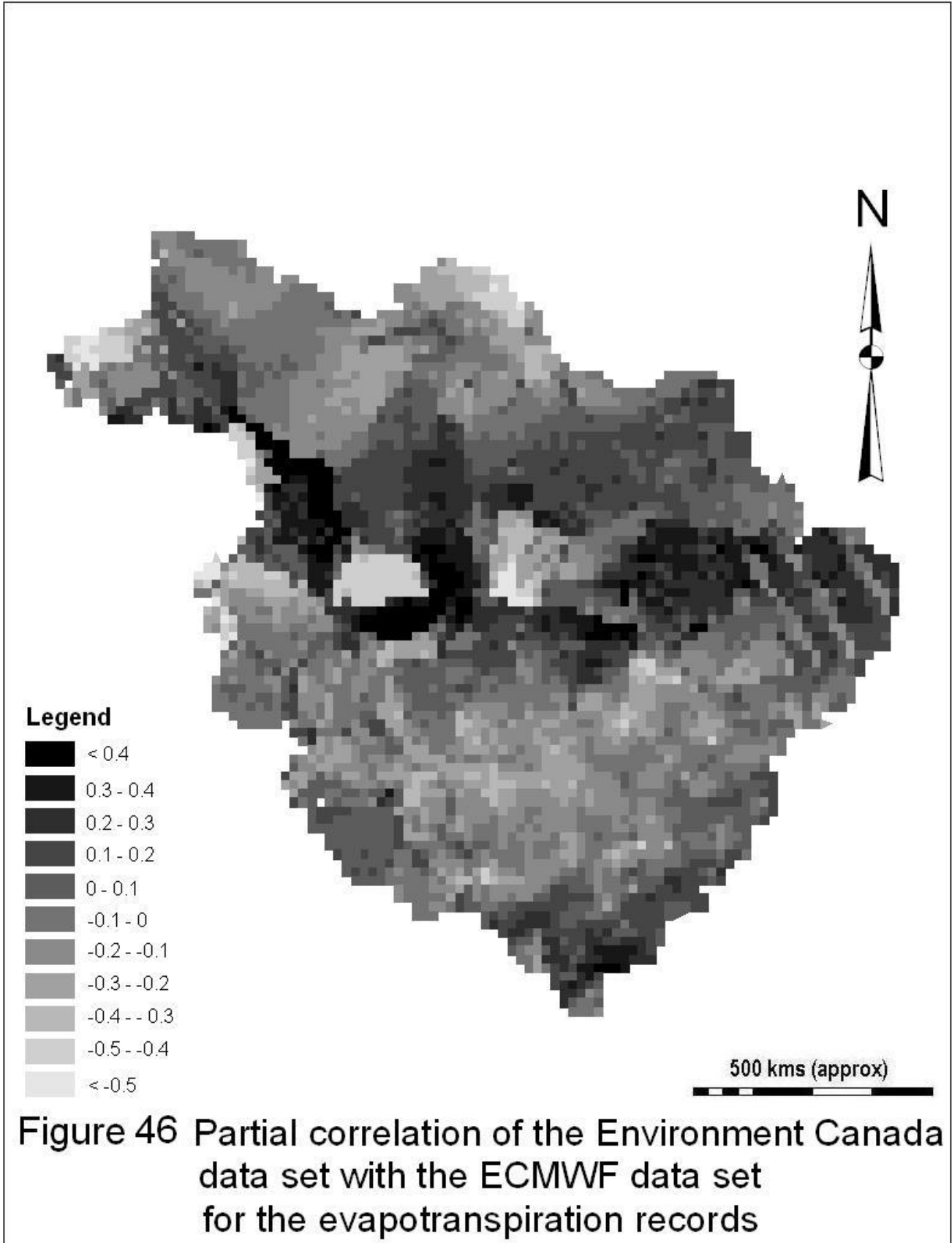


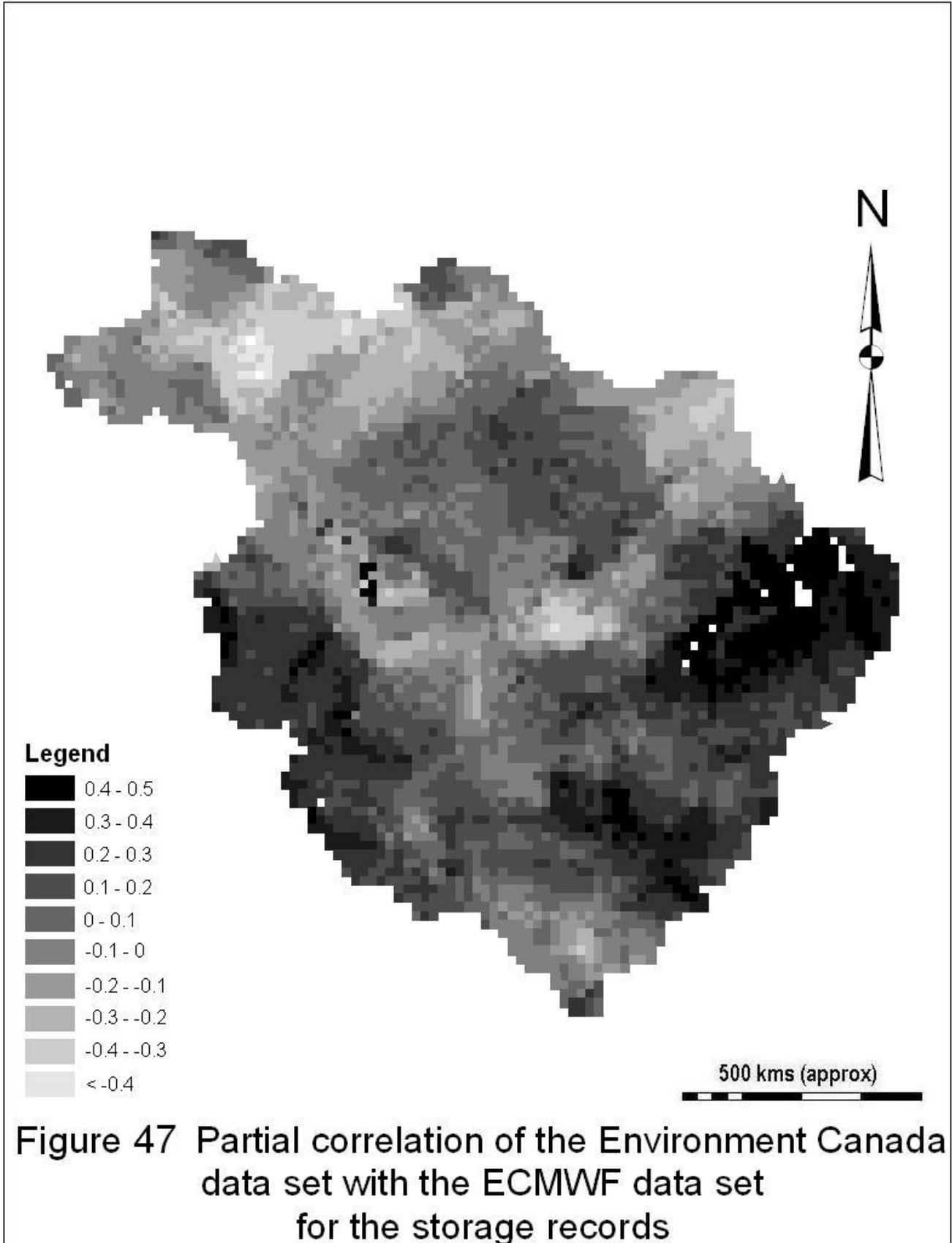
Figure 43 Box plots of 4635 estimated partial correlation of the Environment Canada data set with the ECMWF data set

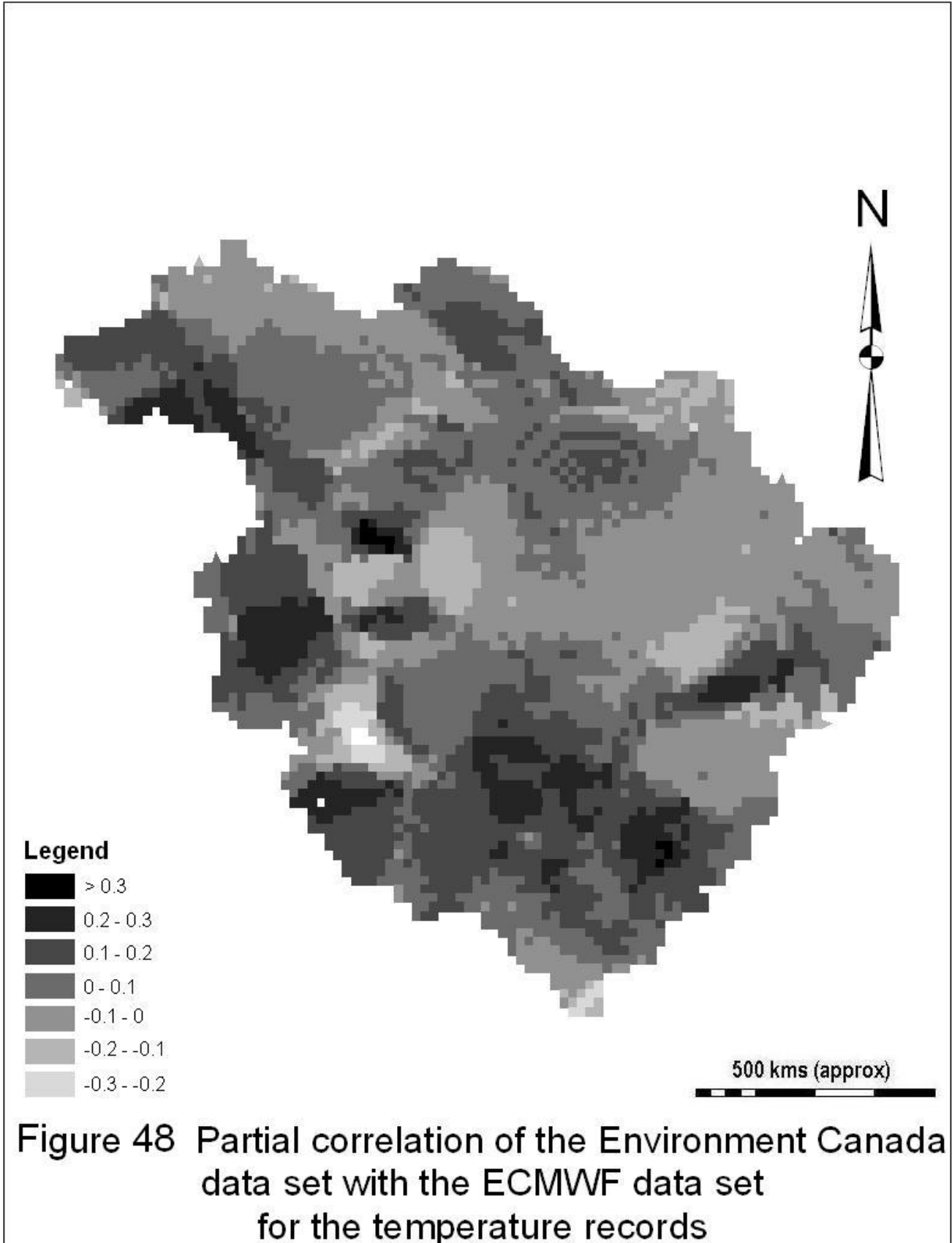
Note: The boxes show the first quartile, median, and the third quartile, which contains 50% of the values. The whiskers extend from the box to the highest and lowest values, excluding outliers.











7 COMPARISONS WITH OTHER STUDIES

Temperature

Similar to other trend detection studies for North America (e.g. Kite (1993); Kwong and Gan (1994); Blarcum *et al.* (1995); Lettenmaier *et al.* (1994); Gan (1998); Zhang *et al.* (2000); Nijssen *et al.* (2001); and Gedney *et al.* (2006)), regional warming temperature and increasing precipitation has been detected in the MRB. Most of these studies indicated that the greatest warming in higher latitude occurs during the winter months. Zhang *et al.* (2000) observed the warming trend is the strongest during winter and early spring in the west. Gan (1995) also reported significant warming trends in January to June and a cooling trend in October over western Canada. Specifically in the MRB, Nijssen *et al.* (2001) and Abdul Aziz (2004) have investigated the climate trends. The former predicted a strong increase in winter and spring temperature and a relatively weaker increase in summer temperature. The latter observed a very strong increase in temperature in winter months of December to April and some cooling trends in October. These observed temperature trends are the same as the finding in this thesis.

Precipitation

This study indicates a weak decrease in winter precipitation and a strong increase in summer precipitation. Blarcum *et al.*'s (1995) results are very close to this study. Under doubled CO₂ climate, his model predicted a strong increase in summer precipitation, followed by increase in autumn and spring precipitation, and a very weak decrease in winter precipitation in the MRB. In addition, the spatial distribution of monthly precipitation in this study is roughly the same as the trends in precipitation found by Abdul Aziz (2004). These results are closer to the pattern of the trend results obtained from the ECMWF data set in this study.

There are some discrepancies in the monthly distribution of precipitation between this study and Zhang *et al.*'s (2000) study. Zhang *et al.* (2000) observed increasing precipitation in all four seasons in the southern MRB during the twentieth century. These trends are statistically significant, at 5% significance level, during fall and winter but insignificant in spring and summer. These observations are closer to the finding from the ECMWF data set. However, the trends from the ECMWF data set are significant during the summer months only. The discrepancies may result from the length of the observation period. Gedney *et al.* (2006), for

example, observed the change in annual precipitation in North America from two different record lengths (1901-1994 and 1960-1994). They found that the precipitation increase for 1960-1994 was double the rate of that for the entire period. The findings from this study and Zhang *et al.*'s (2000) study may suggest the summer precipitation exhibited a strong increase after 1960 and the increase in winter and autumn precipitation were more important in the first half of the century. The observed change in the annual precipitation is in general agreement in both studies.

Runoff

Most of the studies indicate a general increase in runoff in North America (e.g. Gleick (1987); Kite (1993); Lettenmaier *et al.* (1994); Lins and Slack (1999); Douglas *et al.* (2000); and Gedney *et al.* (2006)). Yue *et al.* (2001), Zhang *et al.* (2001a), and Burn and Hag Elnur (2002) detected a general upward trend in the MRB region. Déry and Wood (2005) also detected a 2% increase of river discharge to the Arctic Ocean, although the trend is statistically insignificant at 5% significant level.

Specifically in the MRB region, Blarcum *et al.*'s (1995) and Nijssen *et al.*'s (2001) models predicted increasing runoff in winter, spring and autumn but a slight decrease in summer runoff. Burn *et al.* (2004a) and Abdul Aziz (2004) found similar results from observational data in the MRB for the period of 1960 to 2000. These results are consistent with the trends detected from the Environment Canada data set in this study. Moreover, the spatial distributions of monthly runoff from the Environment Canada data set are also consistent with the location reported by Abdul Aziz (2004).

The conditions in the MRB, with slightly increasing runoff from the ECMWF data set, are consistent with results reported from Soulis (2007), Louie *et al.* (2002), and many other studies done on North America. Soulis (2007) found that the basin is “getting wetter” between 1994 and 2004. Although the time periods are different and the magnitude is much larger than this study, the results are in very close agreement with the results from the ECMWF data set.

Evapotranspiration

Most studies predicted an overall increase in evapotranspiration in response to the warmer

temperature (e.g. Loaiciga *et al.* (1996); Trenberth (1998); Douville *et al.* (2002); Labat *et al.* (2004); and Huntington (2006)). This study indicates that evapotranspiration has also increased in the MRB. Nijssen *et al.* (2001), Louie *et al.* (2002), and Soulis (2007) obtained a similar result for the MRB from their models. Nijssen *et al.* (2001) predicted most of the increase in evapotranspiration to take place during the summer months. This result is similar to the finding in this study.

Storage

The increase in storage for the ECMWF data set is in general agreement with the WATFLOOD modelled storage from Soulis (2007). The Environment Canada data set, with decrease in storage, is consistent with the findings from Louie *et al.* (2002).

Sensitivity

Similar to Karl and Riebsame (1989) and Nijssen *et al.* (2001), runoff is more sensitive to changes in precipitation than to changes in temperature. The sensitivity of runoff to precipitation is an order of magnitude higher than that to temperature. The sensitivity of runoff to precipitation is 1.2 to 1.5, which is in good agreement with the estimates of 1.0 by Blarcum *et al.* (1995) and Gedney *et al.* (2006). The sensitivity of runoff to temperature, on the other hand, is opposite in direction. Nijssen *et al.* (2001) has projected a similar response with increasing temperature, with the exception of spring runoff. This pattern is also similar to the finding in this study: runoff broadly followed the spatial pattern of precipitation but the pattern of changes in spring and autumn runoff is mainly affected by temperature.

Wigley and Jones (1985) have shown that changes in runoff are everywhere more sensitive to changes in precipitation than to changes in evapotranspiration. This theory is consistent with the results obtained from the Environment Canada data set. For the ECMWF data set, however, the sensitivity of runoff to evapotranspiration is stronger than that to precipitation.

8 DISCUSSION

Water balance changes

Recall the simple water balance for the basin from Eq. 1. The water balance would become non-stationary if any one of the water balance components is non-stationary. Warming temperature has increased evapotranspiration during summer. The amount of water vapor increased due to increased evapotranspiration would lead to increased precipitation amount within the basin during summer. Consequently, the change in summer runoff also increased.

The largest hydrological change occurred in the summer months but hydrological change in winter, in fact, is a very important process in a snow-dominated basin, such as the MRB. Among the three water balance components, precipitation changes were the largest during winter. Since runoff and evapotranspiration are limited during winter, any changes in the precipitation amount affect the water storage in the snow pack. The snow pack thus integrates the effects of hydrological change during the winter months. This water storage becomes available for runoff or evapotranspiration on the following spring and summer.

For the Environment Canada data set, the strong decrease in regional winter precipitation would decrease the moisture storage during winter. Consequently, the total amount of snowmelt runoff is decreased. However, the regional runoff remains unchanged during the spring months for the Environment Canada data set. This result may suggest warmer spring temperature has increased glacier melt and snowmelt that used to occur in later months. Reduced snowmelt process in the following summer months of May and June has led to decreased runoff in these months.

For the ECMWF data set, the weak decrease in regional winter precipitation did not alter the hydrologic cycle in a great manner during winter. Thus, the spatial pattern of changes in runoff follows more closely, as compared to the Environment Canada data set, with the pattern of changes in precipitation for most of the remaining months. Changes in the amount of runoff for most of the months are also larger in spatial extent and more sensitive to changes in precipitation as compared to the Environment Canada data set. One interpretation would be that a lesser amount of the increased precipitation was used to replenish the soil moisture storage (because of

increasing soil moisture deficit from the Environment Canada record), thus causing more runoff generated in each grid.

Overall, increasing regional winter runoff but decreasing regional winter precipitation was detected from both data sets. Moreover, there was less connection between the spatial patterns of changes in runoff and the spatial patterns of changes in precipitation during winter. This behaviour may suggest a larger proportion of the precipitation in winter fell as rain, leading to increasing amount of winter runoff.

Evapotranspiration was more related to precipitation and runoff than temperature. The seasonal pattern, the evapotranspiration elasticity to runoff, and the spatial pattern of the partial correlation between the two data sets followed better with precipitation and runoff in both data sets. This is physically possible because evapotranspiration is a direct measure of moisture loss from the region that is both water-limited and energy-limited, whereas, temperature only represents an energy balance component in a region.

Sensitivity

In this study, the climate elasticity was calculated based on annual values. The results indicated that the annual runoff is affected primarily by precipitation. In addition, Abdul Aziz (2004) investigated the correlation between the hydrological and meteorological variables in the MRB. He found that all monthly flows, except January flow, are strongly correlated to changes in mean monthly temperature. These results are in close agreement with Gleick's (1987) findings: the annual runoff is affected primarily by precipitation changes while the seasonal distribution of runoff is affected by changes in mean monthly temperature.

The sensitivity analysis indicated that the ϵ_P and ϵ_{PET} values are quite similar, in terms of magnitude and direction; both of these elasticities have a more distinct pattern than ϵ_T . Both of the ϵ_P and ϵ_{PET} values varied across the basin from west to east, with the lowest value around the Rocky Mountain on the west and highest value on the central zone in the basin. A similar but opposite pattern on moisture flux convergence (such that high value of elasticity is associated with low value of moisture flux convergence, and vice-versa) was observed by Liu *et al.* (2002).

They have also shown the linkage of moisture flux convergence with precipitation, evaporation, and discharge. This implies that ε_P and ε_{PET} in the MRB is likely to be affected by the moisture flux convergence. Another interpretation would be that ε_P and ε_{PET} are related to the topography and/ or physiographic features of the MRB since the values varied between Mountains, Plain, and Shield. On the other hand, ε_T varied with the latitude. This behaviour is expected since temperature varies with latitude.

The elasticity values always varied in the Shield upland in the MRB. This behaviour is not surprising since Woo and Marsh (2005) noted that the runoff ratio from the Shield upland is highly variable. Thus, the ε_P and ε_{PET} are also highly variable because the amount of runoff generated in each grid largely depends upon the runoff ratio. A distinct positive ε_T region in the Shield upland indicated that runoff generated in that region is largely due to the glacier melt. Since Shield upland is extensively glaciated, this area is very sensitive to temperature change.

Large-scale climate anomalies

Large-scale climate anomalies can play a crucial role in changes in temperature (Mantua *et al.*, 1997; Cunderlik and Burn, 2004), precipitation (Mantua *et al.*, 1997; Harshburger *et al.*, 2002), and streamflow (Neal *et al.*, 2002; Burn *et al.*, 2004b; Déry and Wood, 2005) records. In Figure 3, the years with blue colour indicate the combination of La Nina-cold-PDO phase, which is recognized to be associated with cooler and wetter years. The years with orange colour indicate the combination of El Nino-warm-PDO, which is recognized to be associated with warmer and drier year. It is also obvious from the figure that La Nina-cold-PDO phase mostly occurred before 1977 and El Nino-warm-PDO mostly occurred after 1977. Thus, the baseline condition is cooler and wetter. Subsequently, all climate and hydrological changes calculated relative to this baseline condition will be significantly warmer and drier, especially the El Nino-warm PDO phase after 1977 are generally associated with warmer and drier years. Similar to the finding from the Environment Canada data set, Abdul Aziz (2004) and Burn *et al.* (2004b) found that streamflow is generally decreasing from 1960 to 1999. However, streamflow in other study periods (1965-1999, 1970-1999, 1975-1999) were increasing. This behaviour may be an indication of significant relationship between trends in hydrological variables and large-scale climate anomalies.

Model performance/ model evaluation

Performance of the model may vary according to seasons, land-cover type and model resolution. It is also important to note that the model only produced runoff and evapotranspiration fields under changing climate. However, anthropogenic impacts and the combined effect of climate change and anthropogenic impacts can largely affect runoff and evapotranspiration in the basin.

Among the two modelled water balance components, evapotranspiration is the least reliable. Cranmer *et al.* (2001), for example, have concluded that WATFLOOD is capable of accurately modelling the nonlinear rainfall-runoff processes for increasing rainfall intensities. Bingeman *et al.* (2006), however, showed that the WATFLOOD model tends to overestimate the evaporation at the BOREAS study sites. Overestimation of evapotranspiration would lead to less runoff generated in each grid.

It is important to note that there can be many uncertainties feeding into the hydrological model other than the uncertainties within the model itself. For example, uncertainties in the non-climate inputs such as changes in land use or vegetation (Merritt *et al.*, 2006) and uncertainties in the climate inputs (Jones *et al.*, 2006) can have a larger effect on the simulation outputs than the inaccuracy of the models themselves.

From the partial correlation analysis in this study, the two data sets were highly uncorrelated. Since the uncertainties in the model itself and in the non-climate inputs were lurking in both simulation runs, the uncertainties in the climate inputs were responsible for most of the differences between the two data sets. In other words, the low correlation is likely due to the differences in the precipitation and temperature calculation using station and gridded data.

9 CONCLUSIONS AND RECOMMENDATIONS

This study examined changes in surface water components over the MRB basin during 1961-2002. The hydrologic cycle in the MRB appears to be strongly influenced by climate change. The results from the two data sets show that: 1) significant warming has occurred during 1961 to 2002, with the greatest warming during the spring and winter months; 2) there were some cooling trends in the October temperature; 3) the winter precipitation has decreased while the summer precipitation has increased; and 4) the summer evapotranspiration was significantly increased.

In both data sets, there were strong spatial and seasonal structures in the trend results. In general, temperature has significantly increased across much of the basin. For precipitation, increasing trends were mostly in the central basin between the latitude of approximately 60° and 66°. However, differences in the spatial pattern were observed between the two data sets. First, stronger signals of increasing trends were always found in the ECMWF data set. Also, the trends in the ECMWF data set are usually larger in spatial extent and they are positive most of the time. For the Environment Canada data set, on the other hand, there are mixes of increasing and decreasing trends.

There are large discrepancies between the two data sets on runoff and storage. Decreasing trends were detected on both runoff and storage for the Environment Canada data set while increasing trends were detected for the ECMWF data set. This is mainly because the observed increase in basin-averaged annual precipitation was compensated by the relatively strong increase of regional evapotranspiration for the Environment Canada data set, leading to a decrease in runoff and storage. The combination of ENSO and PDO may also lead to decrease in runoff. Since most of the trend detection studies done on the MRB reported a reduction in streamflow, the runoff time series from the Environment Canada data set and observations are in better agreement compared to the ECMWF data set. However, it is important to note that the nature of streamflow responses to trends in precipitation is more complex than changes in direct runoff (Lettenmaier *et al.*, 1994). Thus, a direct comparison between streamflow and runoff may not be valid.

The trends in runoff and evapotranspiration reflected both changes in precipitation and changes in temperature. Sensitivity analysis indicated that the regional annual runoff was strongly sensitive to the regional annual precipitation and less sensitive to regional annual temperature. This result is also indicated in the seasonal pattern and spatial pattern. Both seasonal pattern and spatial pattern of runoff matched better to that of changes in precipitation, particularly from July to November. The runoff-precipitation relationship was stronger in the central zone of the Interior Plain and weaker in the Rocky Mountain chains on the west.

The effect of changes in temperature is much more noticeable in the spring and autumn runoff than that of changes in precipitation. Sensitivity analysis indicated that the regional runoff was negatively correlated with regional temperature, indicating losses due to evapotranspiration caused by increases in temperature was the dominate process (over permafrost or glacier melt) over the MRB. There is one distinct region where runoff is positively correlated with temperature. This region is located in the Shield upland region in the MRB, which is extensively glaciated. The positive temperature elasticity value indicated that losses due to evapotranspiration caused by increases in temperature were offset by increase in melt runoff from glaciers in the Shield upland.

The spatial distribution of evapotranspiration, in general, matched better with the pattern of changes in temperature; yet its seasonal pattern followed closer to that of precipitation. Moreover, the spatial distribution of evapotranspiration elasticity was also similar to that of precipitation. Although regional annual runoff was negatively correlated with regional annual temperature, runoff was positively correlated with evapotranspiration. This unexpected relationship would suggest that increased storage caused more runoff generation in each grid and provided more moisture available for evapotranspiration. The spatial distribution of the change in annual storage also confirmed the runoff-storage relationship. The increases in annual runoff were in roughly the same vicinity as the upward trends in annual storage.

The largest hydrologic changes occurred in summer. These changes were mainly due to large increase in summer precipitation. However, the effects and phenomena of hydrologic changes

during winter should not be overlooked since runoff from glacier, permafrost and snow have a significant contribution to water resources in a snow-dominated basin.

The difference of ε_T with ε_P and ε_{PET} is more than their direction. ε_T varied with latitude while ε_P and ε_{PET} varied across the basin from west to east. The ε_P and ε_{PET} values were lower along the Rocky Mountain chains and progressively increased from the mountain chains to the central zone of the basin. The central zone usually has the highest ε_P and ε_{PET} values. In the Shield upland region in the basin, the ε_P and ε_{PET} values were highly varied. This pattern may be related to the moisture flux convergence, topography, and/ or physiographic features in the MRB. The ε_T values, on the other hand, were usually negative below 55° , zero between 55° and 63° , and positive between 63° and 68° (in the Shield upland region). This pattern may be related to the changing temperature due to changing latitude. Moreover, the distinct region with positive correlation between temperature and runoff indicated that glacier melt is the dominant process (over the losses due to evapotranspiration) in that area.

Many studies have proven that WATFLOOD is capable of simulating runoff and evapotranspiration with reasonable accuracy. However, low partial correlations between the two data sets were obtained. A low partial correlation coefficient suggests that the agreement between the two data sets is weak or non-existent, at least at the grid-cell level. Since there were broad consistencies in the seasonal and spatial patterns of trends between the two data sets, the low correlation was likely due to differences in the precipitation and temperature calculation using station and gridded data. Thus, the data are more reliable for identifying hydrological changes on a regional scale than at grid-cell level. Future improvements in climate input data could greatly enhance our confidence in the results.

Based on the results presented in this study, the intensification of the hydrologic cycle is evident in the basin. These results have important implications for future scenarios, as a continued warming will undoubtedly result in dramatic changes in the hydrologic cycle in the MRB. Climatic warming is likely to further increase the precipitation amount, thereby increasing the evapotranspiration, and affect the timing and amount of runoff and storage in the MRB, particularly as the rate of warming in the 21st century is expected to be several times greater than

in the 20th century (Nijssen *et al.*, 2001). Moreover, climate change itself could trigger additional increases in greenhouse gases and reduction in surface albedo, which further amplify the effects of a change in climate forcing. Thus, detection and attribution studies should be a permanent exercise as the changes of hydrological processes may be stronger and last longer. It is also important to be aware of the consequences of climatic change and its impacts on the planning and management strategies for future water resources system.

The hydrologic cycle must be studied from start to finish if the final impact on the hydrologic cycle is to be assessed. Future research should include the monthly storage term and the ratio of snowfall to total precipitation. Since the presence or absence of glaciers, permafrost, and snow fundamentally changes the nature of the land surface water balance, these data will provide important information needed to better understand the hydrological changes during winter. A next step would be to examine the climate impacts on runoff variability and extreme events. Karl and Riebsame (1989) noted changes in precipitation and temperature could lead to only a small change in mean runoff but a large change in minimum or maximum runoff. It would also be useful to analyze changes in the hydrologic cycle as they relate to other variables. Wigley and Jones (1985) indicated that increasing CO₂ effects on plant transpiration would make more water available as runoff. This phenomenon is only beginning to be quantified (e.g. Gedney *et al.* (2006)). Future studies are needed to test this phenomenon as it applies in the context of the MRB. Future work should also be directed toward developing a method for distinguishing the natural climate variability and the human-induced climate change impacts on the hydrologic cycle.

REFERENCES

- Abdul Aziz, O. I. (2004). *Climate change impacts on the hydrological regime in the Mackenzie River Basin*. MAsC thesis, Department of Civil Engineering, University of Waterloo, Waterloo, ON., Canada.
- Anonymous (2007a, February 1). *Tough words may fight global warming*. Toronto Star.
- Anonymous (2007b, February 4). *46 nations back action on climate*. Toronto Star.
- Anonymous (2007c, February 6). *Gore sharply criticizes global warming critics*. CNN.com.
- Anonymous (2007d, June 5). *Present Positions: Where Various Countries Stand on climate Initiatives*.
- Attenborough, D. (2007). *A change in the moral climate? Interview by Randerson, J. (2007, June 2)*. Retrieved on June 2, 2007, from the World Wide Web, <http://environment.guardian.co.uk/climatechange/story/0,,2093804,00.html>.
- Bayley, G. V. and Hammersley, J. M. (1946). The 'effective' number of independent observations in an autocorrelated time series. *Journal of Royal Statistics Society* 8(2): 184-197.
- Bedient, P. B. and Huber, W. C. (2002). *Hydrology and Floodplain Analysis Third Edition*, Prentice Hall, Upper Saddle River, New Jersey.
- Bingeman, A. K., Kouwen, N. and Soulis, E. D. (2006). Validation of the Hydrological Processes in a Hydrological Model. *Journal of Hydrologic Engineering* 11(5): 451-463.
- Blarcum, S. C. V., Miller, J. R. and Russel, G. L. (1995). High latitude river runoff in a doubled CO₂ Climate. *Climatic Change* 30: 7-26.
- Bonsal, B. R., Zhang, X., Vincent, L. A. and Hogg, W. D. (2001). Characteristics of Daily and Extreme Temperatures over Canada. *Journal of Climate* 14: 1959-1976.
- Borenstein, S. (2007, February 2). *Climate change to last centuries: Report*. Toronto Star, quoted Italy's environment minister Alfonso Pecoraro Scanio.
- Bouwer, L. M., Aerts, J. C. J. H., Droogers, P. and Dolman, A. J. (2006). Detecting the long-term impacts from climate variability and increasing water consumption on runoff in the Krishna river basin (India). *Hydrological and Earth System Sciences* 10: 703-713.
- Buishand, T. A. (1982). Some methods for testing the homogeneity of rainfall records. *Journal of Hydrology* 58: 11-27.
- Burn, D. H. (1994). Hydrologic effects of climatic change in west-central Canada. *Journal of Hydrology* 160: 53-70.
- Burn, D. H. and Hag Elnur, M. A. (2002). Detection of hydrologic trends and variability. *Journal of Hydrology* 255: 107-122.
- Burn, D. H., Abdul Aziz, O. I. and Pietroniro, A. (2004a). A Comparison of Trends In Hydrological Variables for Two Watersheds in the Mackenzie River Basin. *Canadian Water Resources Journal* 29(4): 283-298.
- Burn, D. H., Cunderlik, J. M. and Pietroniro, A. (2004b). Hydrological trends and variability in the Liard River Basin. *Hydrological Sciences Journal* 49(1): 53-67.
- Burn, D. H. and Hesch, N. M. (2006). A Comparison of Trends in Potential and Pan Evaporation for the Canadian Prairies. *Canadian Water Resources Journal* 31(3): 173-184.
- Burn, D. H. and Hesch, N. M. (2007). Trends in evaporation for the Canadian Prairies. *Journal of Hydrology* 336: 61-73.
- Callaway, J. M. and Currie, J. W. (1985). *Water Resource Systems and Changes in Climate and*

- Vegetation*. M.R. White, Washington, DC, Characterization of Information Requirements for Study of CO₂ Effects: Water Resources, Agriculture, Fisheries, Forests, and Human Health. U.S. Department of Energy. DOE/ER-0236.
- Cao, Z., Wang, M., Proctor, B. A., Strong, G. S., Stewart, R. E., Ritchie, H. and Burford, J. E. (2002). On the Physical Process Associated with the Water Budget and Discharge of the Mackenzie Basin during the 1994/95 Water Year. *Atmosphere-Ocean* 40(2): 125-143.
- Chahine, M. T. (1992). The hydrological cycle and its influence on climate. *Nature* 359: 373-380.
- Chalise, S. R. (2002). *Management of water resources for poverty alleviation in the Hindu-Kush Himalayas*, in van Lanen, H. A. J. and Demuth, S., eds., Friend 2002 -- Regional Hydrology: Bridging the Gap between Research and Practice, IAHS Press, P.27-32.
- Chiew, F. H. S. and McMahon, T. A. (1993). Detection of trend or change in annual flow of Australian rivers. *International Journal of Climatology* 13: 643-653.
- Chiew, F. H. S. (2006). Estimation of rainfall elasticity of streamflow in Australia. *Hydrological Sciences Journal* 51(4): 613-625.
- Chingombe, W., Gutierrez, J. E., Pedzisai, E. and Siziba, E. (2005). A study of hydrological trends And variability Of Upper Mazowe catchment-Zimbabwe. *Journal of Sustainable Development in Africa* 7(1): 1-17.
- Cororan, T. (2006, November 14). *Big new push for new gas taxes*. National Post.
- Cranmer, A. J., Kouwen, N. and Mousavi, S. F. (2001). Proving WATFLOOD: modelling the nonlinearities of hydrologic response to storm intensities. *Can. J. Civ. Eng.* 28: 837-855.
- Cunderlik, J. M. and Burn, D. H. (2002). Local and Regional Trends in Monthly Maximum Flows in Southern British Columbia. *Canadian Water Resources Journal* 27(2): 191-212.
- Cunderlik, J. M. and Burn, D. H. (2004). Linkages between Regional Trends in Monthly Maximum Flows and Selected Climatic Variables. *Journal of Hydrologic Engineering* 9(4): 246-256.
- Daniel, W. W. (1978). *Applied Nonparametric Statistics*, Boston, U.S.
- Darken, P. F., Holtzman, G. I., Smith, E. P. and Zipper, C. E. (2000). Detecting changes in trends in water quality using modified Kendall's tau. *Environmetrics* 11: 423-434.
- Déry, S. J. and Wood, E. F. (2005). Decreasing river discharge in northern Canada. *Geophysical Research Letters* 32: L10401, doi: 10.1029/2005GL022845.
- Dibike, Y. B. and Coulibaly, P. (2004). Hydrologic Impact of Climate Change in the Saguenay Watershed. *57th Canadian Water Resources Association Annual Congress*.
- Dingman, S. L. (2002). *Physical Hydrology second edition*, Prentice Hall, New Jersey.
- Dispatch, D. C. (2006, June 6). *The Politics of Global Warming*. National Journal.
- Dornes, P., Pietroniro, A., Toth, B. and Töyrä, J. (undated). *Future Climate Change Scenarios for the Mackenzie Basin*. National Water Research Institute, Environment Canada, Saskatoon, Canada.
- Douglas, E. M., Vogel, R. M. and Kroll, C. N. (2000). Trends in floods and low flows in the United States: impact of spatial correlation. *Journal of Hydrology* 240: 90-105.
- Douville, H., Chauvin, F., Planton, S., Royer, J.-F., Salas-Melia, D. and Tyteca, S. (2002). Sensitivity of the hydrological cycle to increasing amounts of greenhouse gases and aerosols. *Climate Dynamics* 20: 45-68.
- Downeswell, J. A., Hagen, J. O., Björnsson, H., Glazovsky, A. F., Harrison, W. D., Holmlund, P., Jania, J., Koerner, R. M., Lefauconnier, B., Ommanney, C. S. L. and Thomas, R. H.

- (1997). The Mass Balance of Circum-Arctic Glaciers and Recent Climate Change. *Quaternary Research* 48: 1-14.
- Durance, I. and Ormerod, S. J. (2007). Climate change effects on upland stream macroinvertebrates over a 25-year period. *Global Change Biology* 13: 942-957.
- ECMWF (2006). *ECMWF Re-Analysis ERA-40* European Centre for Medium-Range Weather Forecasts. Retrieved on October 1, 2005, from the World Wide Web, <http://www.ecmwf.int/products/data/archive/descriptions/e4/index.html>.
- Environment Canada (2001). *Climate Change and Canada's Water Resources: Predicting the future*. Retrieved on February 15, 2007, from the World Wide Web, http://www.ec.gc.ca/science/sandenov01/article3_e.html.
- Environment Canada (2004). *Hydrology of Canada*. Retrieved on February 15, 2007, from the World Wide Web, http://www.wsc.ec.gc.ca/hydrology/main_e.cfm?cname=hydro_e.cfm.
- Environment Canada and NSERC CRSNG (2004). *The Mackenzie GEWEX Study*. Retrieved on September 1, 2005, from the World Wide Web, http://www.usask.ca/geography/MAGS/index_e.htm.
- Fleming, S. W. and Clarke, G. K. C. (2002). Autoregressive noise, deserialization, and trend detection and quantification in annual river discharge time series. *Canadian Water Resources Journal* 27(3): 335-354.
- Frank, D. A. (2007). Drought effects on above- and belowground production of a grazed temperate grassland ecosystem. *Ecosystem Ecology* 152: 131-139.
- Frich, P., Alexander, L. V., Della-Marta, P., Gleason, B., Haylock, M., Klein Tank, A. M. G. and Peterson, T. (2002). Observed coherent changes in climatic extremes during the second half of the twentieth century. *Climate Research* 19: 193-212.
- Gan, T. Y. (1995). Trends in Air-temperature and Precipitation for Canada and North-eastern USA. *International Journal of Climatology* 15(10): 1115-1134.
- Gan, T. Y. (1998). Hydroclimatic trends and possible climatic warming in the Canadian prairies. *Water Resources Research* 34(11): 3009-3015.
- Gedney, N., Cox, P. M., Betts, R. A., Boucher, O., Huntingford, C. and Stott, P. A. (2006). Detection of a direct carbon dioxide effect in continental river runoff records. *Nature* 439(16): 835-838.
- Gibson, J. J. and Edwards, T. W. D. (2002). Regional water balance trends and evaporation-transpiration partitioning from a stable isotope survey of lakes in northern Canada. *Global Biogeochemical Cycles* 16(2): 10-1--10-14.
- Gleick, P. H. (1986). Methods for Evaluating the Regional Hydrologic Impacts of Global Climatic Changes. *Journal of Hydrology* 88: 97-116.
- Gleick, P. H. (1987). Regional Hydrologic Consequences of Increases of Atmospheric CO₂ and Other Trace Gases. *Climatic Change* 110: 137-161.
- Gorrie, P. (2007, February 3). *Getting warmer...Stephen Harper's environmental conversion continues as he recognizes the 'enormous threat of global warming. But emission cuts? Not so fast.* Toronto Star.
- Groisman, P. Y., Karl, T. R. and Knight, R. W. (1994). Observed impact of snow cover on the heat balance and the rise of continental spring temperatures. *Science* 263: 198-200.
- David, L., Bender, L. and Burns, S. Z. (producer), & Guggenheim, D. (director) (2006). *An Inconvenient Truth* [Motion picture]. Paramount Classics.
- Hall, P., Horowitz, J. L. and Jing, B. (1995). On blocking rules for the bootstrap with dependent data. *Biometrika* 82(3): 561-574.

- Hamed, K. H. and Rao, A. R. (1998). A modified Mann-Kendall trend test for autocorrelated data. *Journal of Hydrology* 204: 182-196.
- Hamlet, A. F. and Lettenmaier, D. P. (1999). Columbia River streamflow forecasting based on ENSO and PDO climate signals. *Journal of Water Resources Planning Management* 125(6): 333-341.
- Hargreaves, G. H. and Samani, Z. A. (1982). Estimating potential evapotranspiration. *J. Irrig. Drain. Div.* 108(3): 225-230.
- Harshburger, B., Ye, H. and Dzialoski, J. (2002). Observational evidence of the influence of Pacific SSTs on winter precipitation and spring stream discharge in Idaho. *Journal of Hydrology* 264: 157-169.
- Helsel, D. R., Mueller, D. K. and Slack, J. R. (2006). *Computer Program for the Kendall Family of Trend Tests: U.S. Geological Survey Scientific Investigations Report, P.4.*
- Hirsch, R. M., Slack, J. R. and Smith, R. A. (1982). Techniques of trend analysis for monthly water quality data. *Water Resources Research* 18: 107-121.
- Hirsch, R. M. and Slack, J. R. (1984). A nonparametric trend test for seasonal data with serial dependence. *Water Resources Research* 20: 727-732.
- Hirsh, R. M., Slack, J. R. and Smith, R. A. (1982). Techniques of trend analysis for monthly water quality data. *Water Resources Research* 18(107-121).
- Holman, I. P. (2006). Climate change impacts on groundwater recharge-uncertainty, shortcomings, and the way forward. *Hydrogeology Journal* 14: 637-647.
- Huntington, T. G. (2006). Evidence for intensification of the global water cycle: Review and synthesis. *Journal of Hydrology* 319: 83-95.
- IPCC. (1995). *Climate Change 1995: Second Assessment Report*, Intergovernmental Panel on Climate Change, 73pp.
- IPCC. (1997). *The Regional Impacts of Climate Change: An assessment of vulnerability*, in Watson, R. T., Zinyowrea, M. L. and Moss, R. H., eds., A Special Report of IPCC Working Group II, International Panel on Climate Change.
- IPCC. (2001a). *Climate Change 2001: Synthesis Report -- Summary for Policymakers*, Intergovernmental Panel on Climate Change, P.34pp.
- IPCC (2001b). *Climate Change 2001: The Scientific Basis*. Retrieved on February 15, 2007, from the World Wide Web, http://www.grida.no/climate/ipcc_tar/wg1/025.htm.
- IPCC. (2007a). *Climate Change 2007: Climate Change Impacts, Adaptation and Vulnerability*, Contribution of Working Group II to the Fourth Assessment Report of the Intergovernmental Panel on Climate Change, Intergovernmental Panel on Climate Change.
- IPCC (2007b). *Climate Change 2007: The Physical Basis*. Retrieved on February 15, 2007, from the World Wide Web, <http://www.ipcc.ch/>.
- IUCN, IWMI, Rasmussen Convention Bureau and WRI (2003). *Water Resources eAtlas*. Retrieved on July 5, 2007, from the World Wide Web, <http://www.iucn.org/themes/wani/eatlas/html/na9.html>.
- Jackson, R. B., Carpenter, S. R., Dahm, C. N., McKnight, D. M., Naiman, R. J., Postel, S. L. and Running, S. W. (2001). Water in a changing world. *Ecological Applications* 11(4): 1027-1045.
- John F. Kennedy School of Government (2001). *Chronology of the Climate Change Issue*, reprinted from the book *Learning to Manage Global Environmental Risks -- Volume 1: A Comparative History of Social Responses to Climate Change, Ozone Depletion, and Acid*

- Rain, by the Social Learning Group (MIT Press, 2001), and is reprinted by permission of the MIT Press. Retrieved on May 14, 2007, from the World Wide Web, http://www.ksg.harvard.edu/sl/docs/SL_Apdx2B.3_CCchronology.pdf.*
- Johnson, R. A. (2000). *Miller & Freund's Probability and Statistics for Engineers*, Prentice Hall, Upper Saddle River, New Jersey.
- Jones, R. N., Chiew, F. H. S., Boughton, W. C. and Zhang, L. (2006). Estimating the sensitivity of mean annual runoff to climate change using selected hydrological models. *Advances in Water Resources* 29: 1419-1429.
- Källberg, P., Berrisford, P., Hoskins, B., Simmons, A., Uppala, S., Lamy-Thépaut, S. and Hine, R. (2005). *ERA-40 Project Report Series No. 19*. Retrieved on July 15, 2007, from the World Wide Web, <http://www.ecmwf.int/publications/library/do/references/list/192>.
- Karabörk, M. C. (2007). Trends in drought patterns of Turkey. *J. Environ. Eng. Sci.* 6: 45-52.
- Karl, T. R. and Riebsame, W. E. (1989). The Impact of Decadal Fluctuations in Mean Precipitation and Temperature on Runoff: A Sensitivity Study Over the United States. *Climatic Change* 15: 423-447.
- Kendall, M. G. (1975). *Rank Correlation Methods*, Charles Griffin, London.
- Kingston, D. G., Lawler, D. M. and McGregor, G. R. (2006). Linkages between atmospheric circulation, climate and streamflow in the northern North Atlantic: research prospects. *Progress in Physical Geography* 30(2): 143-174.
- Kite, G. (1993). Analyzing Hydrometeorological Time-Series for Evidence of Climatic-change. *Nordic Hydrology* 24(2-3): 135-150.
- Kouwen, N. (1972). WATFLOOD, Hydrological Model Routing & Flow Forecasting System, University of Waterloo and Environment Canada.
- Kouwen, N., Soulis, E. D., Pietroniro, A., Donald, J. and Harrington, R. A. (1993). Grouped response units for distributed hydrologic modelling. *Journal of Water Resources Planning Management* 119(3): 289-305.
- Kouwen, N. (1996). WATFLOOD/ WATROUTE -- *Hydrological Model Routing & Flow Forecasting System*, Surveys and Information Branch -- Ecosystem Science and Evaluation Directorate, Environment Canada, P.1 - 217.
- Kouwen, N., Ritchie, H., Donaldson, N., Joe, P. and Soulis, E. D. (2000). Toward the Use of Coupled Atmospheric and Hydrologic Models at Regional Scale. *Monthly Weather Review* 128(6): 1681-1708.
- Kulkarni, A. and Von Storch, H. (1995). Monte Carlo experiments on the effect of serial correlation on the Mann-Kendall test of trend. *Meteorologische Zeitschrift* 4(2): 82-85.
- Kundzewicz, Z. W. and Robson, A. J. (2004). Change detection in hydrological records -- a review of the methodology. *Hydrological Sciences Journal* 49(1): 7-19.
- Kwong, Y. T. J. and Gan, T. Y. (1994). Northward Migration of Permafrost Along the Mackenzie Highway and Climatic Warming. *Climatic Change* 26(4): 399-419.
- Labat, D., Godd eris, Y., Probst, J. L. and Guyot, J. L. (2004). Evidence for global runoff increase related to climate warming. *Advances in Water Resources* 27: 631-642.
- Langbein, W. B. (1949). *Annual Runoff in the United States*, U.S. Geological Survey Circular 5, U.S. Department of Interior, Washington, DC.
- Legates, D. R., Lins, H. F. and McCabe, G. J. (2005). Comments on "Evidence for global runoff increase related to climate warming" by Labat et al. *Advances in Water Resources* 28: 1310-1315.
- Lettenmaier, D. P., Wood, E. F. and Wallis, J. R. (1994). Hydro-Climatological Trends in the

- Continental United States, 1948-88. *Journal of Climate* 7: 586-607.
- Lins, H. F. and Slack, J. R. (1999). Streamflow trends in the United States. *Geophysical Research Letters* 26(2): 227-230.
- Liu, J., Cho, H. R. and Stewart, R. E. (2002). Characteristics of the Water Vapour Transport over the Mackenzie River Basin during the 1994/95 Water Year. *Atmosphere-Ocean* 40(2): 101-111.
- Livezey, R. E. and Chen, W. Y. (1983). Statistical Field Significance and its Determination by Monte Carlo Techniques. *Monthly Weather Review* 111: 46-59.
- Loaiciga, H. A., Valdes, J. B., Vogel, R., Garvey, J. and Schwartz, H. (1996). Global warming and the hydrologic cycle. *Journal of Hydrology* 174: 83-127.
- Louie, P. Y. T., Hogg, W. D., MacKay, M. D., Zhang, X. and Hopkinson, R. F. (2002). The Water Balance Climatology of the Mackenzie Basin with Reference to the 1994/95 Water Year. *Atmosphere-Ocean* 40(2): 159-180.
- Loukas, A. and Quick, M. (1996). Effect of Climate Change on Hydrologic Regime of Two Climatically Different Watersheds. *Journal of Hydrologic Engineering* 1(2): 77-87.
- Loukas, A. and Quick, M. (1999). The effect of climate change on floods in British Columbia. *Nordic Hydrology* 30(3): 231-256.
- Mann, H. B. (1945). Nonparametric Tests Against Trend. *Econometrica* 13(3): 245-259.
- Mantua, N. J., Hare, S. R., Zhang, Y., Wallace, J. M. and Francis, R. C. (1997). A Pacific Interdecadal Climate Oscillation with Impacts on Salmon Production. *Bulletin of the American Meteorological Society* 78(6): 1069-1079.
- Matalas, N. C. and Langbein, W. B. (1962). Information content of the mean. *Journal of Geophysical Research* 67(9): 3441-3448.
- Matthews, D. (2006). The water cycle freshens up. *Nature* 439: 793-794.
- Merritt, W. S., Alila, Y., Barton, M., Taylor, B., Cohen, S. and Neilsen, D. (2006). Hydrologic response to scenarios of climate change in subwatersheds of the Okanagan basin, British Columbia. *Journal of Hydrology* 326(2006): 79-108.
- Merz, J., Nakarmi, G. and Weingartner, R. (2003). Potential solutions to water scarcity in the rural watersheds of Nepal's Middle Mountains. *Mountain Research and Development* 23(1): 14-18.
- Metcalfe, J. R., Ishida, S. and Goodison, B. E. (1994). *A corrected precipitation archive for the Northwest Territories Mackenzie Basin Impact Study Interim Report No. 2.*, Environment Canada, Downsview, Ontario, P.110-117.
- Mimikou, M. A., Baltas, E., Varanou, E. and Pantazis, K. (2000). Regional impacts of climate change on water resources quantity and quality indicators. *Journal of Hydrology* 234: 95-109.
- Mitchell, J. F. B. (1989). The "greenhouse" effect and climatic change. *Reviews of Geophysics* 27: 115-139.
- Mittelstaedt, M. (2007, June 4). *Canada's green record assailed.* Globe and Mail.
- MRBB (2001). *Mackenzie River Basin Board.* Retrieved on February 26, 2007, from the World Wide Web, <http://www.mrbb.ca/>.
- MRBB. (2004). *State of the Aquatic Ecosystem Report 2003*, Mackenzie River Basin Board.
- National Climate Data and Information Archive (2005). *2002 CD CD West CD* Meteorological Service of Canada [MSC], Environment Canada. Retrieved on October 1, 2005, from the World Wide Web, http://www.climate.weatheroffice.ec.gc.ca/prods_servs/cdcd_iso_e.html.

- Neal, E. G., Walter, M. T. and Coffeen, C. (2002). Linking the pacific decadal oscillation to seasonal stream discharge patterns in Southeast Alaska. *Journal of Hydrology* 263: 188-197.
- Neilsen Company and University of Oxford (2007). *Global Nielsen Survey: Consumers Look to Governments to Act on Climate Change*. Retrieved on June 9, 2007, from the World Wide Web, www.eci.ox.ac.uk/news/070605pr-nielsensurvey.pdf.
- Nemec, J. and Schaake, J. (1982). Sensitivity of Water Resources to Climate Variations. *Hydrological Sciences Journal* 27: 327-343.
- Nicholls, N., Gruza, G. V., Jouzel, J., Karl, T. R., Ogallo, L. A. and Parker, D. E. (1996). *Observed climate variability and change*, Houghton, J. T., ed., in *Climate Change 1995, The Science of Climate Change*, Cambridge University Press, New York, P.132-192.
- Nijssen, B., O'Donnell, G. M., Hamlet, A. F. and Lettenmaier, D. P. (2001). Hydrologic Sensitivity of Global Rivers to Climate Change. *Climatic Change* 50: 143-175.
- Norwich Union (2007). *What does the Climate Change Bill mean for businesses*. Retrieved on March 15, 2007, from the World Wide Web, <http://www.nurs.co.uk/news/articles/cms/1173955410212694732418.htm>.
- Official Tourism Site of British Columbia (2007). *Northern British Columbia*. Retrieved on September 1, 2007, from the World Wide Web, <http://www.hellobc.com/en-CA/SightsActivitiesEvents/Attractions/BridgesBuildingsStructures/NorthernBritishColumbia.htm>.
- Önöz, B. and Bayazit, M. (2002). The Power of Statistical Tests for Trend Detection. *Turkish J. Eng. Evn. Sci.* 27: 247-251.
- Overpeck, J., Hughen, K., Hardy, D., Bradley, R., Case, R., Douglas, M., Finney, B., Gajewski, K., Jacoby, G., Jennings, A., Lamoureux, S. L., A., MacDonald, G., Moore, J., Retelle, M., Smith, S., Wolfe, A. and Zielinski, G. (1997). Arctic environmental change of the last four centuries. *Science* 278(5341): 1251-1256.
- PEW Center on Global Climate Change (2004). *Climate Change: Overcoming the Barriers to Action*. Retrieved on February 1, 2007, from the World Wide Web, http://www.pewclimate.org/press_room/speech_transcripts/overcoming_barriers.cfm.
- Priestley, C. H. B. and Taylor, R. J. (1972). On the assessment of surface heat flux and evaporation using large-scale parameters. *Monthly Weather Review* 100(2): 81-92.
- Radziejewski, M. and Kundzewicz, Z. W. (2004). Detectability of changes in hydrological records. *Hydrological Sciences Journal* 49(1): 39-51.
- Raschke, K. and Kühl, U. (1969). Stomatal Responses to Changes in Atmospheric Humidity and Water Supply: Experiments with Leaf Sections of Zea mays in CO₂-Free Air. *Planta* 87(1-2): 36-48.
- Redmond, K. T. and Koch, R. W. (1991). Surface climate and streamflow variability in the western United States and their relationship to large-scale circulation indices. *Water Resources Research* 27(9): 2381-2399.
- Revelle, R. R. and Waggoner, P. E. (1983). *Effect of a Carbon Dioxide-Induced Climatic Change on Water Supplies in the Western United States*, in *Changing Climate*, Report of the Carbon Dioxide Assessment Committee, National Academy Press, Washington, DC, P.419-431.
- Rizzo, B. and Wiken, E. (1992). Assessing the sensitivity of Canada's ecosystems to climatic change. *Climatic Change* 21: 37-55.
- Robson, A. J., Jones, T. K., Reed, D. W. and Bayliss, A. C. (1998). A Study of National Trend

- and Variation in UK Floods. *International Journal of Climatology* 18: 165-182.
- Salas, J. D., Delleur, J. W., Yevjevich, V. and Lane, W. L. (1980). *Applied Modeling of Hydrologic Time Series*, Water Resources Publications, Littleton, CO, USA.
- Sankarasubramanian, A., Vogel, R. M. and Limbrunner, J. F. (2001). Climate elasticity of streamflow in the United States. *Water Resources Research* 37(6): 1771-1781.
- Scafetta, N. and West, B. J. (2006). Phenomenological solar contribution to the 1900-2000 global surface warming. *Geophysical Research Letters* 33: L05708.
- Schindler, D. W. (2001). The cumulative effects of climate warming and other human stresses on Canadian freshwaters in the new millennium. *Canadian Journal of Fish and Aquatic Science* 58: 18-29.
- Searcy, C., Dean, K. and Stringer, W. (1996). A river-coastal sea ice interaction model: Mackenzie River delta. *Journal of Geophysical Research* 101(C4): 8885-8894.
- Seber, G. A. F. (1982). *The Estimation of Animal Abundance*, Macmillan, New York.
- Serreze, M. C., Walsh, J. E., Chapin III, F. S., Osterkamp, T., Dyurgerov, M., Romanovsky, V., Oechel, W. C., Morison, J., Zhang, T. and Barry, R. G. (2000). Observational evidence of recent change in northern high-latitude environment. *Climatic Change* 46: 159-207.
- Shabbar, A., Bonsal, B. R. and Khandekar, M. (1997). Canadian precipitation patterns associated with the Southern Oscillation. *Journal of Climate* 10: 3016-3027.
- Singh, P., Arora, M. and Goel, N. K. (2006). Effect of climate change on runoff of a glacierized Himalayan basin. *Hydrological Processes* 20: 1979-1992.
- Smith, R. L. and Smith, T. M. (2000). *Element of Ecology*, Addison Wesley Longman, Inc., San Francisco, United States.
- Soulis, E. D., Solomon, S. I., Lee, M. and Kouwen, N. (1994). Changes to the Distribution of Monthly and Annual Runoff in the Mackenzie Basin Under Climate Change using a Modified Square Grid Approach. *Mackenzie Basin Impact Study (MBIS) Intermin Report #2*.
- Soulis, E. D., Kouwen, N., Pietroniro, A., Seglenieks, F. R., Snelgrove, K. R., Peller, P., Shaw, D. W. and Martz, L. W. (2005). *A Framework for Hydrological Modelling in MAGS*. Retrieved on September 15, 2005, from the World Wide Web, http://www.cwra.org/Publications/CWRA_-_Bookstore/PUB_Workshop/07_Soulis.pdf.
- Soulis, E. D. (2007). *Personal communication about water budget in the Mackenzie River Basin*, July 10, 2007
- Soulis, E. D. and Seglenieks, F. R. (2007). The MAGS Integrated Modeling System. In *Cold Region Atmospheric and Hydrologic Studies. The Mackenzie GEWEX Experience. Volume 2: Hydrologic Processes*, Springer Berlin Heidelberg, P. 445-473.
- Sparks, T. H. (2007). Lateral thinking on data to identify climate impacts. *Trends in Ecology and Evolution* 22(4): 169-171.
- Spence, C. (2002). Streamflow Variability (1965-1998) in Five Northwest Territories and Nunavut Rivers. *Canadian Water Resources Journal* 27(2): 135-154.
- Spence, C., Saso, P. and Rausch, J. (2007). Quantifying the Impact of Hydrometric Network Reductions on Regional Streamflow Prediction in Northern Canada. *Canadian Water Resources Journal* 32(1): 1-20.
- Steffen, W. (2006). The Arctic in an Earth System Context: From Brake to Accelerator of Change. *Ambio* 35(4): 153-159.
- Stern, N. (2006). *Stern Review on the Economics of Climate Change*. Retrieved on May 4, 2007, from the World Wide Web, <http://www.hm->

treasury.gov.uk/independent_reviews/stern_review_economics_climate_change/sternreview_index.cfm.

- Stewart, R. E., Leighton, H. G., Marsh, P., Moore, G. W. K., Ritchie, H., Rouse, W. R., Soulis, E. D., Strong, G. S., Crawford, R. W. and Kochtubajda, B. (1998). The Mackenzie GEWEX Study: The Water and Energy Cycles of a Major North American River Basin. *Bulletin of the American Meteorological Society* 1998: 2665-2693.
- Stewart, R. E., Bussi eres, N., Cao, Z., Cho, H. R., Hudak, D. R., Kochtubajda, B., Leighton, H. G., Louie, P. Y. T., MacKay, M. D., Marsh, P., Strong, G. S., Szeto, K. K. and Burford, J. E. (2002). Hydrometeorological Features of the Mackenzie Basin Climate System during the 1994/95 Water year: A Period of Record Low Discharge. *Atmosphere-Ocean* 40(2): 257-278.
- Stockton, C. W. and Boggess, W. R. (1979). *Geohydrological Implication of Climate Change on Water Resource Development*, U.S Army Coastal Engineering Research Center, Ft. Belvoir, VA, and University of Arizona, Tucson, AZ, P.206.
- Sung, R. Y.-J., Burn, D. H. and Soulis, E. D. (2006). A Case Study of Climate Change Impacts on Navigation on the Mackenzie River. *Canadian Water Resources Journal* 31(1): 57-68.
- Tchobanoglous, G. and Schroeder, E. D. (1985). *Water Quality*, Addison-Wesley Publishing Company, Inc., United States.
- Tett, S. F. B., Jones, G. S., Stott, P. A., Hill, D. C., Mitchell, J. F. B., Allen, M. R., William, J. I., Johns, T. C., Johnson, C. E., Jones, A., Roberts, D. L., Sexton, D. M. H. and Woodage, M. J. (2002). Estimation of natural and anthropogenic contributions to twentieth century temperature change. *Journal of Geophysical Research* 107(D16): 10-1--10-24.
- Theibaux, H. J. and Zwiers, F. W. (1984). The interpretation and estimation of effective sample size. *Journal of Climate and Applied Meteorology* 23: 800-811.
- Toth, B., Pietroniro, A., Conly, F. M. and Kouwen, N. (2006). Modelling climate change impacts in the Peace and Athabasca catchment and delta: I - hydrological model application. *Hydrological Processes* 20(19): 4197-4214.
- Trenberth, K. E. (1998). Atmospheric moisture residence times and cycling: Implication for rainfall rates and climate change. *Climate Change* 39: 667-694.
- Tynan, C. T. and Demaster, D. P. (1997). Observations and predictions of Arctic climatic change: potential effects on marine mammals. *Arctic* 50(4): 308-336.
- U.S. EPA (2007). *Health and Environmental Effects*. United States Environmental Protection Agency. Retrieved on May 16, 2007, from the World Wide Web, <http://www.epa.gov/climatechange/effects/index.html>.
- UNFCCC (2007). *United Nations Framework Convention on Climate Change*. Retrieved on September 1, 2006, from the World Wide Web, <http://unfccc.int/2860.php>.
- USDA (2005). *What is ENSO*. Retrieved on September 9, 2005, from the World Wide Web, <http://www.csr1.ars.usda.gov/wewc/enso&ag/ensoinfo.htm>.
- USGCRP (2000). *Climate Change Impacts on the United States -- The Potential Consequences of Climate Variability and Change*. Retrieved on January 15, 2007, from the World Wide Web, <http://www.usgcrp.gov/usgcrp/Library/nationalassessment/overview.htm>.
- Viau, E. A. (2003). *Solar Energy for Your World*. Retrieved on May 13, 2007, from the World Wide Web, <http://curriculum.calstatela.edu/courses/builders/lessons/less/biomes/SunEnergy.html>.
- Vincent, L. A. and Mekis,  . (2006). Changes in Daily and Extreme Temperature and

- Precipitation Indices for Canada over the Twentieth Century. *Atmosphere-Ocean* 44(2): 177-193.
- Voisin, N., Leighton, H. G., Soulis, E. D. and Feng, J. (2002) Sensitivity of the Mackenzie River Hydrology to Solar Radiation Uncertainties. *59th Eastern Snow Conference*, Stowe, Vermont, USA.
- Von Storch, H. (1995). Misuses of statistical analysis in climate research. *Analysis of Climate Variability: Applications of Statistical Techniques*, Von Storch, H. and Navarra, A., eds., Springer-Verlag Berlin, 11-26.
- Walsh, J. E., Zhou, X., Portisi, D. and Serreze, M. C. (1994). Atmospheric Contribution to Hydrologic Variations in the Arctic. *Atmosphere-Ocean* 32(4): 733-755.
- Weart, S. and American Institute of Physics (2007). *The Carbon Dioxide Greenhouse Effect*. Retrieved on May 15, 2007, from the World Wide Web, <http://www.aip.org/history/climate/co2.htm>.
- Westmacott, J. R. and Burn, D. H. (1997). Climate change effects on the hydrologic regime within the Churchill-Nelson River Basin. *Journal of Hydrology* 202: 263-279.
- White, D. M., Strang, E. T., Alessa, L., Hinzman, L. and Kliskey, A. (2005). The Potential Impacts of Climate Change on the Quality and Quantity of Freshwater Available to Humans in the Arctic. *American Geophysical Union. ABSTRACT*, 2005AGUFM.U41A0801W.
- WHO (2007). *World Health Organization*. Retrieved on May 21, 2007, from the World Wide Web, <http://www.who.int/en/>.
- Wigley, T. M. L. and Jones, P. D. (1985). Influences of Precipitation Changes and Direct CO₂ Effects on Streamflow. *Nature* 314: 140-152.
- Wikipedia (2007a). *Climate Change*. Retrieved on May 4, 2007, from the World Wide Web, http://en.wikipedia.org/wiki/Climate_change.
- Wikipedia (2007b). *Kyoto Protocol*. Retrieved on May 4, 2007, from the World Wide Web, http://en.wikipedia.org/wiki/Kyoto_Protocol.
- Wikipedia (2007c). *Guy Stewart Callendar*. Retrieved on May 14, 2007, from the World Wide Web, <http://en.wikipedia.org/wiki/Callendar>.
- Woo, M. K. and Thorne, R. (2003). Streamflow in the Mackenzie Basin, Canada. *Arctic* 56(4): 328-340.
- Woo, M. K. and Marsh, P. (2005). Snow, frozen soils and permafrost hydrology in Canada, 1999 - 2002. *Hydrological Processes* 19: 215-229.
- WRI (2007a). *Watersheds of the World: North and Central America -- Mackenzie Watershed*. Retrieved on June 2, 2007, from the World Wide Web, http://earthtrends.wri.org/maps_spatial/maps_detail_static.php?map_select=387&theme=2.
- WRI (2007b). *Water Resource Institute*. Retrieved on February 1, 2007, from the World Wide Web, <http://www.wri.org>.
- Xu, C. Y. (1999). Climate Change and Hydrologic Models: Review of Existing Gaps and Recent Research Developments. *Water Resources Management* 13: 369-382.
- York, G. (2007, February 3). *A canary in the Chinese coal mine*. Globe and Mail.
- Yue, S., Pilon, P., Phinney, B. and Cavadias, G. (2001) Patterns of Trend in Canadian Streamflow. *58th Eastern Snow Conference*, Ottawa, Ontario, Canada.
- Yue, S., Pilon, P. and Cavadias, G. (2002a). Power of the Mann-Kendall and Spearman's rho tests for detecting monotonic trends in hydrological series. *Journal of Hydrology* 259:

254-271.

- Yue, S., Pilon, P., Phinney, B. and Cavadias, G. (2002b). The influence of autocorrelation on the ability to detect trend in hydrological series. *Hydrological Processes* 16: 1807-1829.
- Yue, S. and Wang, C. Y. (2002). Applicability of prewhitening to eliminate the influence of serial correlation on the Mann-Kendall test. *Water Resources Research* 38(6): 4-1--4-7.
- Yue, S. and Pilon, P. (2004). A comparison of the power of the t test, Mann-Kendall and bootstrap tests for trend detection. *Hydrological Sciences Journal* 49(1): 21-37.
- Yue, S. and Wang, C. Y. (2004). The Mann-Kendall Test Modified by Effective Sample Size to Detect Trend in Serially Correlated Hydrological Series. *Water Resources Management* 18: 201-218.
- Yulianti, J. S. and Burn, D. H. (1998). Investigating Links Between Climatic Warming and Low Streamflow in the Prairies Region of Canada. *Canadian Water Resources Journal* 23(1): 45-60.
- Zabarenko, D. (2007, February 3). *Scientist bribes denied*. Toronto Star.
- Zhang, X., Vincent, L. A., Hogg, W. D. and Niitsoo, A. (2000). Temperature and Precipitation Trends in Canada During the 20th Century. *Atmosphere-Ocean* 38(3): 395-429.
- Zhang, X., Harvey, K. D., Hogg, W. D. and Yuzyk, T. R. (2001a). Trends in Canadian streamflow. *Water Resources Research* 37(4): 987-998.
- Zhang, X., Hogg, W. D. and Mekis, É. (2001b). Spatial and Temporal Characteristics of Heavy Precipitation Events over Canada. *Journal of Climate* 14: 1923-1936.

Appendix A

Box plots of estimated monthly trend magnitude

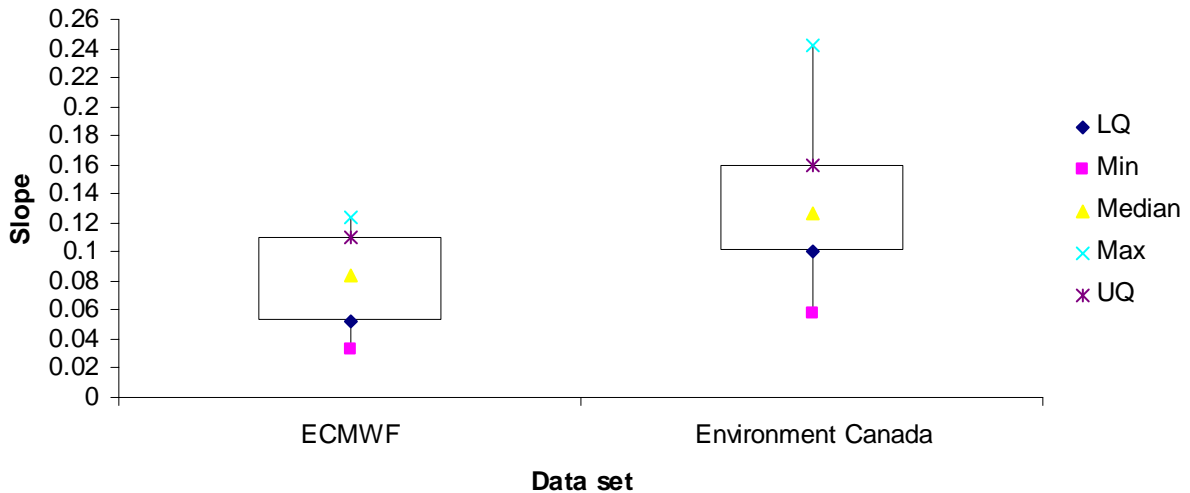


Figure A-1 Box plots of 4635 estimated trend magnitude for January temperature records (in °C/year)

Note: The boxes show the first quartile, median, and the third quartile, which contains 50% of the values. The whiskers extend from the box to the five and 95 percentiles.

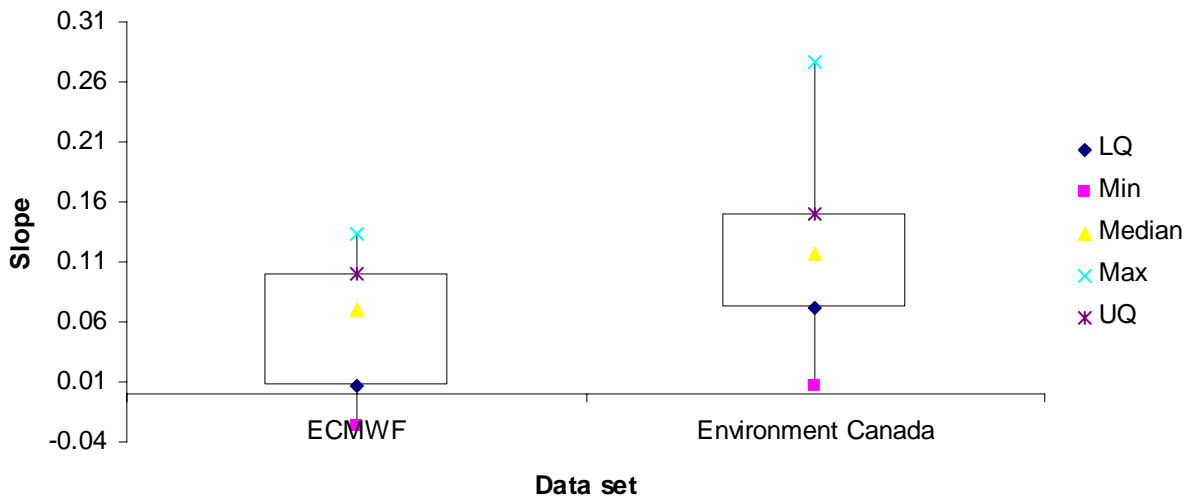


Figure A-2 Box plots of 4635 estimated trend magnitude for February temperature records (in °C/year)

Note: The boxes show the first quartile, median, and the third quartile, which contains 50% of the values. The whiskers extend from the box to the five and 95 percentiles.

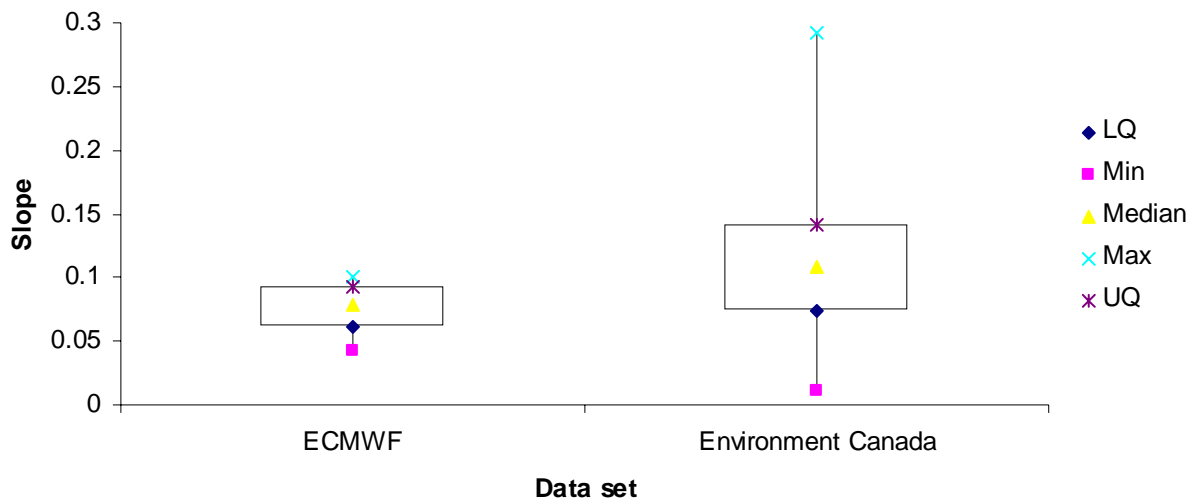


Figure A-3 Box plots of 4635 estimated trend magnitude for March temperature records (in °C/year)

Note: The boxes show the first quartile, median, and the third quartile, which contains 50% of the values. The whiskers extend from the box to the five and 95 percentiles.

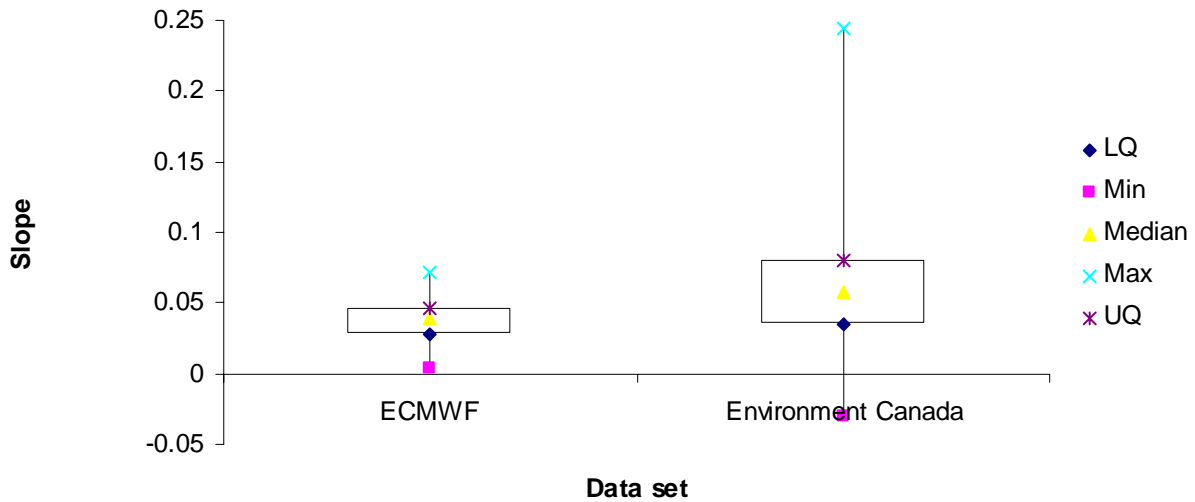


Figure A-4 Box plots of 4635 estimated trend magnitude for April temperature records (in °C/year)

Note: The boxes show the first quartile, median, and the third quartile, which contains 50% of the values. The whiskers extend from the box to the five and 95 percentiles.

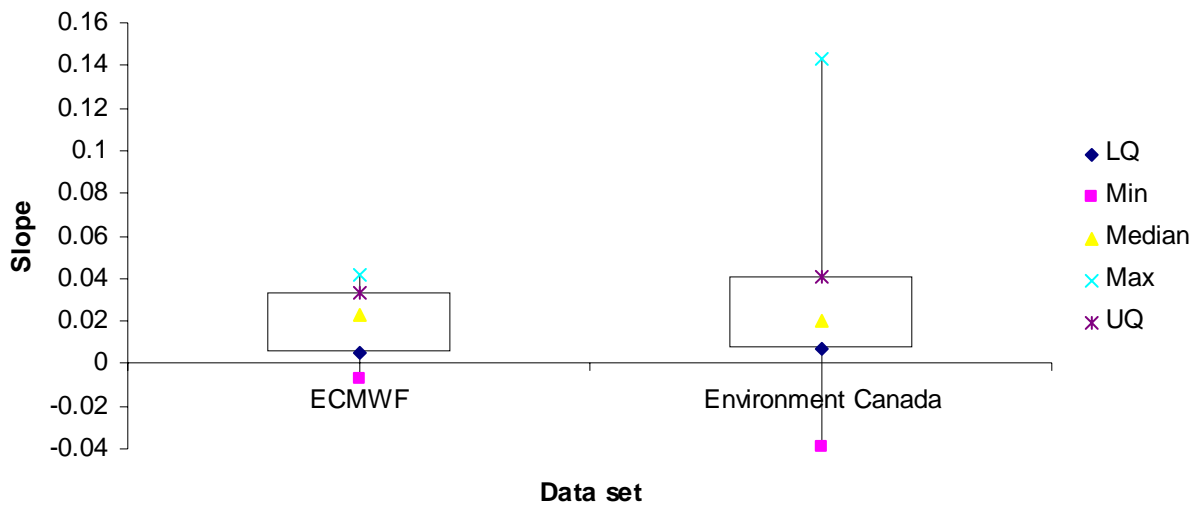


Figure A-5 Box plots of 4635 estimated trend magnitude for May temperature records (in °C/year)

Note: The boxes show the first quartile, median, and the third quartile, which contains 50% of the values. The whiskers extend from the box to the five and 95 percentiles.

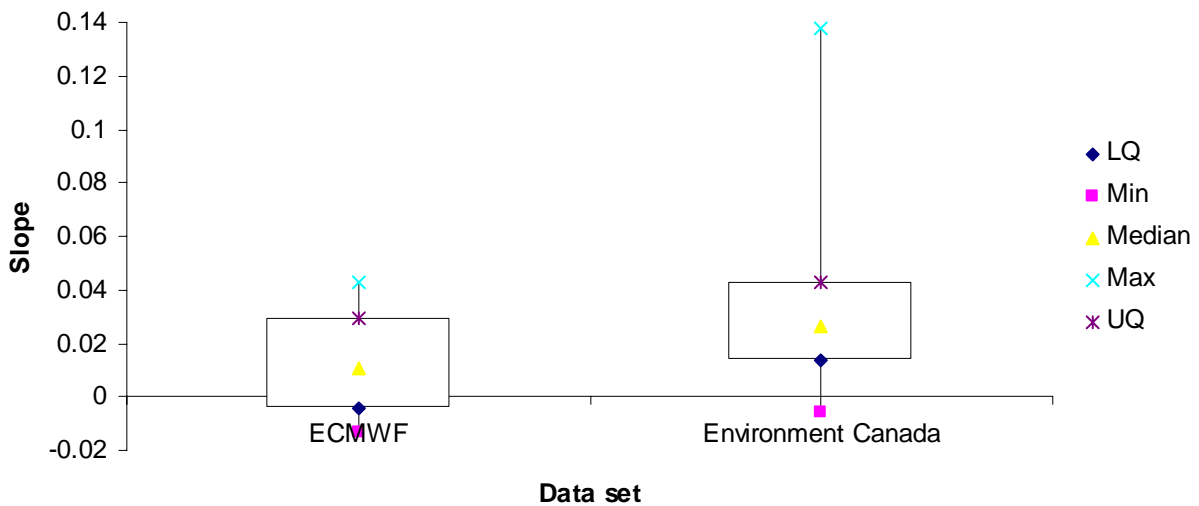


Figure A-6 Box plots of 4635 estimated trend magnitude for June temperature records (in °C/year)

Note: The boxes show the first quartile, median, and the third quartile, which contains 50% of the values. The whiskers extend from the box to the five and 95 percentiles.

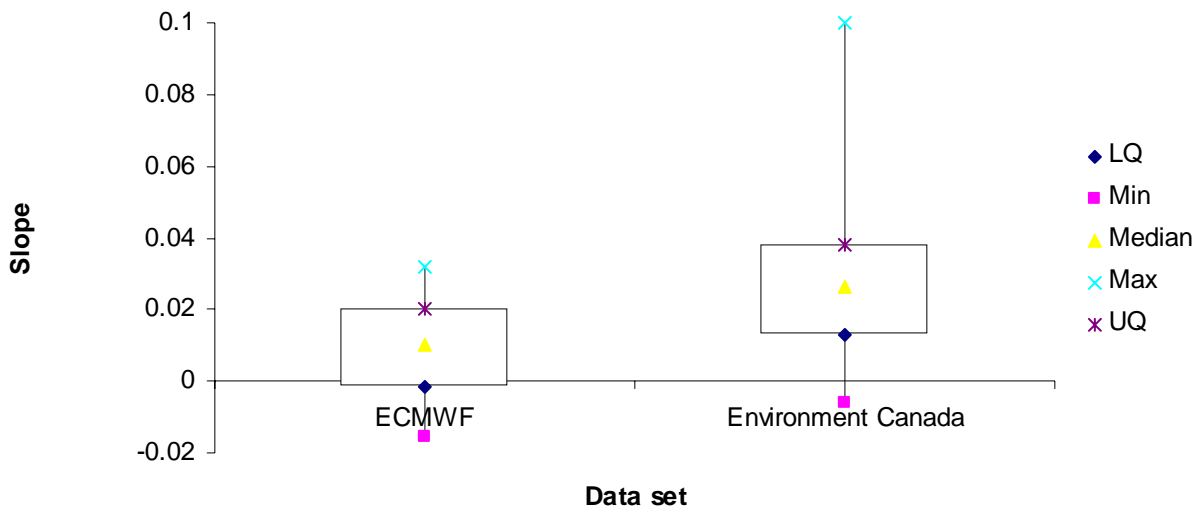


Figure A-7 Box plots of 4635 estimated trend magnitude for July temperature records (in °C/year)

Note: The boxes show the first quartile, median, and the third quartile, which contains 50% of the values. The whiskers extend from the box to the five and 95 percentiles.

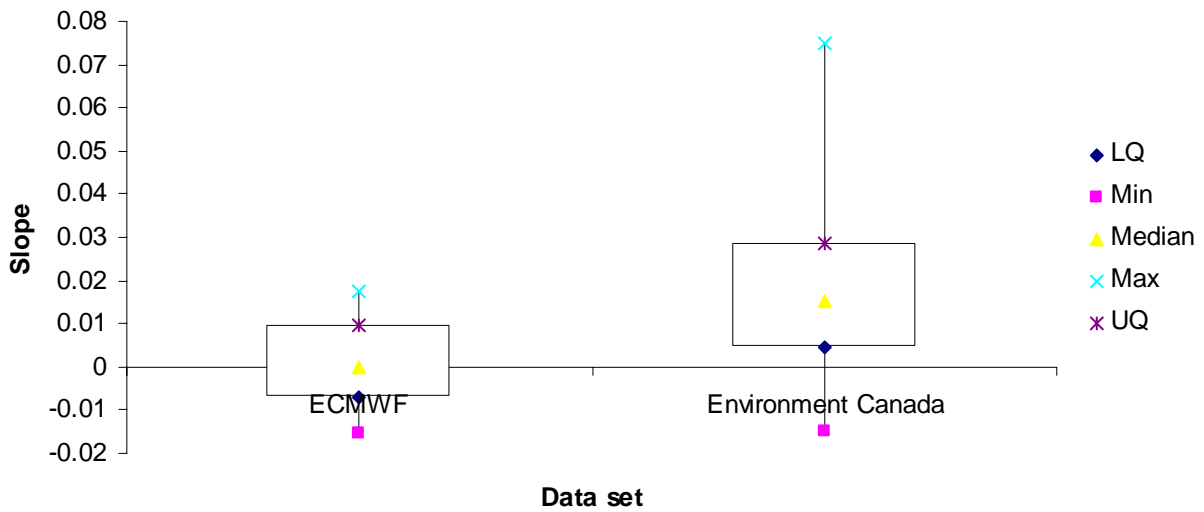


Figure A-8 Box plots of 4635 estimated trend magnitude for August temperature records (in °C/year)

Note: The boxes show the first quartile, median, and the third quartile, which contains 50% of the values. The whiskers extend from the box to the five and 95 percentiles.

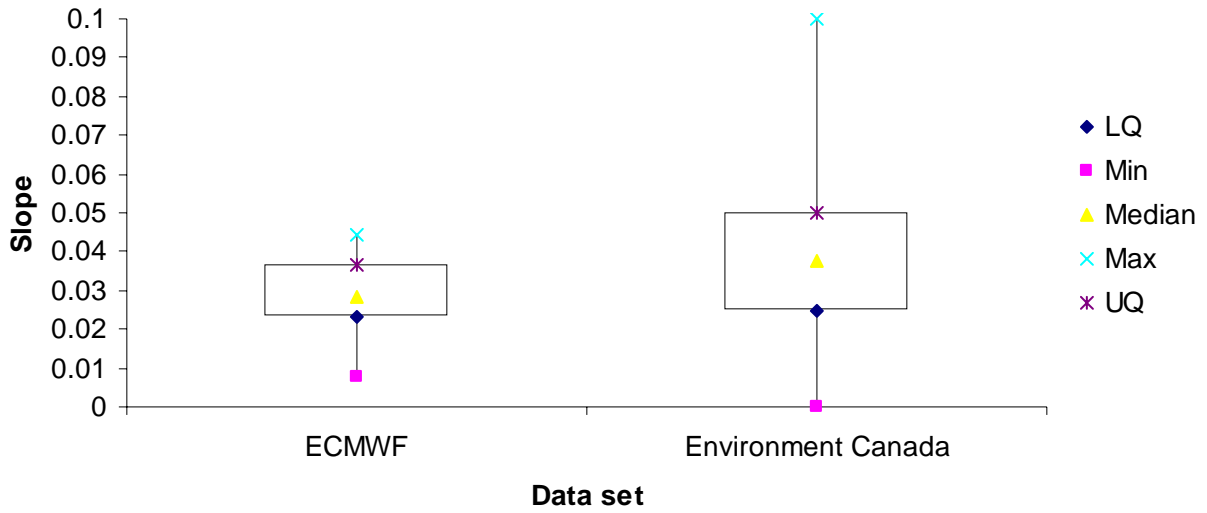


Figure A-9 Box plots of 4635 estimated trend magnitude for September temperature records (in °C/year)

Note: The boxes show the first quartile, median, and the third quartile, which contains 50% of the values. The whiskers extend from the box to the five and 95 percentiles.

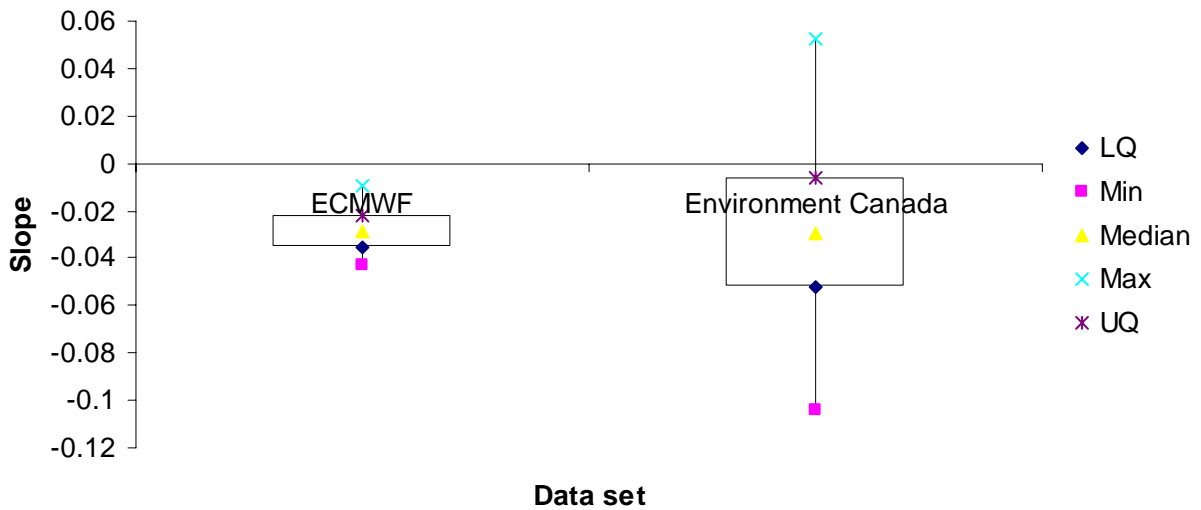


Figure A-10 Box plots of 4635 estimated trend magnitude for October temperature records (in °C/year)

Note: The boxes show the first quartile, median, and the third quartile, which contains 50% of the values. The whiskers extend from the box to the five and 95 percentiles.

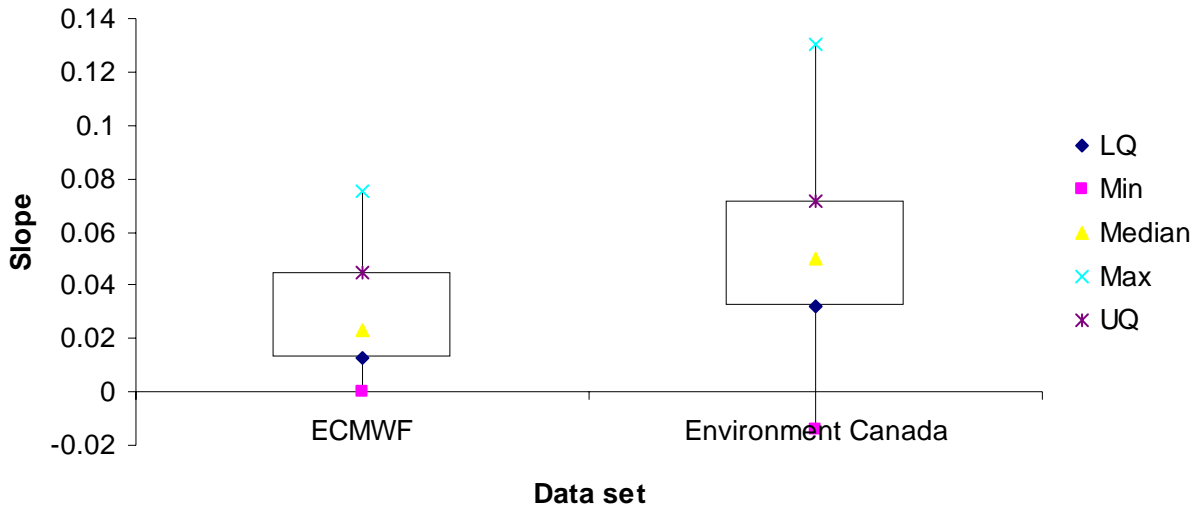


Figure A-11 Box plots of 4635 estimated trend magnitude for November temperature records (in °C/year)

Note: The boxes show the first quartile, median, and the third quartile, which contains 50% of the values. The whiskers extend from the box to the five and 95 percentiles.

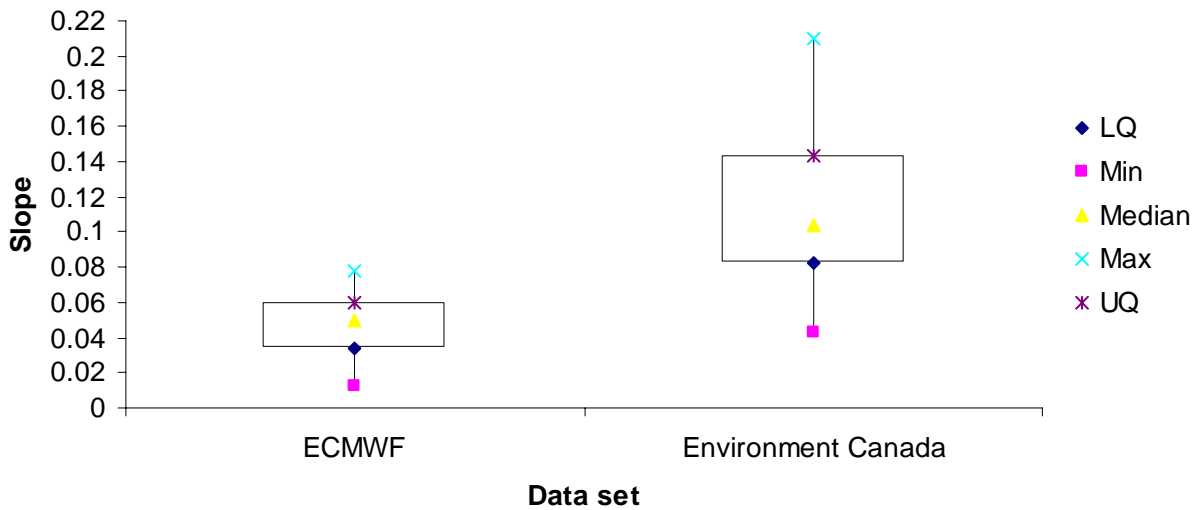


Figure A-12 Box plots of 4635 estimated trend magnitude for December temperature records (in °C/year)

Note: The boxes show the first quartile, median, and the third quartile, which contains 50% of the values. The whiskers extend from the box to the five and 95 percentiles.

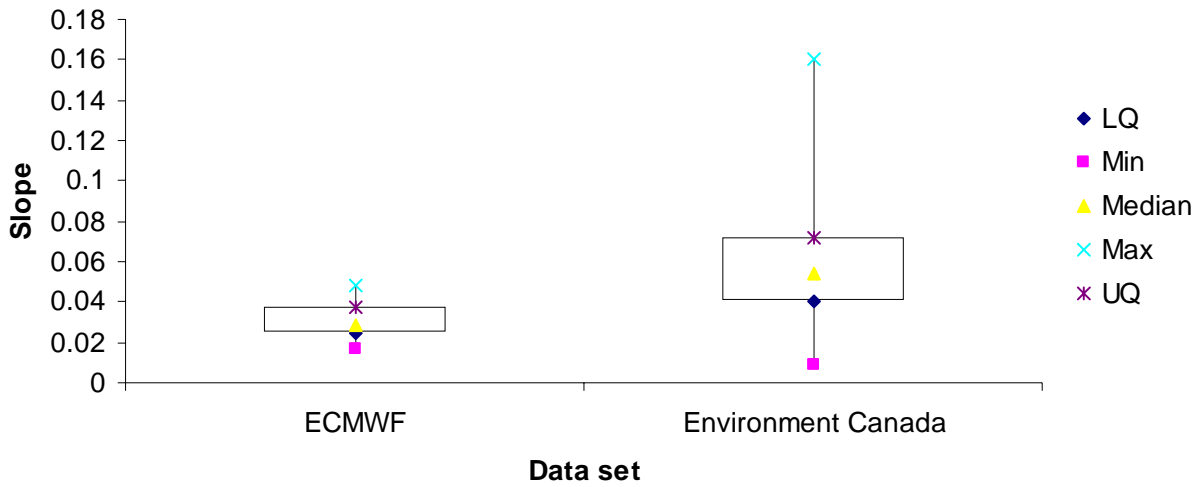


Figure A-13 Box plots of 4635 estimated trend magnitude for annual temperature records (in $^{\circ}\text{C}/\text{year}$)

Note: The boxes show the first quartile, median, and the third quartile, which contains 50% of the values. The whiskers extend from the box to the five and 95 percentiles.

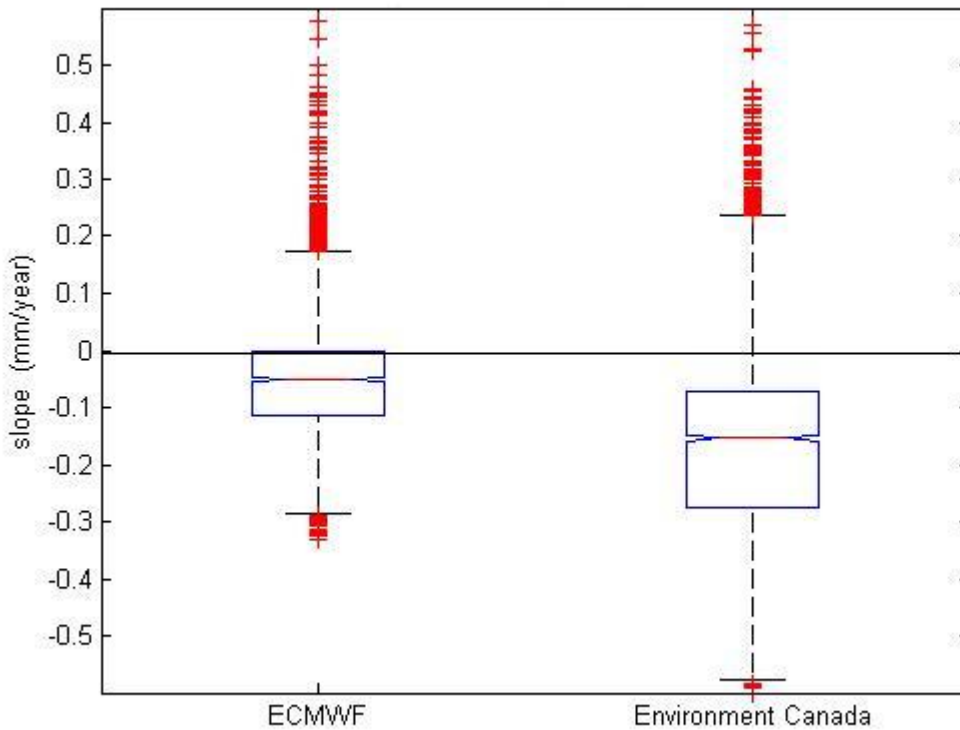


Figure A-14 Box plots of 4667 estimated trend magnitude for January precipitation records (in mm/year)

Note: The boxes show the first quartile, median, and the third quartile, which contains 50% of the values. The whiskers extend from the box to the highest and lowest values, excluding outliers.

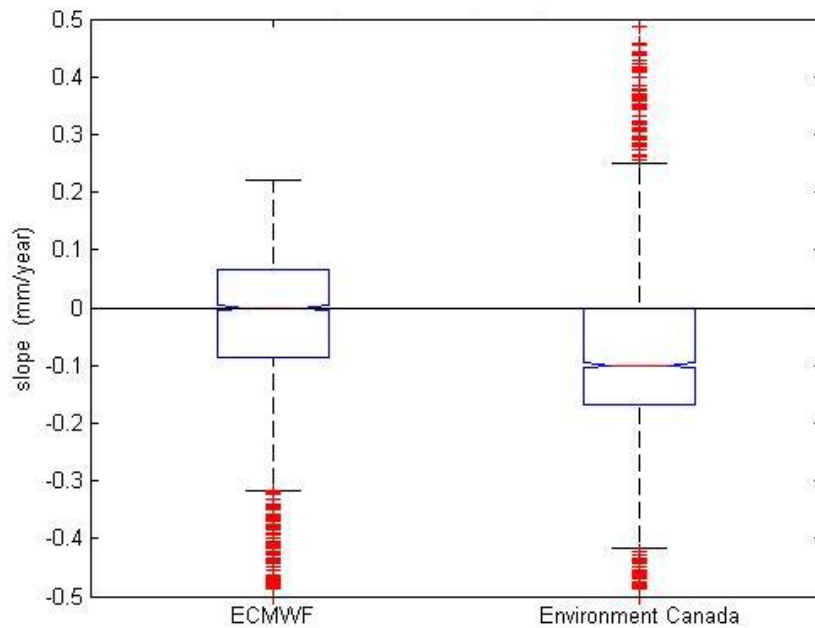


Figure A-15 Box plots of 4667 estimated trend magnitude for February precipitation records (in mm/year)

Note: The boxes show the first quartile, median, and the third quartile, which contains 50% of the values. The whiskers extend from the box to the highest and lowest values, excluding outliers.

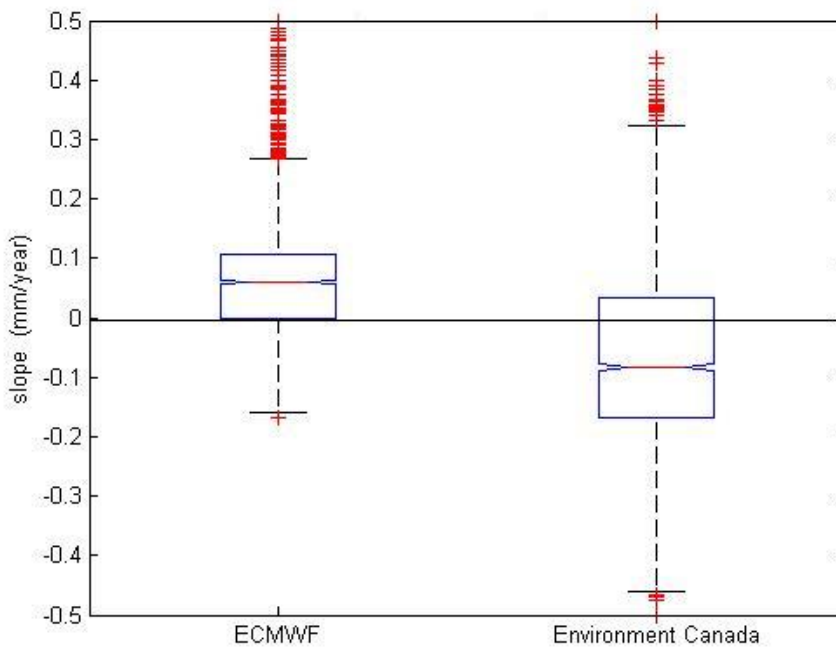


Figure A-16 Box plots of 4667 estimated trend magnitude for March precipitation records (in mm/year)

Note: The boxes show the first quartile, median, and the third quartile, which contains 50% of the values. The whiskers extend from the box to the highest and lowest values, excluding outliers.

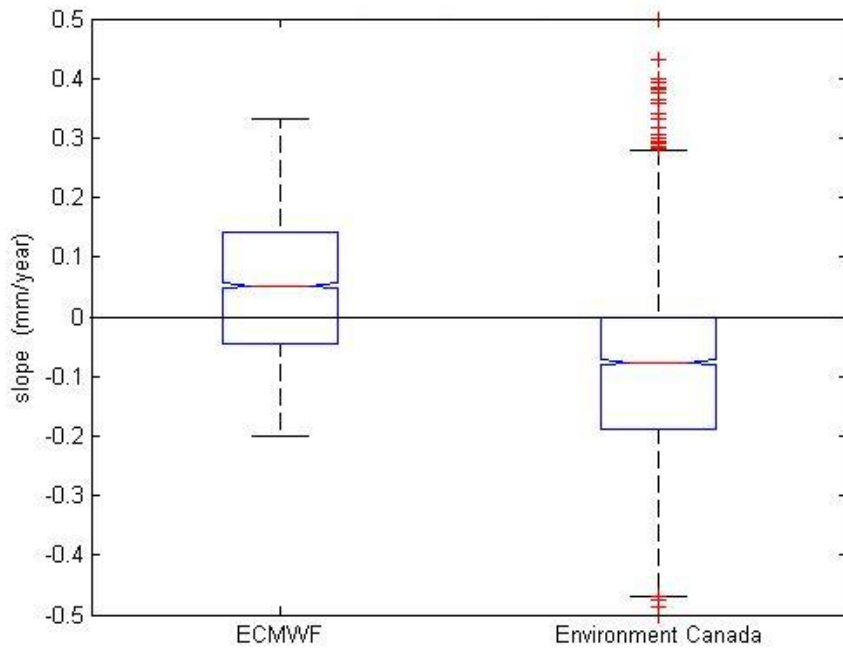


Figure A-17 Box plots of 4667 estimated trend magnitude for April precipitation records (in mm/year)

Note: The boxes show the first quartile, median, and the third quartile, which contains 50% of the values. The whiskers extend from the box to the highest and lowest values, excluding outliers.

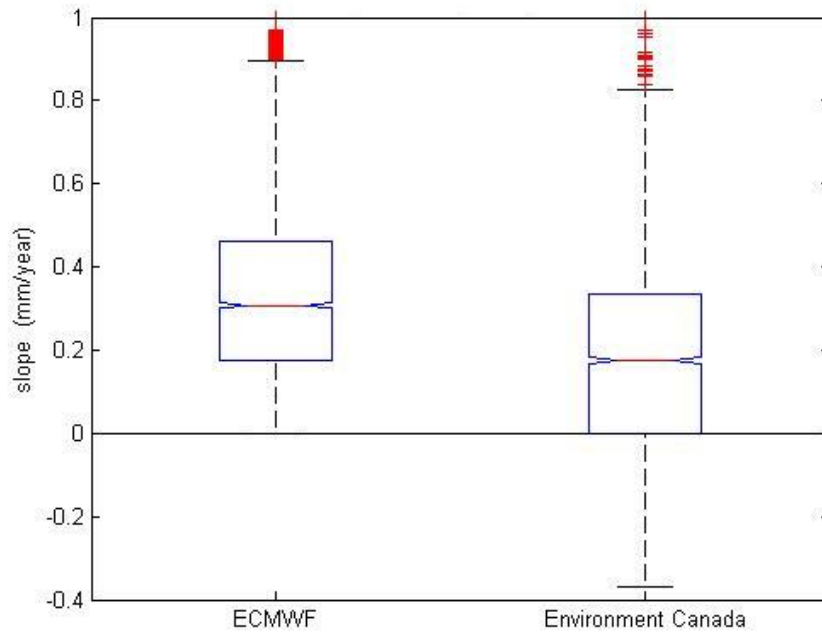


Figure A-18 Box plots of 4667 estimated trend magnitude for May precipitation records (in mm/year)

Note: The boxes show the first quartile, median, and the third quartile, which contains 50% of the values. The whiskers extend from the box to the highest and lowest values, excluding outliers.

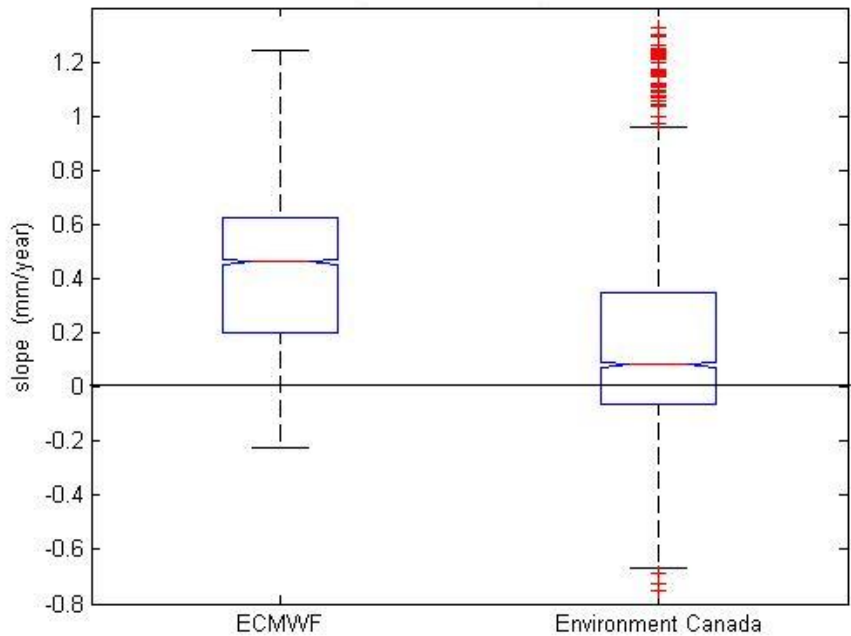


Figure A-19 Box plots of 4667 estimated trend magnitude for June precipitation records (in mm/year)

Note: The boxes show the first quartile, median, and the third quartile, which contains 50% of the values. The whiskers extend from the box to the highest and lowest values, excluding outliers.

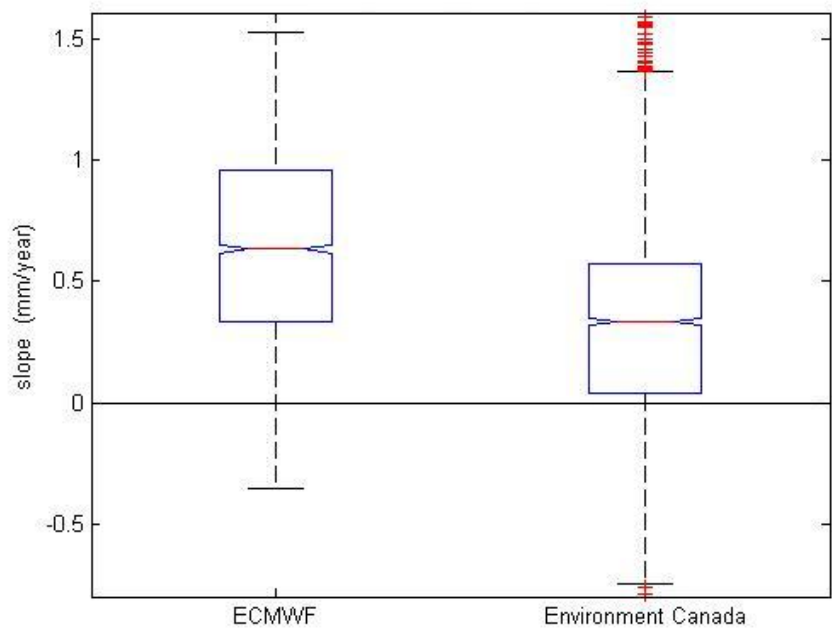


Figure A-20 Box plots of 4667 estimated trend magnitude for July precipitation records (in mm/year)

Note: The boxes show the first quartile, median, and the third quartile, which contains 50% of the values. The whiskers extend from the box to the highest and lowest values, excluding outliers.

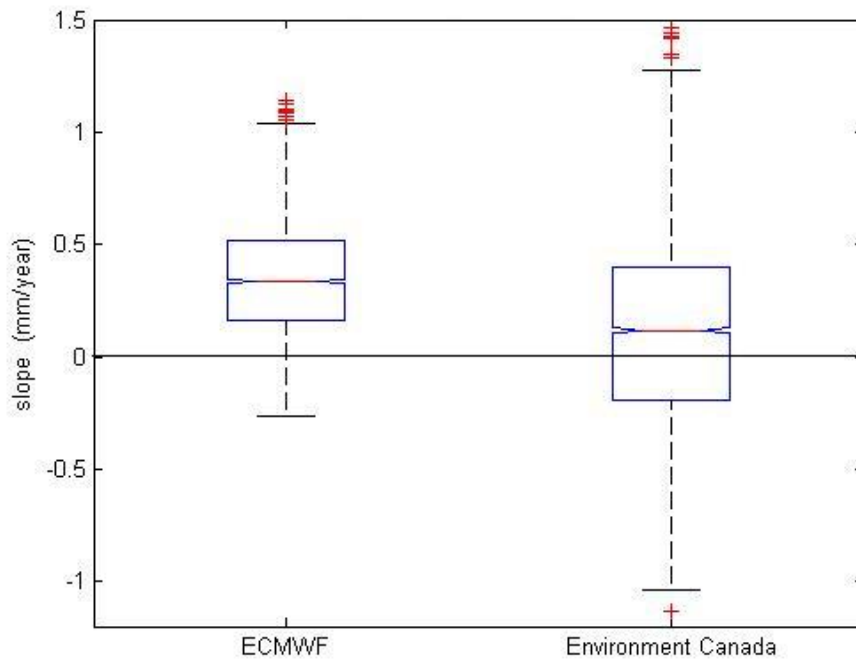


Figure A-21 Box plots of 4667 estimated trend magnitude for August precipitation records (in mm/year)

Note: The boxes show the first quartile, median, and the third quartile, which contains 50% of the values. The whiskers extend from the box to the highest and lowest values, excluding outliers.

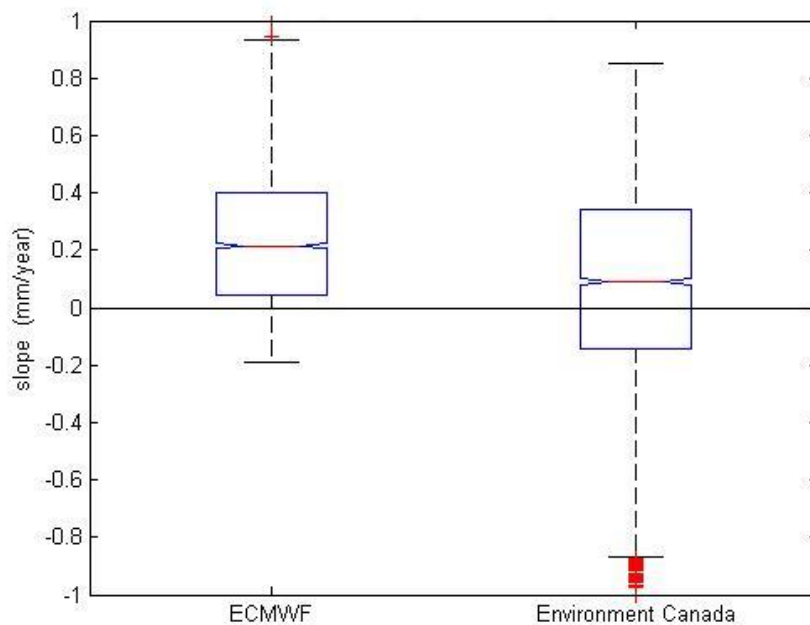


Figure A-22 Box plots of 4667 estimated trend magnitude for September precipitation records (in mm/year)

Note: The boxes show the first quartile, median, and the third quartile, which contains 50% of the values. The whiskers extend from the box to the highest and lowest values, excluding outliers.

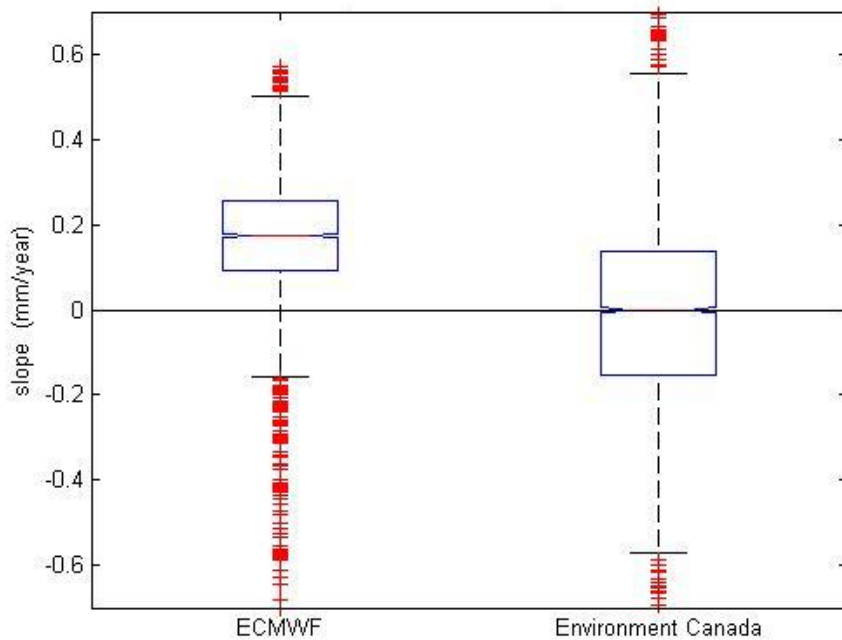


Figure A-23 Box plots of 4667 estimated trend magnitude for October precipitation records (in mm/year)

Note: The boxes show the first quartile, median, and the third quartile, which contains 50% of the values. The whiskers extend from the box to the highest and lowest values, excluding outliers.

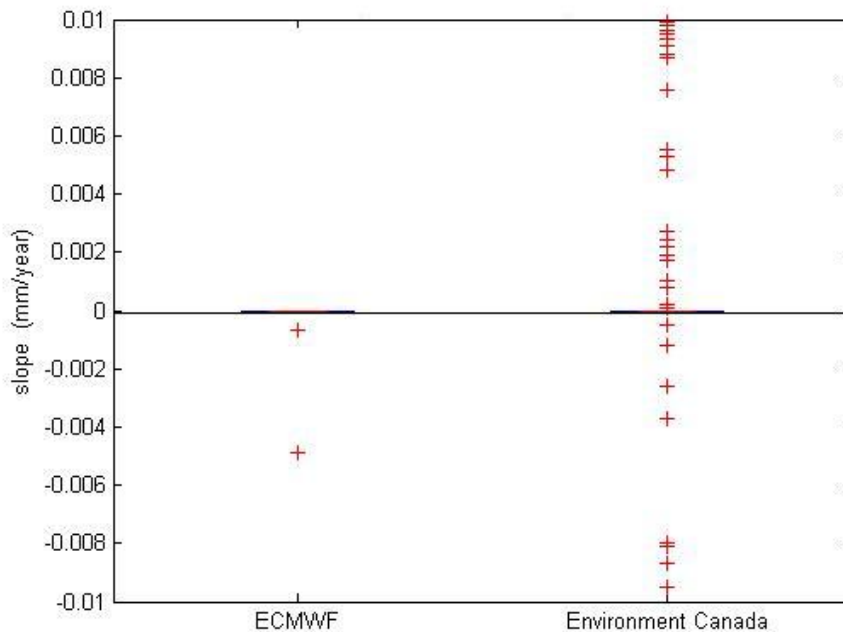


Figure A-24 Box plots of 4667 estimated trend magnitude for November precipitation records (in mm/year)

Note: The boxes show the first quartile, median, and the third quartile, which contains 50% of the values. The whiskers extend from the box to the highest and lowest values, excluding outliers.

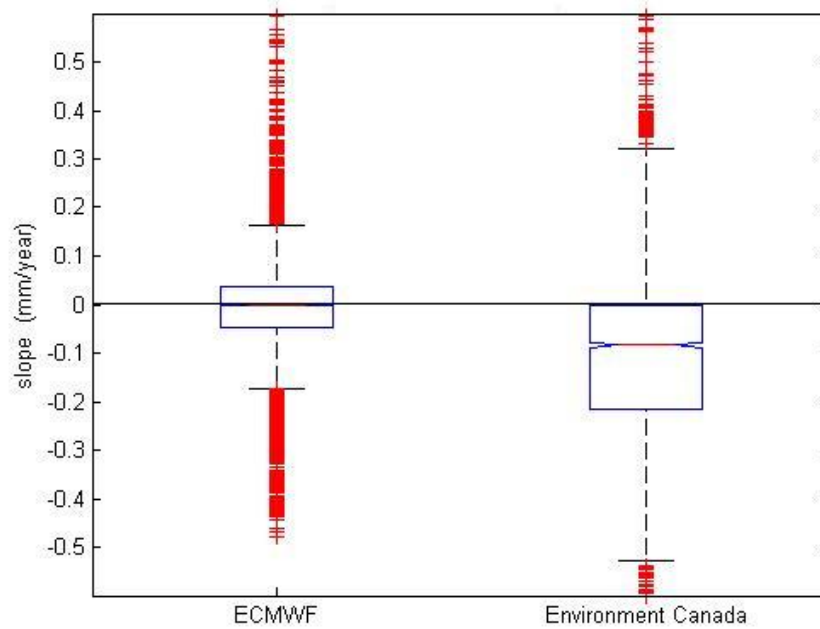


Figure A-25 Box plots of 4667 estimated trend magnitude for December precipitation records (in mm/year)

Note: The boxes show the first quartile, median, and the third quartile, which contains 50% of the values. The whiskers extend from the box to the highest and lowest values, excluding outliers.

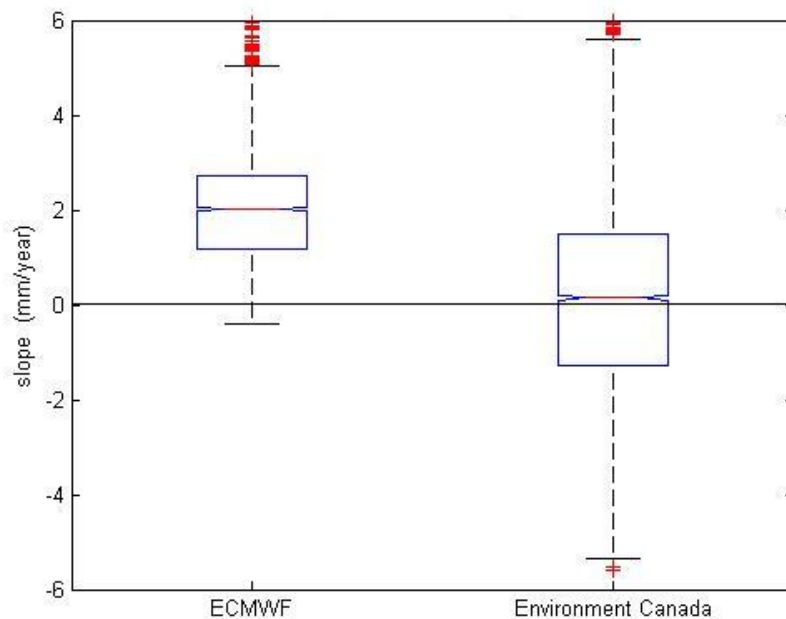


Figure A-26 Box plots of 4667 estimated trend magnitude for annual precipitation records (in mm/year)

Note: The boxes show the first quartile, median, and the third quartile, which contains 50% of the values. The whiskers extend from the box to the highest and lowest values, excluding outliers.

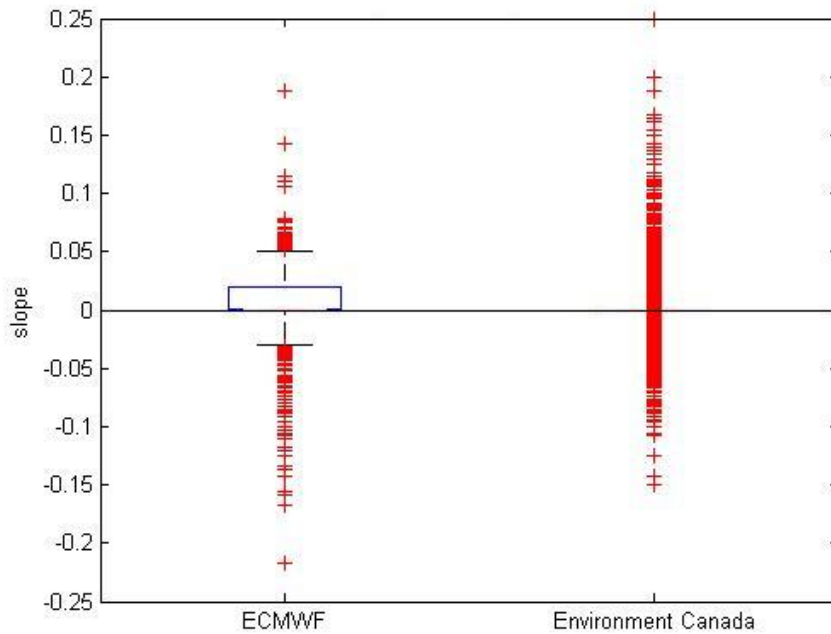


Figure A-27 Box plots of 4667 estimated trend magnitude for January runoff records (in mm/year)

Note: The boxes show the first quartile, median, and the third quartile, which contains 50% of the values. The whiskers extend from the box to the highest and lowest values, excluding outliers.

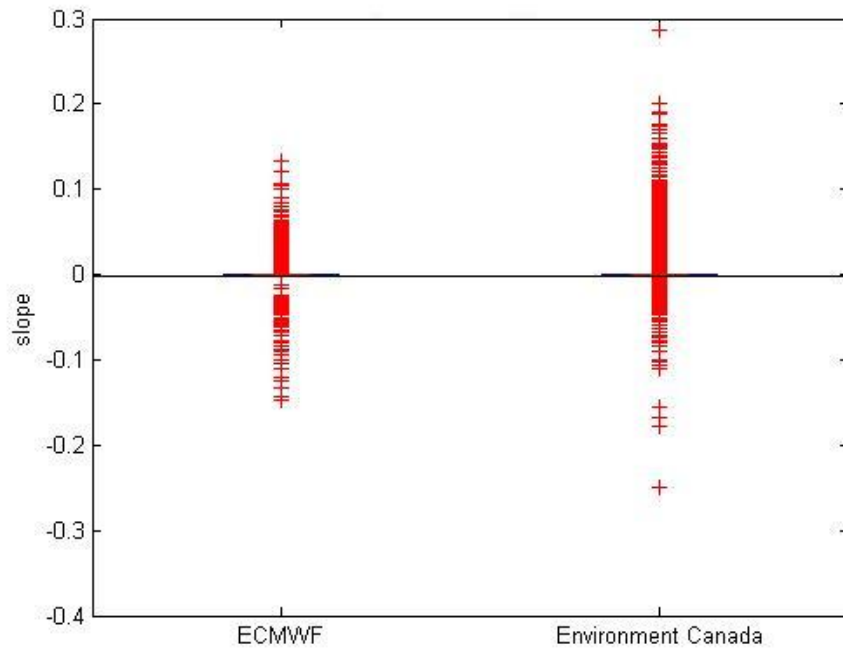


Figure A-28 Box plots of 4667 estimated trend magnitude for February runoff records (in mm/year)

Note: The boxes show the first quartile, median, and the third quartile, which contains 50% of the values. The whiskers extend from the box to the highest and lowest values, excluding outliers.

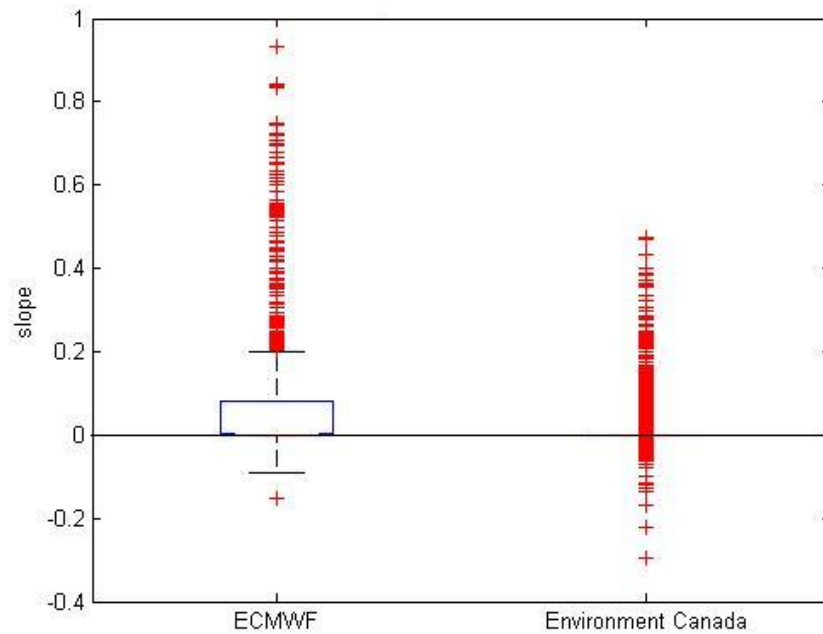


Figure A-29 Box plots of 4667 estimated trend magnitude for March runoff records (in mm/year)

Note: The boxes show the first quartile, median, and the third quartile, which contains 50% of the values. The whiskers extend from the box to the highest and lowest values, excluding outliers.

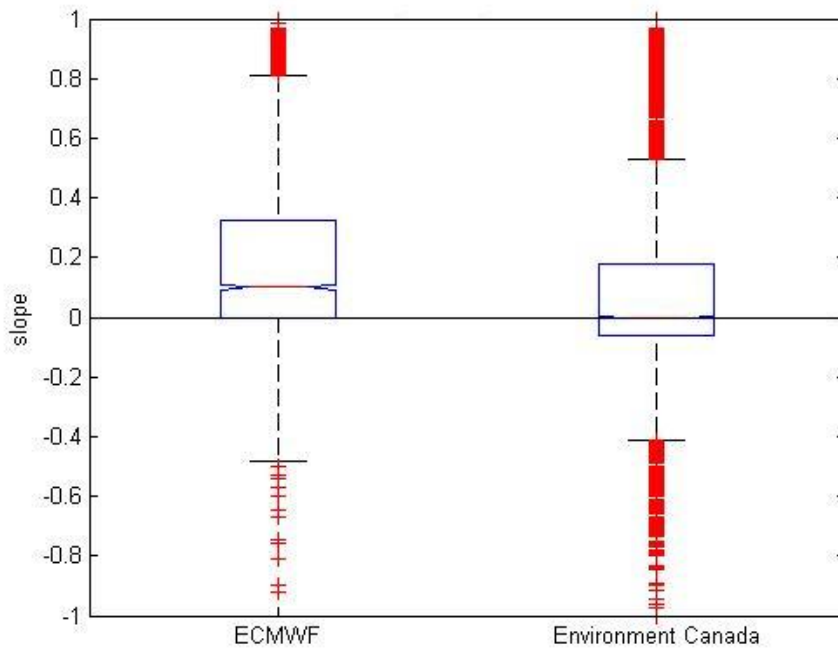


Figure A-30 Box plots of 4667 estimated trend magnitude for April runoff records (in mm/year)

Note: The boxes show the first quartile, median, and the third quartile, which contains 50% of the values. The whiskers extend from the box to the highest and lowest values, excluding outliers.

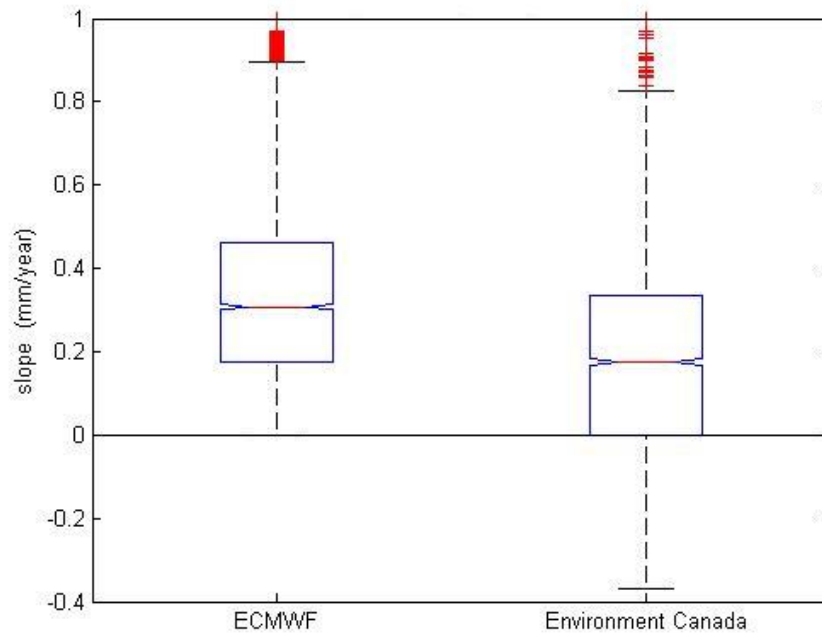


Figure A-31 Box plots of 4667 estimated trend magnitude for May runoff records (in mm/year)
 Note: The boxes show the first quartile, median, and the third quartile, which contains 50% of the values. The whiskers extend from the box to the highest and lowest values, excluding outliers.

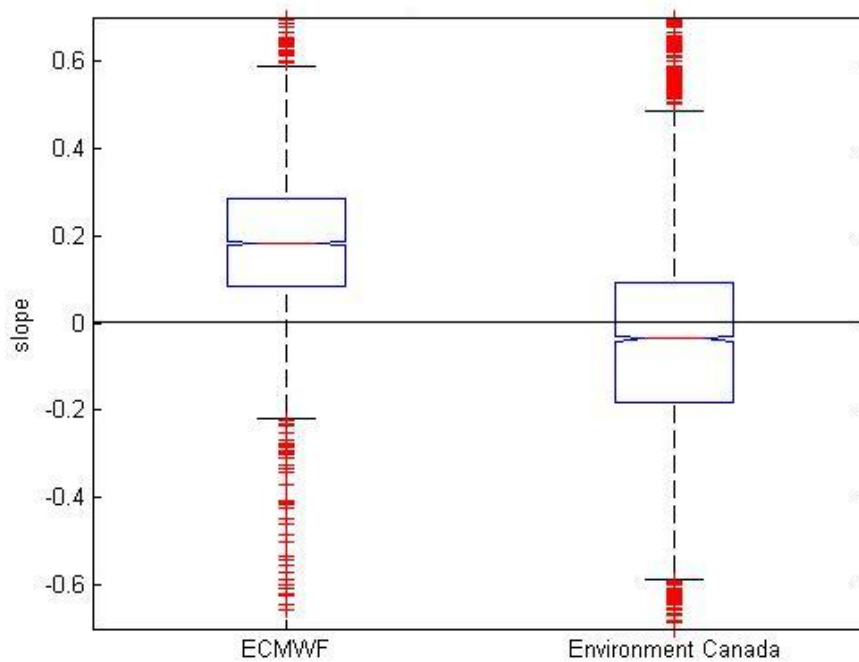


Figure A-32 Box plots of 4667 estimated trend magnitude for June runoff records (in mm/year)
 Note: The boxes show the first quartile, median, and the third quartile, which contains 50% of the values. The whiskers extend from the box to the highest and lowest values, excluding outliers.

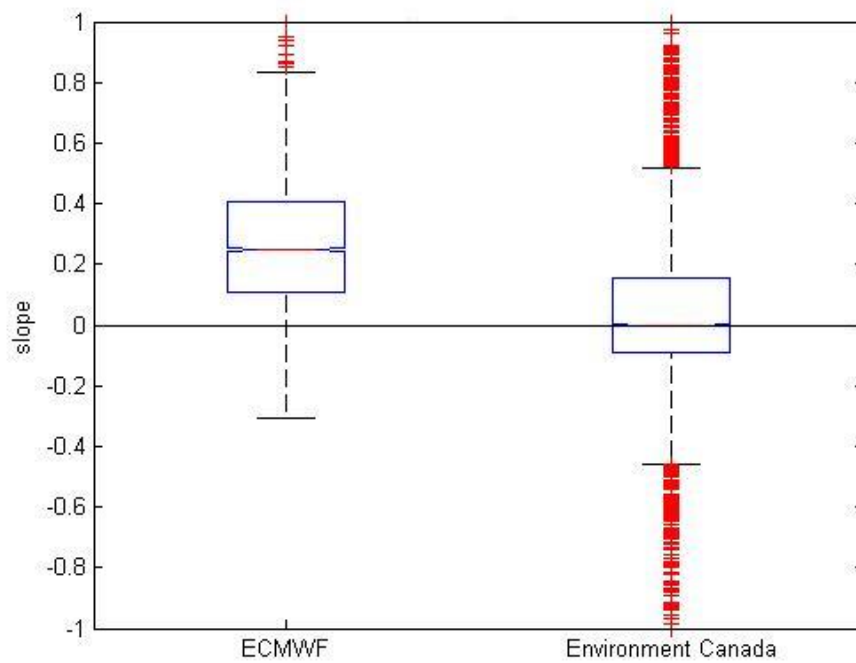


Figure A-33 Box plots of 4667 estimated trend magnitude for July runoff records (in mm/year)
 Note: The boxes show the first quartile, median, and the third quartile, which contains 50% of the values. The whiskers extend from the box to the highest and lowest values, excluding outliers.

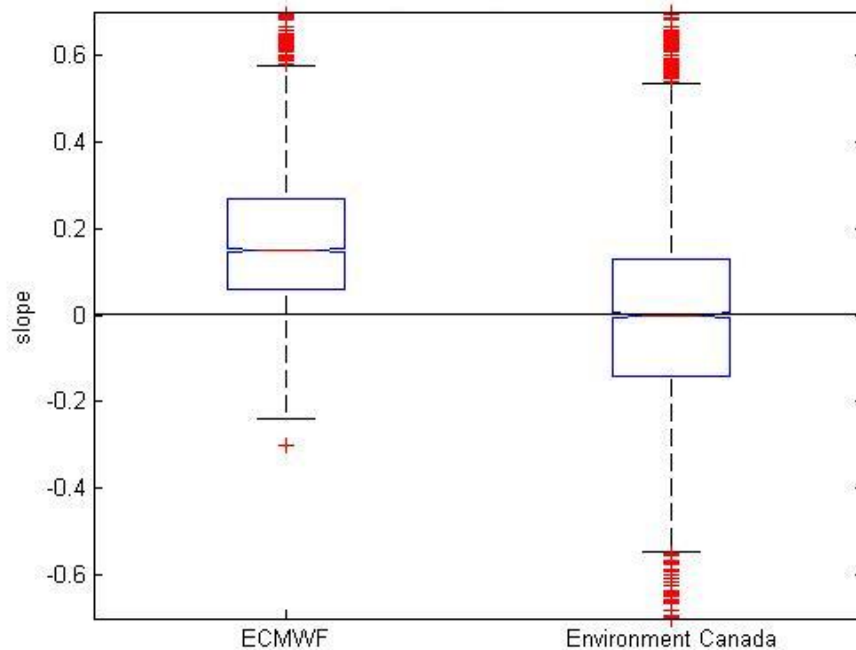


Figure A-34 Box plots of 4667 estimated trend magnitude for August runoff records (in mm/year)

Note: The boxes show the first quartile, median, and the third quartile, which contains 50% of the values. The whiskers extend from the box to the highest and lowest values, excluding outliers.

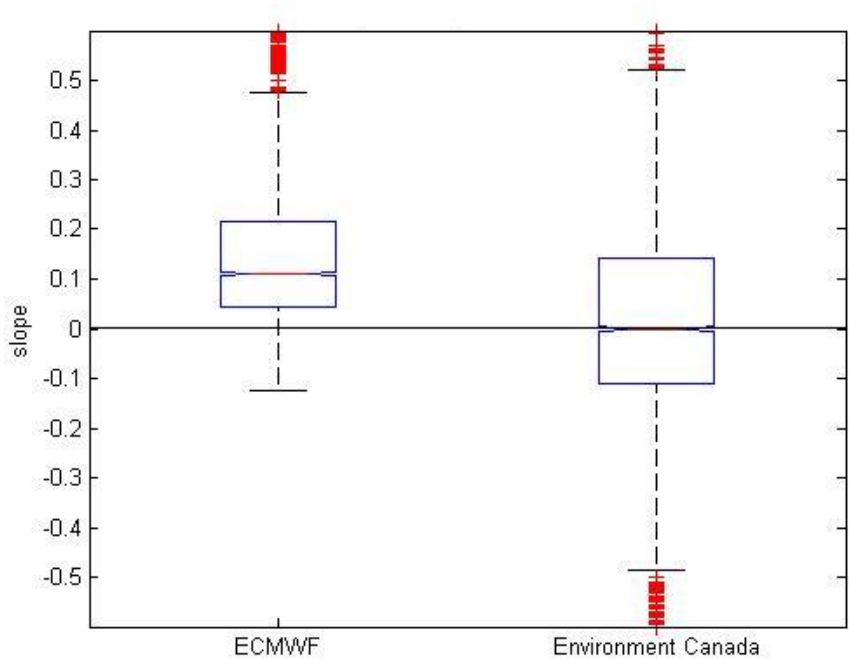


Figure A-35 Box plots of 4667 estimated trend magnitude for September runoff records (in mm/year)

Note: The boxes show the first quartile, median, and the third quartile, which contains 50% of the values. The whiskers extend from the box to the highest and lowest values, excluding outliers.

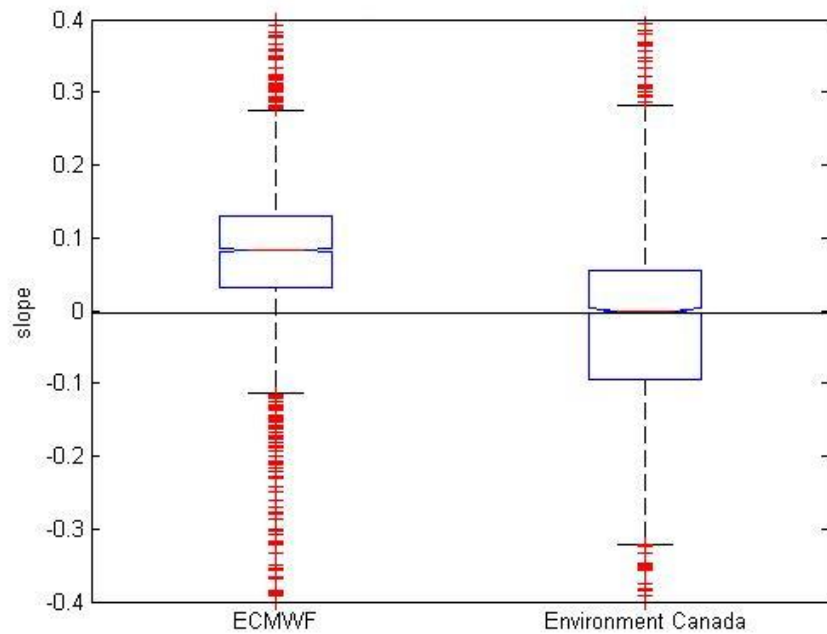


Figure A-36 Box plots of 4667 estimated trend magnitude for October runoff records (in mm/year)

Note: The boxes show the first quartile, median, and the third quartile, which contains 50% of the values. The whiskers extend from the box to the highest and lowest values, excluding outliers.

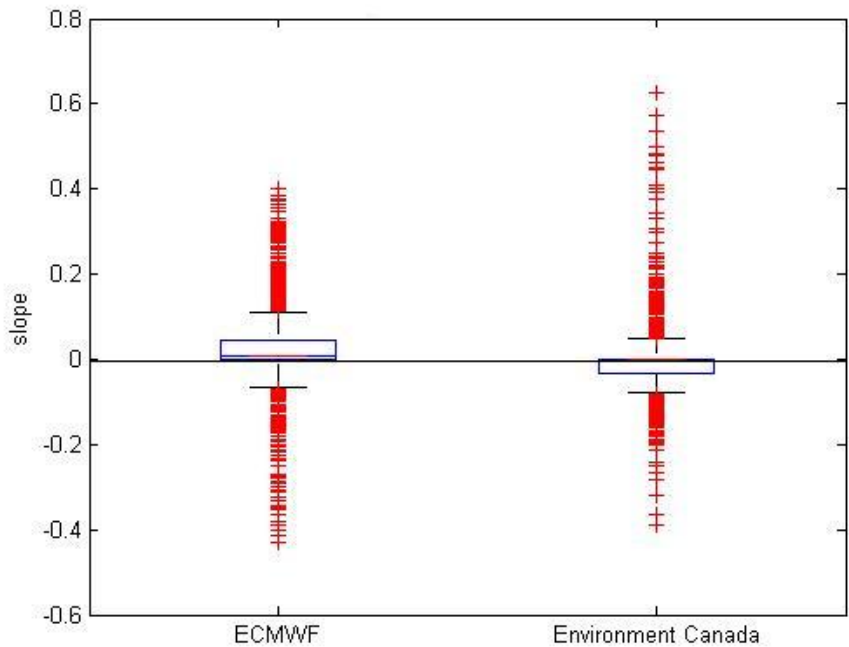


Figure A-37 Box plots of 4667 estimated trend magnitude for November runoff records (in mm/year)

Note: The boxes show the first quartile, median, and the third quartile, which contains 50% of the values. The whiskers extend from the box to the highest and lowest values, excluding outliers.

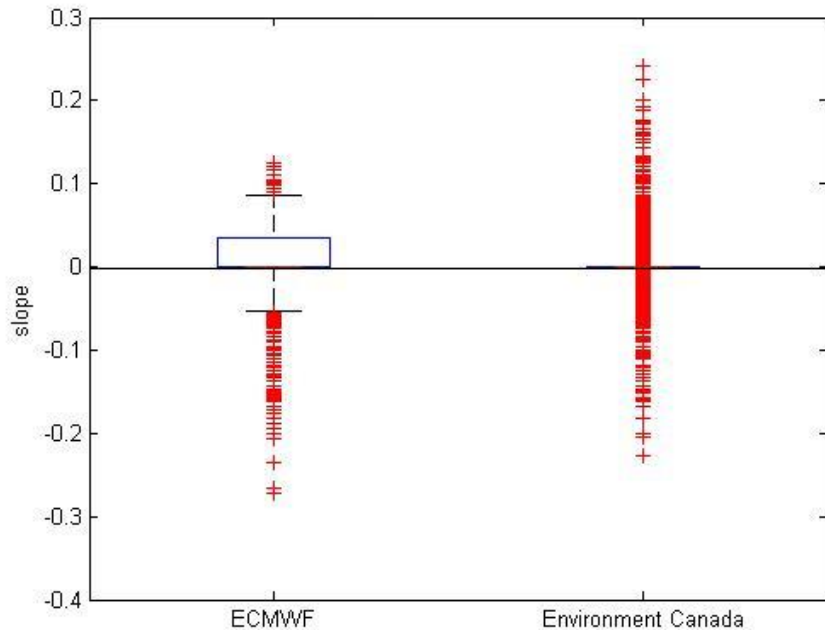


Figure A-38 Box plots of 4667 estimated trend magnitude for December runoff records (in mm/year)

Note: The boxes show the first quartile, median, and the third quartile, which contains 50% of the values. The whiskers extend from the box to the highest and lowest values, excluding outliers.

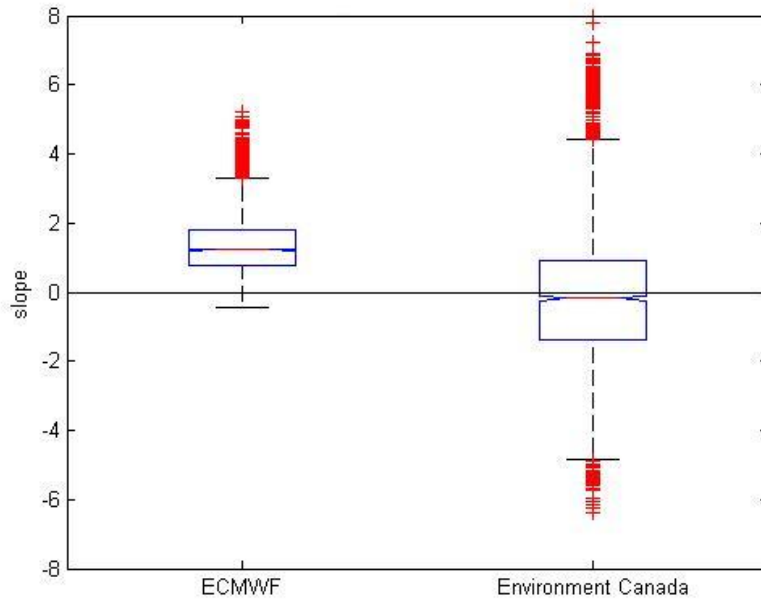


Figure A-39 Box plots of 4667 estimated trend magnitude for annual runoff records (in mm/year)

Note: The boxes show the first quartile, median, and the third quartile, which contains 50% of the values. The whiskers extend from the box to the highest and lowest values, excluding outliers.

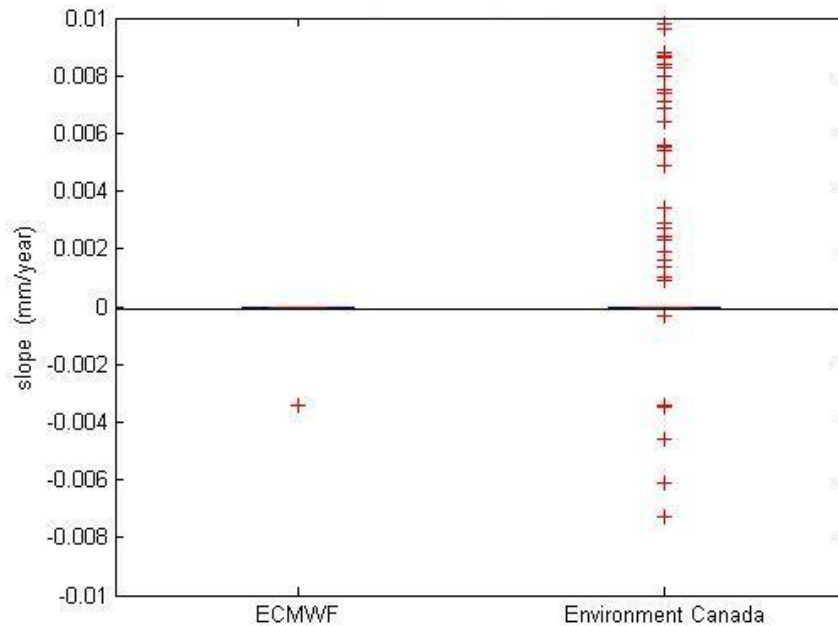


Figure A-40 Box plots of 4667 estimated trend magnitude for January evapotranspiration records (in mm/year)

Note: The boxes show the first quartile, median, and the third quartile, which contains 50% of the values. The whiskers extend from the box to the highest and lowest values, excluding outliers.

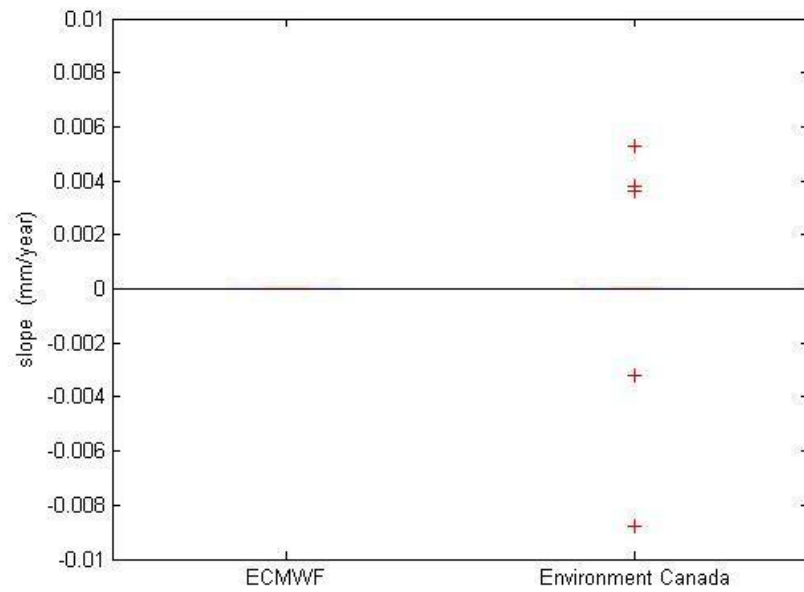


Figure A-41 Box plots of 4667 estimated trend magnitude for February evapotranspiration records (in mm/year)

Note: The boxes show the first quartile, median, and the third quartile, which contains 50% of the values. The whiskers extend from the box to the highest and lowest values, excluding outliers.

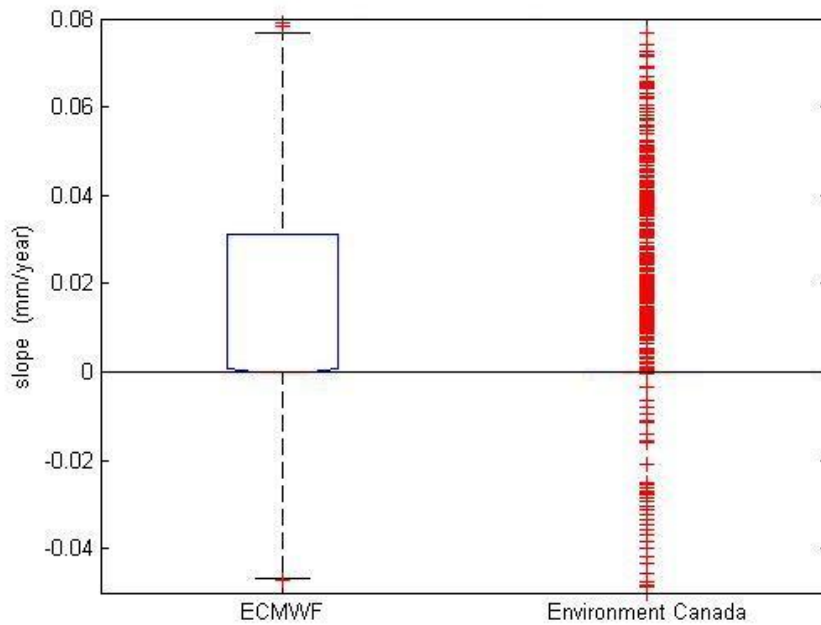


Figure A-42 Box plots of 4667 estimated trend magnitude for March evapotranspiration records (in mm/year)

Note: The boxes show the first quartile, median, and the third quartile, which contains 50% of the values. The whiskers extend from the box to the highest and lowest values, excluding outliers.

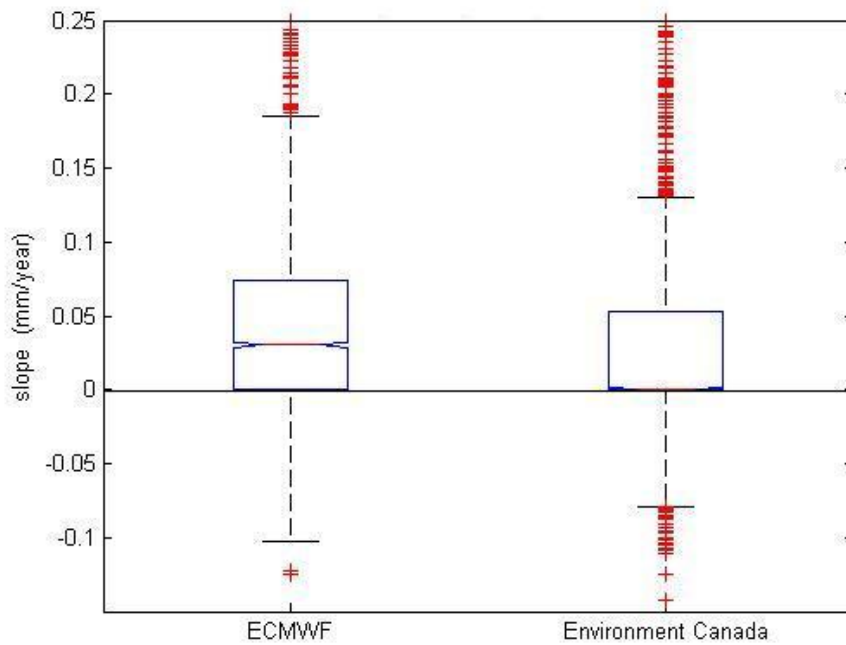


Figure A-43 Box plots of 4667 estimated trend magnitude for April evapotranspiration records (in mm/year)

Note: The boxes show the first quartile, median, and the third quartile, which contains 50% of the values. The whiskers extend from the box to the highest and lowest values, excluding outliers.

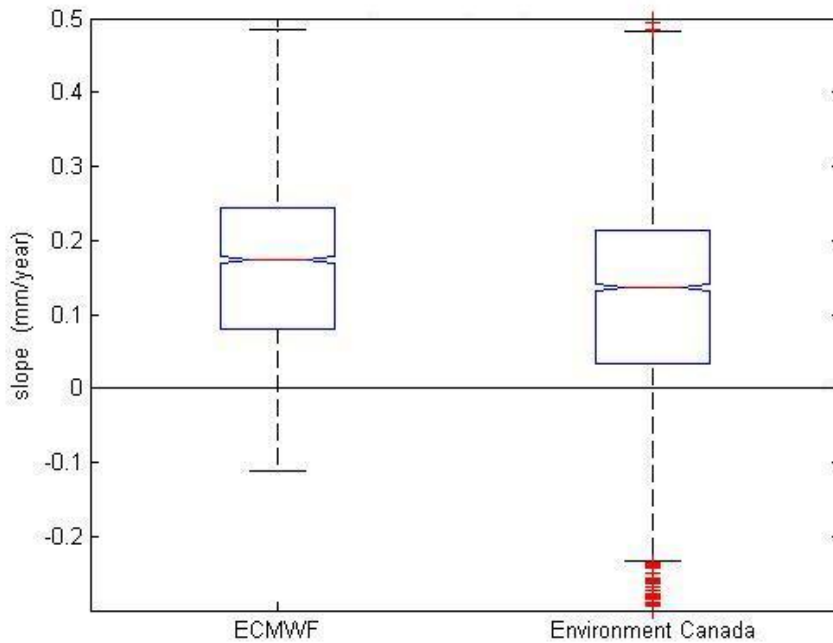


Figure A-44 Box plots of 4667 estimated trend magnitude for May evapotranspiration records (in mm/year)

Note: The boxes show the first quartile, median, and the third quartile, which contains 50% of the values. The whiskers extend from the box to the highest and lowest values, excluding outliers.

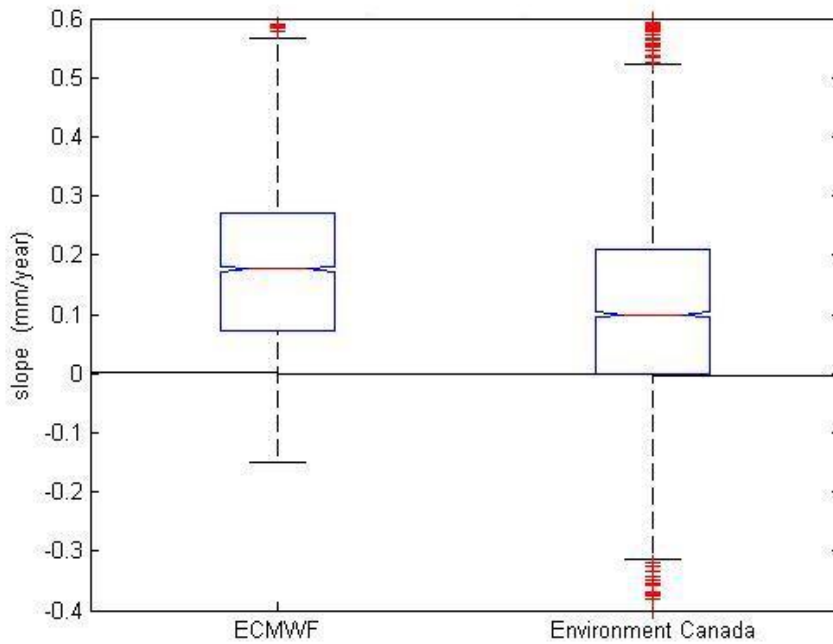


Figure A-45 Box plots of 4667 estimated trend magnitude for June evapotranspiration records (in mm/year)

Note: The boxes show the first quartile, median, and the third quartile, which contains 50% of the values. The whiskers extend from the box to the highest and lowest values, excluding outliers.

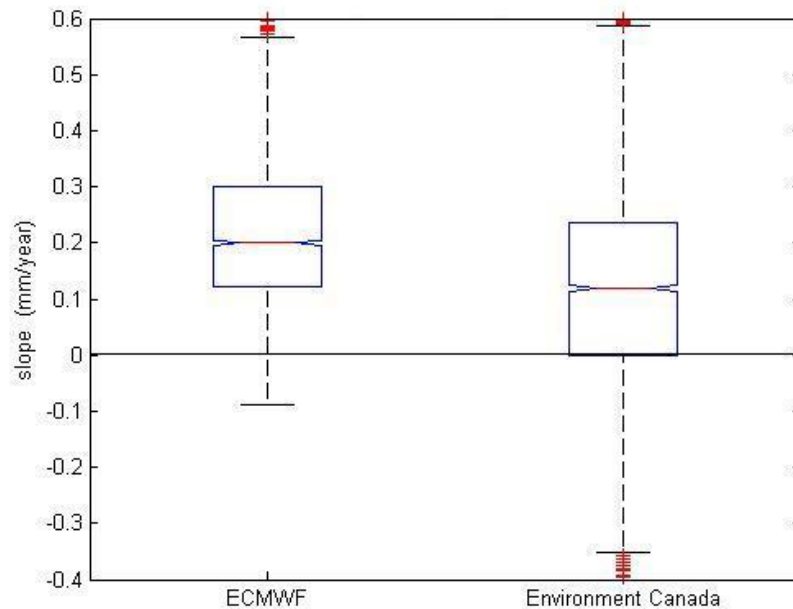


Figure A-46 Box plots of 4667 estimated trend magnitude for July evapotranspiration records (in mm/year)

Note: The boxes show the first quartile, median, and the third quartile, which contains 50% of the values. The whiskers extend from the box to the highest and lowest values, excluding outliers.

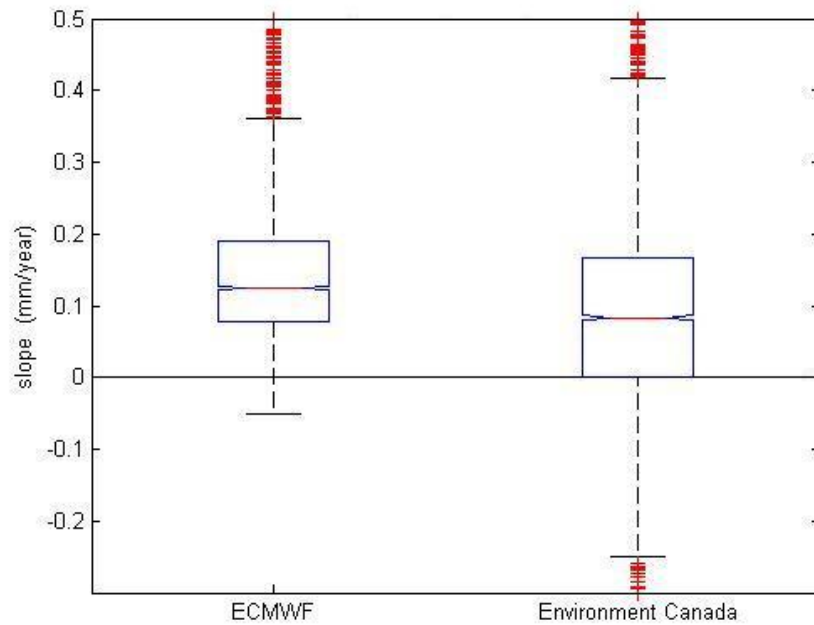


Figure A-47 Box plots of 4667 estimated trend magnitude for August evapotranspiration records (in mm/year)

Note: The boxes show the first quartile, median, and the third quartile, which contains 50% of the values. The whiskers extend from the box to the highest and lowest values, excluding outliers.

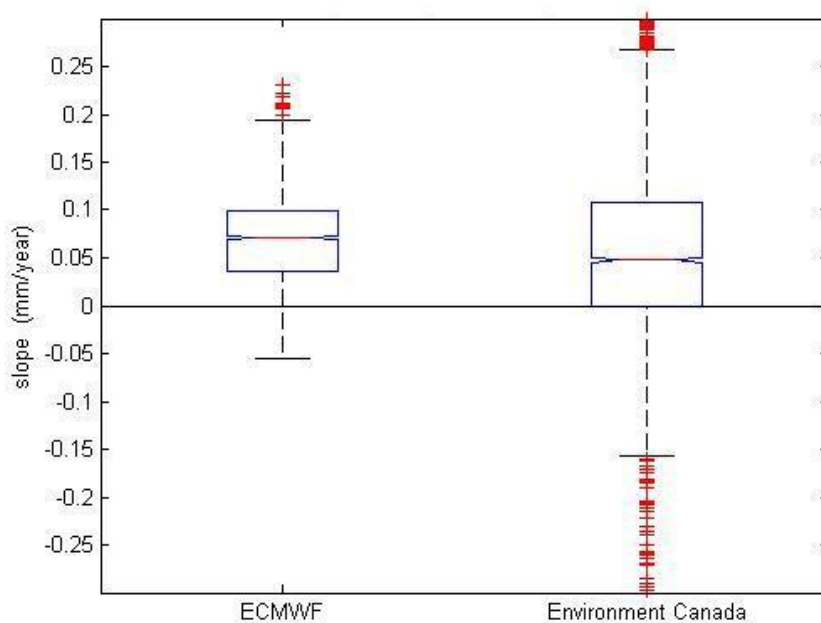


Figure A-48 Box plots of 4667 estimated trend magnitude for September evapotranspiration records (in mm/year)

Note: The boxes show the first quartile, median, and the third quartile, which contains 50% of the values. The whiskers extend from the box to the highest and lowest values, excluding outliers.

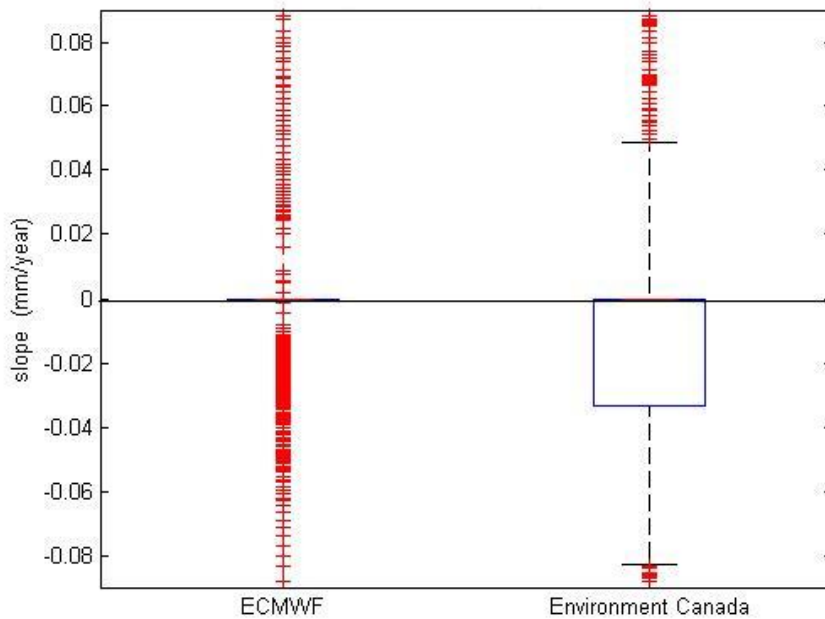


Figure A-49 Box plots of 4667 estimated trend magnitude for October evapotranspiration records (in mm/year)

Note: The boxes show the first quartile, median, and the third quartile, which contains 50% of the values. The whiskers extend from the box to the highest and lowest values, excluding outliers.

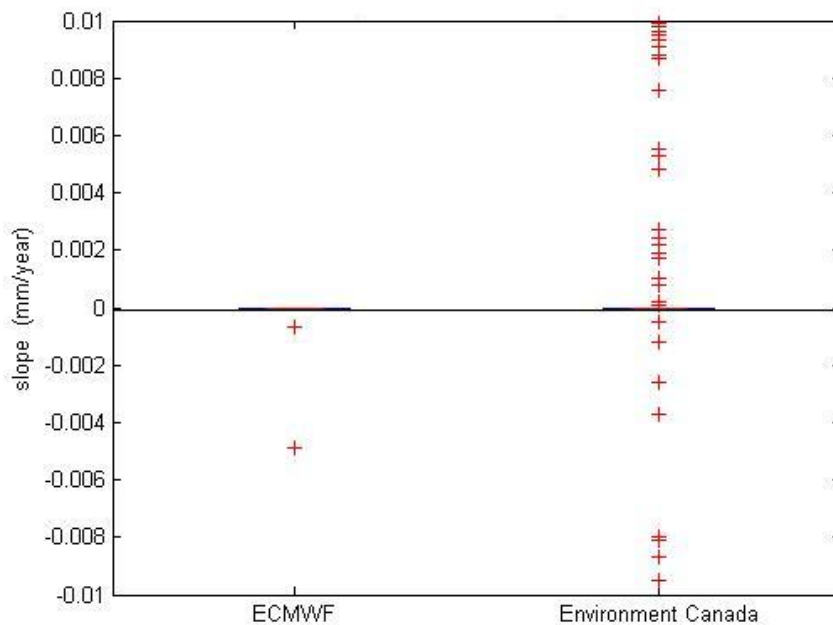


Figure A-50 Box plots of 4667 estimated trend magnitude for November evapotranspiration records (in mm/year)

Note: The boxes show the first quartile, median, and the third quartile, which contains 50% of the values. The whiskers extend from the box to the highest and lowest values, excluding outliers.

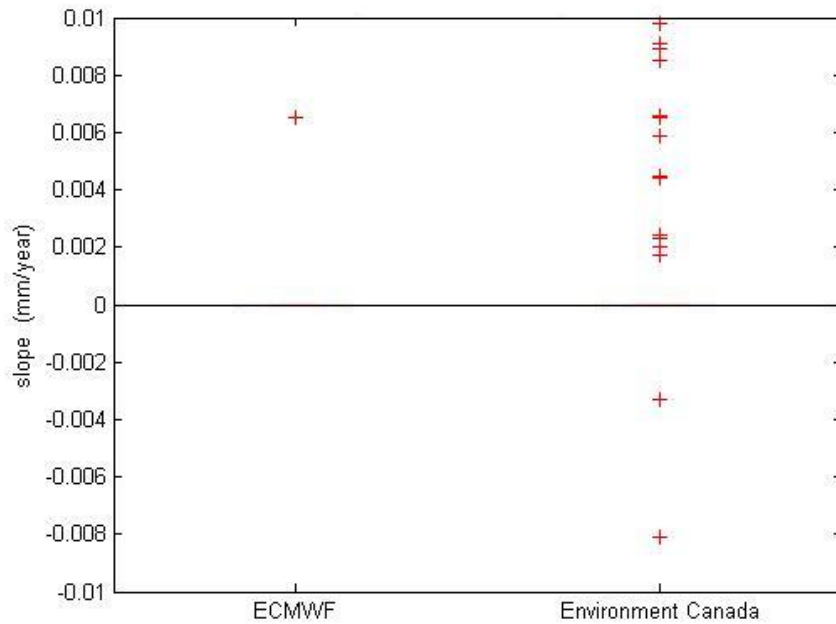


Figure A-51 Box plots of 4667 estimated trend magnitude for December evapotranspiration records (in mm/year)

Note: The boxes show the first quartile, median, and the third quartile, which contains 50% of the values. The whiskers extend from the box to the highest and lowest values, excluding outliers.

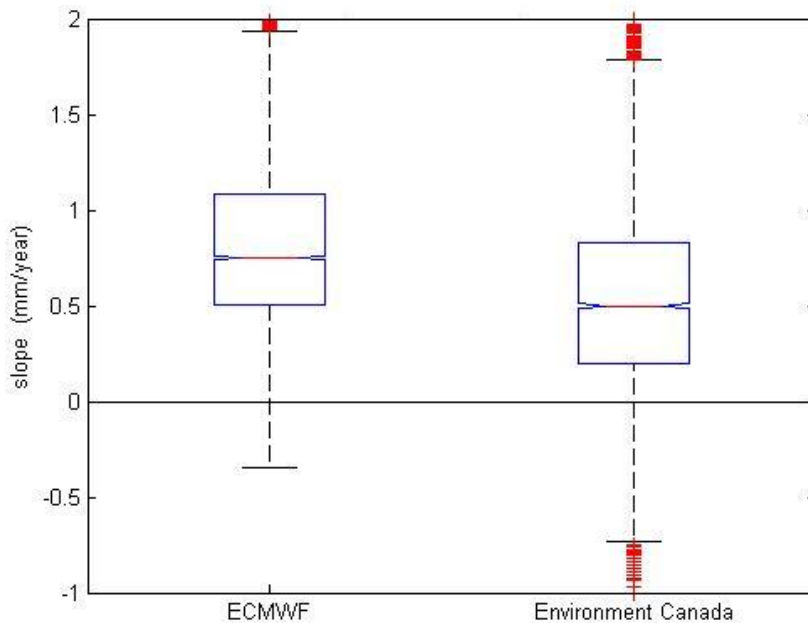


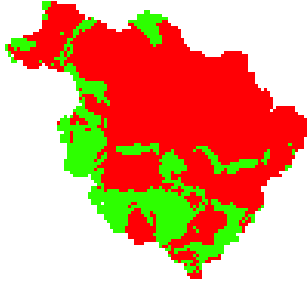
Figure A-52 Box plots of 4667 estimated trend magnitude for annual evapotranspiration records (in mm/year)

Note: The boxes show the first quartile, median, and the third quartile, which contains 50% of the values. The whiskers extend from the box to the highest and lowest values, excluding outliers.

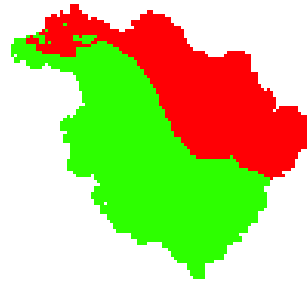
Appendix B
Spatial distribution of monthly trend

Figure B-1 Spatial distribution of temperature trends
Environment Canada ECMWF

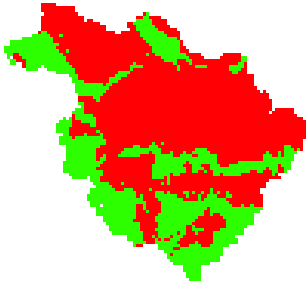
January



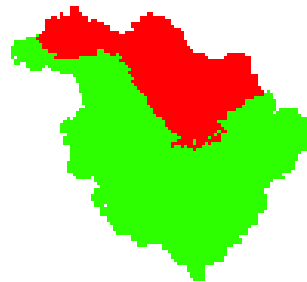
January



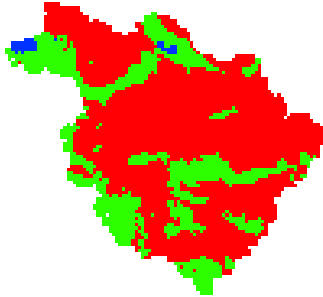
February



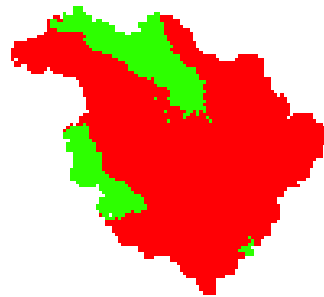
February



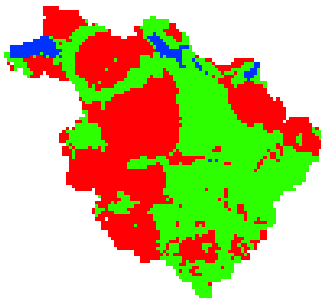
March



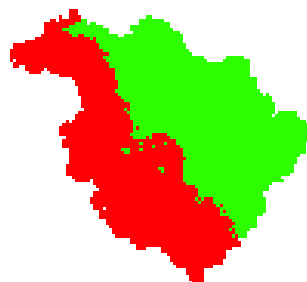
March



April



April



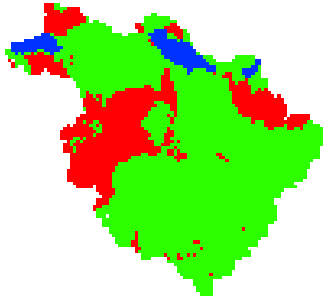
Significant
Negative Trend

No
Significant Trend

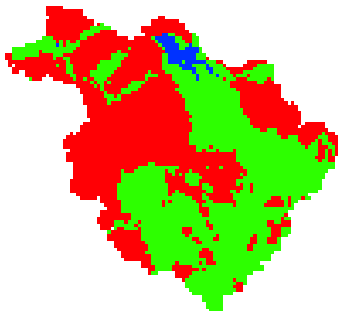
Significant
Positive Trend

Environment Canada

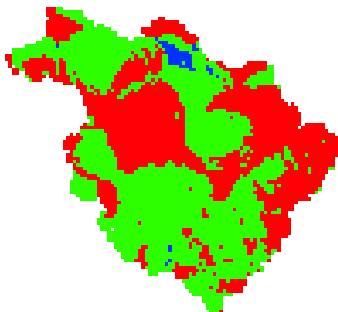
May



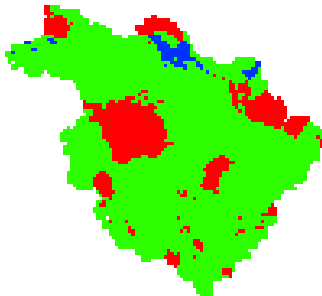
June



July

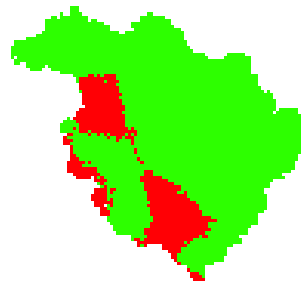


August

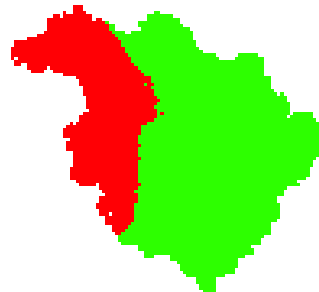


ECMWF

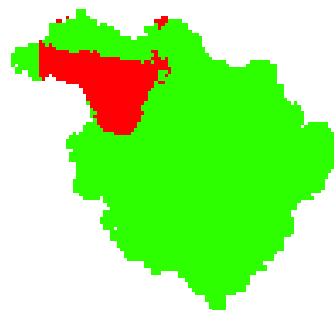
May



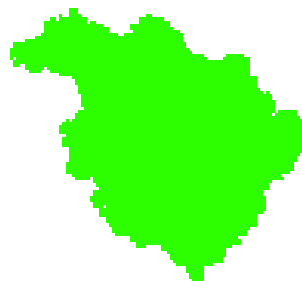
June



July



August



 Significant Negative Trend

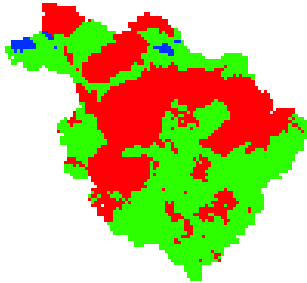
 No Significant Trend

 Significant Positive Trend

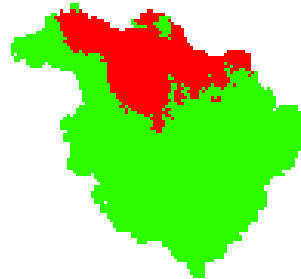
Environment Canada

ECMWF

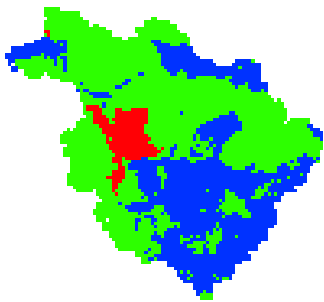
September



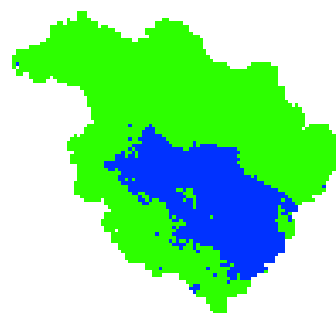
September



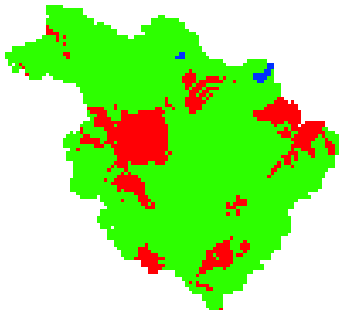
October



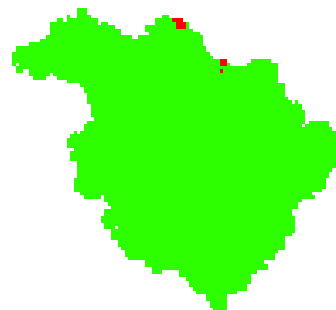
October



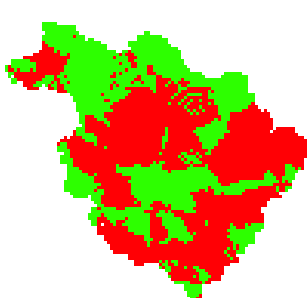
November



November



December



December



 Significant Negative Trend

 No Significant Trend

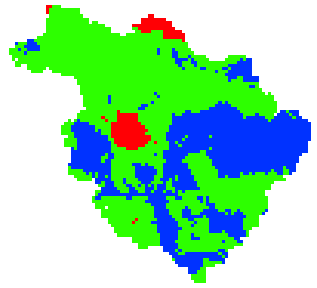
 Significant Positive Trend

Figure B-2 Spatial distribution of precipitation trends

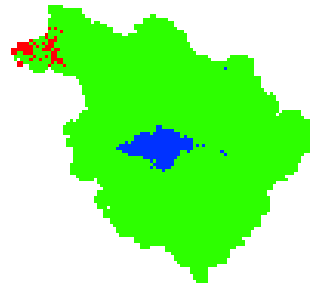
Environment Canada

ECMWF

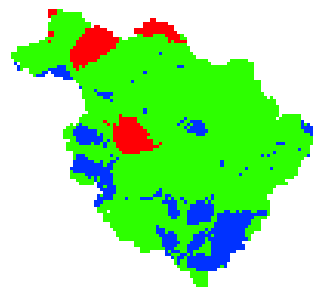
January



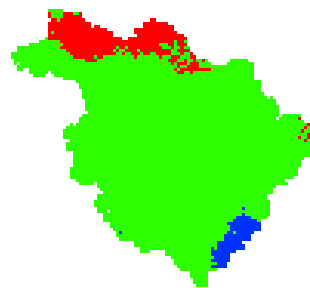
January



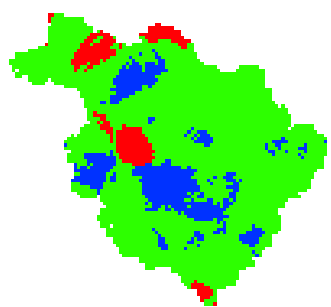
February



February



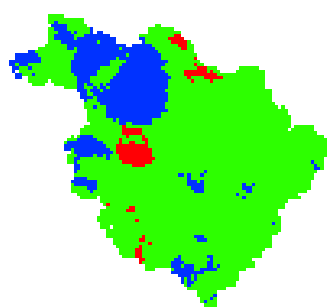
March



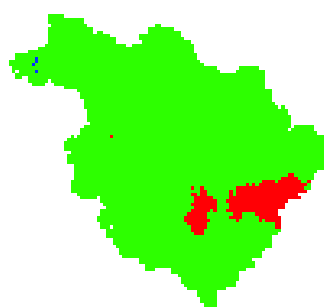
March



April



April



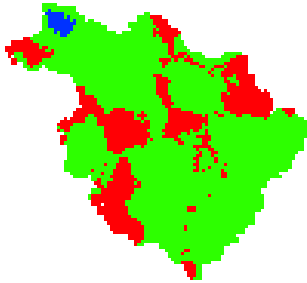
 Significant Negative Trend

 No Significant Trend

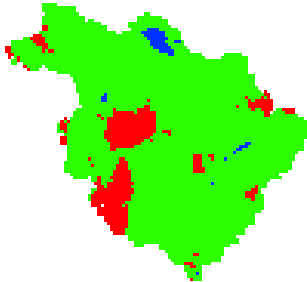
 Significant Positive Trend

Environment Canada

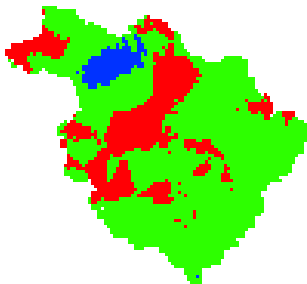
May



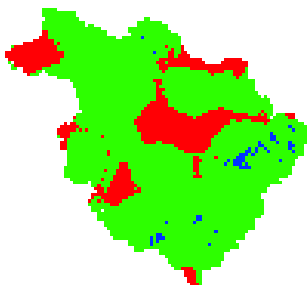
June



July

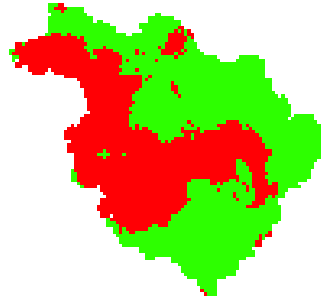


August

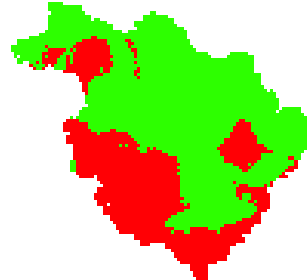


ECMWF

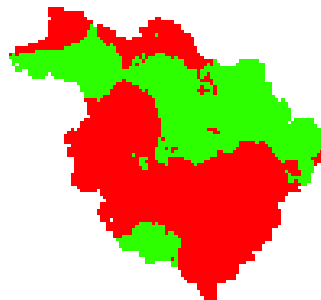
May



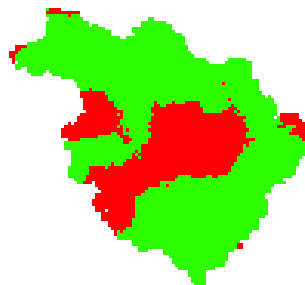
June



July



August



 Significant Negative Trend

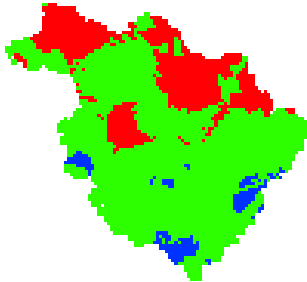
 No Significant Trend

 Significant Positive Trend

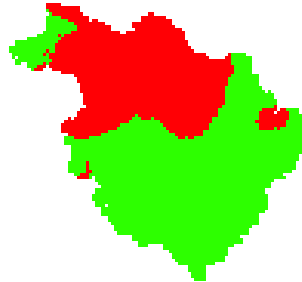
Environment Canada

ECMWF

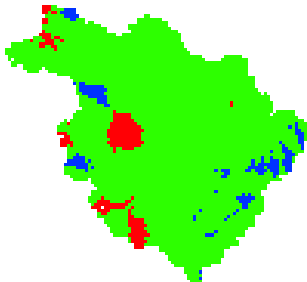
September



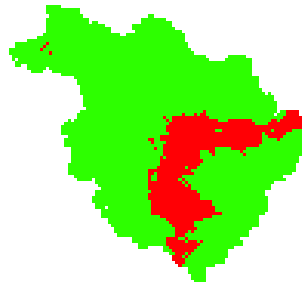
September



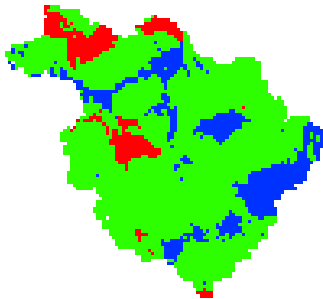
October



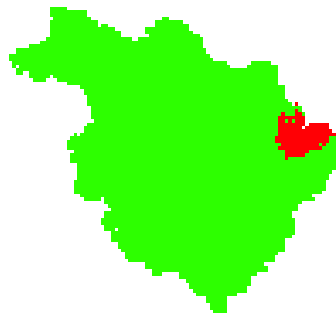
October



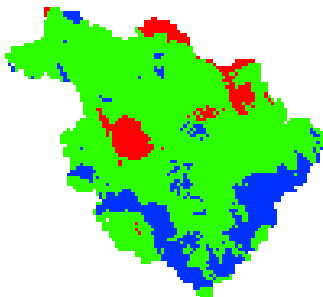
November



November



December



December



 Significant Negative Trend

 No Significant Trend

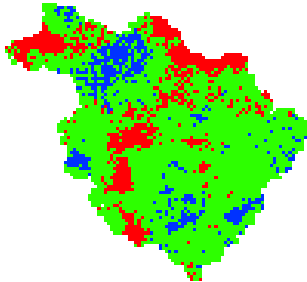
 Significant Positive Trend

Figure B-3 Spatial distribution of runoff trends

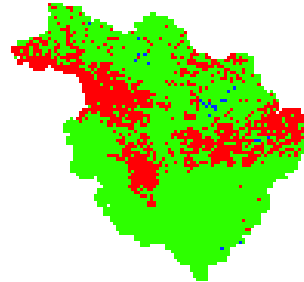
Environment Canada

ECMWF

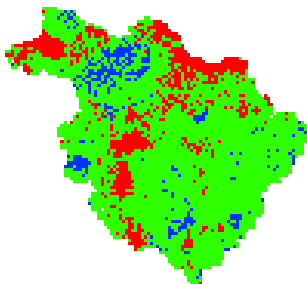
January



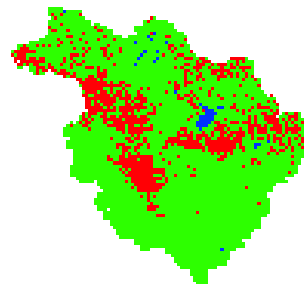
January



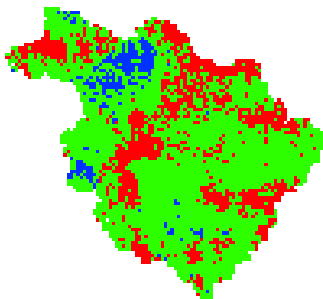
February



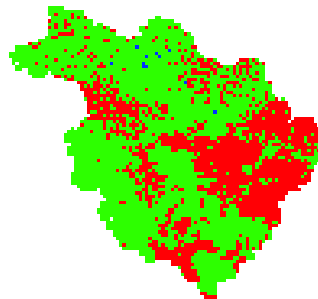
February



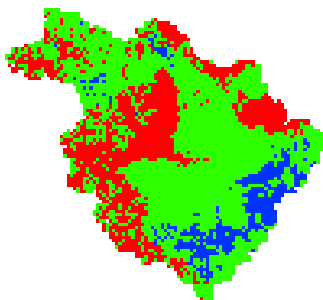
March



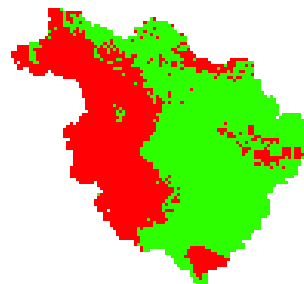
March



April



April



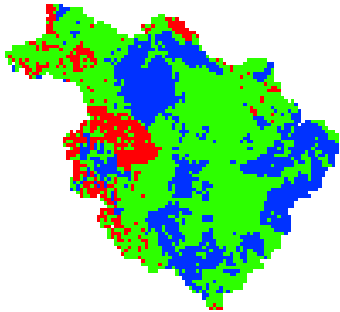
 Significant Negative Trend

 No Significant Trend

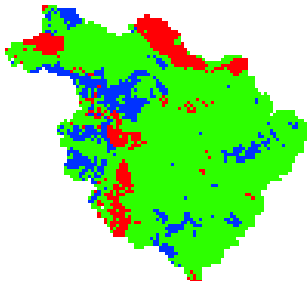
 Significant Positive Trend

Environment Canada

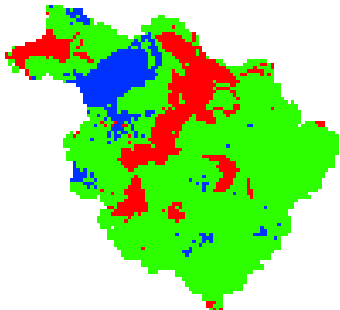
May



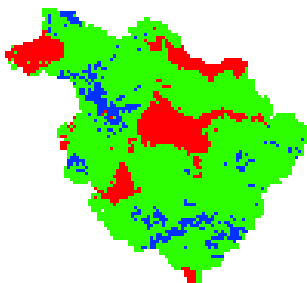
June



July

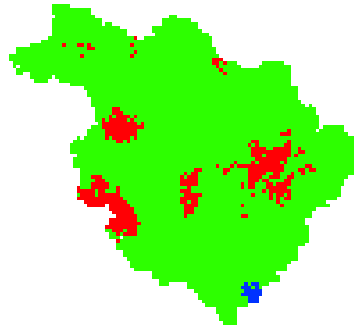


August

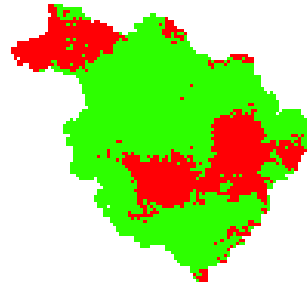


ECMWF

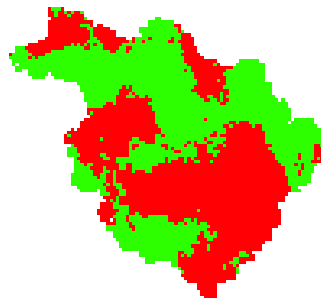
May



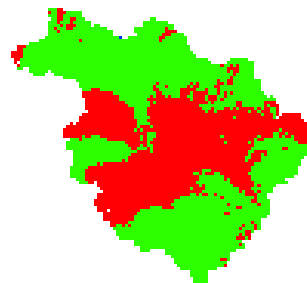
June



July



August



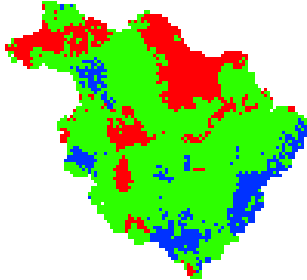
 Significant Negative Trend

 No Significant Trend

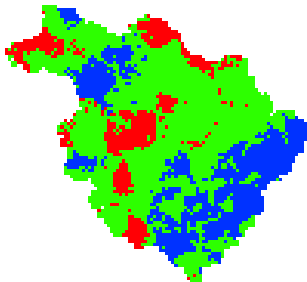
 Significant Positive Trend

Environment Canada

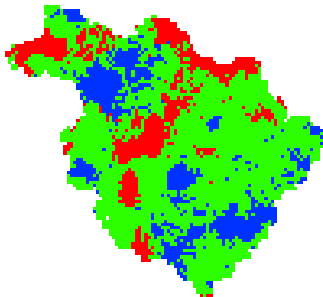
September



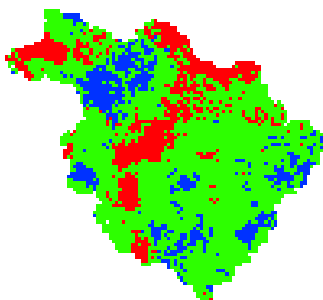
October



November

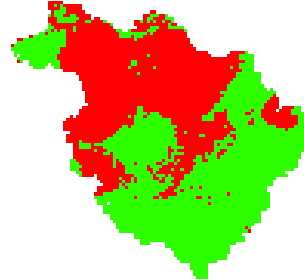


December

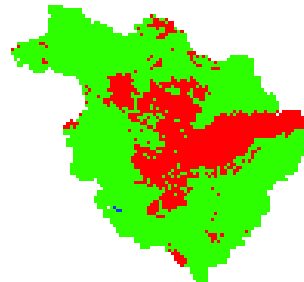


ECMWF

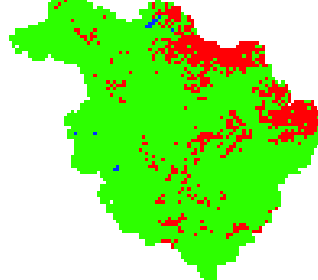
September



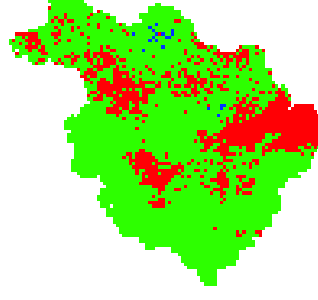
October



November



December



 Significant
Negative Trend

 No
Significant Trend

 Significant
Positive Trend

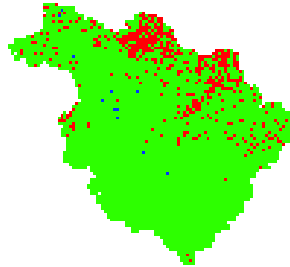
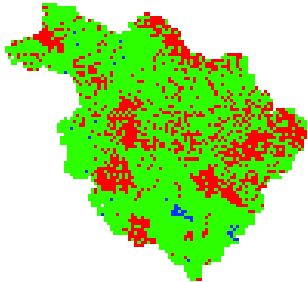
Figure B-4 Spatial distribution of evapotranspiration trends

Environment Canada

ECMWF

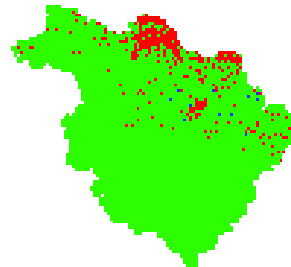
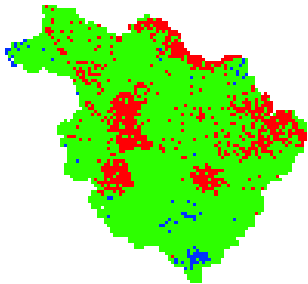
January

January



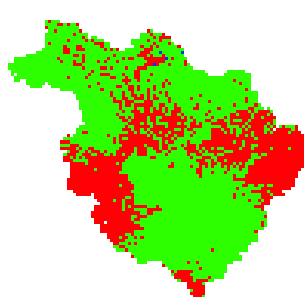
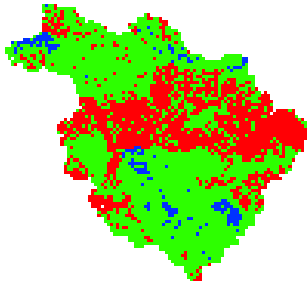
February

February



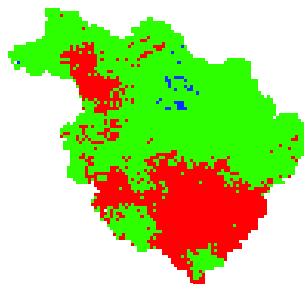
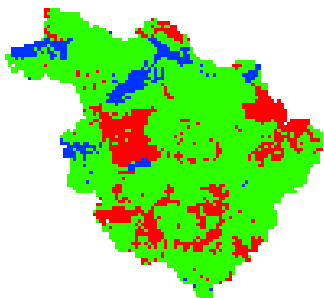
March

March



April

April



Significant
Negative Trend

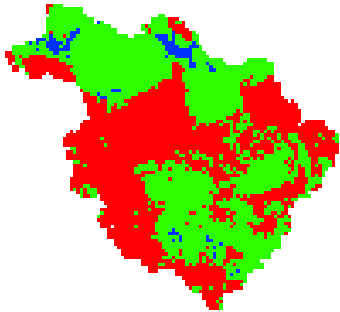
No
Significant Trend

Significant
Positive Trend

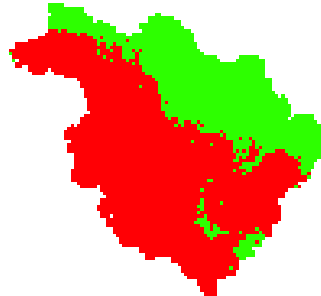
Environment Canada

ECMWF

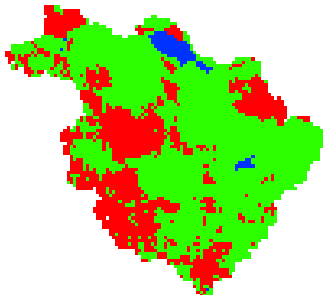
May



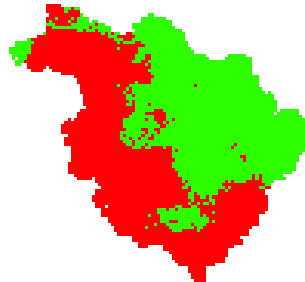
May



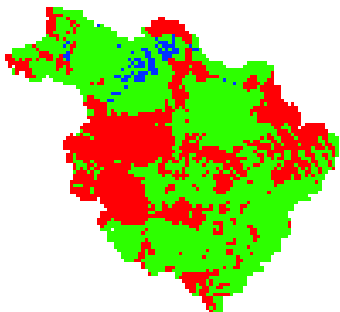
June



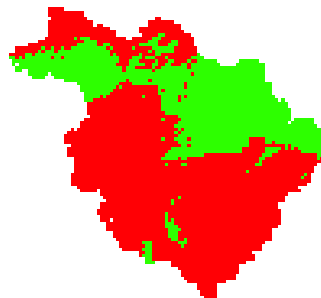
June



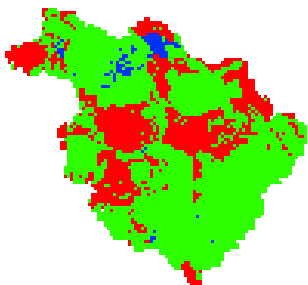
July



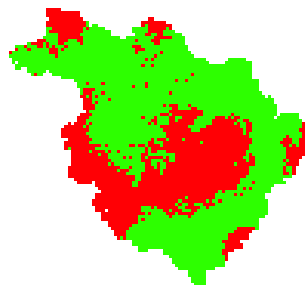
July



August



August



 Significant Negative Trend

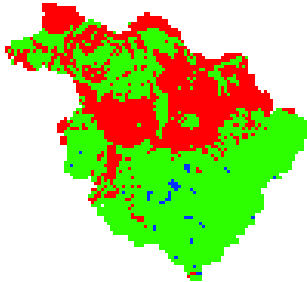
 No Significant Trend

 Significant Positive Trend

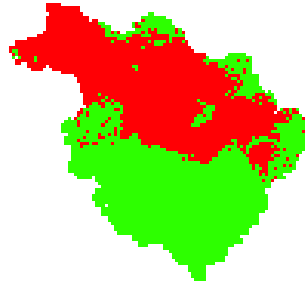
Environment Canada

ECMWF

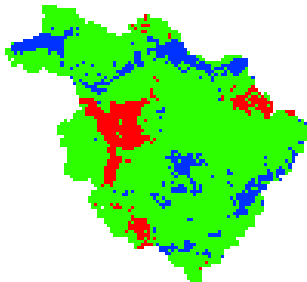
September



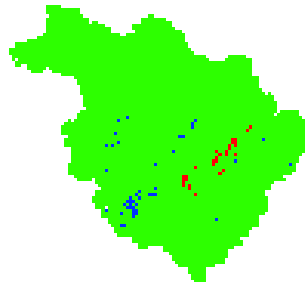
September



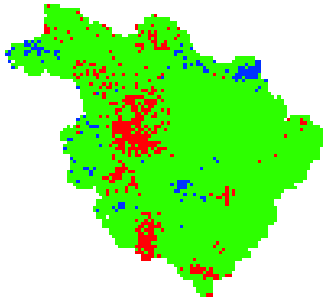
October



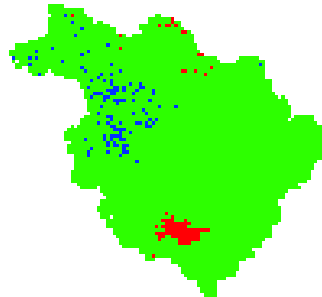
October



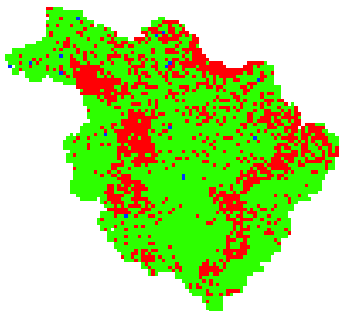
November



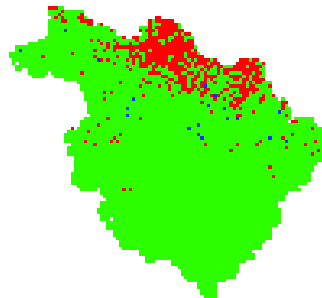
November



December



December

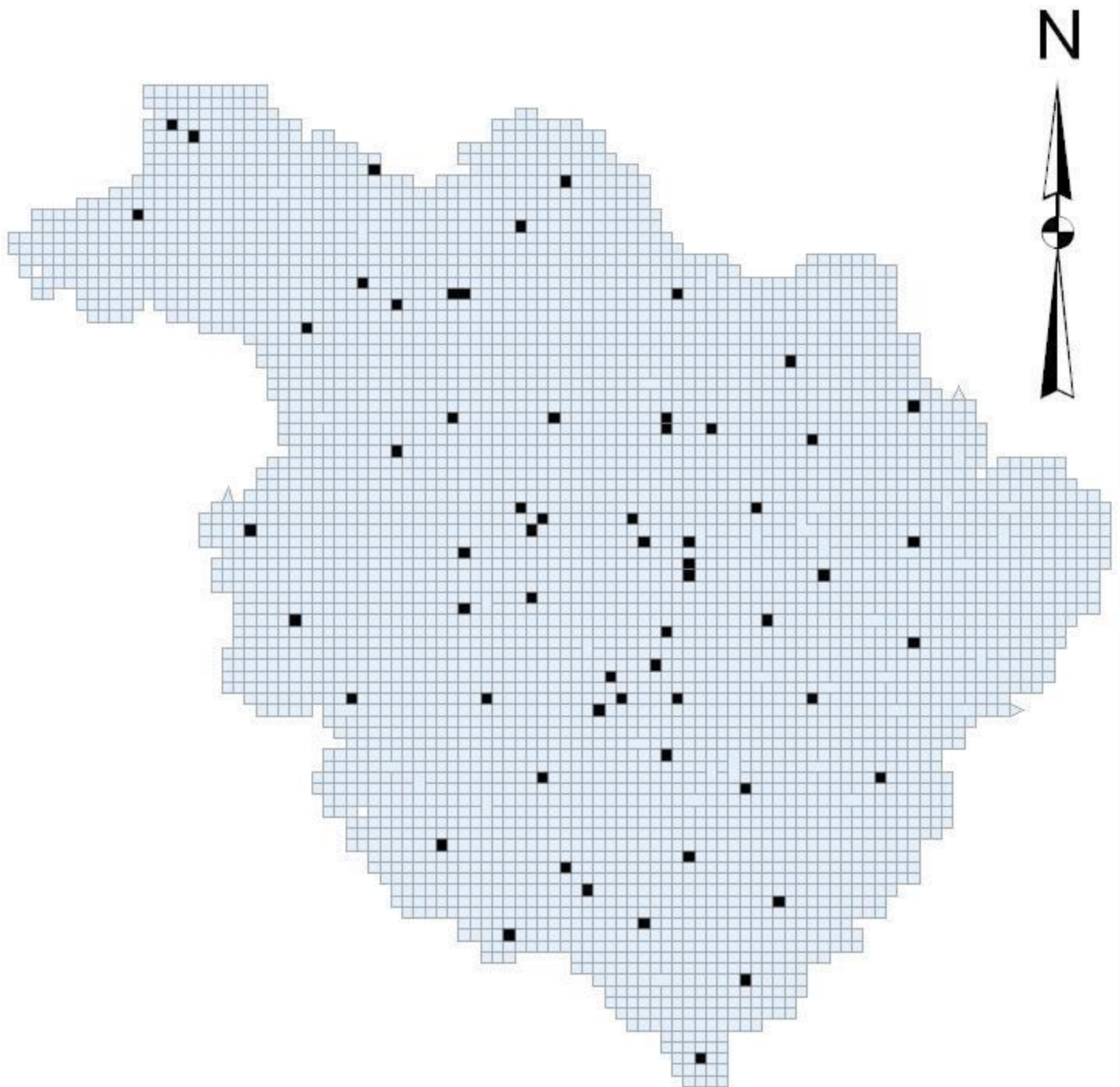


 Significant Negative Trend

 No Significant Trend

 Significant Positive Trend

Appendix C: 60 randomly selected sample sites
for the Mackenzie River Basin
(black grid indicate locations of the sample site)



Not to scale

Appendix D

Summary of original data averaged over the 60 sample sites

Table 1 Summary of runoff data over 60 sample sites (in mm)

Month	Environment Canada	ECMWF
Jan	4.00 (4.62)	4.00 (4.40)
Feb	4.00 (4.18)	3.00 (3.35)
Mar	4.00 (5.52)	5.00 (8.43)
Apr	18.00 (19.92)	33.00 (33.27)
May	15.00 (19.05)	47.00 (55.87)
Jun	6.00 (19.23)	16.00 (19.05)
Jul	13.50 (17.12)	17.50 (17.67)
Aug	9.00 (18.62)	11.00 (9.58)
Sep	14.50 (19.78)	7.00 (9.03)
Oct	7.00 (8.05)	7.00 (10.60)
Nov	4.50 (6.37)	6.00 (8.52)
Dec	4.00 (6.45)	6.00 (9.80)
Annual	120.50 (148.90)	167.00 (189.57)

Table 2 Summary of precipitation data over 60 sample sites (in mm)

Month	Environment Canada	ECMWF
Jan	20.00 (20.02)	9.00 (13.40)
Feb	7.00 (9.37)	18.50 (29.73)
Mar	10.50 (12.72)	27.50 (32.38)
Apr	6.00 (11.58)	17.00 (20.98)
May	36.00 (37.20)	45.50 (44.07)
Jun	32.50 (47.92)	46.50 (51.20)
Jul	57.00 (59.25)	54.50 (57.13)
Aug	49.00 (58.98)	36.50 (37.50)
Sep	54.50 (55.52)	31.00 (31.78)
Oct	14.00 (16.68)	19.00 (22.05)
Nov	20.00 (20.22)	12.50 (14.67)
Dec	16.50 (34.53)	23.50 (34.18)
Annual	337.00 (383.98)	367.00 (389.08)

Table 3 Summary of evapotranspiration data over 60 sample sites (in mm)

Month	Environment Canada	ECMWF
Jan	0.00 (0.60)	0.00 (0.55)
Feb	1.00 (1.38)	0.00 (0.33)
Mar	2.00 (3.05)	2.00 (4.97)
Apr	8.00 (8.80)	6.00 (8.75)
May	29.50 (30.80)	29.00 (31.05)
Jun	36.50 (42.37)	50.50 (51.25)
Jul	41.00 (44.40)	48.00 (50.50)
Aug	38.00 (40.63)	38.00 (39.25)
Sep	26.50 (28.60)	26.50 (27.50)
Oct	11.00 (11.87)	14.50 (15.57)
Nov	3.00 (3.42)	4.00 (4.08)
Dec	0.00 (0.53)	1.50 (2.87)
Annual	195.50 (216.45)	226.50 (236.67)

Table 4 Summary of storage data over 60 sample sites (in mm)

Month	Environment Canada	ECMWF
Annual	53.50 (49.83)	38.00 (34.80)

Table 5 Summary of temperature data over 60 sample site (in °C)

Month	Environment Canada	ECMWF
Jan	-24.15 (-24.13)	-20.75 (-20.59)
Feb	-15.85 (-15.12)	-30.00 (-28.21)
Mar	-12.65 (-12.87)	-11.80 (-12.00)
Apr	3.50 (1.24)	-3.90 (-4.29)
May	8.80 (7.67)	5.30 (4.68)
Jun	14.25 (13.43)	11.60 (11.06)
Jul	15.25 (14.54)	16.55 (16.28)
Aug	12.80 (12.21)	14.15 (13.82)
Sep	5.25 (4.95)	8.70 (8.26)
Oct	2.45 (2.30)	1.50 (1.38)
Nov	-9.25 (-9.21)	-5.70 (-5.50)
Dec	-28.95 (-27.15)	-14.45 (-15.05)
Annual	-2.20 (-2.68)	-2.20 (-2.51)